

UNIVERSITA' DEGLI STUDI DI SIENA
DIPARTIMENTO DI MEDICINA MOLECOLARE E DELLO SVILUPPO

DOTTORATO DI RICERCA IN
MEDICINA MOLECOLARE

CICLO XXIX

COORDINATORE PROF.SSA ANTONELLA NALDINI

TITOLO DELLA TESI: Overexpressed genes in Malignant Pleural Mesothelioma: possible role in tumourigenesis and evaluation of their use as a prognostic marker.

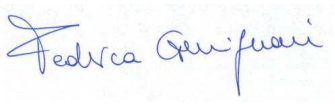
SETTORE SCIENTIFICO-DISCIPLINARE: BIO/18

DOTTORANDA: DR. ELISA BARONE



_____

TUTOR: PROF.SSA FEDERICA GEMIGNANI



_____

ANNO ACCADEMICO: 2015/2016

Index

Abstract **6**

1 Introduction 8

Malignant Pleural Mesothelioma 8

1.1 The normal mesothelium 9

1.2 Aetiology of MPM **11**

1.2.1 Asbestos 11

1.2.2 SV40 infection 17

1.2.3 Exposure to Ionizing Radiations 17

1.2.4 Predisposing Genetic Factors 18

1.3 MPM: clinical features 20

1.4 Molecular alterations in MPM **21**

1.4.1 Somatic genetic alterations in MPM 21

1.4.2 Other molecular pathways involved in the MPM 24

1.4.2.1 Apoptosis and Cell cycle 24

1.4.2.2 Proliferation and angiogenesis 25

1.5 Diagnosis of MPM 26

1.6 Prognostic marker for MPM **30**

1.7 Therapeutic approaches for MPM 32

2 RNAi approach for the identification of new potential biomarkers and therapeutic targets for MPM **32**

3 Backgroud: identification of overexpressed genes in MPM 33

4 Aim **35**

5. Materials and Methods 36

5.1 Selection of putative target genes **36**

5.2 RNAi phenotypic screening **36**

5.2.1 Cell cultures 36

5.2.2 Transfection efficiency 36

5.2.3 siRNA transfection protocols 37

5.2.4 Silencing RNA oligonucleotide 40

5.2.5 RNA isolation and cDNA synthesis 41

5.2.6 Primer design and quantitative Real-Time PCR (QPCR) 41

5.2.7 Protein extraction and Western Blotting 43

5.2.8 Sulphorhodamine (SRB) assay 44

5.2.9 Colony formation assay (CFA) 44

5.2.10 Flow cytometry (FACS) 44

5.2.11 Caspase - Glo® 3/7 assay 45

5.2.12 Wound-Healing Assay 45

5.2.13 Senescence assay 45

5.2.14 Statistical analysis 46

5.3 Tissue Microarray Immunohistochemistry 46

5.3.1 Ethics and consent 46

5.3.2 Antibodies 46

5.3.3 Evaluation of antibody specificity: western blot analysis 47

5.3.4 Characteristic of the MPM Tissue microarray employed 48

5.3.5 Immunohistochemistry 49

5.3.6 Scoring and statistical analysis 49

5.4 Evaluation of THBS2 and MCT4 expression in normal pleura samples **50**

6. Results **51**

6.1 Selection of putative target genes **51**

6.2 RNAi phenotypic screening **51**

6.2.1 CCNO phenotypic analysis 51

6.2.2 CFB phenotypic analysis 56

6.2.3 THBS2 phenotypic analysis 60

6.2.4 TIMP3 phenotypic analysis 65
6.2.5 SULF1 phenotypic analysis 72
6.2.6 PDGFRB phenotypic analysis 79
6.2.7 ASS1 phenotypic analysis 86
6.2.8 SOD1 phenotypic analysis 91
6.2.9 RAN phenotypic analysis 96
6.2.10 CDH11 phenotypic analysis 103
6.2.11 IMP3 phenotypic analysis 107
6.2.12 EIF4G1 phenotypic analysis 114
6.2.13 MCT4 phenotypic analysis 120
6.3 Tissue Microarray Immunohistochemistry **127**
6.3.1 Evaluation of antibody specificity: western blot analysis 127
6.3.2 BSG 129
6.3.3 CAIX 130
6.3.4 MCT1 131
6.3.5 MCT4 131
6.3.6 THBS2 133
6.3.7 Survival analysis 133
6.4 Evaluation of THBS2 and MCT4 expression in normal pleura samples 134

7. Discussion **136**
7.1 *CCNO* **136**
7.2 CFB **136**
7.3 THBS2 137
7.4 TIMP3 139
7.5 SULF1 142
7.6 PDGFRB **144**
7.7 ASS1 145
7.8 SOD1 ..... **147**
7.9 RAN **149**
7.10 CDH11 151
7.11 IMP3 ..... **152**

7.12 EIF4G1 154
7.13 MCT4 and MCT1, CAIX, BSG **156**
8. Conclusions and future perspectives **158**

REFERENCES 159

Abstract

Malignant Pleural Mesothelioma (MPM) is a very aggressive cancer poorly responsive to current therapies. The prognosis is very poor as the development of MPM leads to a median survival of less than one year from the time of diagnosis (Bertino et al. 2009). Moreover, the rapidly growing nature of this cancer, the non-specific onset of symptoms and the lack of an accurate biomarker do not lead to a sufficiently early diagnosis for a radical treatment of the disease. Thus, the identification of novel diagnostic and prognostic biomarkers and therapeutic targets is needed. The knowledge of the genes involved in the triggering/progression of MPM is still limited. In recent years a number of aberrantly expressed genes were suggested, but with a poor consistency among studies. To identify the relevant genes potentially involved in MPM, recently, our group carried out an extensive literature review focused on transcriptome studies whose results were intersected with those from a data mining approach (Melaiu et al. 2012). The results underwent to validation on MPM tissues and cell lines (Melaiu et al. 2015). The study led to the identification of a group of 21 deregulated genes in MPM. Among the 21 genes identified we focused our attention on those up-regulated in MPM tissues and at least in one MPM cell line (i.e. *THBS2, CCNO, CFB, TIMP3, SULF1, PDGFRB, ASS1, SOD1, RAN, CDH11, EIF4G1).* In addition, we made an extensive literature search to identify the most promising novel diagnostic and therapeutic target for MPM and we undertook the study of *IMP3* (Hanley et al.2008; Ikeda et al. 2010; Ikeda et al. 2011; Shi et al.2011; Lee et al. 2013; Okazaki et al. 2013; Minato et a. 2014) , *MCT4* (Mogi et al. 2013), *MCT1* (Mogi et al. 2013), *BSG* (Pinheiro et al. 2012) and *CAIX* (Ramsey et al. 2012; Capkova et al. 2014).
In order to investigate the role of these genes in the carcinogenesis of MPM we performed a phenotypic screening of five MPM cell lines (Mero14, Mero25, IstMes2, NCI-H28, REN) and one non-malignant mesothelial cell line (Met5A) following gene-silencing. We analysed the changes in the proliferation rate, in the caspase3-7 activity, in the migration ability, in the colony formation ability, in the level of senescence and in the cell cycle after transient siRNA transfections.
The RNAi screening highlighted a role in MPM malignant phenotype for *ASS1, CDH11, EIF4G1, IMP3, MCT4, PDGFRB, RAN, SOD1, SULF1, THBS2, TIMP3.*
Moreover, we evaluated the potential prognostic role of THBS2, CDH11, ITGA4, MCT4, MCT1, BSG and CAIX through a tissue microarray (TMA) immunohistochemistry on a series of 135 MPM samples. None of the target analysed showed a statistical significant association, after multiple correction, between protein expression and the overall survival. The weak staining of THBS2 and the negative staining of MCT4 on six normal pleura samples compared to MPM tissues prompted

us to further investigate on protein expression levels: we increased the analysis of protein expression to 15 normal pleura samples.

These results highlights the role of a group of genes, overexpressed in MPM, in the carcinogenetic process suggesting potential novel therapeutic approaches for the treatment of MPM.

1 Introduction

Malignant Pleural Mesothelioma

Malignant pleural mesothelioma is an aggressive tumour arising in the pleura from mesothelial cells and showing a diffuse pattern of growth over the pleural surfaces. Mesothelioma is the most frequent neoplasm affecting the pleura and remains a major health threat for many years to come. Although the causation by asbestos is firmly established since more than 50 years, in many world regions, the use of this dangerous carcinogen peaked between 1970 and 1990. Although now banned in the USA and most European countries, incidence and mortality rates are still climbing. (Robinson and Lake 2005; Tomasson et al 2016) In Italy the peak of mortality from malignant pleural mesothelioma is expected in the period 2012–2024 with about 800 mesothelioma annual deaths (Fig. 1 Marinaccio et al. 2005). Besides the clear established role of the asbestos, other risk factors were suggested, such as the exposure to ionizing radiations (Zucali and Giaccone 2006; Carbone and Bedrossian 2006), the infection to SV40 (Rivera et al., 2008), as well as an enhanced individual genetic susceptibility (Carbone et al., 2012; Roushdy-Hammady et al., 2001; Landi et al., 2007).

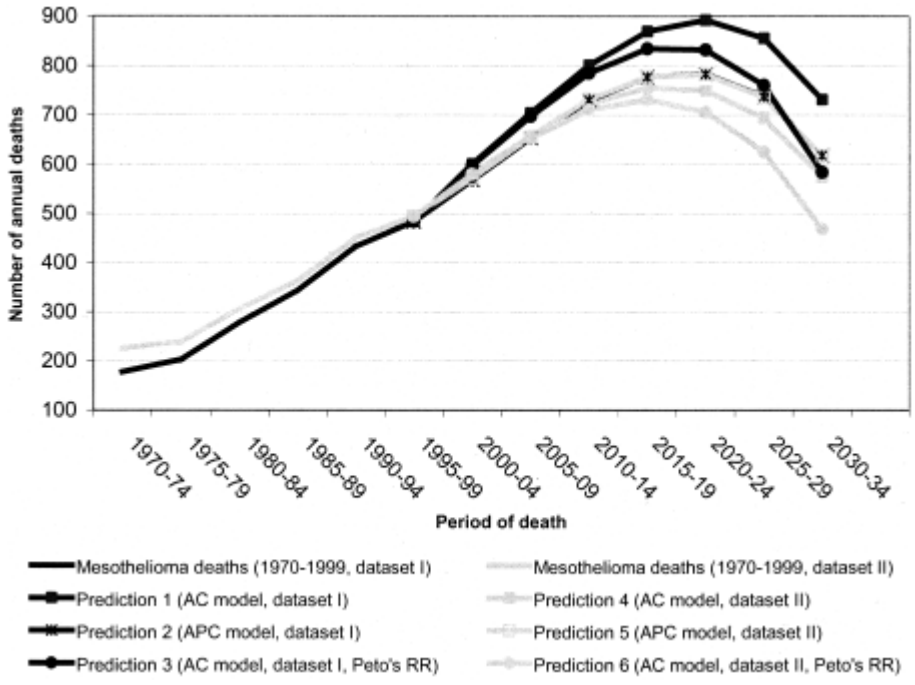


Fig. 1: Pleural mesothelioma deaths (1970–1999) from data set 1 (pleural cancer deaths corrected using the ratio of mesothelioma to pleural cancer mortality derived from the Tuscan mesothelioma register) and data set 2 (pleural cancer deaths corrected using the above ratio and the estimate of misdiagnosis) and predicted (2000–2030) deaths among men aged 25–89 years, Italy, according to different age-period-cohort models (Marinaccio et al. 2005)

Due to its aggressive nature and resistance to chemotherapy, development of MPM leads to a median survival of approximately 14 months from the time of diagnosis in patients undergoing surgery (Flores et al., 2008). But, generally, MPM patients candidates for surgery are those with less advanced disease. Total survival, including patients who are not candidates for surgical resection, is less than 1 year from diagnosis (Bertino et al., 2009).

Survival is influenced by stage, and in 663 consecutive patients (538 men, 125 women) who underwent pleurectomy or extrapleural pneumectomy from 1990 until 2006, median survival was 38 months for stage I, 19 months for stage II, 11 months for stage III and 7 months for stage IV (Flores et al., 2008).

They may be seen clinically as localized pleural tumours or as diffuse pleural disease with effusion and encasement of the lung and obliteration of the pleural space.

The overall outcome of this disease remains not encouraging: it does not respond well to chemotherapy and resection remains still the treatment of choice. Malignant pleural mesotheliomas are locally aggressive and difficult to treat, treatment is generally unsatisfactory, and long-term survival is rare indeed for the majority of patients, MPM is diagnosed at late stages when the tumour remains unresectable, the prognosis is poor, and an efficient management strategy for this cancer is still absent.

1.1 The normal mesothelium

The mesothelium is a membrane, consisting of a monolayer of specialized pavement-like cells that line the body's serous cavities and internal organs. It takes the name of pleura, if it surrounds the lung, peritoneum for the abdominal cavity, and pericardium for the heart sac. Mesothelial tissue also surrounds the male, and female internal reproductive organs (the tunica vaginalis testis, and the tunica serosa uteri, respectively). The visceral mesothelium is the mesothelium that covers the internal organs, while the layer that surrounds the body walls is the parietal mesothelium (Mutsaers, 2002). Mesothelial cells are derived from the embryonic mesoderm cell layer, that lines the coelom (body cavity) in the embryo (Tiedemann, 1976). Numerous are their functions. The mesothelium forms a barrier against pathogen agents, and injury due to the inflammation, keeping the integrity of the serosal space, it surrounds (Mutsaers, 2004). The second important function of the mesothelium is the transport of fluid and cells across the serosal cavities.

The pleura is a thin serous membrane which turns back on itself to form a double layer: the visceral and the parietal (Fig.2). The visceral pleura covers the surface of the lungs and the parietal pleura covers the inner surface of the chest wall, mediastinum and diaphragm. Under normal

circumstances the cavity contains 5-20ml of fluid (Fig.2). The lining of the pleura is composed of a continuous layer of flat or low cuboidal cells- the mesothelium.

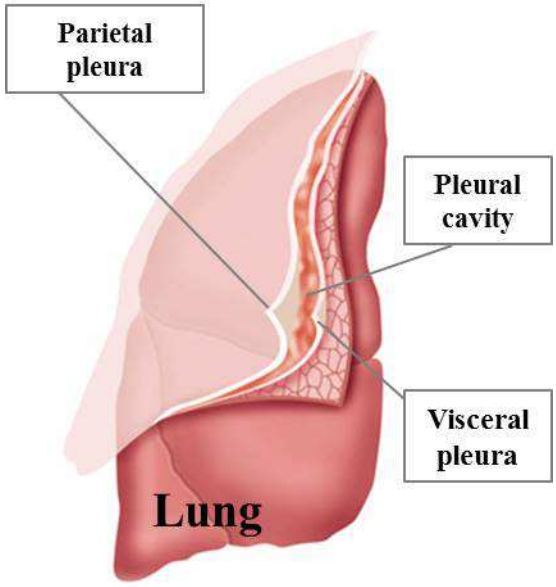


Fig.2 Lung and pleura: The lung is surrounded by a thin serous membrane, called pleura, that turning on itself forms a double layer: the parietal and the visceral pleura. The cavity created between them is called pleural cavity and it contains the pleural fluid.

The pleurae are continuous with each other at the hilum. The parietal pleura is divided into three parts: rib, which adheres to the coast; mediastinal, which lies medial to the heart; diaphragm, which is located along the diaphragm. The visceral pleura starts from the hilum into the lung, along the bronchi and blood vessels, and allows the distinction in the pulmonary lobules. The visceral and parietal pleura delimit a space, called "pleural cavity", containing the pleural fluid which, during the respiratory activity, allows the two pleurae to slide over each other (Fig.2). Between the two layers there is a negative pressure, required to keep the lung stretched, within the pleural sac, and to allow the modification of volume during breathing movements. Pleural fluid is a serous fluid produced by the normal pleurae in order to provide a slippery, non-adhesive, and protective surface to facilitate intra-coelomic movement (Peek et al., 2000). The parietal layer secretes 2400 ml of fluid daily, which is reabsorbed by the visceral layer.

Malignant mesothelioma occurs in the pleural cavity and usually in the lower half of the hemithorax on the right side more often than the left. It encases the lung and direct extension into the subpleural lung is common

1.2 Aetiology of MPM

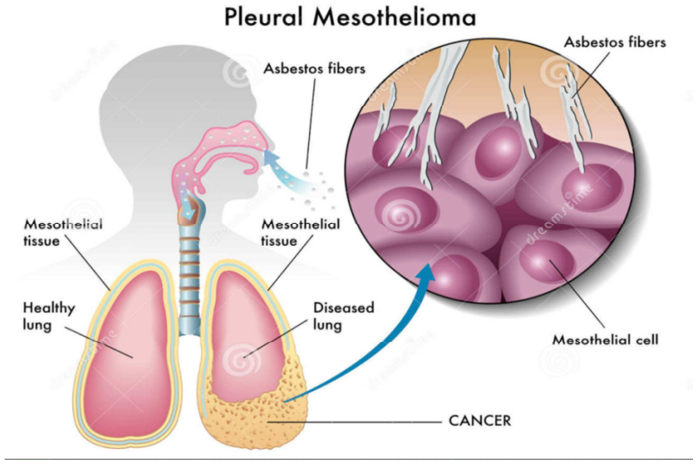


Fig. 4: Asbestos: the main cause of MPM. The exposure to asbestos fibres occurs mainly through inhalation. Normally, the inhaled external agents are removed by phagocytosis and transported by the dense network of lymphatic vessels to the pulmonary hilum. Some of the amphibolic asbestos fibres are removed with this mechanism but, most of them are retained in the lung causing asbestosis. Long-term inhalation of asbestos fibres increases the risk of lung cancer and mesothelioma

1.2.1 Asbestos

Asbestos is considered the main cause of mesothelioma: according to the World Health Organization (WHO), "asbestos is one of the most important occupational carcinogens causing about half of the deaths from occupational cancer" (Concha-Barrientos et al. 2004; Driscoll et al. 2005; World Health Organization 2006).

Asbestos is the commercial name for a group of hydrated mineral silicate fibres including two major forms: serpentine, represented by chrysotile (white asbestos) and amphibole, which includes crocidolite (blue asbestos), amosite (brown asbestos), anthophyllite, actinolite and tremolite (Park et al., 2012; Straif et al., 2009)(Fig. 5).

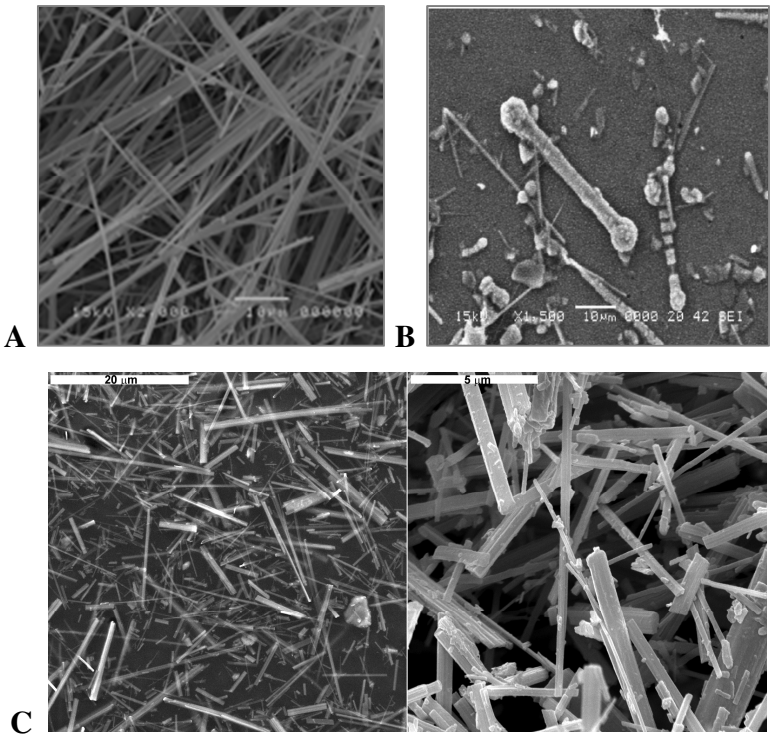


Fig 5: A Chrysotile fibres (white asbestos); B Crocidolite fibres (blue asbestos) from the lung of an asbestos miner (Phillips et al. 2012); **C Amosite (brown asbestos);** usually it is found in materials used as fire retardants in thermal insulation products.

The association between amphibole asbestos exposure and MPM development is well accepted. In particular, crocidolite is considered to be one of the most toxic forms of asbestos due to its high iron content; moreover the long and thin fibres (especially ≥ 8 µm in length ≤ 0.25 µm in width) are thought to be more dangerous, because they have longer biopersistance in the pleura. These fibres are able to penetrate the lung and cause repeated damage, tissue repair and local inflammation (Gibbs 1990; Steyner et al. 2008; Berman et al. 2008).

It is currently stated that the time periods elapsing between first exposure to asbestos and diagnosis of mesothelioma are 20-40 years. However some studies conducted on large mesothelioma series reveal that latency periods are generally longer (Bianchi et al. 1997; Marinaccio et al. 2007;

Asbestos fibres can cause tissue damage trough essentially three mechanisms: ingestion, skin contact, and inhalation. It is the inhalation of the fibres the main route of exposure. The main diseases associated with inhalation of asbestos fibres are asbestosis, lung cancer, MPM, pleural effusions, and rounded atelectasis.

Normally, the pleura is protected from the inhaled external agents, which are trapped in the alveoli or interstitium. The inhaled particles are removed by phagocytosis and transported by the dense

network of lymphatic vessels to the pulmonary hilum. The amphibolic asbestos fibres are able to overcome, exceptionally, the barrier lung-pleura, and the lymphatic drainage of them is difficult.

The exact mechanism by which asbestos fibres migrate to the pleural surface is not known yet. Moreover, it is not possible to explain why the same substance, once in the pleural space, may cause pleural effusions in some individuals, whereas plaques, pleural fibrosis, or MPM in others. The explanation probably lies in a delicate combination of mechanical, biological, and genetic events.

At the present time, the most accredited hypothesis is that the asbestos fibres accumulate within the tissue and lead to the activation of a chronic inflammatory status of the mesothelium (Donaldson 2010). The inflammation, it is thought, induces mesothelial cells to continuously release reactive oxygen species (ROS), as well as cytokines and growth factors, such as the hepatocyte growth factor (HGF), the epidermal growth factor (EGF), the platelet-derived growth factors (PDGFs) (Lee et al., 2007), and the vascular endothelial growth factor (VEGF) (Pasello and Favaretto 2009). An elevated expression of PDGF (chains A and B) were observed in the early response to asbestos and were found to be mitogens for normal mesothelial cells (Gerwin et al., 1987; Langerak et al., 1996), and to act as paracrine stimulators for the proliferation of the MPM (Metheny-Barlow et al., 2001; Pass and Mew 1996). However, asbestos may also cause auto-phosphorylation of EGFR (Zanella et al., 1996), resulting in activation of mitogen-activated protein (MAP) kinase cascade and phosphorylation of extra cellular signal-regulated kinases 1 and 2 (ERK1/ERK2). Studies of transforming growth factor (TGF)-β in both cell lines and MPM samples have shown the over-expression of three isoforms, including both active and latent forms of TGF-β1 and TGF-β2 (Fitzpatrick et al., 1994).

On the other hand, the asbestos fibres which interact with the alveolar macrophages, are captured and entrapped within lysosomes (Matsuzaki et al., 2012). It seems that this leads to the activation of NLRP3 inflammasome, to cleave procaspase 1 to an active form, followed by the activation of pro-interleukin (IL)-1β, and production of ROS, and reactive nitrogen species (RNS) in the macrophages. The consequential apoptotic death of the alveolar macrophages, and the liberation of various cytokines/chemokines, such as IL-1β, tumour necrosis factor (TNF)-α, macrophage inflammatory protein (MIP)-1/2, monocyte chemo-attractant protein-1, and IL-8, cause chronic inflammation and proliferation of collagen fibres as well. This mechanism is continuously repeated: indeed, the released silica particles and asbestos fibres from dead alveolar macrophages are recognized by newly nearby macrophages, with the repetition of similar cellular reactions described above (Hamilton et al., 2008, Thakur et al., 2008).

All these elements constituite a proliferative stimulus for the mesothelium (Lee et al., 2007). The continuous exposure to ROS and to proliferative stimuli is a stress for the mesothelial cells and this may lead to long-term DNA damages (Zucali and Giaccone, 2006). It was also suggested that an increased ROS release could be related to the action of Fe-particles present on the surface of asbestos fibres, in particular on the amphibolic type (Simeonova and Luster, 1995).

The DNA lesions accumulated could cause permanent mutations (Alberts at al. 2002) and/or lead to an epigenetic reorganization of the DNA: these events represent one of the most important molecular changes for reprogramming cells towards a malignant phenotype. The picture below summarizes how the asbestos fibres lead to malignant transformation of mesothelial cells (Fig. 6).

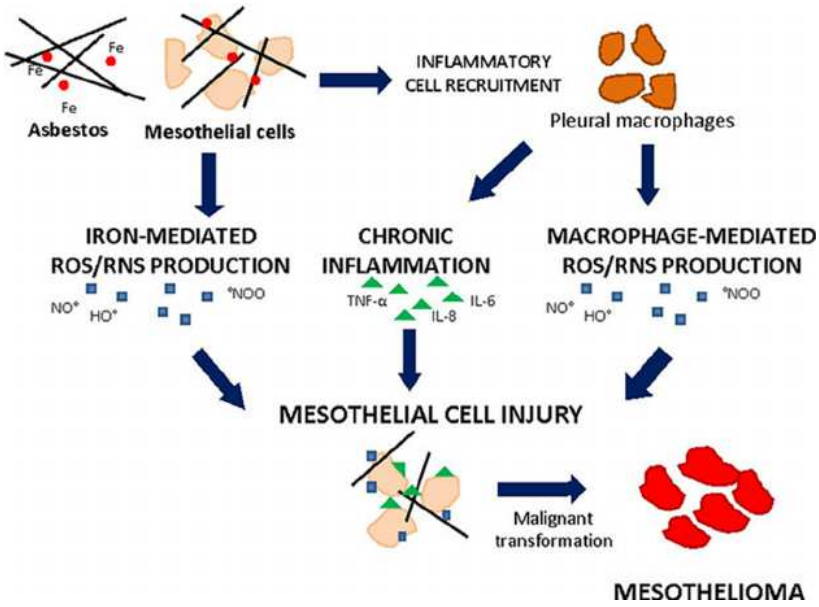


Fig. 6: Mechanisms of action of asbestos fibres: The exposition of mesothelial cells to iron and macrophage-mediated ROS/RNS production and inflammatory cytokines can induce cell injury and malignant transformation giving rise to mesothelioma. (Benedetti et. al 2015)

Since MPM arises most frequently in workers exposed to asbestos fibres, this neoplasm is considered an occupational disease (Mazzoni et al., 2012). Indeed, it is thought that about the 80% of cases is caused by asbestos exposure (McDonald and McDonald 1996).

The first case of MPM has been described in 1947 (Yang et al., 2008). The relationship between MPM and asbestos was first documented in a study conducted in South Africa, on a group of miners of asbestos in 1960 (Wagner et al., 1960). From then, the scientific community has continued to demonstrate the relationship between exposure to asbestos and development of MPM (Selikoff et al., 1968; Spirtas et al., 1994; Hansen et al., 1998; Kurumatani and Kumagai, 2008), and

the developed countries started to collect epidemiological data on asbestos and MPM to confirm the relationship between the incidence of the disease, and the asbestos exposure.

The latency period for MPM after initial exposure to asbestos is typically longer than 30 years, and the median survival time after diagnosis is 9–12 months (Robinson et al., 2005). For this reason, although the use of asbestos has been banned in the Western world since 1980, the incidence of MPM is expected to increase in countries such as Italy (Peto et al., 1999), Great Britain (Tan et al., 2010), and Australia (Kao et al., 2011). On the contrary, the United States has already reached the peak of cases of MPM because asbestos was banned earlier than elsewhere (Price and Ware 2004), although it is expected a further increase in incidence in the aftermath of the World Trade Center (Ismail-Khan et al., 2006), which was partly built with asbestos (insulation, partitions).

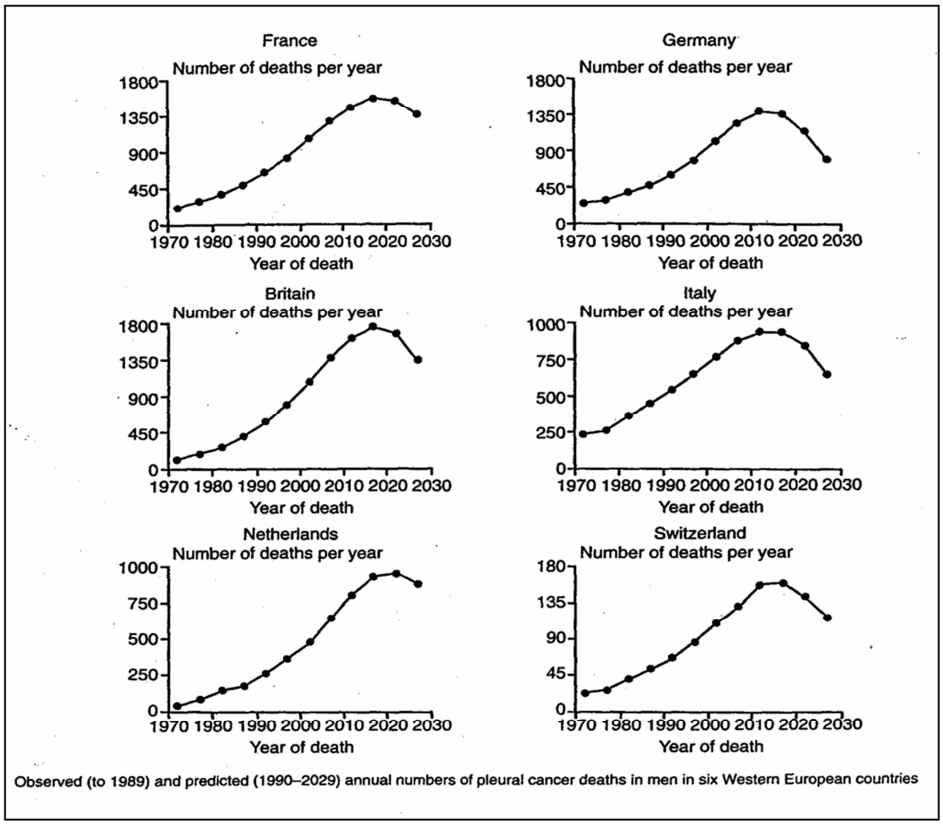


Fig. 7: Estimations of MPM death in Western Europe countries (Peto et al. 1999)

Delgermaa et al., have summarized data on MPM death reported by the World Health Organization database since 1994 to 2008 (Delgermaa et al., 2011). However, it should be noticed that, because

the MPM is a rare disease, few international data are available. A brief extract of the recorded observations are reported below.

In total, 92.253 MPM deaths were reported by 83 countries. Crude and age-adjusted mortality rates were 6.2 and 4.9 per million, respectively. The mean age at death was 70 years, and it has been reported that the incidence is much higher in men than women. Regarding the geographical distribution of deaths, the United States of America reported the highest number, while over 50% of all deaths occurred in Europe. In contrast, less than 12% occurred in middle- and low-income countries.

Although the asbestos was banned or restricted in most of the industrialized world, its use is increasing in some parts of Asia, South America, and the former Soviet Union. The asbestos exports from Canada, Russia, Brazil to countries such as India, Indonesia, and Philippines, is creating an epidemic that may take decades to peak. Moreover, no data were available for China, India, Kazakhstan, the Russian Federation or Thailand, which have produced, or consumed asbestos, at substantial levels for many years.

Regarding the Italian background, in 1992 (Law No. 257), each mining, trade, import, export and production of asbestos, or products containing asbestos have been banned from the entire Italian territory. Epidemiological surveillance of MPM cases is entrusted to the National Register of Mesothelioma (ReNaM), established at the National Institute for Occupational Safety and Prevention (ISPESL). The fifth report of the ReNaM, published in 2015, reports the incidence and exposition to asbestos data of the 21,463 mesothelioma cases diagnosed from 1993 to 2012. Until 45 years the disease is very rare (only 2% of the total number of cases) and the average age at diagnosis is 69.2 years (DS: ± 10,7) without significant difference between gender (70.2 years in women and 68.8 in men). The 93% of the registered mesothelioma cases are pleural mesotheliomas. The standardized rate for mesothelioma (per 100,000 individuals) is equal to 3.64 in men, and 1.32 in women in 2011. In all the cases detected by the registry, 69.5% have occupational exposure, 4.8% family exposure, 4.2% environmental and 1.6% exposure linked to leisure or hobbies activities. For the 20% of the cases the exposure was unlikely or unknown.

The number of cases varies considerably from region to region: the higher number of cases have been diagnosed in Lombardy followed by Piedmont and Liguria . The lowest number of cases have been reported in Molise, Calabria, Basilicata, and Umbria.

1.2.2 SV40 infection

In addition to asbestos exposure, Simian virus 40 (SV40) infection seems to be an additional cause of MPM (Klein et al., 2002; Cristaudo et al., 2005). Indeed, a transforming synergistic action between asbestos fibres and SV40 has been proved in human, hamster, and murine mesothelial cells and in animal models (Pietruska et al., 2007; Robinson et al., 2006; Kroczynska et al., 2006). However, not all the authors agree with this view (Aoe et al., 2006) and the role of SV40 in the aetiology of MPM for humans is still to be ascertained completely. The SV40 is a DNA virus, found in both monkeys, and humans. The virus was firstly identified by Dr. Eddy in 1964 in cultures of rhesus monkey kidney cells, employed to produce polio vaccine (Eddy, 1964). It has been hypothesized that the virus was transmitted from monkeys to humans mainly in the period 1955-1963, through the administration, worldwide, of anti-polio vaccines contaminated with SV40 (Strickler et al., 1998). However Carbone et al., have suggested also a possible virus transmission directly by person-to-person contact (Powers and Carbone, 2002). Once inside the host, the SV40 produces two proteins: the large T antigen (Tag), and the small t antigen (tag). Tag has been shown to bind and inactivate both p53 and pRB in mesothelial cells (Carbone et al., 1997; Gazdar et al., 2002), thus stimulating cell proliferation (Testa and Giordano, 2001). Regarding tag protein, it promotes the MAP signalling pathway, inhibiting the protein phosphatase 2A (PP2A), involved in de-phosphorylation of many protein substrates, including regulators of the cell cycle (Rundell and Parakati, 2001). Mazzoni E et al., have found that in 97 MPM serum samples, the prevalence of antibodies against SV40 viral capsid protein antigens is significantly higher (26%, $P = 0.043$) than in the control group (15%, $n = 168$). Taken with caution, this result could suggest that new therapeutic/preventive strategies could be also applied with antiviral drugs or vaccines (Mazzoni et al., 2012).

1.2.3 Exposure to Ionizing Radiations

It was showed that in rats exposed to asbestos and ionizing radiations (IR) the probability to develop MPM is increased, compared to rats exposed only to asbestos (Warren et al., 1981), suggesting a carcinogenic synergistic effect between radiations and asbestos (Zucali and Giaccone 2006; Carbone et al., 2002; Carbone et al., 2006). The MPM is a well-known consequence of radiation therapy used for the treatment of primary malignancy, like lymphoma, breast cancer, lung cancer and other malignancies. Interestingly, most of the reported cases were not previously exposed to asbestos. Teta and collaborators have shown that patients suffering Hodgkin's disease have a 20 times greater risk of developing MPM following radiotherapy (Teta et al., 2007).

Interestingly recent data from several laboratories indicate that asbestos exposure and SV40 infection are co-carcinogens in causing mesothelioma in rodents and in causing malignant transformation of human mesothelial cells in tissue culture.

1.2.4 Predisposing Genetic Factors

An exciting new development comes from the discovery that genetic susceptibility to mineral fibre carcinogenesis plays a critical role in the incidence of this cancer in certain families. Thus the individual genetic factors seem to be important in the development of MPM. This has been demonstrated firstly, in a study conducted in three villages of Cappadocia, where erionite, a mineral of the zeolite family, was extracted from quarries, and used as building material. In these villages an "epidemic" of MPM was recorded, and more than 50% of the inhabitants died for the disease (Carbone et al., 2007); initially, the erionite has been considered as the only etiologic factor, but in 2001 Roushdy-Hammady and colleagues investigated whether some families of the villages were genetically predisposed to the development of the malignancy. Through a deep analysis of the pedigree, until the sixth generation (526 individuals in total), the authors highlighted the possibility that MPM was genetically transmitted, as an autosomal dominant disease (Roushdy-Hammady et al., 2001). The suspicion about familiarity to MPM comes also from observations of families with a history of environmental exposure to asbestos such as that reported by Musti and collaborators: the entire family (mother, father and 4 children) has lived for 13 years in Casale Monferrato, very close to the factory where the father worked, the only one with a real occupational exposure to asbestos. Two sisters have developed MPM, the other one has developed peritoneal mesothelioma, and the brother, pleural plaques, whereas the mother was not affected (Musti et al., 2002). Moreover, in 2011, mutations within *BAP1* were reported to be causative for a rare familial form of MPM (Testa et al., 2011). At the present time, this is the only gene identified to confer an increased susceptibility to MPM. Biallelic inactivation of *BAP1* was found in two US families with high incidence of MPM. In one of them, Testa et al., sequenced *BAP1* in germline DNA identifying that six affected members had identical mutations, whereas unaffected family members did not. In the second analyzed family, germline DNA from three individuals with MPM reported C/G-to-T/A transition in exon 16, creating a stop codon. Moreover the authors have identified that in addition to MPM, some *BAP1* mutation carriers developed uveal melanoma.

Some studies have also suggested that low-penetrant polymorphisms of genes involved in the metabolism of xenobiotics may constitute a risk factor for the development of sporadic MPM.

Associations between risk of MPM, and polymorphisms in specific genes have been reported: for example, it has been observed that the absence of the polymorphic gene *GSTM1*, that encodes for the enzyme "Glutathione S-transferase", in some studies it has been shown that the absence of the gene increases the risk of MPM (Hirvonen et al., 1995; Landi et al., 2007).
which combines the glutathione to a wide range of electrophilic substances, such as ROS, easily released from the cells and excreted.
Moreover, for individuals having simultaneously the null genotype for the *GSTM1* gene, and the slow acetylator alleles for *NAT2* gene, the risk of developing MPM doubles, compared to subjects with a present genotype for *GSTM1*, and rapid acetylator for *NAT2* (Hirvonen et al., 1996).
The *NAT2* gene encodes the N-acetyltransferase. The enzyme catalyzes the transfer of the acetyl group from acetyl-CoA on the amino groups. Aromatic and heterocyclic amines are some of its substrates. The response against oxidative stress induced by asbestos fibres, involves products also of other genes, such as manganese superoxide dismutase (MnSOD), one of the most important antioxidant enzymes in mammals (Hayes et al., 2005). It has been shown that the activity of MnSOD is almost absent in normal mesothelial cells of the pleura, while it is higher in MPM cells (Kinnula et al., 1996). The most common polymorphism of MnSOD results in an Alanine (Ala) to Valine (Val) amino acid change at codon 16, producing a conformational change in the protein secondary structure that may impair the transport of the protein into the mitochondria. (Sutton et al., 2003). Ninety cases of MPM and 395 controls were genotyped using the arrayed-primer extension technique. The Ala/Ala genotypes at codon 16 within MnSOD was showed to be associated with the risk of MPM, and a stronger effect of MnSOD was observed among patients without a clear exposure to asbestos fibres (Landi et al., 2007). Other potentially involved polymorphisms are within the genes involved in DNA repair. In particular *XRCC3* was found associated with MPM. This gene encodes a protein involved in homologous recombination and repair of DNA damage. In a case-control study in Casale Monferrato, variants of *XRCC3* (*XRCC3-241T, XRCC1-399Q*) were associated with an increased risk of MPM (Dianzani et al., 2006). This has been also confirmed by a study with a larger sample size, extended to the city of Turin (Betti et al., 2011).
The studies conducted to date do not clarify in a definitive way what are the susceptibility alleles for MPM. This is also due to the rarity of the tumour, and the consequent difficulty in carrying out studies of case-control with a sample size sufficient to guarantee the desired statistical significance.

1.3 MPM: clinical features

The neoplastic cells are initially localized in the basal pleural segments, then the tumour spreads involving the pleural spaces, as well as with the direct invasion of the thoracic structures. The affected lung is permeated and surrounded by a thick layer of gelatinous neoplastic tissue. Three main histological subtypes are known (Fig.8): epithelioid mesothelioma is the most common histological subtype (about 50-70% of all mesothelioma cases) and it is the most treatable, while the sarcomatoid is the most rare subtype and it accouts for only 10-15 percent of all the mesothelioma cases; approximately 30% of all cases are biphasic/mixed histological subtype (Travis et al., 2004.). These groups show significant differences in their histological and clinical features:

- Epithelioid: characterized by cuboidal, cylindrical or flattened cells, conferring to the structure a shape tubular, papillary, or tubulo-papillary. The epithelial cells have an acidophilus cytoplasm, and vesicular nuclei with prominent nucleoli.
- Sarcomatoid: it shows interwoven bundles of spindle cells (fibroblast-like) in a stroma collagen.

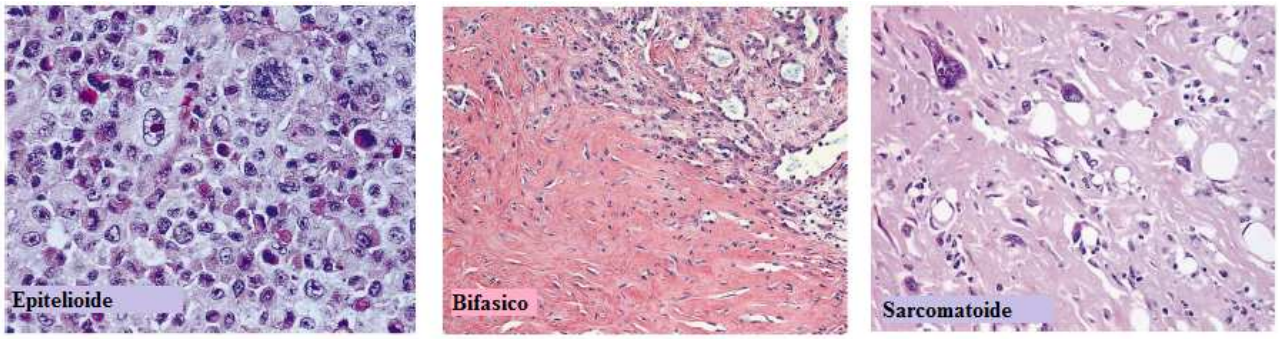


Fig.8: Haematoxylin-eosin staining to identify the histology of MPM, from left to right Epithelioid MPM, Biphasic MPM and Sarcomatoid MPM

According to the TNM staging system, the evolution of the MPM goes through four stages (Moore et al., 2008):

1. Stage I (localized MPM): the cancer interested the right or left pleura and may also spread to the lung, pericardium, or diaphragm, on the same side. Lymph nodes are not involved.
2. Stage II: the cancer spreads from the pleura, on one side, to the lymph nodes next to the lung, on the same side. It may also spread to the lung, pericardium, or diaphragm, on the same side.

3. Stage III: the cancer invaded the chest wall, muscle, ribs, heart, esophagus, or other organs in the chest, on the same side, with or without lymph node involvement, on the same side as the primary tumour.
4. Stage IV: the cancer spreads to the lymph nodes in the chest on the side opposite to the primary tumour, or extends to the pleura or lung on the opposite side, or directly to the organs of the abdominal cavity or neck. At this stage, there are distant metastases.

1.4 Molecular alterations in MPM

1.4.1 Somatic genetic alterations in MPM

The knowledge of the molecular-genetic alterations underlying MPM is an important guide for proper diagnostic orientation, prognosis and therapy. Since the typical MPM tumour biology has a broad spectrum of heterogeneity, as demonstrated by both the morphology and, even more, by the various chromosomal abnormalities in the various subtypes, it is not easy to identify a common pattern, which differentiates this pathology (Krismann, et al., 2002). Cytogenetic studies have revealed complex karyotypic changes in the MPM, involving all chromosomes with chromosomal losses more frequent than chromosomal gains. Frequent losses are localized on chromosome arms 1p, 3p, 4q, 6q, 9p, 13q, 14q, and 22q and gains involve chromosome arms 1q, 5p, 7p, 8q, and 17q. (Krismann et al., 2002; Lindholm et al., 2007; Taniguchi et al., 2007; Ivanov et al., 2009; Cheung et al., 2010; Christensen et al., 2010; Jean et al., 2011). Mutations of proto-oncogenes and, deletions, loss of heterozygosity, or inactivation of tumour supressor genes occur frequently in basically all human cancers. Interestingly, mutations within p53 and pRb, among the most frequently mutated genes in cancer, are rare in the MPM (Lee et al., 2007). However, one of the predominant genetic abnormality in the MPM is the homozygous inactivation of the gene CDKN2A within the 9p21 region, occurring at a frequency of greater than 70%, (Prins et al., 1998; Chiosea et al., 2008). CDKN2A is regulated in order to allow stem cells to proliferate and plays a critical role also in the cellular senescence of mature cells, through the regulation of both the pathways pRb and p53 (Gil and Peters, 2006). The locus encodes two distinct proteins (overlapping genes), p16INK4a and p14ARF, originating from different transcription start sites and translated from mRNA undergone to alternative splicing. p16INK4A and p14ARF are involved in major networks "tumour suppressor" that govern fundamental physiological processes, such as replicative senescence of mature cells, apoptosis, the self-renewal of SCs (stem cells), but however, they are inactivated in tumours (Gil and Peters, 2006). p14ARF inactivates the human homolog of mouse double minute 2

(MDM2), which is an upstream regulator of p53 (Sekido, 2008), thus allowing the stabilization and activation of p53 (Yoshitaka, 2008) p16INK4a exerts its tumour suppressive effect by inhibiting the cyclin-D-dependent kinases (CDKs), thus preventing the CDK-mediated hyper-phosphorylation and the inactivation of pRB, that normally leads to the cell cycle arrest at the G1-phase (Zucali and Giaccone, 2006). The figure below summarizes the signaling pathways downstream CDKN2A (Fig. 9).

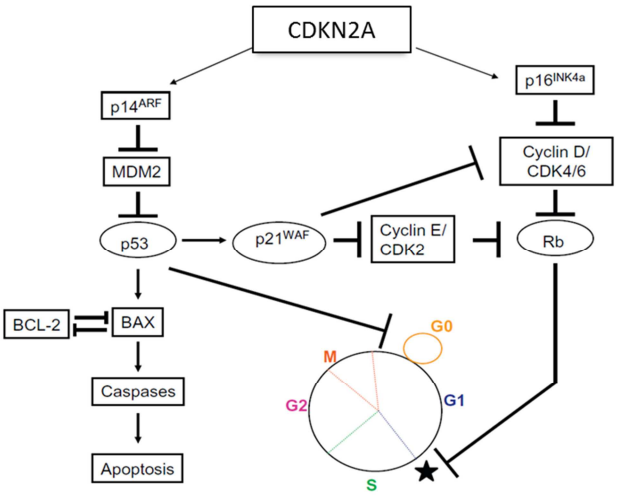


Fig. 9: Signaling pathways downstream CDKN2A. The locus of CDKN2A gene encodes two distinct proteins: p16INK4a and p14ARF that are both involved in the tumor suppressor networks. p16INK4a exerts its tumour suppressive effect by inhibiting the cyclin-D-dependent kinases (CDKs), thus preventing the CDK-mediated hyper-phosphorylation and the inactivation of pRB, that normally leads to the cell cycle arrest at the G1-phase while p14ARF inactivates the human homolog of mouse double minute 2 (MDM2), which is an upstream regulator of p53, thus allowing the stabilization and activation of p53.

The main cause of p16 inactivation is the homozygous deletion of the CDKN2A locus / ARF, although some cases of promoter hypermethylation events, which make it transcriptionally inactive, have been found (Kobayashi et al., 2008).

Frequently the gene *NF2*, coding for the tumor suppressor protein Merlin, is inactivated in MPM (Thurneysen et al. 2009). The loss of merlin in MPM has been associated not only to increased proliferation, but also increased invasiveness, spreading and migration (Poulikakos et al. 2006).

The Merlin protein acts as a negative regulator of the pathways of Hippo, involved in growth and tissue homeostasis, and PI3K (phosphoinositide 3 kinase) / AKT / mTOR, involved in the regulation of protein and lipid synthesis, metabolism, apoptosis, autophagy, proliferation, cell

motility and cytoskeletal organization (Stamenkovic and Yu , 2010; Laplante and Sabatini, 2012) (Fig. 10).

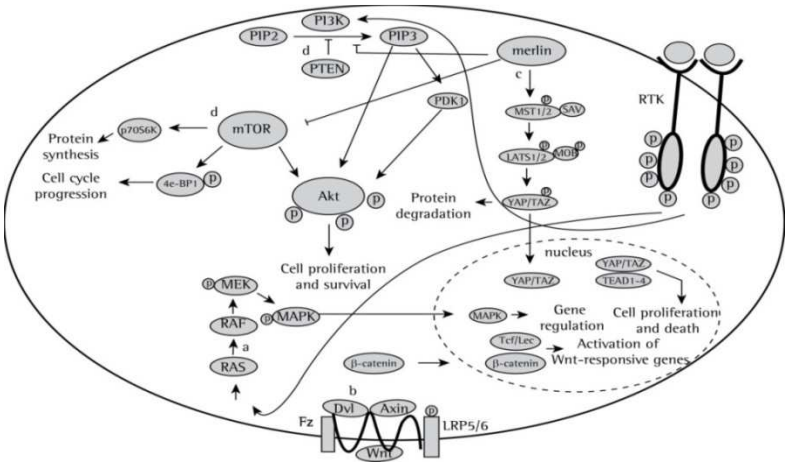


Fig. 10: Overview of the pathways regulated by Merlin

The activation of PI3K occurs in the presence of growth factors that bind tyrosine kinases or G-protein coupled receptors. The activated PI3K phosphorylates the 3'OH of phosphoinositide and phosphatidylinositols, including PIP3 (phosphatidylinositol 3,4, 5-triphosphate), which acts as an intracellular second messenger (Engelman, et al., 2006).

In particular PIP3 promotes AKT translocation (serine-threonine kinase implicated in the survival, apoptosis and metabolism), at the level of the cytoplasmic membrane, where it may undergo an activating phosphorylation (Laplante, et al., 2012). PIP3 activates AKT, which in turn activates mTORC1; mTORC1 is a complex constituited by the catalytic mTOR subunit togheter with these protein components: raptor (regulatory associated protein of mTOR), PRAS40 (proline-rich AKT substrate 40 kDa), and mLST8 (mammalian lethal with sec-13) (Yip et al. 2010).

Studies have shown that about 60% of MPM cell lines has an altered activation of AKT (Suzuki, et al., 2009). The recurrent deletion of PTEN (which encodes a phosphatase that acts as a negative regulator of the membrane translocation of AKT, dephosphorylating PIP2 to PIP3) promotes the expression of AKT (Suzuki, et al., 2009). The presence of mutations in PTEN has been confirmed in 60% of MPM cases (Opitz, et al., 2008).

Another chromosomal alteration involved in MPM is the deletion of 3p21 band. This deleted region carries nine genes including *BAP1*, *PHF7*, *SEMA3G*, *TNNC1*, *NISCH*, *STAB1*, *NT5DC2*, *C3orf78*, and *PBRM1*. Given the role of *BAP1* in the rare familial form of MPM, it is conceivable that an

altered activity of *BAP1* could provide a reasonable explanation for the frequent loss of 3p21 in MPM. *BAP1* encodes a nuclear ubiquitin carboxy-terminal hydrolase (UCH), called "BRCA1 associated protein-1", belonging to one of several classes of de-ubiquitinating enzymes. This gene contains binding domains for BRCA1 (OMIM: 113705) and BARD1 (OMIM: 601593), that form a tumour suppressor heterodimeric complex. Ventii KH et al., have shown that BAP1 exerts its tumour suppressor functions by affecting the cell cycle, speeding the progression through the G1-S checkpoint, and inducing cell death via a process that has characteristics of both apoptosis and necrosis (Ventii et al., 2008). Bott et al., have analyzed 53 samples of MPM patients, looking for additional genes crucial for MPM pathology, and have found that 12 (23%) of them showed somatic mutations inactivating the gene BAP1 (Bott et al., 2011). Yoshikawa and collaborators have analyzed the genomic alterations of BAP1 in 23 samples of MPM (16 epithelioid and 7 non-epithelioid), finding biallelic alterations of BAP1 in 14 samples (61%). Seven of these showed homozygous deletions of the BAP1 (partial or total), five had point mutations (including small deletions), while the other two had homozygous mutations without deletions. Of the 14 samples with mutations in BAP1, 13 were epithelioid and only one biphasic. These results reveal that the inactivation of BAP1 occurs at a very high frequency in patients with epithelioid MPM, and this could be useful for diagnosis of epithelioid type MPM (Yoshikawa et al., 2012).

In summary, the complete pattern of molecular changes will need further studies, integrating knowledge from different type of information in a more systematic approach.

1.4.2 Other molecular pathways involved in the MPM

Numerous molecular pathways involved in the MPM have been studied and identified, including the regulation of cell cycle, apoptosis, cell proliferation, and angiogenesis.

1.4.2.1 Apoptosis and Cell cycle

Apoptosis is a form of cell death essential for development, deletion of damaged cells and the turnover of the cells (Danial and Korsmeyer 2004). Since 1998 it has been reported that the MPM cell lines are more resistant to apoptosis, than the normal mesothelial cells (Narasimhan et al. 1998). The inhibition of apoptosis in MPM may contribute to its resistance to conventional chemotherapy. In MPM, several mechanisms of inhibition of apoptosis have been described, including the stabilization of the mitochondrial membrane (Patergnani et al. 2015) and the inhibition of caspases, through the activity of the inhibitor of apoptosis proteins (IAPs) that have been found highly expressed in MPM (Gordon et al. 2002; Kleinberg et al. 2007). It has been hypothesized that apoptosis can be induced or inhibited by altering the ratio of expression between pro-apoptotic and anti-apoptotic genes, belonging to the Bcl-2 family (Chresta et al., 1996). Inhibitors of Bcl-xL/Bcl-2

emerge as a new class of compounds for disrupting the balance between pro-apoptotic and the anti-apoptotic stimuli. The exposure of tumour cells to inhibitors of Bcl-2/xL, alone or in combination with other chemotherapeutic, has shown a synergistic inhibition of tumour growth, inducing apoptosis and increasing the chemo-sensitivity both in vitro and in vivo, and it may represent a new therapeutic strategy in the treatment of MPM (Cao et al., 2007).

An important factor involved in the immortality of cancer cells is also the transcription factor NF-kB. The exposition to asbestos induces TNF-α release by macrophages and mesothelial cells and consequently, TNF-α dependent, p65 NF-kB nuclear traslocation and activation (Yang et al. 2006).

The activation of NF-kB allows mesothelial cells with asbestos–induced DNA damage to survive rather then to die, concurring to a genetic damage accumulation and to the eventually develop of MPM. This suggests that the therapeutic targeting toward the signaling TNF-α/NF-κB may decrease drug resistance and increase cytotoxicity in MPM cells (Carbone and Bedrossian, 2006).

1.4.2.2 Proliferation and angiogenesis

The particular growth factors that affect MPM cell growth are under investigation.

The hepatocyte growth factor / scatter factor (HGF / SF) is a multifunctional growth factor that can induce many biological functions, critical for the malignant phenotype, including invasion, proliferation and morphogenesis. The receptor c-Met is the only known receptor for HGF / SF. Downstream of c-Met, more signalling pathways are activated, including Ras / Erk, PI3K/Akt, and c-Src kinase pathways. It has been demonstrated an autocrine loop of HGF / SF / c-Met in both cell lines and MPM tissue samples, and the over-expression of HGF and c-Met has been associated with increased microvascular density and an increased expression of matrix metalloproteinases (Tolnay et al., 1998).

It has been noticed that the small molecule SU11274, through the inhibition of c-Met, is able to induce the suppression of cell growth in some MPM cell lines, but not in non-malignant mesothelial cells. In particular, SU11274 inhibits cell migration, and the signal transduction induced by HGF (Jagadeeswaran et al., 2006).

The cytoplasmic tyrosine kinase Src is often expressed and activated in MPM. The activity of SRC kinases family is associated with an advanced stage of MPM, and it may contribute to invasiveness and metastatic spread. In preclinical models, the dasatinib, a potent inhibitor of SRC kinases family, prevents the migration and the invasion of MPM (Tsao et al., 2007). Moreover in MPM, the epidermal growth factor receptor (EGFR) has been found overexpressed especially in the epithelioid subtype and it has been associated with a worst prognosis (Rena et al. 2011). An important molecule, involved in EGFR downstream signalling is the phosphoinositide-3-kinase

(PI3K), whose pathway appears to be active in MPM cell lines (Cacciotti et al., 2001). The PI3K/AKT pathway is involved in the regulation of cell size, proliferation and survival, as well as in the formation of cancer metastasis, angiogenesis and invasiveness. The PI3K/AKT pathway can be tested as a target for inhibiting the growth of MPM cells, although it has been observed that cell lines of human MPM with high constitutive activity of AKT are more resistant to drugs (Ramos-Nino et al., 2005).

The MPM patients have the highest levels of VEGF (vascular endothelial growth factor) compared to patients suffering of any other solid tumour. Indeed, VEGF, VEGF-C and their receptors are over-expressed in the tissue of MPM, in cell lines and in pleural effusions (Strizzi et al., 2001). In addition, elevated levels of VEGF have been observed in the sera of MPM patients, compared to the serum of normal subjects. In particular, MPM cell lines express high levels of VEGF and its receptors (VEGFR-1 and VEGFR-2), compared with normal mesothelial cells. Neutralizing antibodies against VEGF and VEGFR 1-2 reduce significantly the viability and the proliferation of the MPM cells in vitro, while the pre-treatment in vivo with an antibody anti-VEGFR reduces the malignant pleural effusion in a murine model. VEGF may also act in an functional autocrine loop that directly stimulates the growth of cells of MPM. In fact, the production of VEGF can have an impact on patients survival, not only promoting tumour angiogenesis, but also by directly stimulating tumour growth (Zucali et al., 2011). High levels of VEGF in the pleural were associated with reduced survival in patients with MPM (Strizzi et al., 2001). Similarly, the over-expression of VEGF, as detected by immunohistochemical analysis, predicts a shorter survival in patients with MPM (Demirag et al., 2005). To conclude, the expression of VEGF and VEGF-C in MPM is correlated with microvessel density, and high density of microvessels is associated with poor survival. In recent years it has become clear that the MPM is characterized by activation of survival pathway and inhibition of tumour suppressor (Fennell, 2011). Other molecules have been identified (Fox and Dharmarajan, 2006): Among them, WNT (that seems to play an important role in homeostasis and development), mesothelin (regulating apoptosis and cancer cell growth) (Wang et al., 2012), and calretinin, whose up-regulation seems to increase resistance to asbestos cytotoxicity and thereby contributing to fibres carcinogenicity (Henzi et al., 2009).

1.5 Diagnosis of MPM

Malignant mesothelioma is one of the most challenging malignancies to diagnose. The existence of mesothelioma was initially doubted by prominent pathologists prior to the current epidemic from asbestos (Willis, 1960). Symptoms from malignant pleural mesothelioma (MPM) include dyspnea,

weight loss and chest wall pain, and have an insidious onset. Confirmation of the diagnosis is often prolonged as distinguishing MPM from benign pleural effusions related to asbestos or pleural effusions from other malignancies is challenging. Many factors cause this delay including identifying asbestos exposure and, when confirming the diagnosis, there are limitations of imaging, biomarkers and pathological sampling (Madsen et al. 2013). At the present time, improved detection methods for diagnosis of asymptomatic MPM are lacking, but needed for an early and reliable detection and treatment of this disease. A definitive and early diagnosis on effusion samples could be important, because advances in therapy for patients with MPM may result in an improved outcome if they are applied to stage I disease (Pomjanski et al., 2008). The need to detect the MPM at the early stages led several authors to investigate whether tumour-related biomarkers can contribute towards the evaluation of the carcinogenic risk in populations exposed to asbestos. Several biomarkers have been suggested for screening and early diagnosis of MPM.

The calretinin (CALB2) and Wilms'tumour-1antigen (WT1) are cytologic markers useful to distinguish from mesothelial origin or lung parenchyma. The Epithelial membrane antigen (EMA) known as CA15-3 and mucin-1 is able to identify MPM with a sensitivity of 75% and a specificity of 100% compared to the reactive mesothelial tissue (Saad et al.2005); the vimentin seems useful to distinguish MPM from metastasis of lung adenocarcinoma (Duggan et al. 1987) but it is not useful for differential diagnosis of malignant mesothelioma as it did not show significant differences between a group of malignant mesothelioma patients and controls (Creaney et al. 2011 A).

The soluble mesothelin-related peptides (SMRP) is the soluble form of a membrane glycoprotein of mesothelial cells. In 2003 it was suggested as marker for MPM given the high concentrations found in serum of 84% of MPM patients and in less than 2% of patients with other lung or pleural diseases (Robinson et al. 2003). The biological role of mesothelin is still unknown; its levels has been correlated with the trend of the disease and the response to therapeutic treatments but it has shown a low sensitivity (Grigoriu et al. 2003)

The osteopontin, a glicoprotein of mesothelial cells, is considered a negative predictor of survival for MPM (Hollevoet et al. 2011), but it does not seem a powerful diagnostic marker alone (Grigoriu et al.2007). It is able to discriminate patients exposed to asbestos from patients with early MPM (Pass et al. 2005), but it seems not able to differentiate the MPM from others pleural disease (O'Regan et al. 2006).

Currently, high levels of soluble mesothelin-related peptides (SMRP), plasma osteopontin (pOPN) and vimentin have been reported in patients with MPM as promising markers for diagnosis, but their clinical use in monitoring is still discussed (Bonotti et al. 2016).

The VEGF seems to be a more promising diagnostic target: VEGF serum concentration was found significantly higher in 51 cases with MPM compared to 42 controls suffering from asbestosis or pleural plaques (Yasumitsu et al. 2010).

Moreover, miR-126 has been proposed as useful tool for early diagnosis in MPM: high levels have been found in blood of MPM patients while it was absent in patients exposed to asbestos and in healthy people. Interestingly the Mir-126 levels correlate with VEGF levels. Santarelli et al. observed that levels of miR-126 in serum, and its levels in patients' serum in association with SMRPs correlate with subjects at high risk to develop MPM. This suggests the potential screening of Mir-126 and SMRP as a powerful tool for MPM diagnosis (Santarelli et al. 2011). However, to date, biomarkers in MPM are not useful diagnostic tools as happens in other cancers (Bibby et al. 2016) because the MPM biomarkers are still imperfect and of limited clinical use: at present, no tissue or serum marker (including the molecular detection of p16/CDKN2A) has been proved to have sufficient specificity, consistency and reproducibility (Henderson et al. 2013)

The diagnosis of MPM should be considered in any individual with evidence of a diffuse malignant process in the abdomen on initial clinical evaluation. It is confirmed based on suspicion of findings on cross-sectional imaging and tissue biopsy with appropriate immunohistochemical staining. Computer Assisted Tomography or Computerized Tomography (CT) scan is the imaging modality most commonly used although magnetic resonance imaging (MRI) using specific acquisition protocols may be increasingly used in the future (Yan et al. 2005; Low and Barone 2012). The value of positron emission tomography (PET) or PET/CT in initial diagnosis or staging is not clear (Deraco et al. 2008).

To date, specific tests, currently employed in case of suspected MPM are following (Moore et al., 2008):

- Chest X-ray is used to identify changes in the lung or in the pleura, such as variations of the thickness of the pleura, the presence of calcified pleural plaque and the presence of fluid in the space between the lungs and the chest wall.
- CT is used to obtain more detailed images of pulmonary structures. It allows to locate the tumor mass and it can show if it has spread to other organs. Moreover the detailed images allow the identification of characteristic features of MPM, like the presence/absence of circumferential pleural rind or of pleural nodularity, leading to a more clear differentiation between MPM and benign pleural disease. However, the absence of this picture does not exclude the MPM diagnosis (Leung et al., 1990).

- PET scan is not as detailed as CT or MRI scan but, it is helpful to distinguish whether a thickening of the pleura, seen on a CT scan, is more likely cancer or scar tissue because it allows to measure the metabolic activity of a lesion: the value obtained in case of MPM is significantly higher, compared with that from other benign disease (Wang et al., 2004; Bénard et al., 1998).
- MRI is not employed routinely to assess a MPM case. However it can give additional information above CT because it provide very detailed images of soft tissues and, in mesothelioma, is useful to evaluate the possible extension into the diaphragm (Wang et al. 2004).
- Biopsy: it allows to verify, under a microscope, the presence of tumour cells in the pleural sample. The analysis of pleural biopsies allows the diagnosis in 98% of patients (Boutin and Rey, 1993). For this reason it is considered the gold standard for the diagnosis of MPM.

To further ascertain the MPM diagnosis, a useful tool routinely employed is the immune-histochemical analysis, easily reproducible and reliable. The histological investigation is important to distinguish MPM from other types of lung diseases. Positive staining for calretinin, WT-1, cytokeratin 5/6, podoplanin, mesothelin, and thrombomodulin; and negative staining for carcinoembryonic antigen (CAE), and for other epithelial antigens, generally expressed by lung adenocarcinoma, such as TTF-1 (Thyroid Trascription Factor 1) (Scherpereel et al., 2010), can address for the MPM diagnosis.

1.6 Prognostic marker for MPM

The prognosis of MPM is poor due to the difficulty of making diagnosis in the early stage, the high invasiveness and the lack of effective treatment.

The difficulty in finding a single prognostic predictor has favored the development of clinical scoring systems. Table 1 below reassumes the CALGB system, the EORTC system, and the modified version of the latter. These systems classify low- and high-risk subgroups with different survival rates. Currently a new prognostic system is being developed by IASLC (International Association for the Study of Lung Cancer) thanks to a database of more than 3000 surgically managed patients. This system considers at first a group of prognostic factors called "core" factors, together with others supplementary prognostic variables (Table 1; Mineo and Ambrogi 2012): the "core" variables on multivariate analysis were stage, histology, sex, age, white blood cell count, and platelet count.

Serum biomarkers are used mainly for early diagnosis, but it would be useful to employ them to monitor the evolution of the disease and to predict prognosis. Serum mesothelin (variants 1, 2, and 3) is a differentiation antigen in mesothelial cells that is highly expressed in MPM. Abnormal serum levels correlate with metabolically active tumour volume and have proved effective as a prognostic indicator (Cristaudo et al. 2007; Creaney et al. 2011 B; Dipalma et al. 2011; Linch et al. 2014). Moreover, together with Soluble mesothelin, also MPF (Megakaryocite Potentiating Factor) levels has been associated with disease course and has been proposed as a novel prognostic marker in andvanced mesothelioma (Hollevoet et al. 2011; Mori et al. 2013). Both Soluble Mesothelin and MPF originate from the mesothelin gene (Shiomi et al. 2006), that is overexpressed in epithelioid mesothelioma cells. Furthermore different studies highlighted that MPF levels can differentiate between early- and late-stage disease (Shiomi et al. 2008; Hollevoet et al. 2010, 2012). Osteopontin is a glycoprotein involved in the adhesion of cells to the bone matrix. Serum levels of osteopontin are higher in MPM and are related to the duration of exposure to asbestos. Low serum levels of osteopontin are associated with a better overall survival.

	Parameter	Good Prognostic Group	Poor Prognostic Group
CALGB*	Performance status	Good	Poor
	Age	> 75 years	≤75 years
	Platelet count	< 400 x 10^9 /L	≥400 x 10^9 /L
	Chest pain	Absent	Present
	Lactate dehydrogenase level	< 500 IU/L	≥ 500 IU/L
EORTC*	EOCG* performance status	0	1-2
	Histological subtype	Epithelioid	Non epithelioid
	Sex	Female	Male
	Certainty of diagnosis	Definite	Possible
	White blood cell count	< 8.3 x 10^9 /L	≥ 8.3 x 10^9 /L
EORTC revised	Stage	I/II	III/IV
	Histology	Epithelioid	Non epithelioid
	Interval since diagnosis	< 50 days	≥ 50 days
	Platelet count	< 350 x 10^9 /L	≥ 350 x 10^9 /L
	Hemoglobin difference [(a)]	< 1	≥ 1
	Pain	Absent	Present
	Appetite loss	Absent	Present
IALSC*	**Stage**	I/II	III/IV
	Histological subtype	Epithelioid	Non epithelioid
	Sex	Female	Male
	Age	≥ 50 years	< 50 years
	Type of surgery	Curative	Palliative
	Adjuvant therapy	Yes	No
	Smoking history	No	Yes
	Asbestos exposure	No	Yes
	Weight loss	No	Yes
	ECOG performance status	0	1-2
	Chest pain	No	Yes
	Dyspnea	No	Yes
	Hemoglobin	< 14.5 g/dL	≥ 14.5 g/dL
	White blood cell count	< 15.5 x 10^9 /L	≥ 15.5 x 10^9 /L
	Platelet count	< 400 x 10^9 /L	≥ 400 x 10^9 /L

Table 1: Prognostic scoring systems in Malignant Pleural Mesothelioma (Mineo and Ambrogi 2012). (* : CALGB = Cancer and Leukemia Group B; EORTC = European Organisation for Research and Treatment of Cancer; EOCG = Eastern Cooperative Oncology Group; [(a)] Difference between actual value and 16g/dL in males, or between actual value and 14 g/dL in females.)

1.7 Therapeutic approach for MPM

MPM is highly malignant and aggressive: infact if left untreated, the median survival time of the patients is about 4 to 12 months (Jaklitsch 2001). Most patients died of the local invasion of the tumour or the contralateral metastasis. The most promising strategy up to date is the treatment of resecting the visible tumour as much as possible, combined with radiotherapy, chemotherapy and immunotherapy (Rusch 2007; Krug 2009). But we must consider that only a minority of patients are eligible for radical surgery. The combination of pemetrexed and cisplatin is the standard of care in the first-line treatment, while carboplatin is often substituted for cisplatin, due to simpler/shorter administration and less toxicity (Vogelzang et al. 2003; Ceresoli et al. 2006). Unfortunately, the efficacy of treatment is very limited for the tumour is usually diagnosed too late. Moreover after initial chemotherapy, patients almost invariably experience progression (Ceresoli et al. 2010). All of the current therapies have modest impact against MPM and they are only expected to improve the quality of life and prolong survival time of the patients with MPM (Rosenzweig 2013). For these reasons, new agents targeting key factors and molecular pathways involved in chemoresistance are warranted.

2 RNAi approach for the identification of new potential biomarkers and therapeutic targets for MPM

Nowadays the use of "RNA-interference" (RNAi) technique is of increasing interest because it is considered a powerful strategy to study the function of any gene. The RNAi is a biological endogenous mechanism that led to gene expression inhibition throught the degradation of specific mRNA. siRNAs are small RNA of about 21-23 nucleotides, that bind their mRNAs target with a perfect complementarity and trigger their destruction (Baselga, 2006; Carthew and Sontheimer, 2009). They could derive from the cleavage mediated by Dicer (an endoribonuclease belonging to the RNaseIII family) of a long non-coding double-stranded RNAs either produced in the cell, introduced by viruses, or also by transfection (Sashital and Doudna, 2010). The RNAi is an evolutionary conserved mechanism and the great interest resides in the fact that, with a simple transfection of a siRNA, it is possible to knock-down the expression of a specific gene. For this reason, this tool has a wide application in basic research (Lindbo et al., 1993; Tamura et al., 2006). Moreover, siRNA have potentially unlimited therapeutic applications and preliminary studies are ongoing (Dykxhoorn, 2009; Lindbo et al., 1993). Indeed, siRNAs have some distinct advantages over conventional drug therapies: they have high specificity, a potentially enormous number of

targets, and a more rapid method of manufacturing comparing to small molecules (Vaishnaw et al., 2010), as shown in table 2.

	siRNA	Small molecule
Specificity	High, sequence driven	Low-medium, conformation driven
Potency	Typically pM	Variable
Number of accessible targets	>>1000	500 to 1,000
Number of potential leads and backups	>>10 to 100, depending on length of target	<2 to 3
Speed to lead molecule	4 to 8 weeks	2 to 4 years
Species crossreactivity	High	Low
Manufacturing	Common, rapid, scalable methods	Variable, can be complex

Table 2: A comparison of various drug discovery attributes of siRNAs and small molecules (Vaishnaw et al. 2010).

Algorithms have been developed for screening and selection of siRNAs. They allow the identification of double-stranded segments, 19-23 base pairs in length, that have the minimal complementarities with the off-target sequences (Vaishnaw et al., 2010).

In order to better understand the role of genes/pathways in the development of the MPM, gene silencing strategy has been already used, alone or in combination with the conventional chemotherapy (Delage et al. 2010; Lee et al. 2016). These results highlight how the RNAi experimental approach is useful to determine whether a gene could play an important role for sustaining the malignant phenotype.

3 Backgroud: identification of overexpressed genes in MPM

Researchers have actively sought MPM biomarkers for more than 20 years but the late diagnosis and the poor outcome of the disease require the identification of marker for an earlier diagnosis and an effective treatment of MPM. Essentially biomarkers would be helpful in managing three clinical aspects of MPM: early diagnosis, prognosis, and treatment outcome prediction.

The knowledge of the genes involved in the development and progression of MPM is still limited: in recent years several deregulated genes have been suggested, but most of these have been reported in a few studies and often analyzed in a few samples or cell lines.

In order to find a consensus among these data and to identify relevant genes involved in this neoplasm, previously our group, performed an extensive literature review focused on the MPM transcriptome and a data mining (using Coremine, SNPs3D, and GeneProspector). The results from

transcriptome studies and from data mining were intersected (Melaiu et al. 2011) Then, a validation study has been undertaken to verify whether 77 genes could be confirmed in their de-regulation on an independent series of specimens (20 MPM and 20 healthy pleura tissues). Genes showing a differential expression in MPM as compared to healthy pleural tissues, have been further validated on two MPM cell lines (Fig. 11) (Melaiu et al. 2015) This work identified a set of 21 upregulated genes in MPM tissues and in at least one MPM cell line.

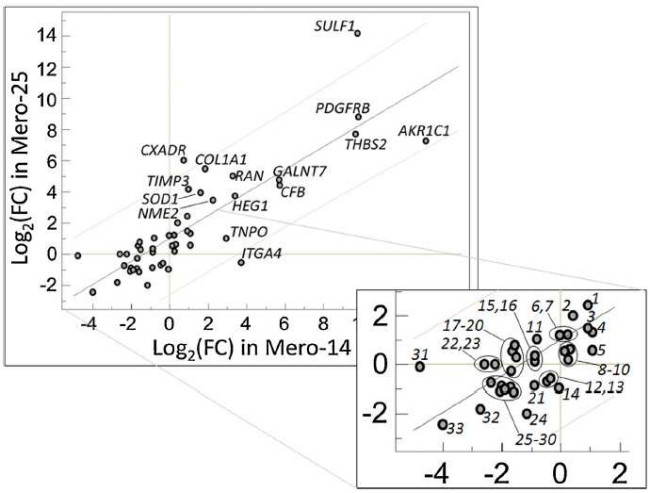


Fig.11 . Fifty-one genes deregulated in a statistically significant way in MPM tissues were assayed in Mero-14 and Mero-25 MPM cell lines. The figure shows the correlation of the results obtained in the two cell lines. Gene expression level (as the logarithm base 2 of the fold change) and its statistical significance are calculated using the non-MPM cell line Met-5A as reference. The correspondence between labels and genes is reported in legend. Three genes, KRT5, CDH11, and PTGIS, showed an up-regulation in Mero25 cells with a Log2(FC) of 1.685, 5.607, and 8.910 and P values of 0.0198, $<10^{-5}$, and $<10^{-5}$, respectively but were undetectable in Mero14 cells. The remaining genes (C10orf116,HCA112, SPINT2, UPK1B, FBLN2, ANK2, AOC3 and COL11A1) were undetectable in both cell lines. Mero 14-cells: ***for P value $\leq 10^{-5}$, **for P values $\leq 10^{-3}$, *for P values ≤0.05;Mero-25 cells:†††for P value $\leq 10^{-5}$,††for P values $\leq 10^{-3}$,†for P values ≤0.05. SULF1******†††; PDGFRB******†††; THBS2******†††; AKR1C1******†††; GALNT7***; CFB******††; CXADR†††; COL1A1†††; RAN†;SOD1†; HEG1; TIMP3*†††; NME2; TNPO2; ITGA4***; 1 = ASS1†††; 2 = MCM4; 3 = CCNO*†††; 4 = XPOT******††; 5 = MSLN; 6 = PCNA; 7 = DSP; 8 = EIF4G1†††; 9 = NMU; 10 = PPARA; 11 = CCNB1†;12 = TACC1*†; 13 = PKM2; 14 = GAPDH†††; 15 = ALDOA; 16 = KRT18*; 17 = HELLS***; 18 = CENPF***†; 19 = SMC4***; 20 = KIF23***; 21 = ACSL1***†; 22 = NUSAP1***; 23 = CHEK1***;24 = EFEMP1*†††; 25 = FEN1***; 26 = MKI67******†††; 27 = TOP2A******†††; 28 = CCNB2***†; 29 = SMARCA4******†††; 30 = BIRC5******†††; 31 = CALB2***; 32 = CDC2******†††; 33 = FANCI******††† (Melaiu et al. 2015)

4 Aim

Given the non-specificity of symptoms with which it occurs, the unavailability of effective marker for an early diagnosis, and given the conventional therapies currently guided by gross tumour characteristics and patient features rather than by the specific biological fingerprint of the tumour, the identification of more effective biomarkers and the knowledge of the mechanisms involved in MPM carcinogenesis and chemo-resistance is necessary.

For this reason:

- we investigated on the role played by overexpressed genes in MPM on the maintenance of malignancy through an RNAi phenotypic approach;
- we evaluated the possible use of some of these overexpressed genes as potential prognostic marker
- we analyzed the expression of two candidate genes in non-malignant pleura compared to MPM tissues at protein level as potential diagnostic markers

5 Materials and Methods

5.1 Selection of putative target genes

To identify the relevant genes potentially involved in MPM, recently, our group carried out an extensive literature review focused on the MPM transcriptome intersected with a data mining (Melaiu et al. 2012) and a validation study on MPM tissues and cell lines (Melaiu et al. 2015). The study led to the identification of a group of 21 deregulated genes in MPM. Among the 21 genes identified we focused our attention on those up-regulated in MPM tissues and at least in one MPM cell line (i.e. *THBS2, CCNO, CFB, TIMP3, SULF1, PDGFRB, ASS1, SOD1, RAN, CDH11, ITGA4, EIF4G1).* In addition, we made an extensive literature search to identify the best promising novel diagnostic and therapeutic target for MPM and we undertook the study of *IMP3* (Hanley et al.2008; Ikeda et al. 2010; Ikeda et al. 2011; Shi et al.2011; Lee et al. 2013; Okazaki et al. 2013; Minato et a. 2014) , *MCT4* (Mogi et al. 2013), *MCT1* (Mogi et al. 2013), *BSG* (Pinheiro et al. 2012) and *CAIX* (Ramsey et al. 2012; Capkova et al. 2014).

5.2 RNAi phenotypic screening

5.2.1 Cell cultures

Five mesothelioma cell lines (Mero-14, Mero-25, IstMes2, NCI-H28 and REN) and one mesothelial non-MPM immortalized cell line (MeT-5A) were used. The Met5A cell line was purchased from ATCC and grown in Medium 199 with HEPES (Life Technologies, Monza, Italy) supplemented with 10% FCS, 3.3 nM epidermal growth factor (EGF, Life Technologies, Monza, Italy), 400 nM hydrocortisone (Sigma Aldrich Corp. St Louis, MO, USA), and 870 nM insulin (Life Technologies, Monza, Italy). Three mesothelioma cell lines Mero-14 (Versnel et al. 1989), Mero-25, and IstMes2 (Orengo et al. 1999), kindly donated by Istituto Tumouri of Genova (National Research Council, Genova, Italy), were cultured in DMEM medium (Lonza, Basel, Switzerland), with 10% of FCS. The others two mesothelioma cell lines NCI-H28 and REN, purchased from ATCC and kindly donated by collaborators of the Pharmaceutical Department of the University of Pisa, were cultured in RPMI medium (Lonza, Basel, Switzerland), with the addiction of 10% of FCS.

5.2.2 Transfection efficiency

To evaluate the optimal transfection conditions for each cell line we performed a series of experiments using the All Star Negative Control siRNA (SI03650318, Qiagen S.p.A, Milano, Italy) as non-targeting negative control (siRNA C-), as it does not affect cell viability, and the AllStars Hs

Cell Death Control (SI04381048, Qiagen S.p.A, Milano, Italy) as positive control (siRNA C+). AllStars Hs Cell Death Control siRNA is a blend of highly potent siRNAs targeting ubiquitously expressed human genes that are essential for cell survival. Knockdown of these genes induces a high degree of cell death, which is visible by light microscopy. siRNA transfection was performed with the HiPerFect® Transfection Reagent (Qiagen, Hilden, Germany). We tested different combinations of siRNA concentrations and volumes of transfection reagent according to the datasheets suggestions.

We tested these siRNA concentrations:

25 nM, 50 nM, 100 nM for MeT5A, Mero25, IstMes2, NCI-H28 and REN cell lines;

20 nM, 40 nM, 80nM for Mero14.

HiPerFect® volumes tested were:

- ✓ 7 µl,
- ✓ 14 µl
- ✓ 21 µl

according to the datasheet suggestions.

We estimated the optimal transfection efficiency by observing morphology, viability and adhesion of cells by straightforward light microscopy, 72 hours after transfection, and selecting the combinations that caused the higher degree of cell death.

5.2.3 siRNA Transfection Protocols

To optimize the condition for an efficient transfection for all the cell lines employed we tested different siRNA and Hiperfect concentrations. The following tables summarize the most efficient protocols for each cell line; pictures show the transfected cells 72h after treatment.

- ***MeT-5A: 50 nM siRNA – 14 µl HiPerFect®***



MeT5A siRNA C-



MeT5A siRNA C+

- ***Mero14: 20 nM siRNA – 7 µl HiPerFect®***



Mero14 siRNA C-

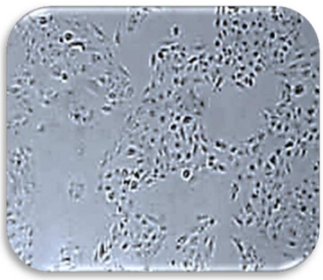


Mero14 siRNA C+

- ***Mero25: 50 nM siRNA – 21 µl HiPerFect®***

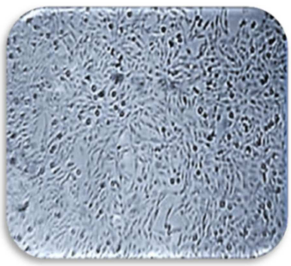


Mero25 siRNA C-



Mero25 siRNA C+

- ***IstMes2: 50 nM siRNA – 21 µl HiPerFect®***



IstMes2 siRNA C-



IstMes2 siRNA C+

- ***NCI-H28: 50 nM siRNA – 21 µl HiPerFect®***

	
NCI-H28 siRNA C-	***NCI-H28 siRNA C+***

Ren: 50 nM siRNA – 7 µl HiPerFect®

	
Ren siRNA C-	***Ren siRNA C+***

5.2.4 Silencing RNA oligonucleotide

Experiments were performed by using a single specific siRNA purchased from Qiagen or Invitrogen (for thrombospondin2):

Gene	*Target sequence*	*So-called*
ASS1	5'-CCCGTGGAGCATGGATGAGAA-3'	si*ASS1*
CCNO	5'-CCGGGCGTTGAAGGTAGTAAA-3'	si*CCNO*
CDH11	5'-ACCGTCGGAATTCATTGTCAA-3'	si*CDH11*
CFB	5'-CAGCTCAATGAAATCAATTAT-3'	si*CFB*
EIF4G1	5'-CTCCATCGATTCTAACAACCA-3'	si*EIF4G1*
IMP3	5'-CACATTTAATTCCTGGATTAA-3'	si*IMP3*
MCT4	5'-TTCGAGACAACGTGACTTTAA-3'	si*MCT4*
PDGFRB	5'-CCGAGCAACTTTGATCAACGA-3'	si*PDGFRB*
RAN	5'-ATCCATTGTCTTCCACCGAAA-3'	si*RAN*
SOD1	5'-ATGGCACTTATTATGAGGCTA-3'	si*SOD1*
SULF1	5'-TCCGTCGAATTTGAAGGTGAA-3'	si*SULF1*
THBS2	5'-CCTCAAGTACGAATGCAGAGATATT-3'	si*THBS2*
TIMP3	5'-CACGCTGGTCTACACCATCAA-3'	si*TIMP3*

Table 3: Target sequences of siRNA used for the gene specific silencing.

And the ''AllStars Negative Control siRNA'' (SI03650318 - the so-called "siCTRL" now-on) was used as non-targeting control.

siRNA oligonucleotides were re-suspended in the provided buffer at a final stock concentration of 20 mM, and employed, in each experiments, at 20nM for Mero14 and 50nM for all the others cell lines, according to the transfection efficiency results. HiPerfect transfection reagent was employed for siRNA trasfection (Qiagen, UK).

5.2.5 RNA isolation and cDNA synthesis

72h after transfection cells were harvested and washed in PBS buffer. Cells were lysated by adding the buffer RLT (Qiagen S.p.A, Milano, Italy), which had been previously added β-mercaptoethanol (10 uL of β-mercaptoethanol in 1 mL of buffer RLT) and homogenized using a sterile syringe and needle. The lysates were directly pipetted into a QIAshredder spin column and washed with specific buffer supplied by the RNeasy kit used (Qiagen S.p.A, Milano, Italy). The eluates were collected in RNAse free Eppendorf. Concentration of clean-up RNA was determined spectrophotometrically (SmartSpec 3000, Bio-Rad Laboratories, Hercules, CA) at 260nm or using the Qubit® Fluorometer with the Qubit® RNA HS Assay Kit. The ratio of readings at 260 and 280 nm (A260/A280) provided an estimate of the purity of RNA with respect to contaminants that absorb in the UV spectrum, such as proteins and DNA. The integrity and purity of total RNA was further verified by electrophoresis on ethidium bromide agarose gel, inspecting the 18 and 28S ribosomal RNA bands.

The reverse transcription (RT) of mRNA to cDNA was performed using the iSCRIPT cDNA Synthesis Kit (Bio-Rad Laboratories, Hercules, CA). cDNA synthesis was carried out from 1 ug of total RNA in a final reaction volume of 20 μl. The reaction is catalyzed by the Moloney Murine Leukemia Virus (MMuLV) reverse transcriptase, an RNA/DNA-dependent DNA polymerase modified and optimized for the synthesis of cDNA, in presence of an mRNA-polyA template and a single-stranded oligo-dT.

5.2.6 Primer design and quantitative Real-Time PCR (QPCR)

To evaluate mRNA expression and silencing in all the cell lines employed for the phenotypic screening were used primers previously tested (Melaiu et al. 2015) in our laboratory for gene expression study on mesothelioma tissues and cell lines. In table 4 are listed the primers sequences used for five target genes.

Gene Symbol (HUGO)	NM	Primers sequences (*foward/reverse*)	T_m (°C)	Amplicon lenght
ASS1	NM_000050	ATT gAC ATC gTg gAg AAC Cg gCC TCg ATg TCT AAA TgA gCA	60	101 bp
CDH11	NM_001797	CTTTgCAgCAgAAATCCACA TgggAgCATTATCgTTgACA	60	86 bp
EIF4G1	NM_198241	CTg TgT gAC gAg Cag AAg gA CCC AAC TgT AgA Agg CAT CC	59	148 bp
RAN	NM_006325	CAg gAg AAA TTC ggT ggA CT ATg CCA gTT Agg CAC ATT CTT	60	111 bp
SOD1	NM_000454	Agg CCC CTT AAC TCA TCT CTA CAg gTA CTT TAA AgC AAC TCT	60	122 bp

Table 4: Primers sequences of five target genes.

For these others target: CFB, CCNO, IMP3 (IGF2BP3), MCT4, PDGFRB, SULF1, THBS2 and TIMP3 the mRNA expression level was evaluated through specific Taqman gene expression assay probes:

CFB ID: 00156060_m1

CCNO ID: 00221731_m1

IMP3 (IGF2BP3) ID: hs00559907_g1

MCT4 ID: 00358829_m1

PDGFRB ID:01019589_m1

SULF1 ID: 00290918_m1

THBS2 ID: 00170248_m1

TIMP3 ID: 00165949_m1

For a precise comparison of mRNA transcription in different samples it is crucial to choose the appropriate reference genes. The optimal reference gene should be constantly transcribed in all types of cells at any time of the cell cycle and of the ontogenesis.

The three housekeeping genes used (TBP, HPRT1, RPLP0) (Tab. 5) have been previously identified by our group through the employment of geNorm (URL: http:// medgen.ugent.be/genorm/), a software that ranks the candidate reference genes based on their stability parameter M, according to the MIQE guidelines (Bustin et al., 2009).

Gene Symbol (HUGO)	NM	Primers sequences (*foward/reverse*)	T_m (°C)	Amplicon lenght	Taqman assay ID
TBP	NM_003194	GCGGTTTGCTGCGGTAATC TCTGGACTGTTCTTCACTCTTGG	57	109	00427620_m1
HPRT	NM_000194	GATGGTCAAGGTCGCAAG GGGCATATCCTACAACAAACTT	62	110	01003267_m1
RPLP0	NM_053275	CCTCATATCCGGGGGAATGTG GCAGCAGCTGGCACCTTATTG	60	95	99999902_m1

Table 5: Primers sequences of housekeeping genes.

QPCR was set up using 2 µl first-strand cDNA template, 16 µl deionized H_2O, 0.3 µM of upstream and downstream primers and 5 µl 5× Eva Green master mix (Solis, Tartu, Estonia). The thermal cycling conditions used with primers were 15 min at 95°C followed by 15 s at 95 °C, 30 s 60°C (40 cycles) and 30 s at 65 °C. For the TaqMan assay, the reaction mixture consisted of 2 µl of cDNA template, 7 µl of deionized H_2O, 1 µl of specific TaqMan Assay probe and primers mixture, and 10 µl of TaqMan® Gene Expression Master Mix (Life Technologies, Monza, Italy). The thermal cycling conditions were: 15 min at 95°C followed by 15 s at 95 °C, (40 cycles) and 60 s at 60 °C. To ensure reproducibility of the experiments, all the reactions were executed in triplicate and the average was used for the statistical analyses.

5.2.7 Protein extraction and Western Blotting

Cells were washed twice with ice-cold PBS and harvested in ice-cold PBS plus EDTA. Cell pellets were re-suspended in ice-cold RIPA buffer containing proteases and phosphatases inhibitors. After 15 min of ice-incubation the extracts were clarified by centrifugation at 16.1 x 10^3 x g for 15 min at 4 °C. The proteins concentration was determined through the Bicinchonic acid assay (BCA) diluting samples with reagents A, B and C from Quantum Micro Protein kit (Euroclone), incubating them at 37°C, for 2h and reading 562nm absorbance with iMark Microplate Reader (Bio-Rad). Lysates were incubated in Laemmli sample buffer plus β-mercaptoethanol (10 min, 95 °C). 50 µg of proteins for each sample was loaded onto 8–15% SDS polyacrylamide gel. Proteins were then transferred onto a nitrocellulose membrane. The membrane was blocked for 1 hour with non-fat dry milk in TBS containing 0.05% Tween 20, washed, and successively incubated with different primary antibodies overnight at 4 °C. The membranes were then washed three times for 8 min and incubated with the HRP-conjugated secondary antibody for 1 h at room temperature (RT). After

washing, the blot was exposed to ECL (GE Healthcare, NJ) and the image was acquired with Chemidoc MP BIORAD.

Densitometry results of western blot were analysed with Image J software (NIH, Bethesda, MD, USA). For quantitative analysis, the signal intensity of each band was normalized with ß-actin densitometry values. Each density was compared to the intensity of the reference cell line (Met5A) and all western blot analyses were replicated twice for the calculation of the average increase.

5.2.8 Sulphorhodamine (SRB) assay

Cells were seeded in five 96 well plates (3 x 10^3 cells/well for Met5A, Mero14, Mero25 and NCI-H28; 1.5 x 10^3 cells/well for IstMes2; as a result of setting tests). After 24h four plates were treated with specific siRNA and one plate was fixed with 100 µL per well of ice-cold 40% (vol/vol) TCA (Sigma Aldrich Corp. St Louis, MO, USA), incubated overnight at 4°C, washed with deionized water and then stained with 0.4% SRB solution (Sigma Aldrich Corp. St Louis, MO, USA) for the evaluation of absorbance at the time of transfection. The remaining plates were analyzed at 2-day intervals for a total of 8 days. After staining, unbound dye was removed by washing five times with 1% acetic acid solution and left to air dry. The bound SRB dye was then solubilized by adding unbuffered Tris-base solution, and plates were then read at OD 492 nm, using a microplate reader (Biorad Imark).

5.2.9 Colony formation assay (CFA)

Cells were seeded in a 96-well plate (4x 10^3 cells/well for Met5A, Mero14 and Mero25; 3 x 10^3 cells/well for IstMes2; as a result of setting tests) and, after 24 h, transfected with a proper concentration of siRNA. After 24h post treatment, cells were transferred in 6-well plates and incubated for a further 14 days. Following 14 day incubation, growth medium was removed and cells fixed and stained in 10% ethanol solution containing 0.1% crystal violet for 1 h. Colonies were then counted and measured with Image J software or with Photoshop.

5.2.10 Flow cytometry (FACS)

After siRNA transfection for 48 h, 10^5 cells were collected, washed in phosphate-buffered saline (PBS), pelleted by centrifugation and fixed in cold 95% ethanol. Then cells were suspended in PBS containing 50 µg/ml of RNAse A (Qiagen, UK), and stained with propidium iodide (final

concentration 100 µg/ml) overnight at 4°C. The percentage of cells in G0/G1, S and G2/M phases were determined from 10,000 cells using the BD FACS Software (Becton Dickinson).

5.2.11 Caspase - GloH 3/7 assay

Caspase-3/7 activation was measured using the Caspase-Glo 3/ 7 Luminescence Assay (Promega Corp. Madison, Wisc., USA) according to the manufacturer's instructions. Cells were seeded in a 6 well plate (2 x 10^5 cells/well for Met5A, Mero14, Mero25; 3 x 10^5 cells/well for NCI-H28; 1.5 x 10^5 cells/well for IstMes2; as a result of setting tests). The day after, the cells were treated with siRNAs for 72 h. Then, the cells were collected by trypsinization, and approximately 15 x 10^3 cells were transferred in a 96-well white plate. Caspase-3/7-Glo reagent was added, and the samples were incubated at constant room temperature for 1 h. The luminescence that is proportional to the caspase 3/7 activities was determined by luminometer (FLUOstar OPTIMA, BMG LABTECH).

5.2.12 Wound-Healing Assay

About 2.5 x 10^3 cells were seeded in a 6-well plate and, after 24h, transfected with siRNAs. A linear scratch in the confluent cell monolayer was made with a sterile pipette tip 24h after transfection when cells reached confluency. Then, cells were rinsed and incubated in full medium. Finally, cells were photographed with an optical microscope at 10X magnification connected to the computer. The migration was then evaluated on the images, and measured with Image J or with Zen software.

5.2.13 Senescence assay (β-galactosidase assay)

To evaluate the senescence of treated cells we used the Senescence β-Galactosidase Staining Kit (Cell Signaling Technology®) that is designed to detect β-galactosidase activity at pH 6, a known characteristic of senescent cells not found in presenescent, quiescent or immortal cells. After setting tests we seeded, in chamber-slides, these quantities of cells:

- 40,000 cells/well for IstMes2;
- 50,000 cells/well for Mero25 and MeT-5A.
- 100,000 cells/well for Mero14

After 24 h at 37 °C the cells were transfected with siCTRL and the target specific siRNA; 96 h after treatment the medium has been removed and the chambers-slides were washed with 2 ml/well of 1X PBS; subsequently the chambers-slides were incubated for 15' at room temperature with 1 ml/well of 1X Fixative Solution to fix the cells.

Then the chambers were washed two times with 2 ml/well of 1X PBS and 1 ml/well of β-Galactosidase Staining Solution was added. The β-Galactosidase Staining Solution has been previously prepared with 930 µl of 1X Staining Solution, 10 µl of Staining Supplement A, 10 µl of Staining Supplement B and 50 µl 20 mg/ml X-gal in DMF.
The chambers were incubated overnight at 37 °C in a dry incubator (no CO_2) and to avoid the evaporation of the solution the chambers were wrapped with parafilm. The day after we observed the staining through the microscope. Each experiment has been repeated three times.

5.2.14 Statistical analyses

The measurements of gene expression performed on cell lines, and the results obtained from the in vitro assays were statistically evaluated using a two-tailed Student's t-test and a multifactor analysis of variance (MANOVA) model, for the analysis of curves with multiple data-points. The statistics were performed with the software Statgraphics Centurion XV (StatPoint, Inc.).

5.3 Tissue Microarray Immunohistochemistry

5.3.1 Ethics and consent

The study was approved by the Research Ethics Committee of the Papworth Hospital (Cambridge, UK) (REC reference 09/H0311/21). Patients diagnosed with malignant mesothelioma between 2005 and 2010 were identified from hospital records. Their histology slides and FFPE (formalin-fixed paraffin-embedded) biopsy tissue blocks were retrieved from the pathology department and clinical data relating to each case were extracted from hospital records.

5.3.2 Antibodies

The antibodies used in this study were:
ABCAM cat. n. ab49493 (AB1843) gene BSG, R&D SYSTEMS cat. n. MAB21881 (303104) gene CA9 (CAIX), Chemicon (Millipore) cat. n. AB3538P gene SLC16A1 (MCT1), Santa Cruz Biotechnology cat. n. sc-376101 (F-10) gene SLC16A3 (MCT4) and Santa Cruz Biotechnology cat. n. sc-7655 gene Thrombospondin 2 (N-20). The following antibodies were tested using various conditions in cell lysates through WB analysis and in tissues blocks but were ineffective in detecting the correct target: R&D SYSTEMS cat. n. MAB1790 (283416) gene CDH11, NOVUS BIOLOGICALS cat. n. NB110-66654 (EPR1355Y) gene ITGA4. For this reason these antibodies were no longer used for TMA staining.

5.3.3 Evaluation of antibody specificity: western blot analysis

Mero14, Mero25, A549, Hela and Jurkat cells were used to test antibodies specificity through immunofluorescence western blot with secondary LI-COR antibodies (LI-COR Biosciences, USA). Cells were lysated with Harvest Buffer (containing 50mM NaCl, 0.5M sucrose, 10mM Hepes pH 7.9, 0.5% triton X-100 and 0.1mM EDTA). From the supernatant of lysates we obtained the cytosolic extracts while from the pellets of lysates we isolated the nuclear extracts with buffer A (10mM KCl, 0.1mM EGTA, 0.1mM EDTA, 10mM Hepes pH 7.9) and with buffer C (containing 500mM NaCl, 10mM Hepes pH 7.9 , 0.1mM EGTA, 0.1mM IGEPAL and 0.1mM EDTA). Cytosolic and nuclear extracts were quantified through Bradford protein assay using a spectrophotometer.

Extracts were incubated in loading buffer plus DTT (8 min, 70 °C). 50 µg of proteins for each sample was loaded onto 10% SDS polyacrylamide gel. Proteins were then transferred onto a nitrocellulose membrane. The membrane was blocked for 1 hour with non-fat dry milk in TBS containing 0.05% Tween 20, washed, and successively incubated with different primary antibodies overnight at 4 °C. The membranes were then washed three times for 8 min and incubated with the LI-COR secondary antibody for 1 h at room temperature (RT). After washing, image was acquired with Licor Odyssey (LI-COR Biosciences, USA). The blot incubated with the primary THBS2 antibody was incubated with ECL and the image was acquired in dark room. In Table 6 are listed all the optimized WB protocols for all the antibodies tested.

To evaluate BSG specificity we treated the extracts with PNGase F (NEB), that is an endoglycosidase optimized for the efficient release of N-linked oligosaccharides, with the following protocol: (Denaturing Reaction Conditions)

1. Combine 1-20 µg of glycoprotein, 1 µl of Glycoprotein Denaturing Buffer (10X) and H_2O (if necessary) to make a 10 µl total reaction volume.
2. Denature glycoprotein by heating reaction at 100°C for 10 minutes.
3. Chill denatured glycoprotein on ice and centrifuge 10 seconds.
4. Make a total reaction volume of 20 µl by adding 2 µl GlycoBuffer 2 (10X), 2 µl 10% NP-40 and 6 µl H_2O.
5. PNGase F is inhibited by SDS, therefore it is essential to have NP-40 in the reaction mixture under denaturing conditions. Failure to include NP-40 into the denaturing protocol will result in loss of enzymatic activity.
6. Add 1 µl PNGase F, mix gently.
7. Incubate reaction at 37°C for 1 hour.

Target	Antibody	Molecular weight; theoretical weight	Optimized WB Protocol
BSG	ab49493	42 KDa; 29 KDa	Primary Ab 1/250; ON 4°C Secondary 1/5000; 1h RT
CAIX	MAB21881	49.9 KDa; 55 KDa	Primary Ab 1/250; ON 4°C Secondary 1/5000; 1h RT
CDH11	MAB1790	110 KDa	Primary Ab 1/250; ON 4°C Secondary 1/5000; 1h RT
ITGA4	NB110-66654	150 KDa; 114,89 KDa	Primary Ab 1/250; ON 4°C Secondary 1/5000; 1h RT
MCT1	AB3538P	40 KDa	Primary Ab 1/500; ON 4°C Secondary 1/5000; 1h RT
MCT4	sc-376101	43 KDa	Primary Ab 1/500; ON 4°C Secondary 1/5000; 1h RT
THBS2	sc-7655	129 KDa; 180 KDa	Primary Ab 1/250; ON 4°C Secondary 1/10000; 1h RT

Table 6: WB optimized protocols of the antibodies used for TMA IHC staining.

5.3.4 Characteristic of the MPM Tissue microarray employed

Thanks to the collaboration with Doris Rassl and Stefan Marciniak the MPM TMA slides employed in this study derived from the MPM TMA blocks already used in Dalton et al. study (Dalton et al. 2013). Tissue blocks from 135 patients diagnosed of malignant mesothelioma were included in the study. For each tissue block at least three representative regions of tumour were identified following a haematoxylin and eosin staining and a re-examination by an experienced histopathologist. Three TMA were built from cores of tissue measuring 0.6 mm in diameter taken from each region of each block. At random intervals, sections of normal pleura, liver and kidney controls were distributed throughout the TMA. Cores were monitored for morphology and quality by a staining, one every 50th section, with haematoxylin and eosin.

5.3.5 Immunohistochemistry

Sections were baked in an oven at 65 °C for 1 h. PT link tanks (Dako, Glostrup, Denmark) were used to perform deparaffinisation and heat-induced epitope retrieval (EnVision FLEX Target Retrieval Solution High pH; Dako). As a result of optimization tests, PT link solutions with high or low pH have been used for the different antibodies (see Table 7). All the slides were incubated for 20 min at 97 °C and left in buffer (EnVision FLEX wash buffer; Dako) at room temperature for a minimum of 10 min to cool down. Staining was performed using an automated immunostainer (AutostainerLink48; Dako). All the slides were incubated for 5 min in an EnVision FLEX peroxidase-blocking reagent (Dako) and then incubated with antibody; some antibodies required an additional incubation with EnVision FLEX/mouse or rabbit LINKER (Dako); the detailed protocols are listed in Table 7. MNF116 had an additional step of incubating sections with mouse linker (EnVision FLEX/mouse (linker); Dako) for 15 min. Then all sections were incubated for 30 min in EnVision FLEX/HRP (Dako). Each individual stage was followed by buffer rinses (EnVision FLEX wash buffer; Dako). Staining was visualised using the chromogen 3,3′-diaminobenzidine for 10 min, counterstained with haematoxylin (EnVision FLEX; Dako) for 5 min and manually cover-slipped (Surgipath) with DePeX mounting medium (VWR International, Poole, UK).

Target	Antibody	Antigen retrival pH	Antibody diluition and protocol
BSG	ab49493	HIGH pH	1/200; Incubation = 1h, RT.
CAIX	MAB21881	LOW pH	1/ 7; Incubation = 1h, RT
MCT1	AB3538P	LOW pH	1/400; Overnight incubation at 4°C.
MCT4	sc-376101	HIGH pH	1/1200; Incubation = 1h, RT; with LINKER
THBS2	sc-7655	LOW pH	1/50; Overnight incubation at 4°C

Table 7: Immunohistochemistry staining protocols.

5.3.6 Scoring and statistical analysis

Scoring has been performed trough PathXL software by EB with the supervision of an experienced histopathologist. Survival was assessed from the date of histological diagnosis. Data analysis was performed with SPSS v17.0 (SPSS Inc., Woking, UK) and the R software environment. The analysis had the aim of testing whether there was a significant association between membrane and cytoplasm score of five different biomarkers, and survival time. For each biomarker we fitted a Cox

proportional hazard model (coxph() function in R) with survival time as the outcome and membrane scoring at baseline, cytoplasm scoring at baseline, age at diagnosis, gender, and stage of disease as covariates. Individuals who did not die during the follow-up time were right censored at the time they were last seen.

As the baseline score was missing for a substantial number of individuals, we used multiple imputation by chained equations with 20 replicates (using the mice library in R (Buuren et al. 2011)) to account for missing data. We did not formally adjust for multiple testing, so any marginally significant results should be interpreted with caution.

5.4 Evaluation of THBS2 and MCT4 expression in normal pleura samples.

The antibodies and the protocol used for the staining were the same used for TMA IHC.

Fifteen normal pleura samples has been stained together with some selected cases of MPM, previously studied in TMA IHC in order to compare the intensity and the localization of staining.

The cases include lung tissue with some surface visceral pleural mesothelial cells and strips of parietal pleura from pneumothorax patients.

6 Results

6.1 Selection of putative target genes

Following an extensive literature search we identified a set of overexpressed genes in MPM that could potentially be explored as a new therapeutic and diagnostic target. Thus, we focused our attention on *ASS1, BSG, CAIX, CCNO, CDH11, CFB, EIF4G1, IMP3, ITGA4, MCT1, MCT4, PDGFRB, RAN, SOD1, SULF1, THBS2, TIMP3* genes.

6.2 RNAi phenotypic screening

In order to ascertain whether these genes, upregulated in mesothelioma tissues, play a role in the maintenance of malignant phenotype, we adopted a gene silencing-RNA approach. After the evaluation of mRNA and protein levels of the target genes, we evaluated the effects of silencing in the proliferation, in the caspase activity, in senescence, in the cell cycle, in the migration and in the colony formation ability.

6.2.1 CCNO phenotypic analysis

***CCNO*: mRNA levels.**

Three mesothelioma cell lines show statistical significant higher levels of *CCNO* mRNA compared to Met5A: Mero14 (p-value = 0.035), Mero25 (p-value = 0.027) and NCI-H28 (p-value = 0.020); REN (0.073) and IstMes2 cell line did not show upregulation. (Fig. 12)

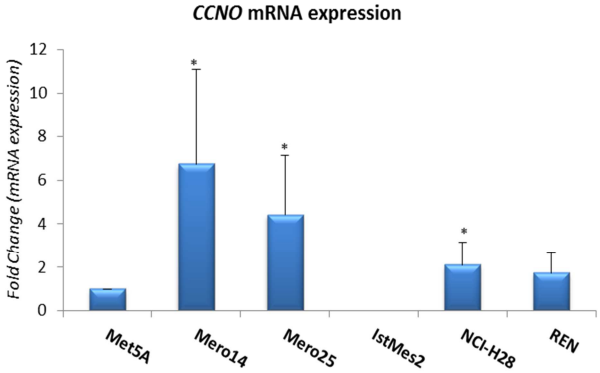


Fig.12 Basal expression level of *CCNO* in five MPM cell lines. On the left, RTqPCR showing fold change of quantitative mRNA levels of *CCNO* measured on MPM cell lines versus MeT-5A cells. Mean of *RPLP0*, *HPRT*, and *TBP* was used for normalization. Errors bars are SEM of the fold change from three independent experiments, each in triplicate. Mero14 cells showed the highest expression levels of *CCNO* (p=0.035), followed by Mero25 (p =0.027) and NCI-H28 (p=0,020)

mRNA expression after *CCNO* silencing

CCNO knockdown was statistically significant in Mero-14 (p-value = 0.01) with 59% reduction of CCNO mRNA, in NCI-H28 (p-value = 0.04) with a reduction of 32%, in REN (p-value= 0.001) with a reduction of 60% and in Met-5A (p-value = 0.007) with 42% of reduction of CCNO mRNA. In Mero25 cell line silencing was not effective (Fig. 13).

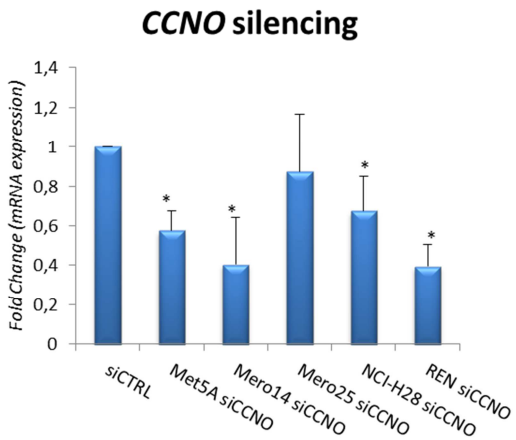


Fig. 13: Silencing of *CCNO*. On the left, RTqPCR showing fold change of quantitative mRNA levels of *CCNO* in Met5A, Mero14, Mero25, NCI-H28 and REN cell lines treated with si*CCNO* versus the corresponding cell line treated with siCTRL. Mean of *RPLP0*, *HPRT*, and *TBP* was used for normalization. Errors bars are SEM of the fold change from three independent experiments, each in triplicate

CCNO silencing and proliferation

The sulphorodamine assay showed a significant increment of proliferation (p-value= 0.037) in REN cell line treated with siCCNO compared to the treatment with siCTRL (Fig. 14). Met5A, Mero14 and NCI-H28 cell lines did not show any significant difference between cells treated with si*CCNO* and siCTRL.

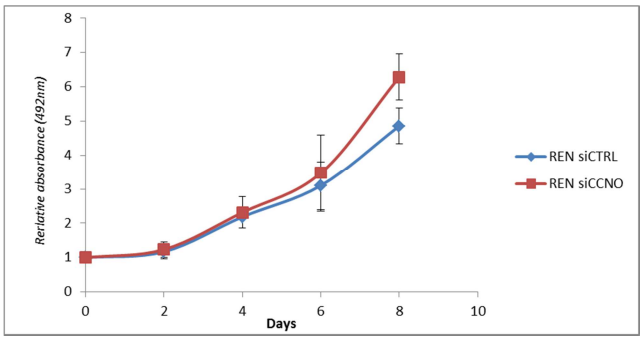
A 

Fig. 14: Effects of *CCNO* on REN proliferation: Proliferation curve of REN cells treated with 50 nM of siCTRL and si*CCNO*. The acquisition of optical density has been made every two days (day 0, 2, 4, 6, 8) starting from the time of transfection (= day 0). Error bars represent SEM of three independent experiments, each done in triplicate.

CCNO silencing and migration

We did not observe any significant difference in migration ability after CCNO silencing in none of the cells treated (Met5A, Mero14, NCI-H28 and REN).

CCNO silencing and colony formation ability

The Colony Formation ability of REN increased (fold change compared to the siCTRL= 6.55) after CCNO silencing (p-value = 0.05) as shown in figure 15; while Mero14, NCI-H28 and Met5A did not show any significant change.

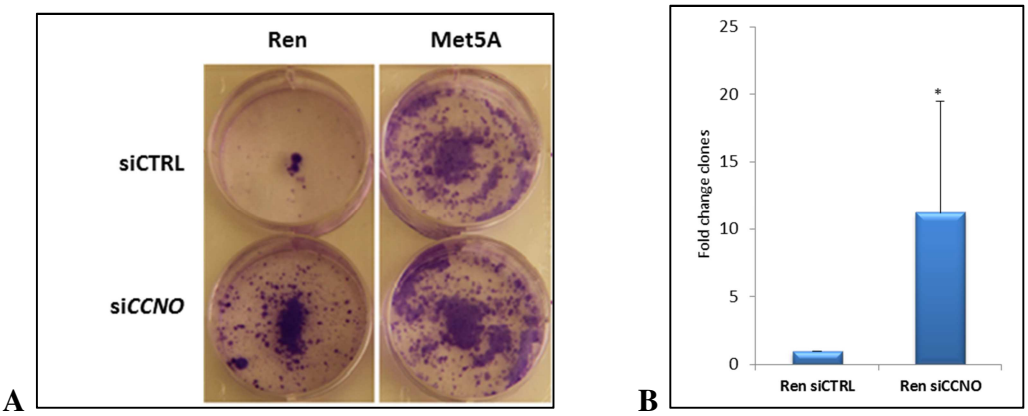


Fig. 15: Effects of *CCNO* on Met5A and REN colony formation ability: **A** pictures showing the colonies fixed 14 days after treatment; **B** the histogram highlights the increment of colonies measured 14 days after *CCNO* silencing. Errors bars are SEM of the fold change from three independent experiments

CCNO silencing and apoptosis

In all the cell lines treated with siCCNO we did not observe any statistically significant change in caspase 3/7 activity, 72 h after treatment, compared to the treatment with siCTRL (Fig. 16).

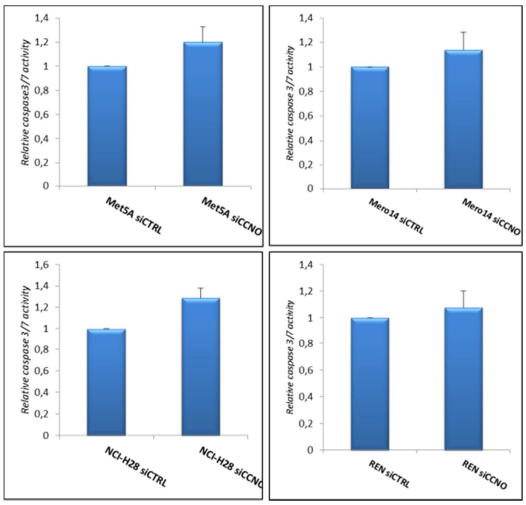


Fig.16 Effects of *CCNO* on caspase 3/7 activity Relative fold change of caspase 3/7 activity measured 72h after transfection with 50nM of siCTRL and si*CCNO* for Met5A, NCI-H28 and REN, or with 20nM of siCTRL and si*CCNO* for Mero14, according to efficiency results. Errors bars are SEM of the fold change from three independent experiments.

6.2.2 *CFB* phenotypic analysis

***CFB*: mRNA and protein levels.**

Mero14 cell line shows a significant higher expression of *CFB* levels compared to Met5A (p-value = 0.009), while Mero25, IstMes2, NCI-H28 and Ren show a lower expression of this gene compared to the non malignant cell line. For this reason we decided to focus CFB RNAi phenotypic screening on Mero14 cell line.

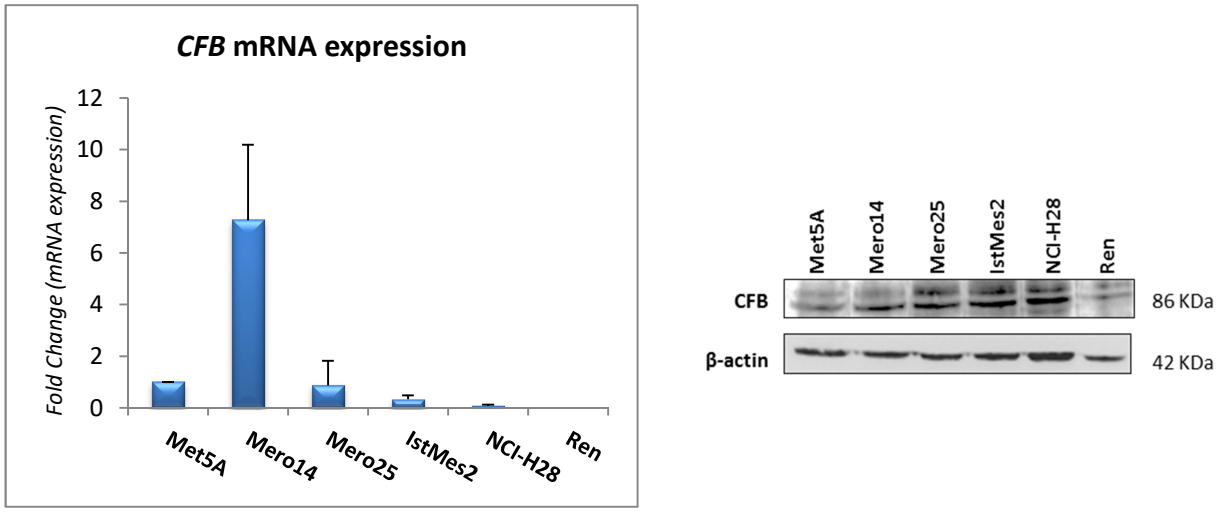


Fig. 17 Basal expression level of *CFB* in five MPM cell lines. On the left, RTqPCR showing fold change of quantitative mRNA levels of *CFB* measured on MPM cell lines versus MeT-5A cells. Mean of *RPLP0*, *HPRT*, and *TBP* was used for normalization. Errors bars are SEM of the fold change from three independent experiments, each in triplicate. Mero14 cells showed the highest expression levels of *CFB* (p= 0.009). On the right, the protein levels of CFB on MeT-5A, Mero-14, Mero 25, IstMes2, NCI-H28 and REN cells. β-Actin was used as loading control. The protein levels were confirmed with two independent experiments.

mRNA and protein expression after *CFB* silencing

We evaluated the expression levels after CFB depletion in Met5A and in Mero14. We observed a significant decrease of CFB levels in Mero14 cell line treated with siCFB compared to the control (p-value = 2 x10^{-5}) with 84% reduction of expression while in Met5A cell line the reduction of CFB levels was of 45% (p-value = 0.02). We analyzed the protein levels after silencing in Met5A, Mero14 and Mero25: the knockdown of the protein was statistically significant only in Mero14.

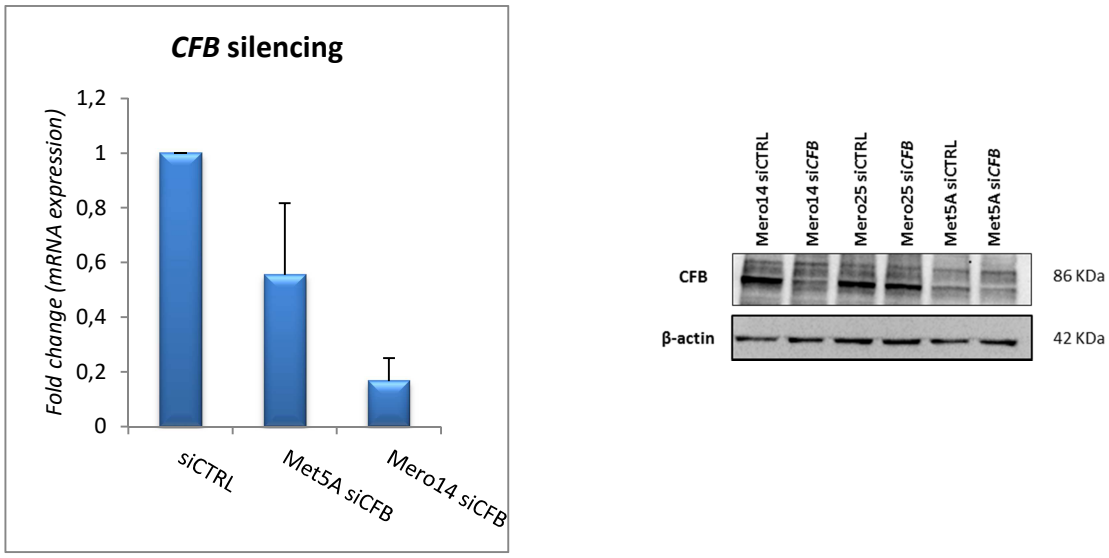


Fig. 18: Silencing of *CFB*. On the left, RTqPCR showing fold change of quantitative mRNA levels of *CFB* in Met5A (p=0.02), Mero14 (p=2 x 10^{-5}) cell lines treated with si*CFB* versus the corresponding cell line treated with siCTRL (All Star Negative control siRNA). Mean of *RPLP0*, *HPRT*, and *TBP* was used for normalization. Errors bars are SEM of the fold change from three independent experiments, each in triplicate. On the right, the protein levels of CFB after its depletion with si*CFB* versus the control, β-Actin was used as loading control. The protein levels were confirmed with two independent experiments.

CFB silencing and proliferation

The sulphorodamine assay did not show significant differences between cells treated with siCFB and siCTRL.

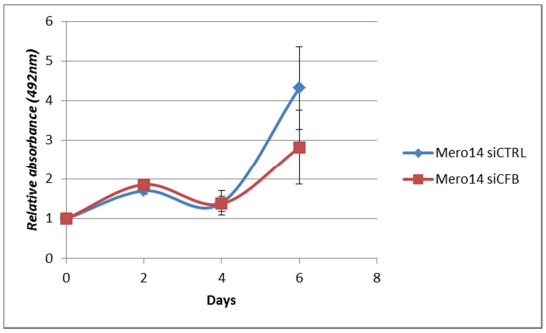


Fig. 19: Effects of *CFB* on Mero14 proliferation: the proliferation curve of Mero14 cells treated with 20 nM of siCTRL (All star negative siRNA) and si*CFB*. The acquisition of optical density has been made every two days (day 0, 2, 4, 6, 8) starting from the time of transfection (= day 0). Error bars represent SEM of three independent experiments, each done in triplicate.

CFB silencing and migration

The Wound Healing Assay did not show significant differences between cells treated with siCFB and siCTRL. Here we report the pictures of Mero14 and Met5A at the time of scratch and 72h after trasfection.

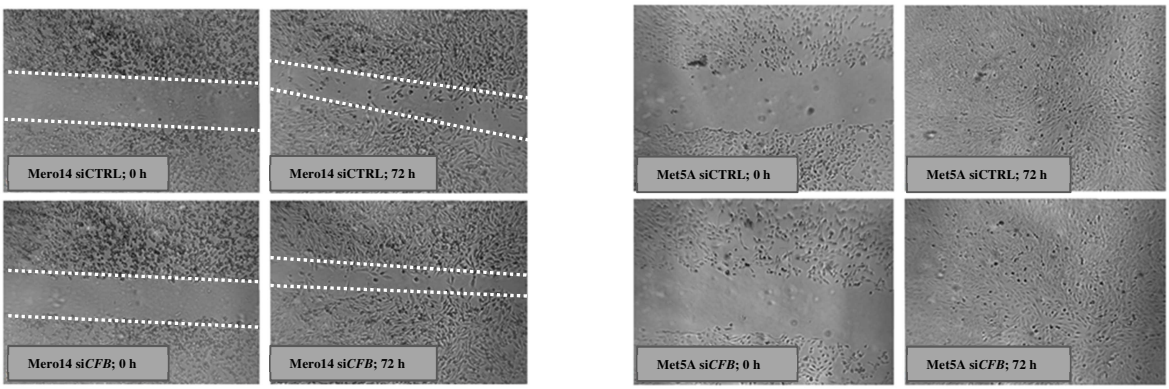


Fig.20: Effects of *CFB* on migration: A on the upper left Mero14 cells treated with 20nM of siCTRL (siRNA C- in picture) at the time of scratch, on the lower left Mero14 cells treated with 20 nM of si*CFB* at the time of scratch, on the right the same cells 72 h after scratch. **B** on the upper left Met5A cells treated with 50nM of siCTRL at the time of scratch, on the lower left Met5A cells treated with 50 nM of si*CFB* at the time of scratch, on the right the same cells 72 h after scratch.

CFB silencing and colony formation ability

The colony formation assay did not show significant differences between cells treated with siCFB and siCTRL.

CFB silencing and apoptosis

We did not observe any significant difference in caspase 3/7 activity between cells treated with siCFB and siCTRL.

6.2.3 *THBS2* phenotypic analysis

***THBS2*: mRNA and protein levels.**

The analysis of the expression levels of THBS2 shows a statistical significant overexpression in three mesothelioma cell lines compared to the non-malignant Met5A: Mero-14 (p-value = 0.032), Mero-25 (p-value = 0.037), IstMes2 (p-value = 0.003) while *THBS2* mRNA level in NCI-H28 and REN was lower than Met5A levels.

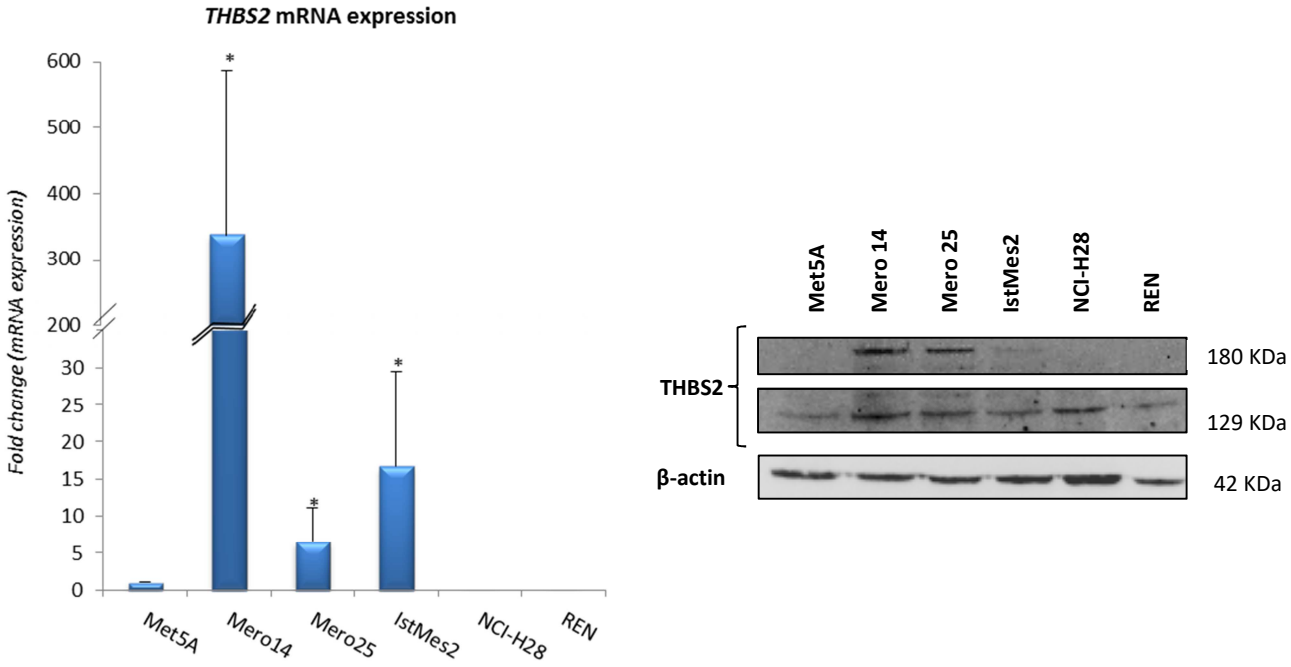


Fig.21: Basal expression level of *THBS2* in five MPM cell lines. On the left, RTqPCR showing fold change of quantitative mRNA levels of *THBS2* measured on MPM cell lines versus MeT-5A cells. Mean of *RPLP0*, *HPRT*, and *TBP* was used for normalization. Errors bars are SEM of the fold change from three independent experiments, each in triplicate. Mero14 cells showed the highest expression levels of *THBS2* (p=0,032), followed by IstMes2 (p = 0,003) and Mero25 (p=0, 037). On the right, the protein levels of THBS2 on MeT-5A, Mero-14, Mero 25, IstMes2, NCI-H28 and REN cells. β-Actin was used as loading control. The protein levels were confirmed with two independent experiments.

mRNA and protein expression after *THBS2* silencing

THBS2 silencing was statistically significant in Mero-14 (p-value = 0.001) with a reduction of 84% of THBS2 mRNA, in IstMes2 (p-value = 0.00002) with a reduction of 62% and in Met5A (p-value = 0.002) with a reduction of 51%. Moreover the silencing was evaluated in cells lysates 72h after transfection through western blot in two independent experiments. The knockdown of the protein was about 99% in Mero14 and about 90% in IstMes2 and Met5A while the silencing in Mero25 was not effective.

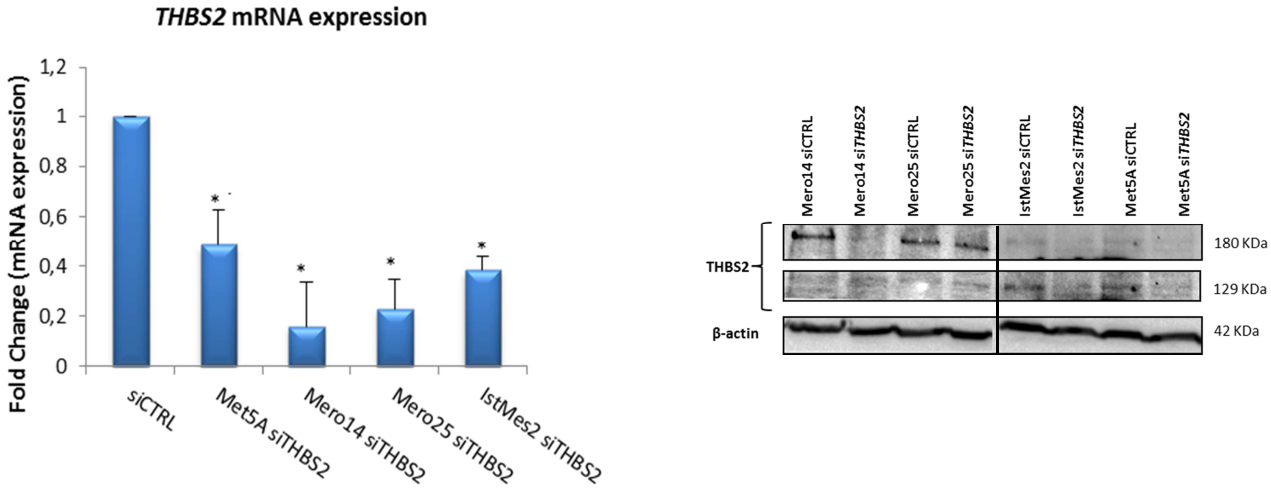


Fig. 22: Silencing of THBS2. On the left, RTqPCR showing fold change of quantitative mRNA levels of *THBS2* in Met5A (p=0.002), Mero14 (p=0.001) and IstMes2 (p=0.00002) cell lines treated with si*THBS2* versus the corresponding cell line treated with siCTRL (All Star Negative control siRNA). Mean of *RPLP0*, *HPRT*, and *TBP* was used for normalization. Errors bars are SEM of the fold change from three independent experiments, each in triplicate. On the right, the protein levels of THBS2 after its depletion with *THBS2* siRNA versus the control, β-Actin was used as loading control. The protein levels were confirmed with two independent experiments.

THBS2 silencing and proliferation

THBS2 silencing caused a statistically significant (p-value = 0.01) decrease in the proliferation rate of IstMes2 (with a reduction of 41% at day 8). Mero-14 and MeT-5A did not show any significant difference.

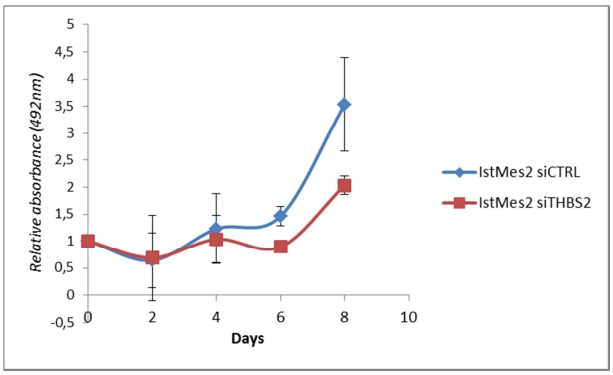


Fig. 23 Effects of *THBS2* on the proliferation: Proliferation curve of IstMes2 cells treated with 50 nM of siCTRL (All star negative siRNA) and si*THBS2*. The acquisition of optical density has been made every two days (day 0, 2, 4, 6, 8) starting from the time of transfection (= day 0). Error bars represent SEM of three independent experiments, each done in triplicate.

THBS2 silencing and migration

The Wound Healing Assay did not show significative differences between cells treated with siCTRL and si*THBS2*. Here we report the acquisitions made at the time of the scratch (on the left of each picture) and 72h after transfection (on the right of each picture) for Mero14 in fig. 24A, for IstMes2 in fig. 24B and for MeT5A in fig. 24C.

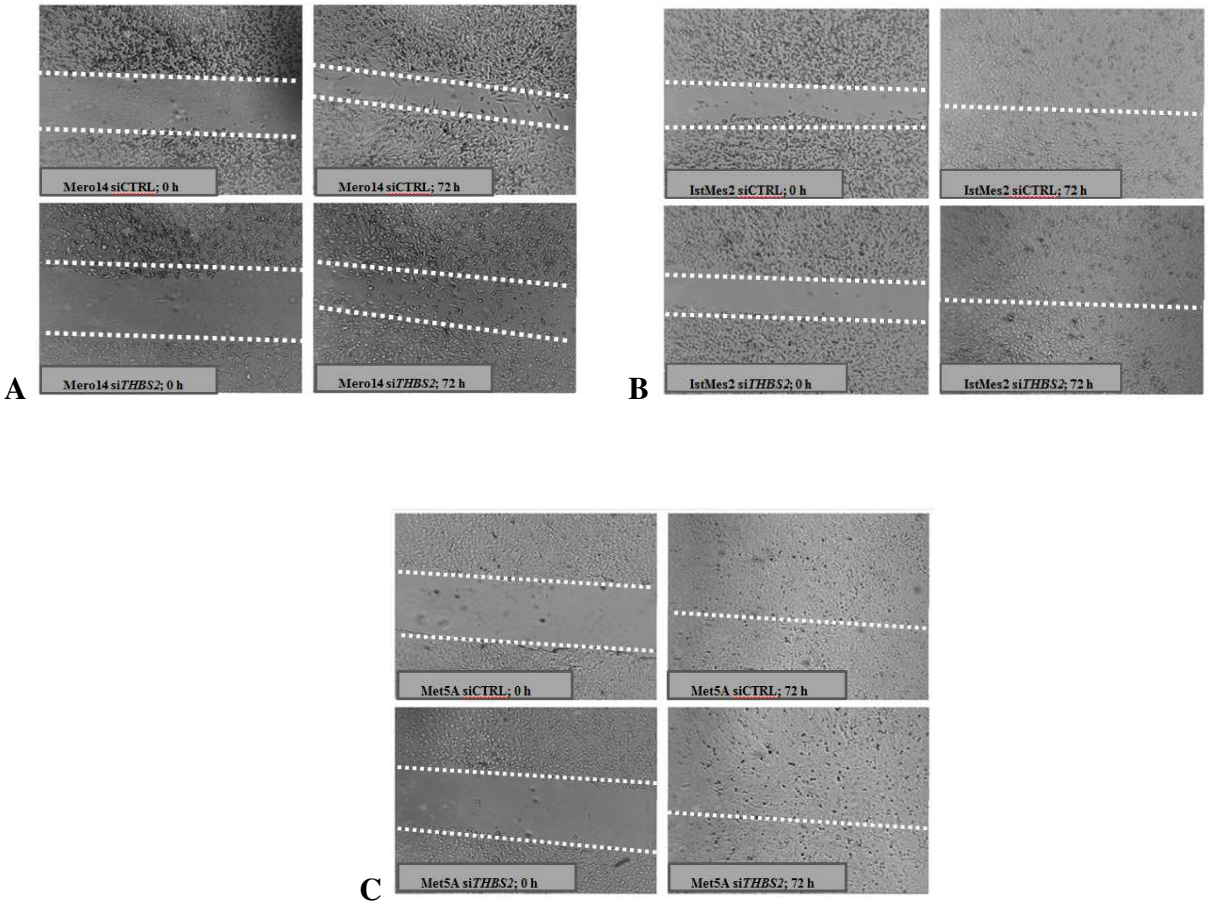


Fig. 24: Effects of *THBS2* on migration: A on the upper left Mero14 cells treated with 20nM of siCTRL (siRNA C- in picture) at the time of scratch, on the lower left Mero14 cells treated with 20 nM of si*THBS2* at the time of scratch, on the right the same cells 72 h after the scratch. **B** on the upper left IstMes2 cells treated with 50nM of siCTRL at the time of scratch, on the lower left IstMes2 cells treated with 50 nM of si*THBS2* at the time of scratch, on the right the same cells 72 h after the scratch. **C** on the upper left Met5A cells treated with 50nM of siCTRL (siRNA C- in picture) at the time of scratch, on the lower left Met5A cells treated with 50 nM of si*THBS2* at the time of scratch, on the right the same cells 72 h after the scratch.

THBS2 silencing and colony formation ability

THBS2 silencing caused a significant (p = 0.020) drop of 66% in colony number in IstMes2 cells while we did not observe any change in colony formation ability of Met5A non malignant cells, as shown in picture (Fig. 25). Mero14 has not been affected by *THBS2* silencing.

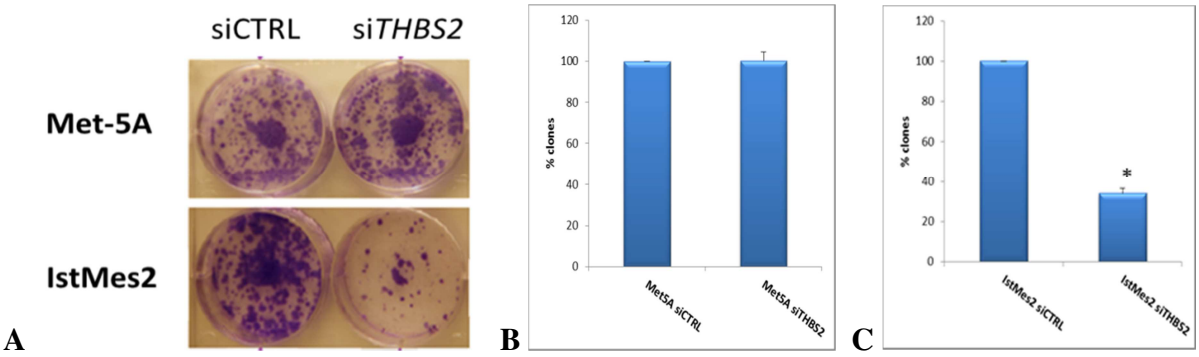


Fig. 25: Effects of *THBS2* on Met5A and IstMes2 colony formation ability. A Pictures show the Met5A and IstMes2 cells, silenced with 50nM of siCTRL and si*THBS2*, fixed and stained 14 days after treatment. **B** The histograms show the percentage of clones measured 14 days after silencing. Errors bars are SEM of the percentage fold change from three independent experiments

THBS2 silencing and apoptosis

The depletion of THBS2 caused a statistical significant increment of caspase 3/7 activity in Mero-14 (p-value = 0.032), with 30% increase of cell death in cells treated with siTHBS2 compared to the control; in IstMes2 and MeT-5A cell lines we did not observe any significant alteration.

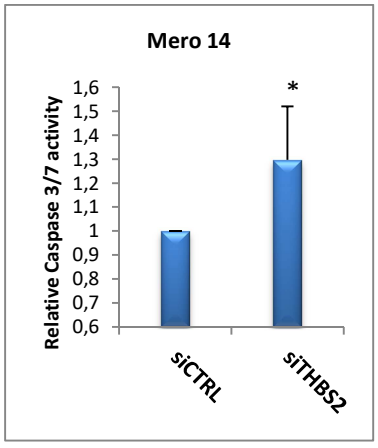


Fig. 26 Effects of THBS2 on caspase 3/7 activity: Relative fold change of caspase 3/7 activity measured 72h after treatment with 20nM of siCTRL and si*THBS2*. Errors bars are SEM of the fold change from three independent experiments

6.2.4 *TIMP3* phenotypic analysis

***TIMP3*: mRNA levels.**

Three of the four mesothelioma cell lines analysed showed statistically significant higher levels of *TIMP3* mRNA compared to Met5A expression levels (Mero14 p = 0,036; Mero25 p = $0{,}22*10^{-3}$; IstMes2 p = 0,013) while in NCI-H28 cells the gene was not expressed.

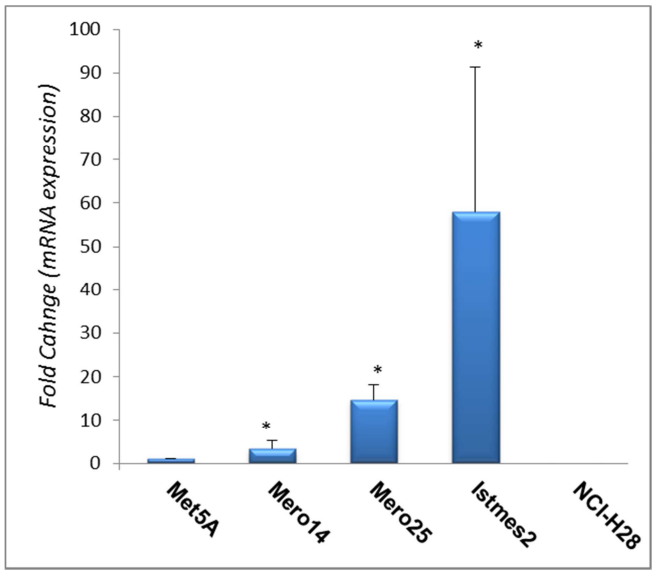


Fig. 27 Basal expression level of *TIMP3* in four MPM cell lines. RTqPCR showing fold change of quantitative mRNA levels of *TIMP3* measured on MPM cell lines versus MeT-5A cells. Mean of *RPLP0*, *HPRT*, and *TBP* was used for normalization. Errors bars are SEM of the fold change from three independent experiments, each in triplicate.

mRNA expression after *TIMP3* silencing

TIMP3 silencing has been effective, at mRNA level, for all the cell lines: Mero14 cells showed the higher decrease of 91,2% ($p = 2,42 \times 10^{-6}$), followed by Met5A with a the decrease of TIMP3 mRNA levels of 80% (p= 0,0008), in of 93,23% (p= 0,0004), in IstMes2 of 65,4% (p= 0,0016) and in Mero25 of 64% (p= 0,001).

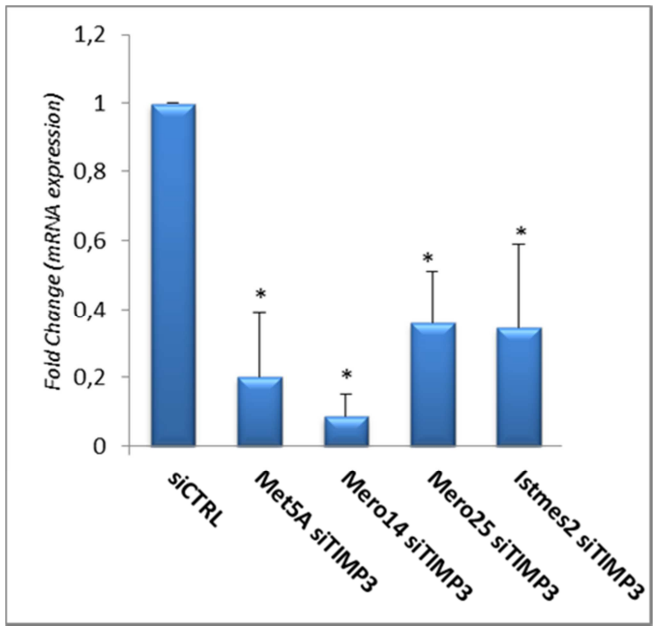


Fig.28: Silencing of *TIMP3*. RTqPCR showing fold change of quantitative mRNA levels of *TIMP3* (72h after tTIMP3sfection) in one mesothelial cell line (Met5A) and four mesothelioma cell lines versus the expression levels observed in the corresponding cell line treated with siCTRL (All Star Negative control siRNA). Mean of RPLP0, HPRT, and TBP was used for normalization. Errors bars are SEM of the fold change from three independent experiments, each in triplicate.

TIMP3 silencing and proliferation

TIMP3 depletion caused a statistical significant decrease of proliferation rate (p=0.014) in Mero14 (decrement at day 8 of 54,2%) and in IstMes2 (p=0.047) with a decrement at day 8 of 49%; while Mero25 and MeT5A did not show any difference in proliferation.

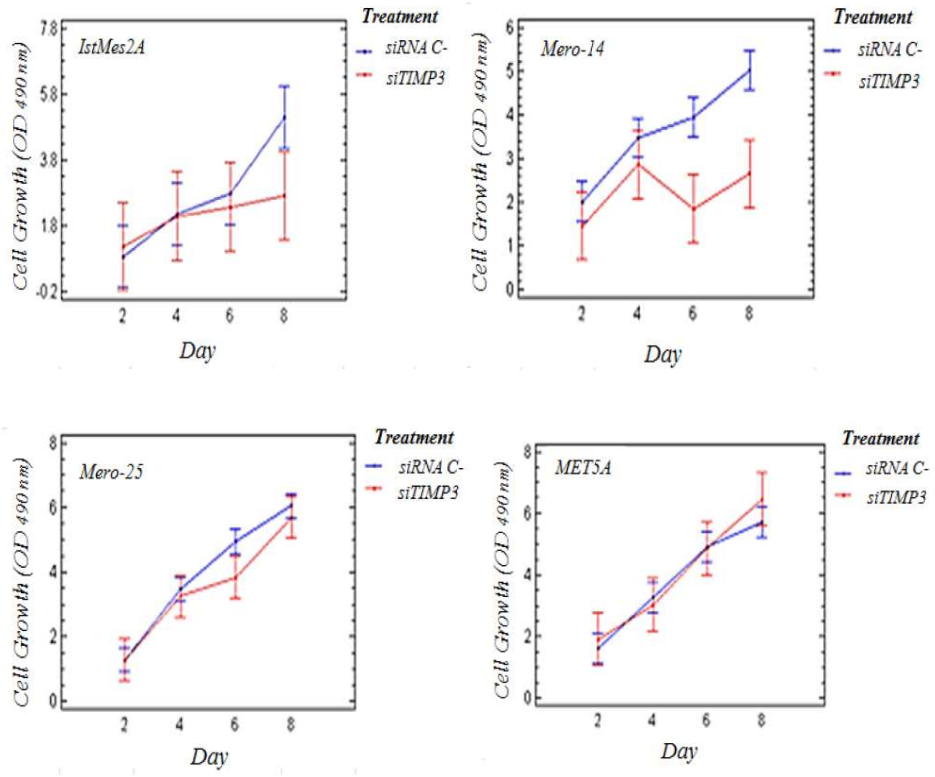


Fig. 29 Effects of *TIMP3* on the proliferation: Proliferation assay curves of IstMes2, Met5A, Mero25, cells treated with 50 nM of siCTRL (All star negative siRNA) and si*TIMP3*. Mero14 has been treated with 20nM of siCTRL and si*TIMP3*, according to the trasfection efficiency results. The acquisition of optical density has been made every two days (day 0, 2, 4, 6, 8) starting from the time of transfection (= day 0). Error bars represent SEM of three independent experiments, each done in triplicate.

TIMP3 silencing and migration

After *TIMP3* silencing we did not observe any change in the migration ability of all the cell lines treated.

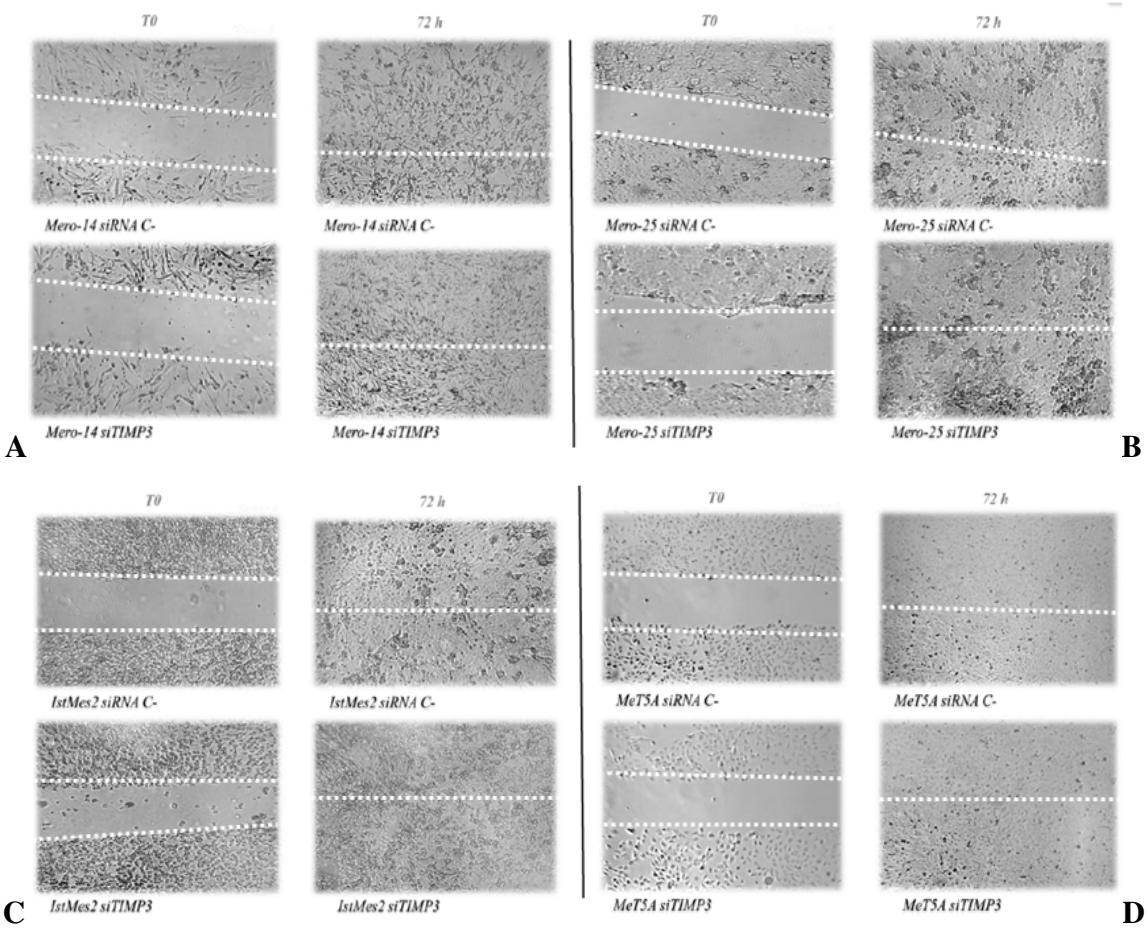


Fig.30 Effects of *TIMP3* on migration: A on the upper left Mero14 cells treated with 20nM of siCTRL (siRNA C- in picture) at the time of scratch, on the lower left Mero14 cells treated with 20 nM of si*TIMP3* at the time of scratch, on the right the same cells 72 h after the scratch. **B** on the upper left Mero25 cells treated with 50nM of siCTRL (siRNA C- in picture) at the time of scratch, on the lower left Mero25 cells treated with 50 nM of si*TIMP3* at the time of scratch, on the right the same cells 72 h after the scratch. **C** on the upper left IstMes2 cells treated with 50nM of siCTRL (siRNA C- in picture) at the time of scratch, on the lower left IstMes2 cells treated with 50 nM of si*TIMP3* at the time of scratch, on the right the same cells 72 h after the scratch. **D** on the upper left Met5A cells treated with 50nM of siCTRL (siRNA C- in picture) at the time of scratch, on the lower left Met5A cells treated with 50 nM of si*TIMP3* at the time of scratch, on the right the same cells 72 h after the scratch.

TIMP3 silencing and colony formation ability

All the MPM cell lines treated showed a statistical significant average decrease of colony formation ability after si*TIMP3* transfection: we observed a decrease of 55.5% in Mero14 (p =0.031), of 15% in Mero25 (p =0.010) e of 95% in IstMes2 (p =0.33 x 10^{-3}), while it was not significant for the non-malignant MeT5A cell line (p=0.129).

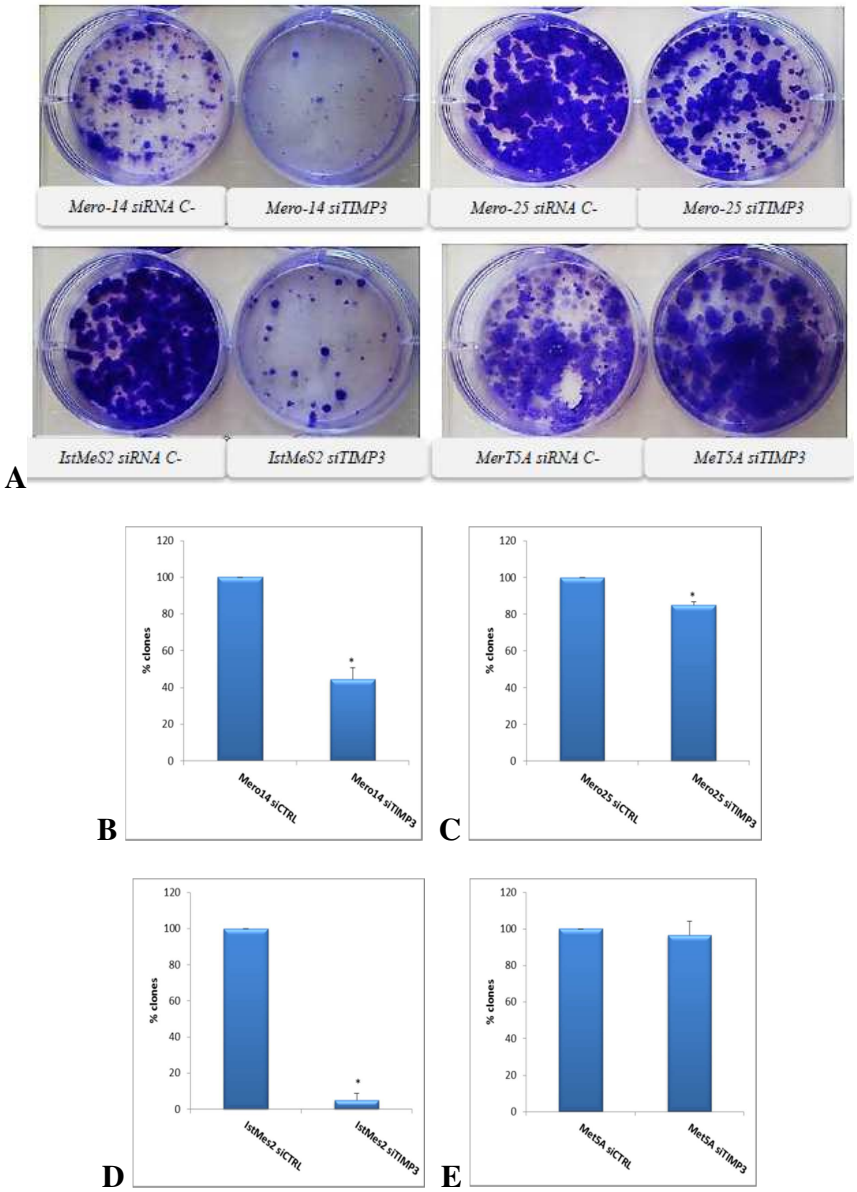


Fig. 31 Effects of *TIMP3* on colony formation ability. A Pictures show the Mero14 cells silenced with 20nM of siCTRL and si*TIMP3* and Mero25, IstMes2 and Met5A cells, silenced with 50nM of siCTRL and si*TIMP3*, fixed and stained 14 days after treatment. **B, C, D, E** The histograms show the percentage of clones measured 14 days after silencing. Errors bars are SEM of the percentage fold change from three independent experiments

TIMP3 silencing and apoptosis

TIMP3 silencing caused a statistical significant decrement of caspase 3/7 activity by 45% in Mero14 cell line ($p < 10^{-3}$) while IstMes2, Met5A and Mero25 seems not to be affected by the treatment.

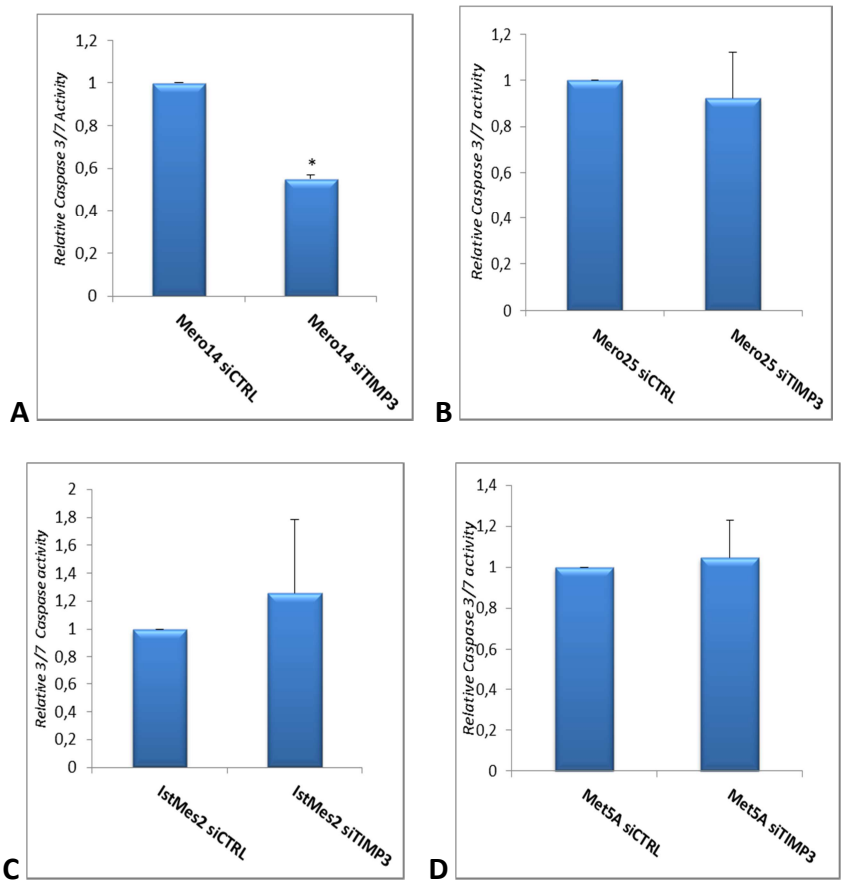


Fig 32 Relative fold change of caspase 3/7 activity measured 72h after TIMP3 transfection with 50nM of siCTRL and si*TIMP3* for Mero25 (p = 0,541) (B), IstMes2 (C) and Met5A (p = 0,339) (D) cell lines; and after TIMP3 transfection with 20nM of siCTRL and si*TIMP3* for Mero14 (A) cell line, according to the TIMP3 transfection efficiency results. Errors bars are SEM of the fold change from three independent experiments.

TIMP3 silencing and senescence

The reduced caspase 3/7 activity observed in Mero14 cells following siTIMP3 prompted us to hypothesize that cells could be more resistant to apoptosis, thereby being more susceptible to die by senescence. Thus, we measured the β-galattosidase activity following TIMP3 silencing and, indeed, we observed an increase (+90%) of Mero14 senescent cells (*p= 0,037*), while we did not observe any difference in the non-malignant Met5A cell line (*p= 0.5*). Here we reports the acquisition made five days after transfection for Mero14 and Met5A.

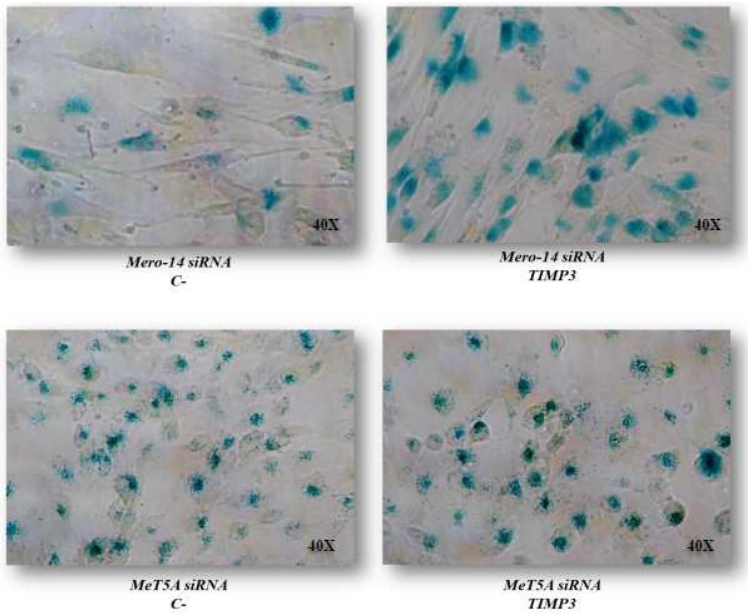


Fig. 33 Effects of *TIMP3* on Met5A and Mero14 senescence: Pictures show Mero14 and Met5A cells 5 days after treatment (Mero14 C- = treated with 20nM of siCTRL; Mero14 siRNA TIMP3 = treated with 20nM of siTIMP3; Met5A C- = treated with 50nM of siCTRL; Met5A siRNA TIMP3 = treated with 50nM of siTIMP3). The ß-galattosidase activity is highlighted by the blue staining of senescent cells.

6.2.5 SULF1 phenotypic analysis

***SULF1*: mRNA levels.**

SULF1 resulted overexpressed compared to Met5A, in two of the four MPM cells analysed.

In particular Mero-25 (p-value =0,048) and Mero-14 (p-value =8,96 x 10^{-7}) showed a statistical significant higher expression level compared to Met5A, while IstMes2 and NCI-H28 did not expressed *SULF1* mRNA.

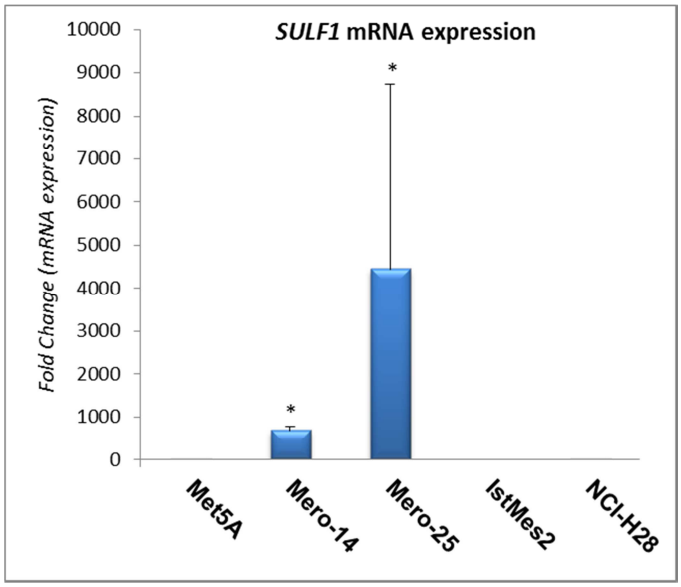


Fig.34 Basal expression level of *SULF1* in four MPM cell lines. A)RTqPCR showing fold change of quantitative mRNA levels of *SULF1* measured on MPM cell lines versus MeT-5A cells. Mean of *RPLP0*, *HPRT*, and *TBP* was used for normalization. Errors bars are SEM of the fold change from three independent experiments, each in triplicate.

mRNA expression after*SULF1* silencing

SULF1 silencing has been effective,at mRNA level, for all the cell lines treated. In Met5A the decrease of SULF1 mRNA levels has been of 35,5% (p=0,045), in Mero14 of 98% (p=7,37 x 10^{-8}) and in Mero25 of 95 % (p=1,16 x 10^{-6}).

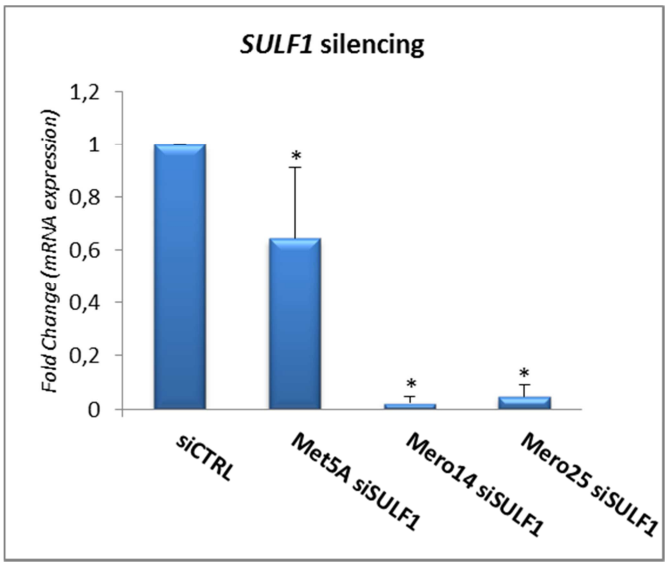


Fig. 35: Silencing of *SULF1*. On the left, RTqPCR showing fold change of quantitative mRNA levels of *SULF1*(72h after si*SULF1* transfection) in one mesothelial cell line (Met5A) and three mesothelioma cell lines versus the expression levels observed in the corresponding cell line treated with siCTRL (All Star Negative control siRNA). Mean of RPLP0, HPRT, and TBP was used for normalization. Errors bars are SEM of the fold change from three independent experiments, each in triplicate.

*SULF1*silencing and proliferation

SULF1 silencing affected in a statistical significant way only Mero-14 proliferation rate (p-value =0.025); Mero25 (p-value =0,658) and MeT5A (p-value =0,378) were not significantly affected by the treatment.

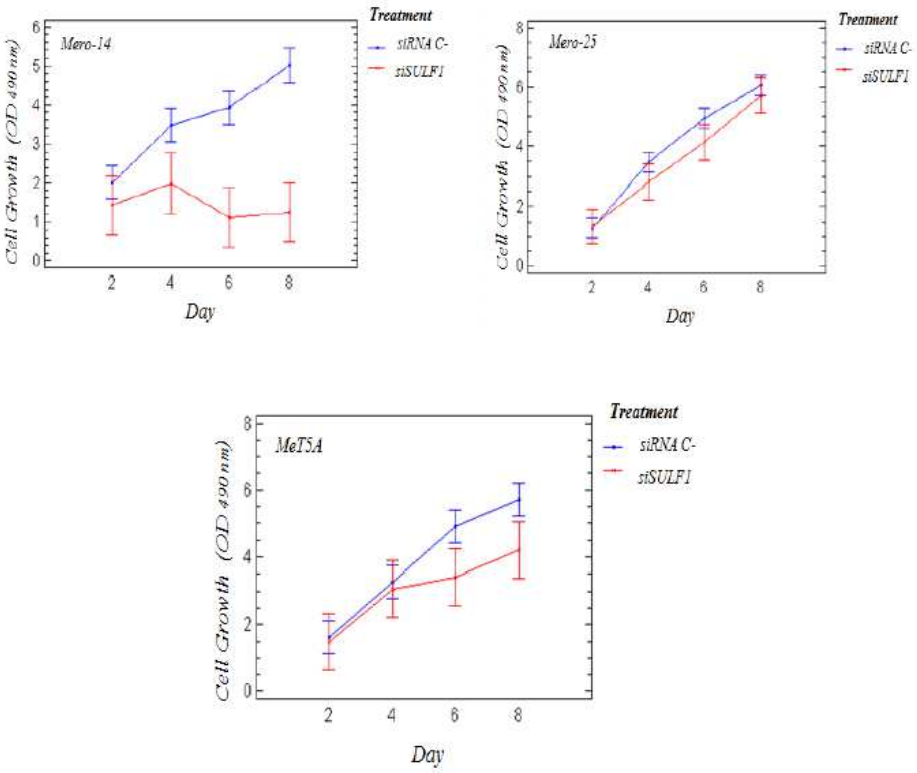


Fig. 36 Effects of *SULF1* on proliferation: Proliferation assay curves of Mero25 and Met5A, cells treated with 50 nM of siCTRL (All star negative siRNA) and si*SULF1*. Mero14 has been treated with 20nM of siCTRL and si*SULF1*, according to the trasfection efficiency results. The acquisition of optical density has been made every two days (day 0, 2, 4, 6, 8) starting from the time of transfection (= day 0). Error bars represent SEM of three independent experiments, each done in triplicate.

SULF1 silencing and colony formation ability

SULF1 knockdown caused a statistical significant decrease of colony formation ability by 96% in Mero14 (p-value=0,99 x 10^{-4}) while Mero25 (p-value=0,587) and MeT5A (pvalue=0,348) colony number did not significantly change after treatment.

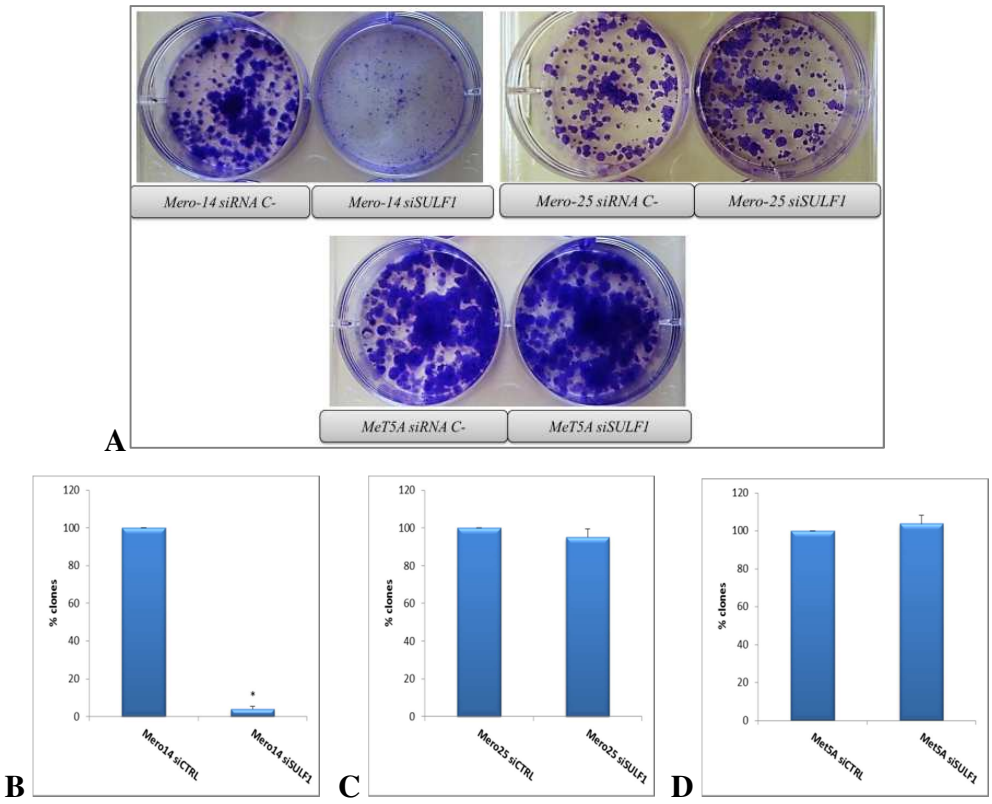


Fig.37:Effects of SULF1silencing in the colony formation ability A Pictures show the Mero14 cells silenced with 20nM of siCTRL and si*TIMP3* and Mero25 and Met5A cells, silenced with 50nM of siCTRL and si*TIMP3*, fixed and stained 14 days after treatment. **B, C, D** The histograms show the percentage of clones measured 14 days after silencing. Errors bars are SEM of the percentage fold change from three independent experiments

SULF1 silencing and apoptosis

SULF1 silencing caused a significant increment of caspase 3/7 activity of 64% in Mero14 (p = 0.046); while MeT5A and Mero25 did not show a significant difference.

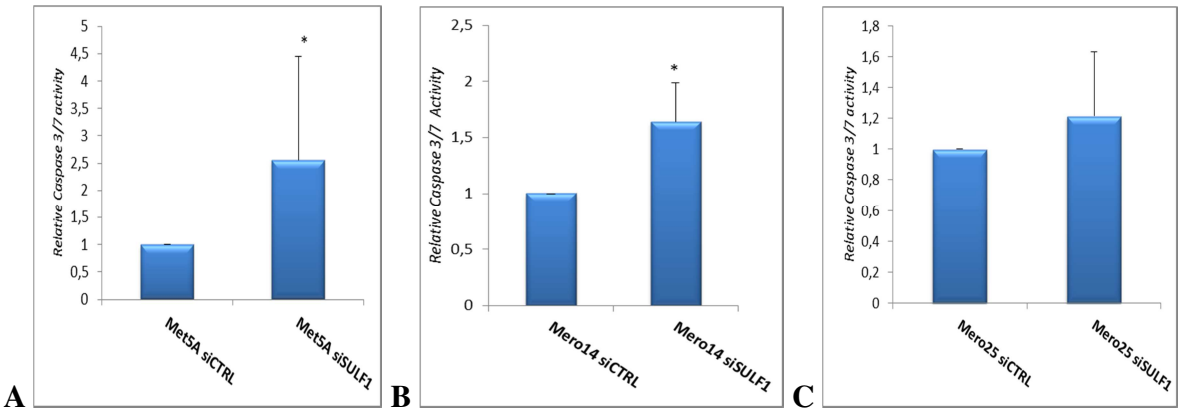
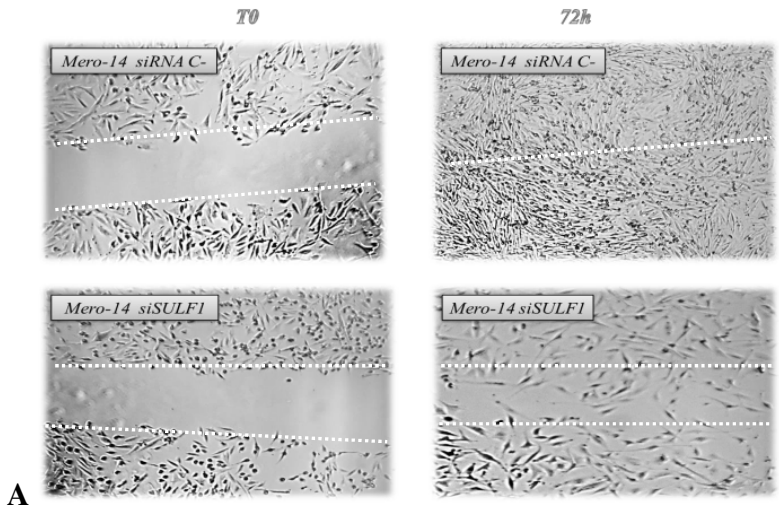


Fig. 38 . **Effects of *SULF1* on caspase 3/7 activity:** Relative fold change of caspase 3/7 activity measured 72h after transfection with 20nM of siCTRL and si*SULF1* for Mero14 (B) cell line and after transfection with 50nM of siCTRL and si*SULF1* for Met5A and Mero25 (B and C). Errors bars are SEM of the fold change from three independent experiments.

*SULF1*silencing and migration

We observed a decreased migration ability of Mero14 of 35,5% but it was not statistically significant (p-value=0.060), while Mero25 and MeT5A (p-value=0.823) did not show any difference.



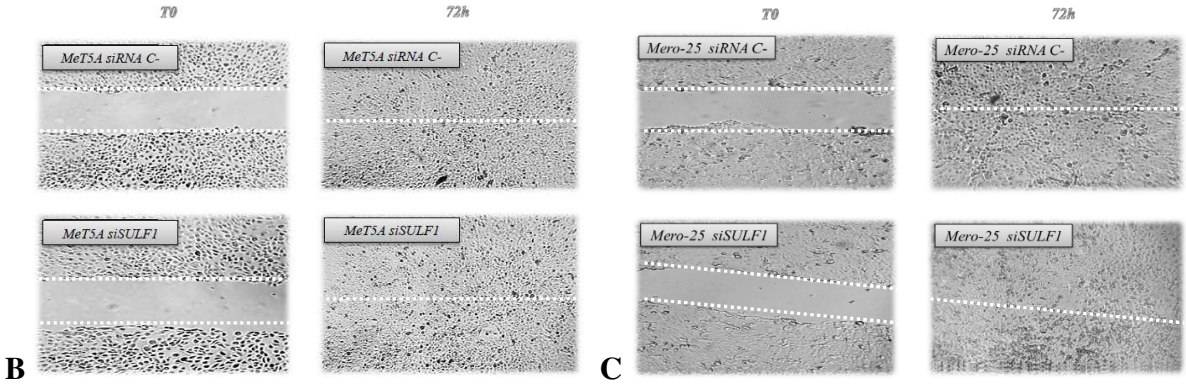


Fig. 39 Effects of *SULF1* on migration: A on the upper left Mero14 cells treated with 20nM of siCTRL (siRNA C- in picture) at the time of scratch, on the lower left Mero14 cells treated with 20 nM of si*SULF1* at the time of scratch, on the right the same cells 72 h after the scratch. **B** on the upper left Met5A cells treated with 50nM of siCTRL (siRNA C- in picture) at the time of scratch, on the lower left Met5A cells treated with 50 nM of si*SULF1* at the time of scratch, on the right the same cells 72 h after the scratch; **C** on the upper left Mero25 cells treated with 50nM of siCTRL (siRNA C- in picture) at the time of scratch, on the lower left Mero25 cells treated with 50 nM of si*SULF1* at the time of scratch, on the right the same cells 72 h after the scratch.

SULF1 silencing and senescence

After *SULF1* silencing has been observed only a slight inhibition of 30% of cell maturation but not statistically significant in Mero14 (p-value = 0.260). We did not observe any difference in the non malignant Met5A and in Mero25

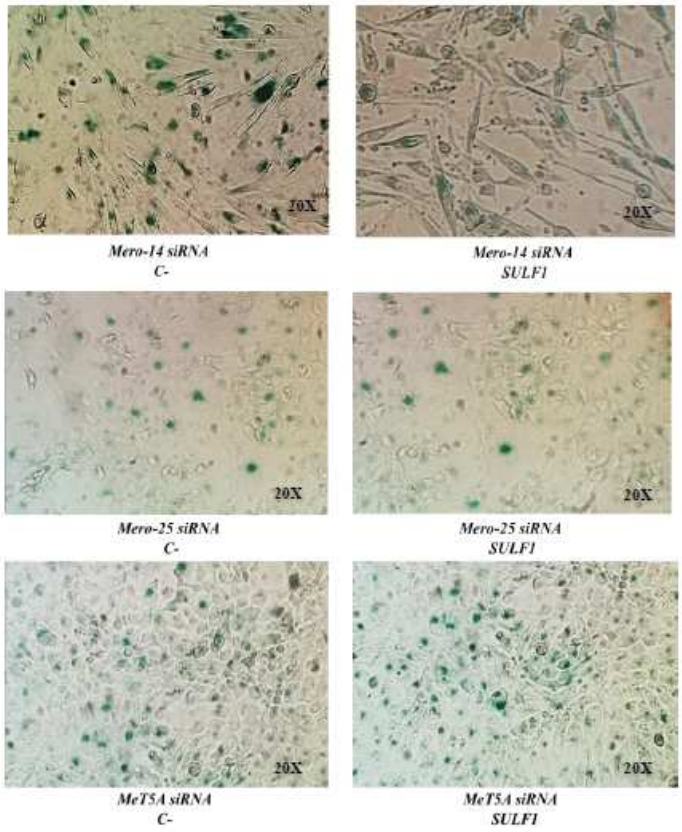


Fig. 40 Effects of *SULF1* on senescence: Pictures show Mero14, Mero25 and Met5A cells 5 days after treatment (Mero14 C- = treated with 20nM of siCTRL; Mero14 siRNA SULF1 = treated with 20nM of siSULF1; Mero25 C- = treated with 50nM of siCTRL; Mero25 siRNA SULF1 = treated with 50nM of siSULF1; Met5A C- = treated with 50nM of siCTRL; Met5A siRNA SULF1 = treated with 50nM of siSULF1). The ß-galattosidase activity is highlighted by the blue staining of senescent cells.

6.2.6 PDGFRβ phenotypic analysis

***PDGFRβ*: mRNA and protein levels.**

Three mesothelioma cell lines showed statistically significant higher levels of PDGFRβ mRNA compared to Met5A expression levels. Mero14 cells showed the higher expression levels with a fold change(fc) ~70 compared to Met5A (p-value =0,006); the higher expression observed in the others two cell lines was lower but still high and significant (Mero25, ~25fc, p-value =0,013; IstMes2 ~10fc, p-value =0,0004). In NCI-H28 cells (p-value =0,043) the gene expression level was significantly lower than Met5A expression level.

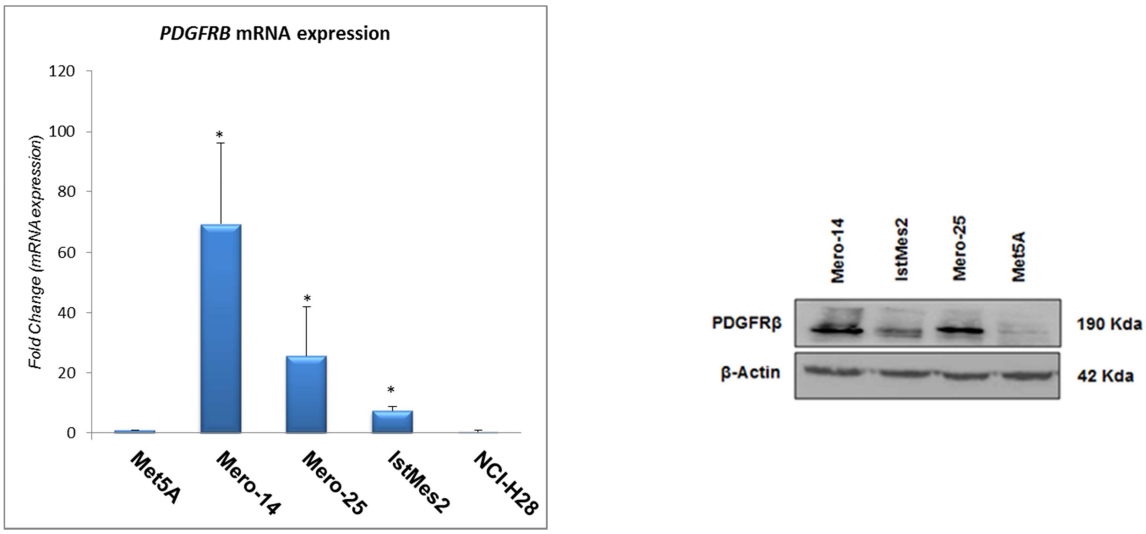


Fig.41 Basal expression level of *PDGFRβ* in four MPM cell lines. On the left, RTqPCR showing fold change of quantitative mRNA levels of *PDGFRβ* measured on MPM cell lines versus MeT-5A cells. Mean of *RPLP0*, *HPRT*, and *TBP* was used for normalization. Errors bars are SEM of the fold change from three independent experiments, each in triplicate. All the MPM cell lines showed significant upregulated levels of *PDGFRβ* mRNA compared to *PDGFRβ* levels in Met5A cell line. Mero14 cells showed the highest expression levels of *PDGFRβ* (p = 0,006) compared to Met5A expression levels, followed by Mero25 (p = 0,013), IstMes2 (p =0,0004). NCI-H28 (p =0,043) were downregulated. On the right, the protein levels of PDGFRβ on MeT5A, Mero14, Mero25 and IstMes2 cells. β-Actin was used as loading control. The protein levels were confirmed with two independent experiments.

mRNA and protein expression after *PDGFRβ* silencing

PDGFRβ silencing has been effective for all the cell lines at mRNA level, we observed a decrease by 70% in Met5A, p=0,004; decrease by 95,1% in Mero14, p=3,33 x 10^{-6}; decrease by 75% in Mero25, p=0,004; decrease by 96,1%, in IstMes2 p= 2,16 x 10^{-8}.

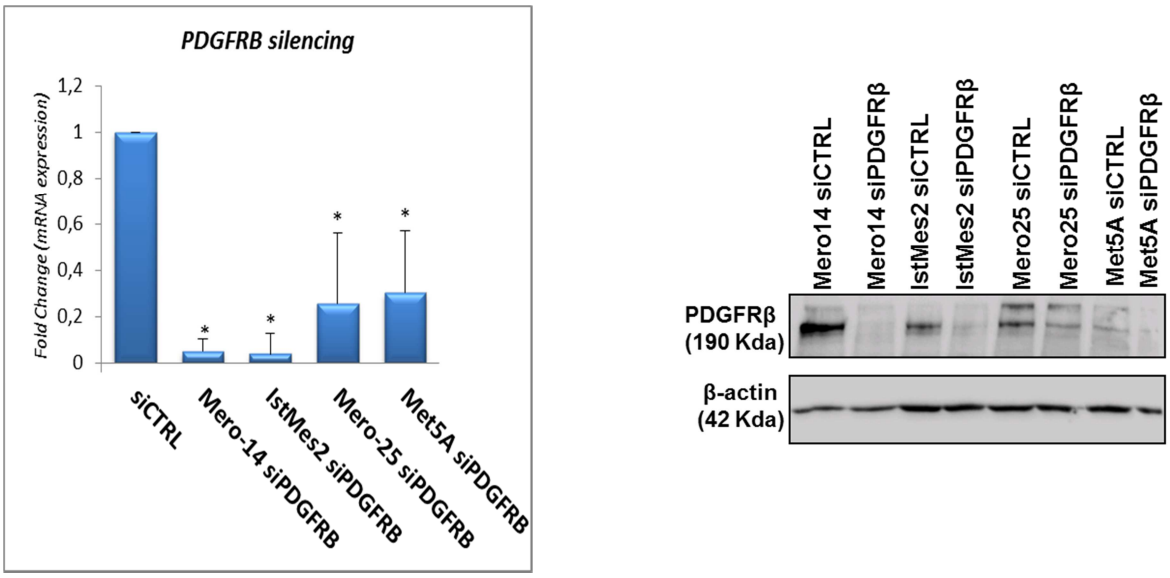


Fig. 42: Silencing of *PDGFRβ*. On the left, RTqPCR showing fold change of quantitative mRNA levels of *PDGFRβ* (72h after transfection) in one mesothelial cell line (Met5A) and four mesothelioma cell lines versus the expression levels observed in the corresponding cell line treated with siCTRL (All Star Negative control siRNA). Mean of RPLP0, HPRT, and TBP was used for normalization. Errors bars are SEM of the fold change from three independent experiments, each in triplicate. On the right, the protein levels of PDGFRβ after its depletion with *PDGFRβ* siRNA versus the control, β-Actin was used as loading control. The protein levels were confirmed with two independent experiments.

***PDGFRβ* silencing and proliferation**

In Met5A and Mero25 we did not observe any significant difference between the proliferation curves of the control and the silenced. The proliferation has been affected, in a statistically significant way, by PDGFRB silencing in Mero14 (p = 0.002) and in IstMes2 (p = 0.0067) cell lines. The proliferation in Mero14 treated with siPDGFRβ decreased by 30% at day 8. In IstMes2 we observed a decrease of proliferation of 34% at day 8.

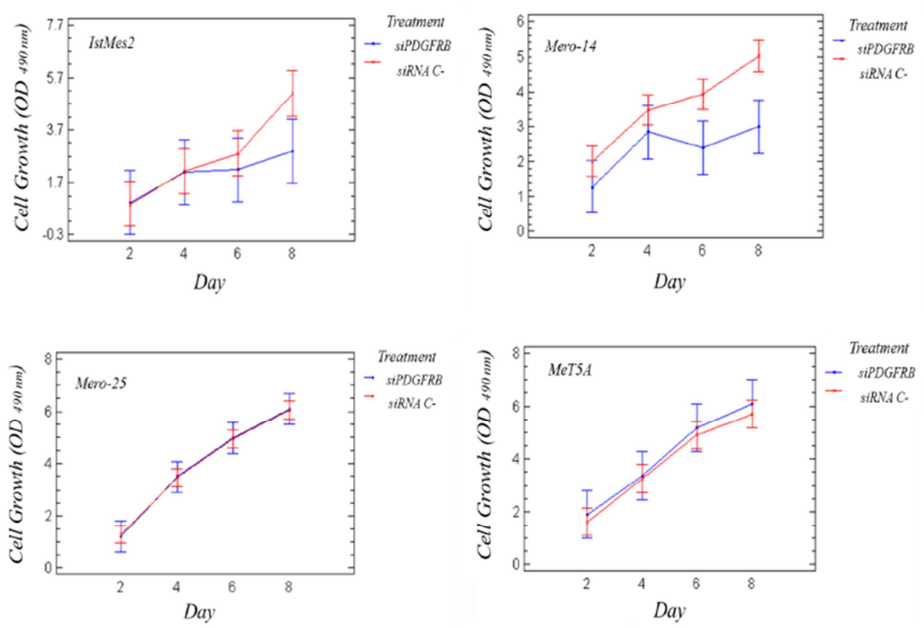


Fig. 43 Effects of *PDGFRβ* on the proliferation: At the top, proliferation assay curves of IstMes2, Mero25 and Met5A cells treated with 50 nM of siCTRL (All star negative siRNA) and si*PDGFRβ*. Mero14 has been treated with 20nM of siCTRL and si*PDGFRβ*, according to the transfection efficiency results. The acquisition of optical density has been made every two days (day 0, 2, 4, 6, 8) starting from the time of transfection (= day 0). Error bars represent SEM of three independent experiments, each done in triplicate.

PDGFRβ silencing and migration

Mero14 cells migration ability has been significantly affected by *PDGFRβ* silencing and showed a decreased migration by 47,24 % (p-value =0,019); we did not observe any difference in Mero25, IstMes2 and in MeT5A (fig. B; p-value =0,723).

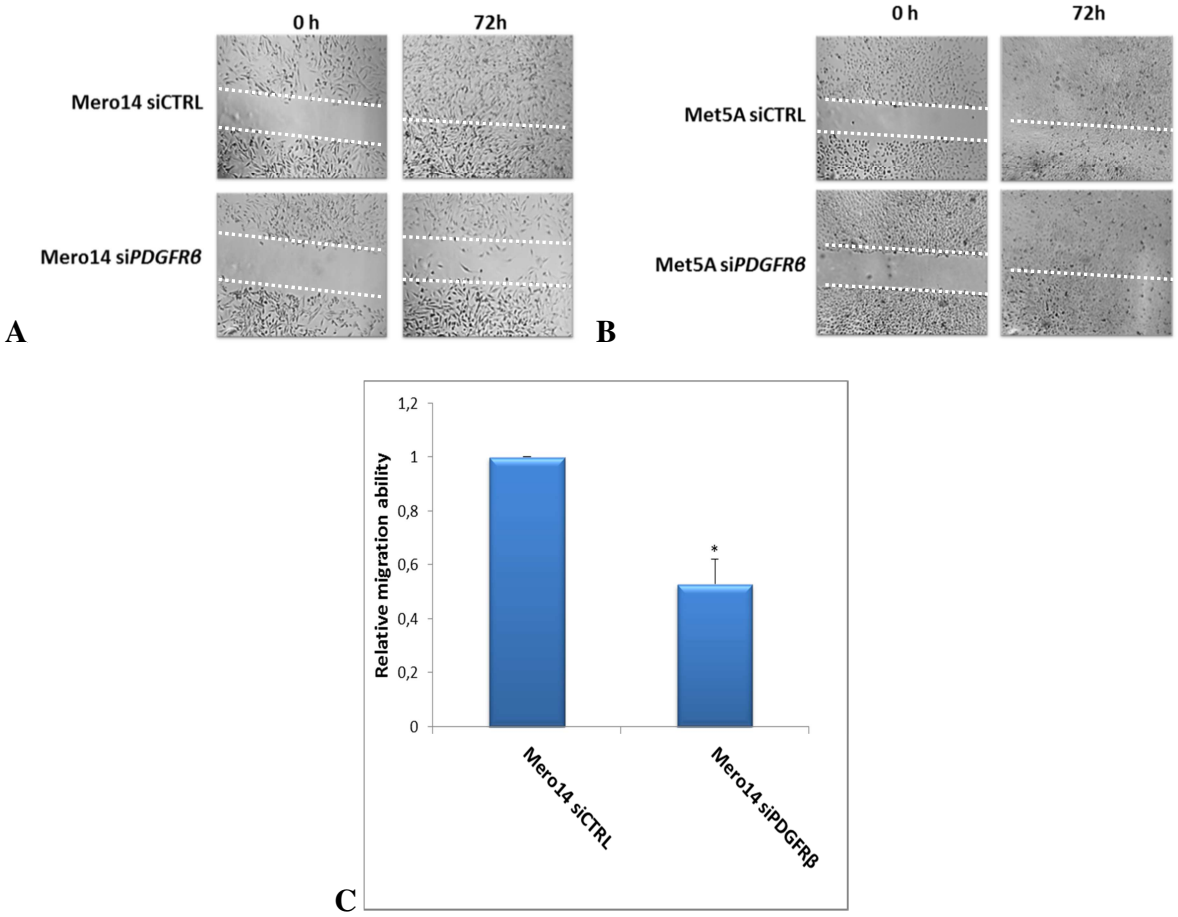


Fig.44 Effects of *PDGFRβ* on migration A on the upper left Mero14 cells treated with 20nM of siCTRL (siRNA C- in picture) at the time of scratch, on the lower left Mero14 cells treated with 20 nM of si*PDGFRB* at the time of scratch, on the right the same cells 72 h after the scratch. **B** on the upper left Met5A cells treated with 50nM of siCTRL (siRNA C- in picture) at the time of scratch, on the lower left Met5A cells treated with 50 nM of si*PDGFRB* at the time of scratch, on the right the same cells 72 h after the scratch. **C** The histogram shows the decreased migration in Mero14 cells after si*PDGFRβ* treatment. Error bars represent SEM of three independent experiments

PDGFRβ silencing and colony formation ability

PDGFRβ silencing significantly affected MPM colony formation ability: Mero-14 (p =0,0029) and IstMes2 cells (p=0,0005) showed a decrease by 80,1% and 86,3% respectively. Mero-25 (p-value =0,107) showed a slight decrease not statistically significant. Interestingly MeT5A did not show any difference.

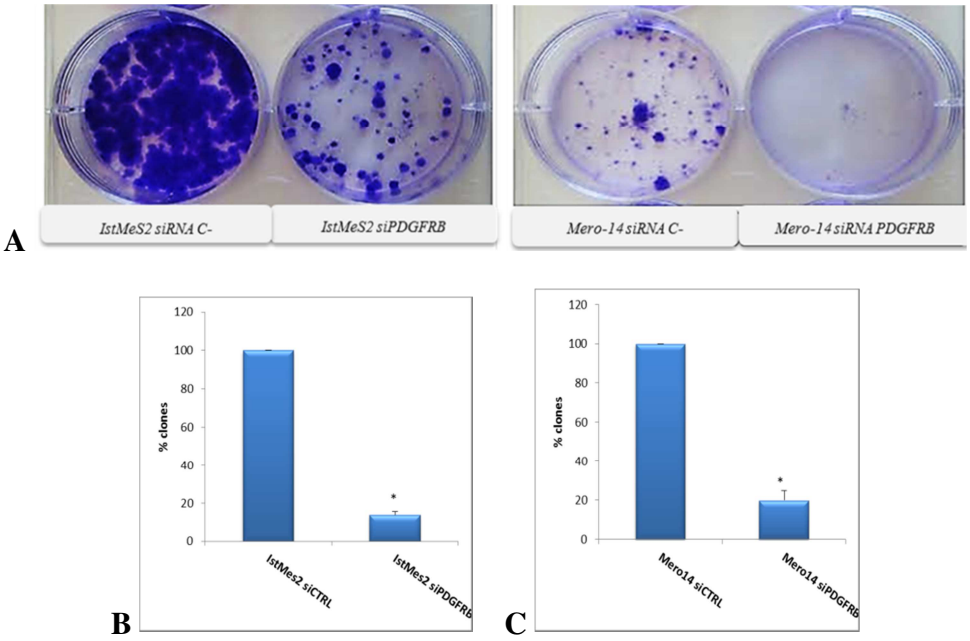


Fig. 45 Effects of *PDGFRβ* on IstMes2 and Mero14 colony formation ability. A Pictures show the IstMes2 cells, silenced with 50nM of siCTRL and si*PDGFRB*, fixed and stained 14 days after treatment and Mero14 cells silenced with 20nM of siCTRL and si*PDGFRB*. **B and C** The histograms show the percentage of clones measured 14 days after silencing. Errors bars are SEM of the percentage fold change from three independent experiments

PDGFRβ silencing and apoptosis

PDGFRβ silencing caused a statistical significant increment of caspase 3/7 activity in two MPM cell lines: Mero14 showed an increment of 62% ($p < 10^{-3}$) and IstMes2 caspase 3/7 activity increased by 34% (p = 0,009). Met5A (p-value=0,345) and Mero25 (p-value=0,604) did not show any phenotypic difference.

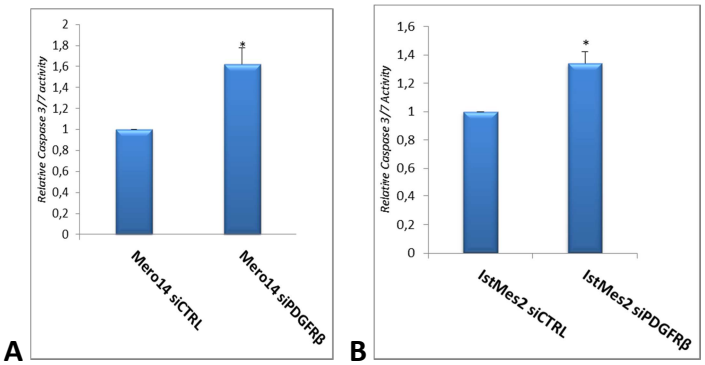


Fig 46. **Effects of *PDGFRB* on caspase 3/7 activity:** Relative fold change of caspase 3/7 activity measured 72h after transfection with 20nM of siCTRL and si*PDGFRβ* for Mero14 (A) cell line and after transfection with 50nM of siCTRL and si*PDGFRβ* for IstMes2 (B). Errors bars are SEM of the fold change from three independent experiments.

PDGFRβ silencing and senescence

The number of senescent cells did not significantly change after si*PDGFRβ* treatment, as shown in picture.

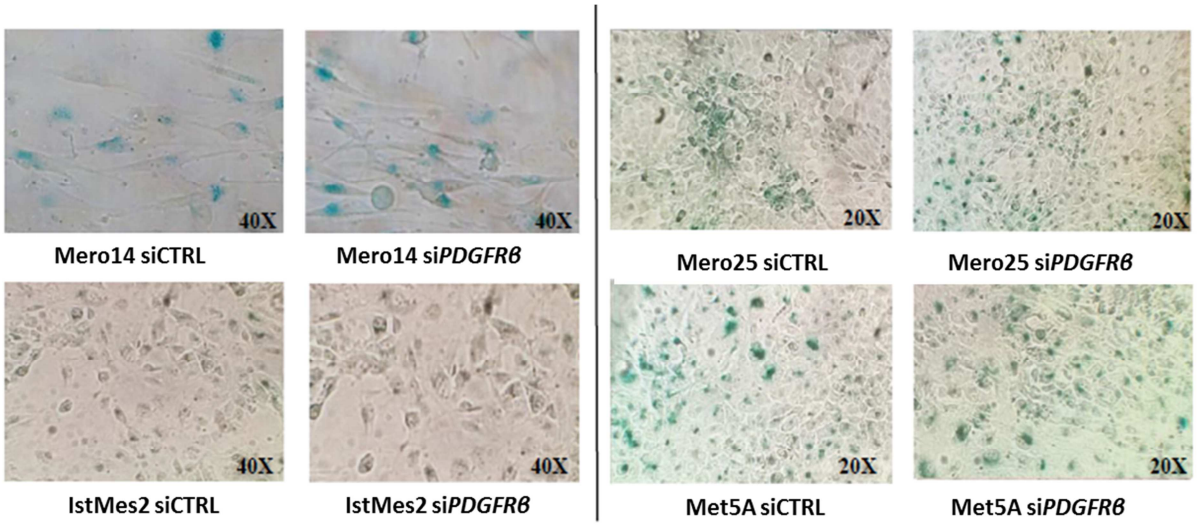


Fig. 47 Effects of *PDGFRB* on senescence: Pictures show Mero14, Mero25, IstMes2 and Met5A cells 5 days after treatment (Mero14 C- = treated with 20nM of siCTRL; Mero14 siRNA PDGFRB = treated with 20nM of siPDGFRB; Mero25 C- = treated with 50nM of siCTRL; Mero25 siRNA PDGFRB = treated with 50nM of siPDGFRB; IstMes2 C- = treated with 50nM of siCTRL; IstMes2 siRNA PDGFRB = treated with 50nM of siPDGFRB; Met5A C- = treated with 50nM of siCTRL; Met5A siRNA PDGFRB = treated with 50nM of siPDGFRB). The ß-galattosidase activity is highlighted by the blue staining of senescent cells.

6.2.7 ASS1 phenotypic analysis

***ASS1*: mRNA and protein levels.**

Only two MPM cell line (Mero25 and IstMes2) showed statistically significant up-regulated levels of *ASS1* mRNA versus Met5A expression

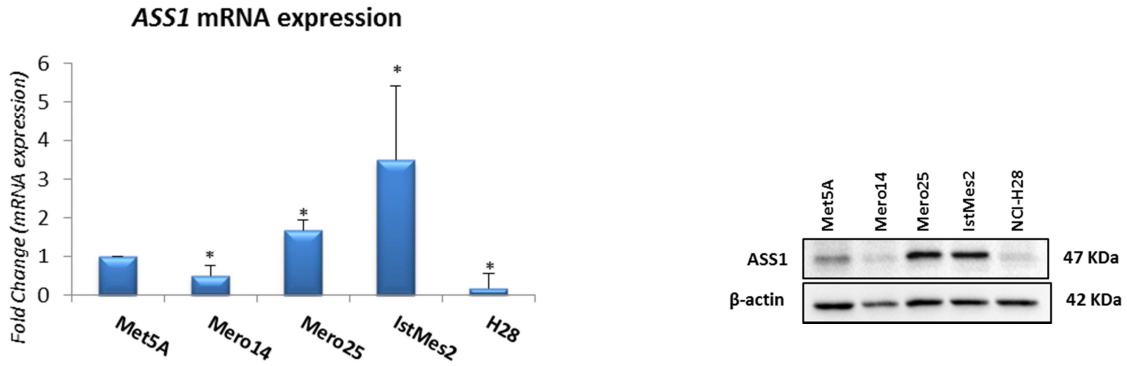


Fig.48 Basal expression level of *ASS1* in four MPM cell lines. On the left, RTqPCR showing fold change of quantitative mRNA levels of *ASS1* measured on MPM cell lines versus MeT-5A cells. Mean of *RPLP0*, *HPRT*, and *TBP* was used for normalization. Errors bars are SEM of the fold change from three independent experiments, each in triplicate. All the MPM cell lines express *ASS1* mRNA but only two MPM cell lines show a significant upregulation compared to *ASS1* levels in Met5A cell line. IstMes2 cells showed the highest expression levels of *ASS1* ($p = 0,029$) compared to Met5A expression levels, followed by Mero25 ($p = 0,0004$). Expression levels in Mero14 ($p = 0,019$) and NCI-H28 ($p = 0,001$) cells were downregulated compared to Met5A levels. On the right, the protein levels of ASS1 on MeT5A, Mero14, Mero25, IstMes2 and NCI-H28 cells. β-Actin was used as loading control. The protein levels were confirmed with two independent experiments.

mRNA and protein expression after *ASS1* silencing

ASS1 silencing has been effective for all the cell lines (in Met5A p= 0,00021; in Mero14 p= 0,002; in Mero25 p= 0,00024; in IstMes2 p= 0,00023) except for the NCI-H28, probably due to the lower expression of ASS1 mRNA in this cell line.

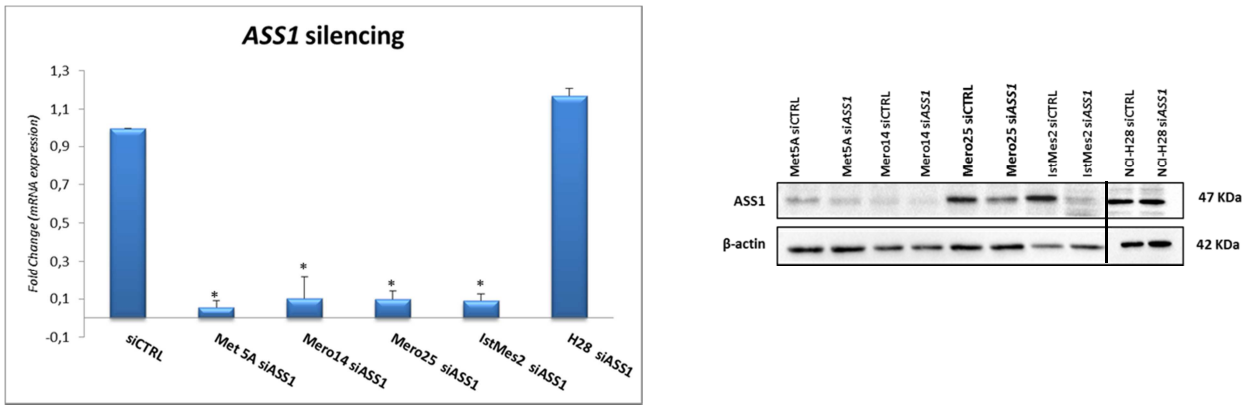
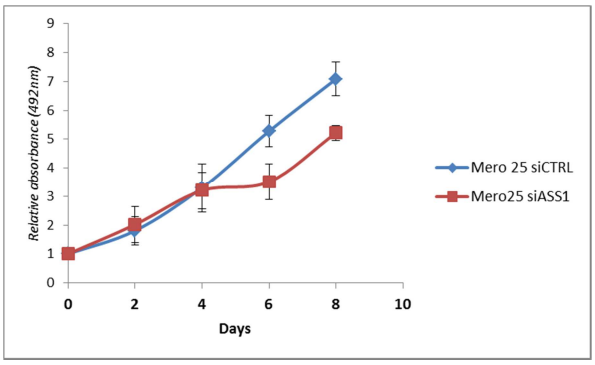


Fig. 49: Silencing of *ASS1*. On the left, RTqPCR showing fold change of quantitative mRNA levels of *ASS1* (72h after transfection) in one mesothelial cell line (Met5A) and four mesothelioma cell lines versus the expression levels observed in the corresponding cell line treated with siCTRL (All Star Negative control siRNA). Mean of RPLP0, HPRT, and TBP was used for normalization. Errors bars are SEM of the fold change from three independent experiments, each in triplicate. On the right, the protein levels of ASS1 after its depletion with ASS1 siRNA versus the control, β-Actin was used as loading control. The protein levels were confirmed with two independent experiments.

ASS1 silencing and proliferation

In Met5A, Mero14 and NCI-H28 we did not observe any significant difference between the proliferation curves of the control and the silenced. The proliferation has been affected, in a statistically significant way, by ASS1 silencing in Mero25 (p = 0,0068) and IstMes2 (p = 0,0022), the two cell lines showing upregulated levels of ASS1 mRNA. The effects of silencing are noticeable from day 6 in both cell lines in all the three experiments performed. The proliferation in Mero25 treated with siASS1 decreased by 46,11% at day 6 and by 38,04% at day 8. A similar trend has been observed in IstMes2 cell line: ASS1 silencing caused a decrease of 38,7% at day 8.

A 

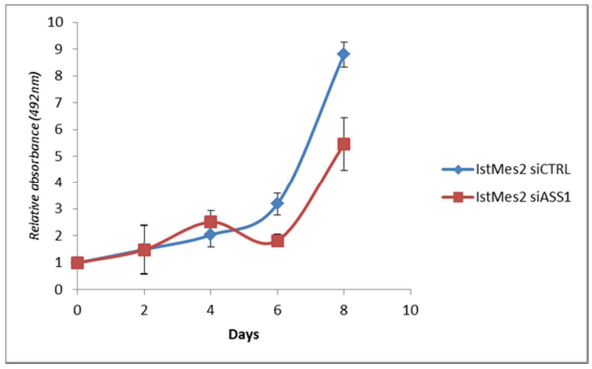
B 

Fig. 50 Effects of *ASS1* on the proliferation: On the left, proliferation assay curves of Mero25 (A) and IstMes2 (B) cells treated with 50 nM of siCTRL and si*ASS1*. The acquisition of optical density has been made every two days (day 0, 2, 4, 6, 8) starting from the time of transfection (= day 0). Error bars represent SEM of three independent experiments, each done in triplicate.

ASS1 silencing and colony formation ability

Only the two cell lines showing upregulated levels of ASS1 mRNA (Mero25 and IstMes2 cell lines) showed a decreased ability in colony formation after ASS1 knockdown; Mero 25 cells showed an average decrease of 31,36% (p = 0,027) and IstMes2 showed an average decrease of % (p = 0,019) (Fig. 51). Mero14 and Met5A did not show any change after *ASS1* silencing.

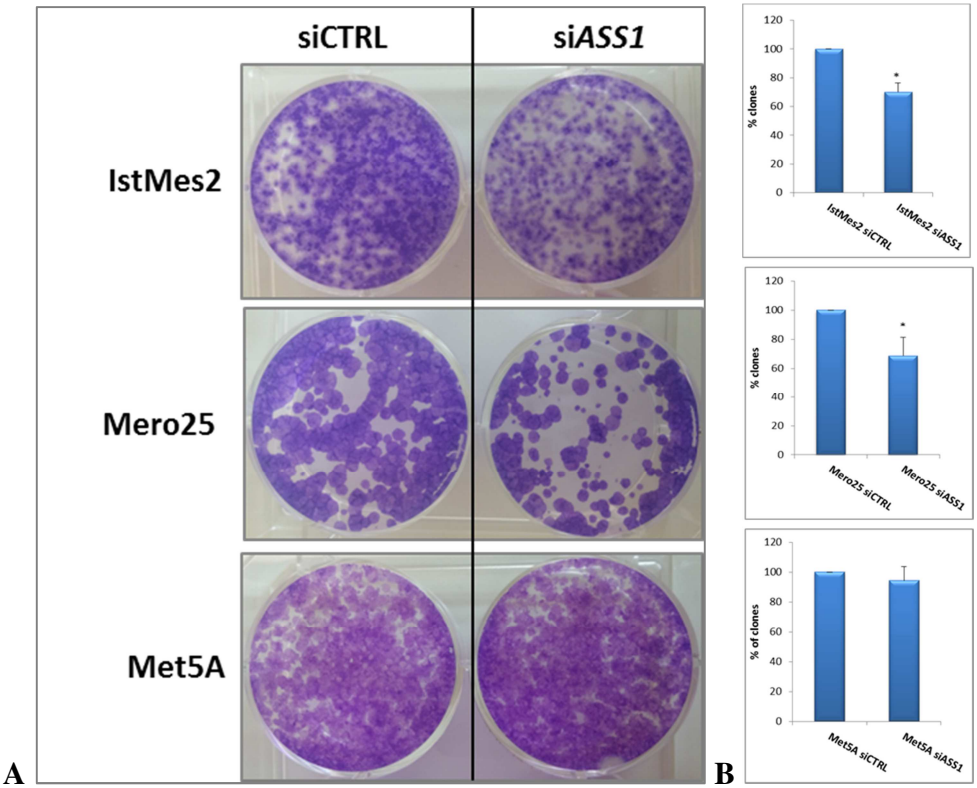


Fig. 51 Effects of *ASS1* on colony formation ability. A Pictures show the IstMes2, Mero25 and Met5A cells, silenced with 50nM of siCTRL and si*ASS1*, fixed and stained 14 days after treatment. **B** The histograms show the percentage of clones measured 14 days after silencing. Errors bars are SEM of the percentage fold change from three independent experiments

***ASS1* silencing and migration**

We did not observe any significant difference in migration ability after ASS1 silencing in none of the cells treated (Met5A, Mero14, Mero25 and IstMes2).

ASS1 silencing and apoptosis

Mero25 cell line showed an increment, not statistically significant (p= 0,08), in caspase activity after treatment with siASS1. In none of the others cells treated (Met5A, Mero14, IstMes2 and NCI-H28) we observed any significant difference in caspase 3/7 activity after ASS1 silencing.

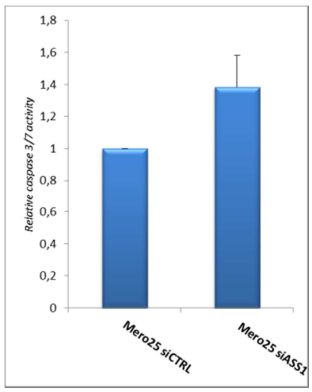


Fig 52. **Effects of *ASS1* on caspase 3/7 activity:** Relative fold change of caspase 3/7 activity measured 72h after transfection with 50nM of siCTRL and si*ASS1*. Errors bars are SEM of the fold change from three independent experiments.

6.2.8 SOD1 phenotypic analysis.

***SOD1*: mRNA and protein levels.**

All the four mesothelioma cell lines analysed showed statistically significant upregulated levels of *SOD1* mRNA compared to Met5A expression levels; the protein levels did not show the same pattern of up-regulation, Met5A showed a high level of SOD1 protein and only NCI-H28 cells showed a comparable high expression.

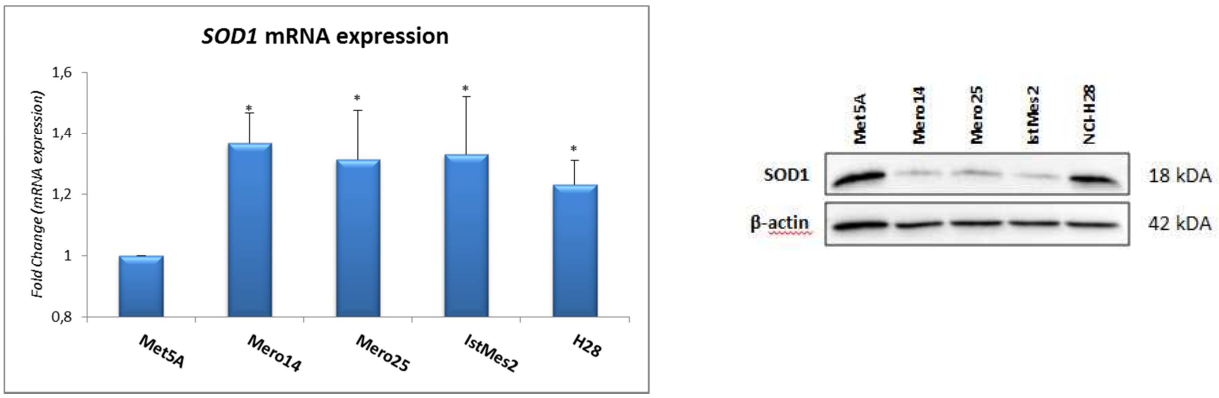


Fig. 53 Basal expression level of *SOD1* in four MPM cell lines. On the left, RTqPCR showing fold change of quantitative mRNA levels of *SOD1* measured on MPM cell lines versus MeT-5A cells. Mean of *RPLP0*, *HPRT*, and *TBP* was used for normalization. Errors bars are SEM of the fold change from three independent experiments, each in triplicate. All the MPM cell lines showed significant upregulated levels of *SOD1* mRNA compared to *SOD1* levels in Met5A cell line. Mero14 cells showed the highest expression levels of *SOD1* ($p = 0,046$) compared to Met5A expression levels, followed by IstMes2 ($p = 0,035$), Mero25 ($p = 0,026$) and NCI-H28 ($p = 0,003$). On the right, the protein levels of SOD1 on MeT5A, Mero14, Mero25, IstMes2 and NCI-H28 cells. β-Actin was used as loading control. The protein levels were confirmed with two independent experiments.

mRNA and protein expression after *SOD1* silencing

SOD1 silencing has been effective for all the cell lines at mRNA level: in Met5A p= 1,9 x 10^{-3}; in Mero14 p= 1,6 x 10^{-4}; in Mero25 p= 7,69 x 10^{-6}; in IstMes2 p= 4,9 x 10^{-4}; in NCI-H28 p= 0,043.

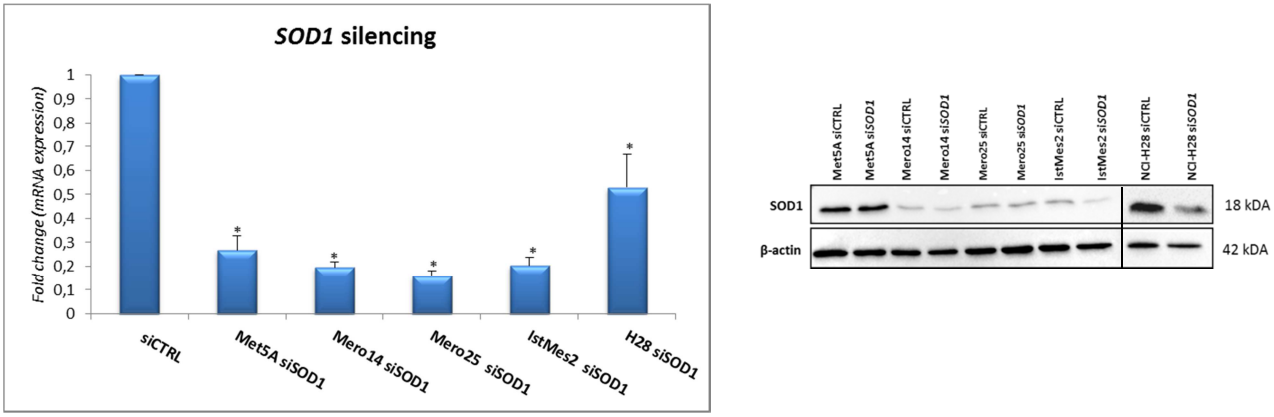


Fig. 54: Silencing of *SOD1*. On the left, RTqPCR showing fold change of quantitative mRNA levels of *SOD1* (72h after transfection) in one mesothelial cell line (Met5A) and four mesothelioma cell lines versus the expression levels observed in the corresponding cell line treated with siCTRL (All Star Negative control siRNA). Mean of RPLP0, HPRT, and TBP was used for normalization. Errors bars are SEM of the fold change from three independent experiments, each in triplicate. On the right, the protein levels of SOD1 after its depletion with SOD1 siRNA versus the control, β-Actin was used as loading control. The protein levels were confirmed with two independent experiments.

SOD1 silencing and proliferation

In Met5A we did not observe any significant difference between the proliferation curves of the control and the silenced. The proliferation has been affected, in a statistically significant way, by SOD1 silencing in Mero25 (p = 0.024), Mero14 (p = 0,015) and NCI-H28 (p = 0,0031) cell lines. The effects of silencing are noticeable from day 6 in these cell lines in all the three experiments performed. The proliferation in Mero25 treated with siSOD1 decreased by 32,7% at day 8. In Mero14 we observed a decrease of proliferation of 27,52% at day 8. The proliferation rate of NCI-H28 cells silenced with siSOD1 dropped at day 8 by 27,95%.

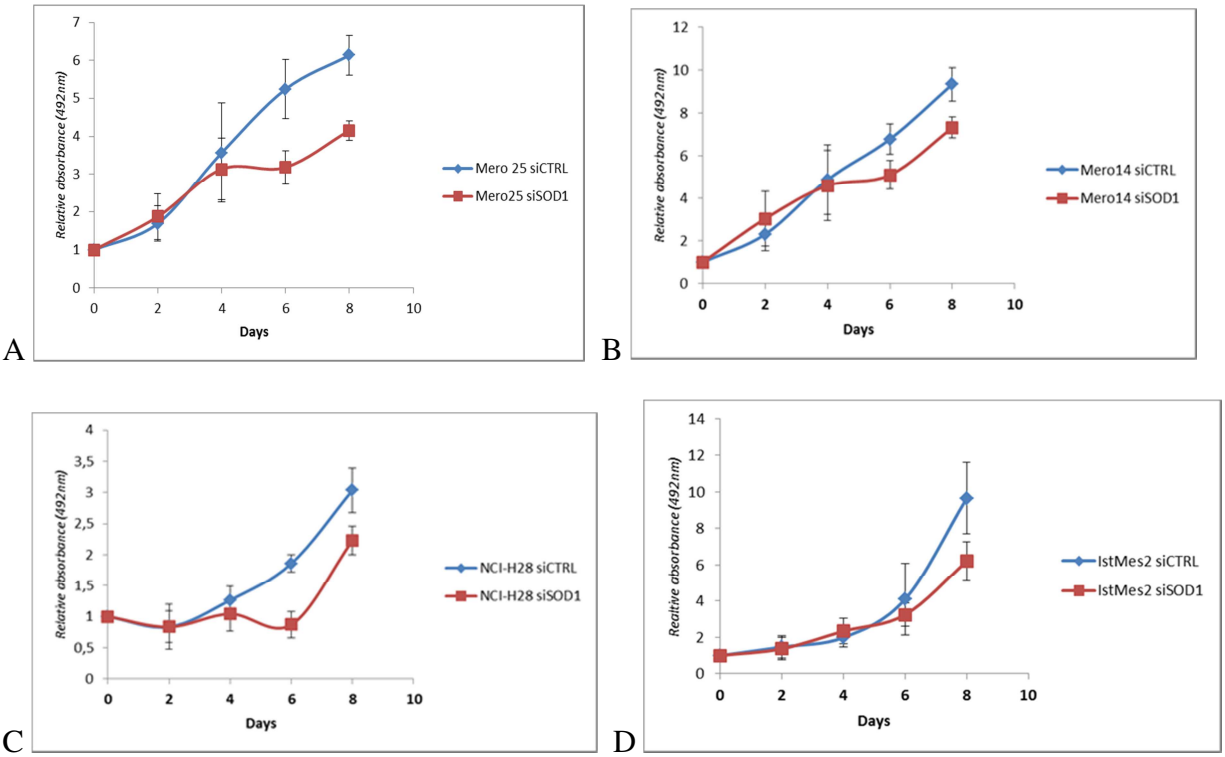


Fig. 55 Effects of *SOD1* on the proliferation: On the left, proliferation assay curves of Mero25 (A), NCI-H28 (C) and IstMes2 (D) cells treated with 50 nM of siCTRL (All star negative siRNA) and si*SOD1*. Mero14 (B) has been treated with 20nM of siCTRL and si*SOD1*, according to the transfection efficiency results. The acquisition of optical density has been made every two days (day 0, 2, 4, 6, 8) starting from the time of transfection (= day 0). Error bars represent SEM of three independent experiments, each done in triplicate.

SOD1 silencing and migration

We did not observe any significant difference in migration ability after SOD1 silencing.

SOD1 silencing and colony formation ability

Only the colony formation ability of Mero25 cells has been affected in a statistically significant way, by *SOD1* knockdown ($p = 0{,}021$); the average decrease observed in three independent experiment was of 44,37% (Fig. 56). Met5A, Mero14 and IstMes2 did not show a significative change in colony formation ability after *SOD1* silencing.

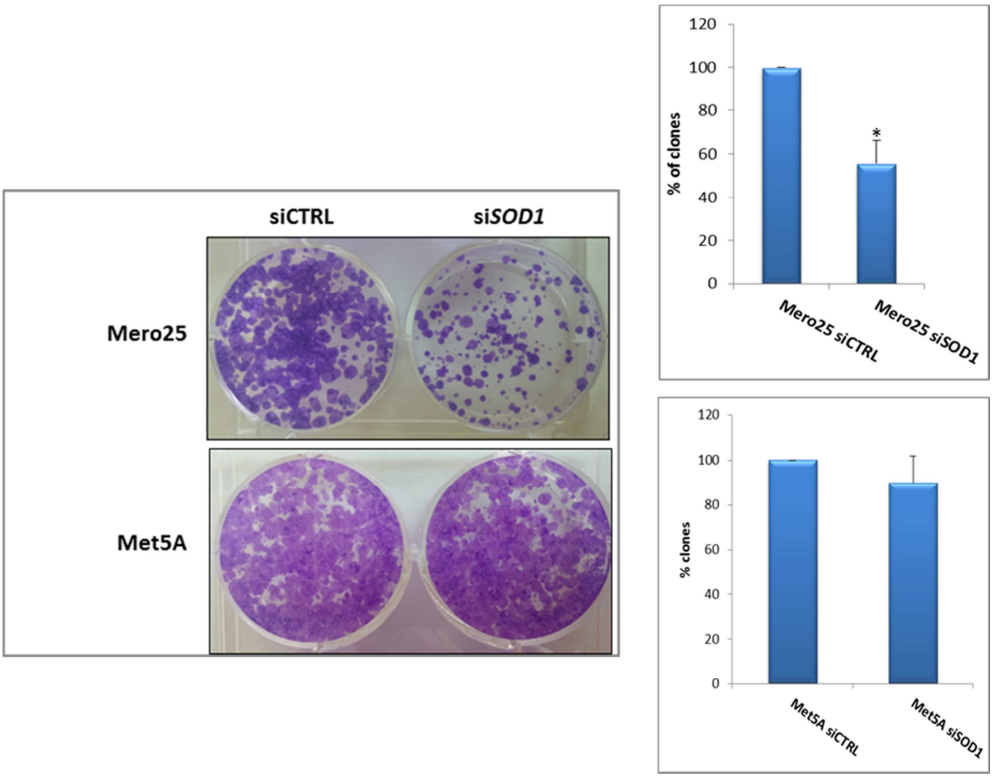


Fig. 56 Effects of *SOD1* on colony formation ability. A Pictures show the Mero25 and Met5A cells, silenced with 50nM of siCTRL and si*SOD1*, fixed and stained 14 days after treatment. **B** The histograms show the percentage of clones measured 14 days after silencing. Errors bars are SEM of the fold change from three independent experiments

SOD1 silencing and apoptosis

SOD1 silencing caused a statistical significant increment of caspase 3/7 activity in all the cell lines treated: Met5A showed an increment of 62,84% (p = 0,0022), in Mero14 caspase 3/7 activity increased by 166,88% (p = 0,014), in Mero25 the increment was of 87,25% (p = 0,0073), in IstMes2 was of 42,64% (p = 0,05) and in NCI-H28 was of 121,54% (p = 0,016).

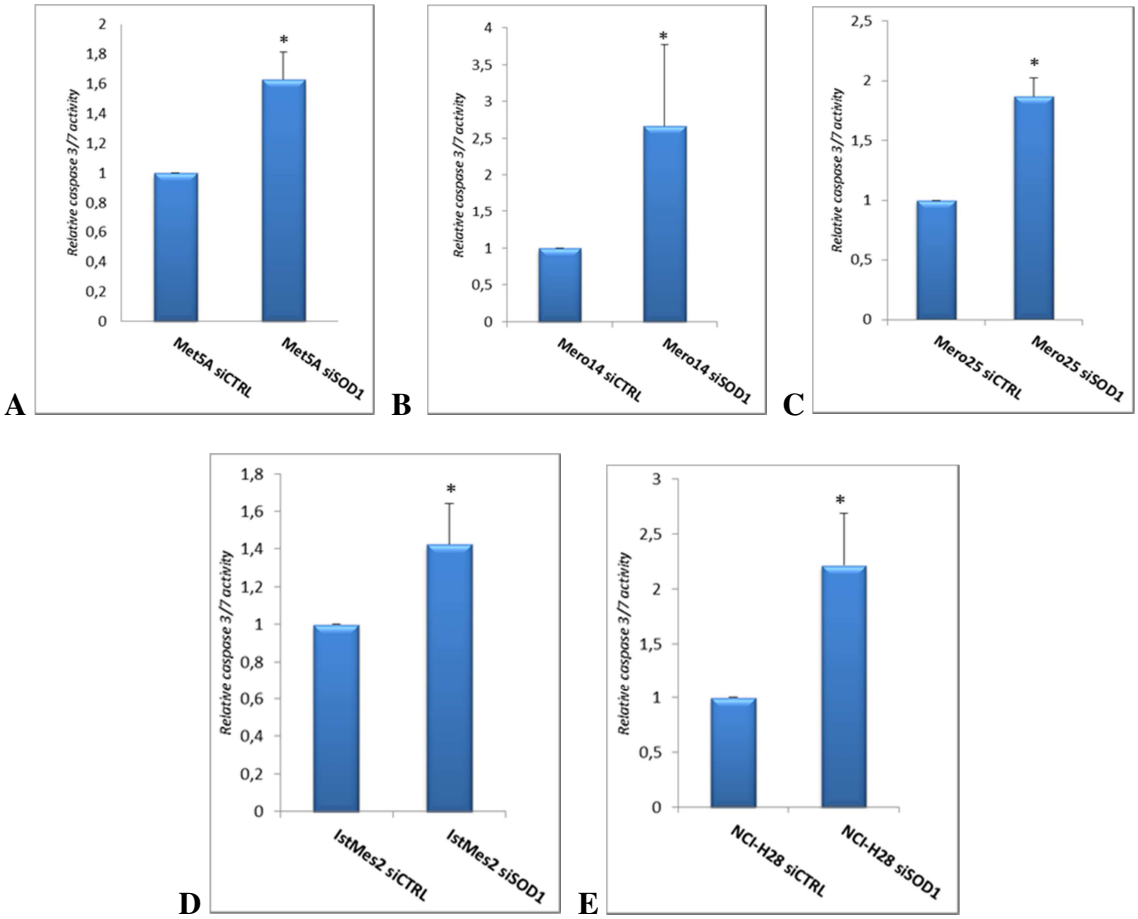


Fig 57. **Effects of SOD1 on caspase 3/7 activity:** Relative fold change of caspase 3/7 activity measured 72h after transfection with 50nM of siCTRL and si*SOD1*for Met5A (A), Mero25 (C), IstMes2 (D) and NCI-H28 (E) cell lines; and after transfection with 20nM of siCTRL and si*SOD1* for Mero14 (B) cell line. Errors bars are SEM of the fold change from three independent experiments.

6.2.9 *RAN* phenotypic analysis

***RAN*: mRNA and protein levels.**

Three of the four mesothelioma cell lines analysed showed statistically significant upregulated levels of *RAN* mRNA compared to Met5A expression levels (Mero14 p = 0,037; Mero25 p = 0,04; IstMes2 p = 0,047).

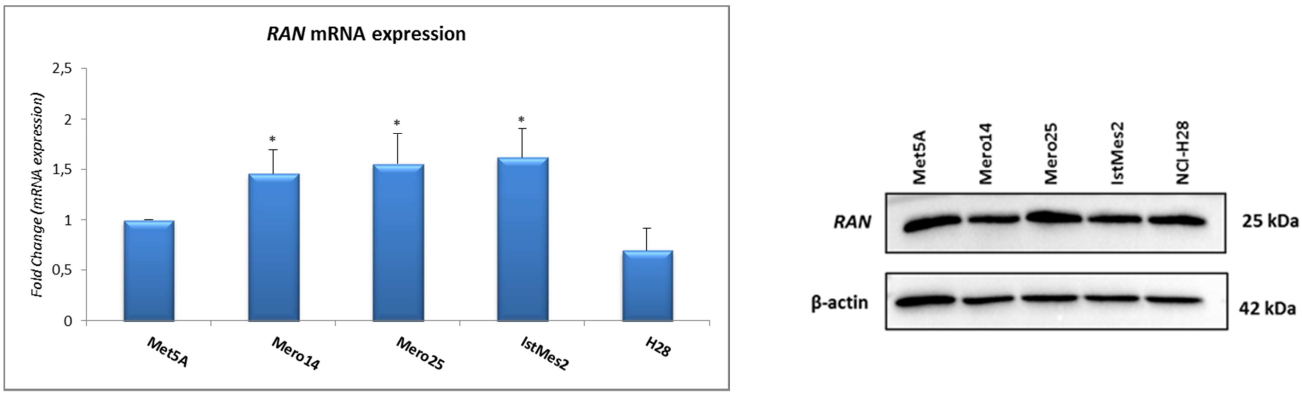


Fig. 58 Basal expression level of *RAN* in four MPM cell lines. On the left, RTqPCR showing fold change of quantitative mRNA levels of *RAN* measured on MPM cell lines versus MeT-5A cells. Mean of *RPLP0*, *HPRT*, and *TBP* was used for normalization. Errors bars are SEM of the fold change from three independent experiments, each in triplicate. Mero14, Mero25 and IstMes2 cell lines showed statistically significant up-regulated levels of *RAN* mRNA compared to Met5A expression levels (Mero14 p = 0,037; Mero25 p = 0,04; IstMes2 p = 0,047). NCI-H28 cell line expressed *RAN* mRNA levels lower than Met5A levels. On the right, the protein levels of RAN on MeT5A, Mero14, Mero25, IstMes2 and NCI-H28 cells. β-Actin was used as loading control. The protein levels were confirmed with two independent experiments.

mRNA and protein expression after *RAN* silencing

RAN silencing has been effective, at mRNA level, for all the cell lines except for NCI-H28 cells in which we obtained a not statistically significant average decrease of 26,51% (p = 0,23). In Met5A the decrease of RAN mRNA levels has been of 82,71% (p= 0,006), in Mero14 of 93,23% (p= 0,0004), in Mero25 of 76,71% (p= 0,01) and in IstMes2 of 89,89% (p= 0,0004).

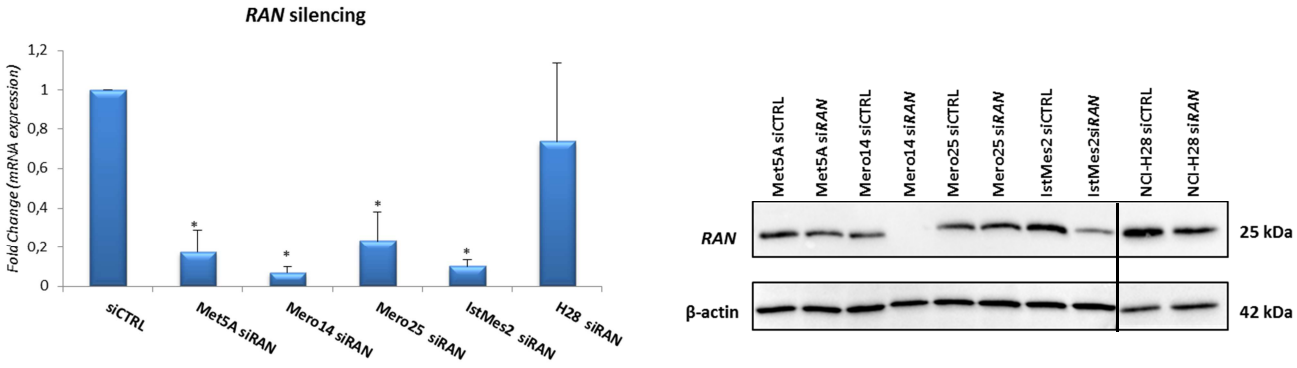


Fig. 59: Silencing of *RAN*. On the left, RTqPCR showing fold change of quantitative mRNA levels of *RAN* (72h after transfection) in one mesothelial cell line (Met5A) and four mesothelioma cell lines versus the expression levels observed in the corresponding cell line treated with siCTRL (All Star Negative control siRNA). Mean of RPLP0, HPRT, and TBP was used for normalization. Errors bars are SEM of the fold change from three independent experiments, each in triplicate. On the right, the protein levels of RAN, 72h after its depletion with *RAN* siRNA, versus the control; β-Actin was used as loading control. The protein levels were confirmed with two independent experiments.

RAN silencing and proliferation

In Met5A and NCI-H28 cells we did not observe any significant difference between the proliferation curves of the control and the silenced. The proliferation has been affected, in a statistically significant way, by RAN silencing in Mero14 ($p < 10^{-4}$), Mero25 (p = 0.0009) and IstMes2 (p = 0.003) cell lines. The effects of silencing are noticeable from day 6 in these cell lines in all the three experiments performed. The proliferation in Mero14 treated with siRAN decreased by 76,82% at day 8. In Mero25 we observed a decrease of proliferation of 57,6% at day 8. The proliferation rate of IstMes2 cells silenced with siRAN dropped at day 8 by 58,97%.

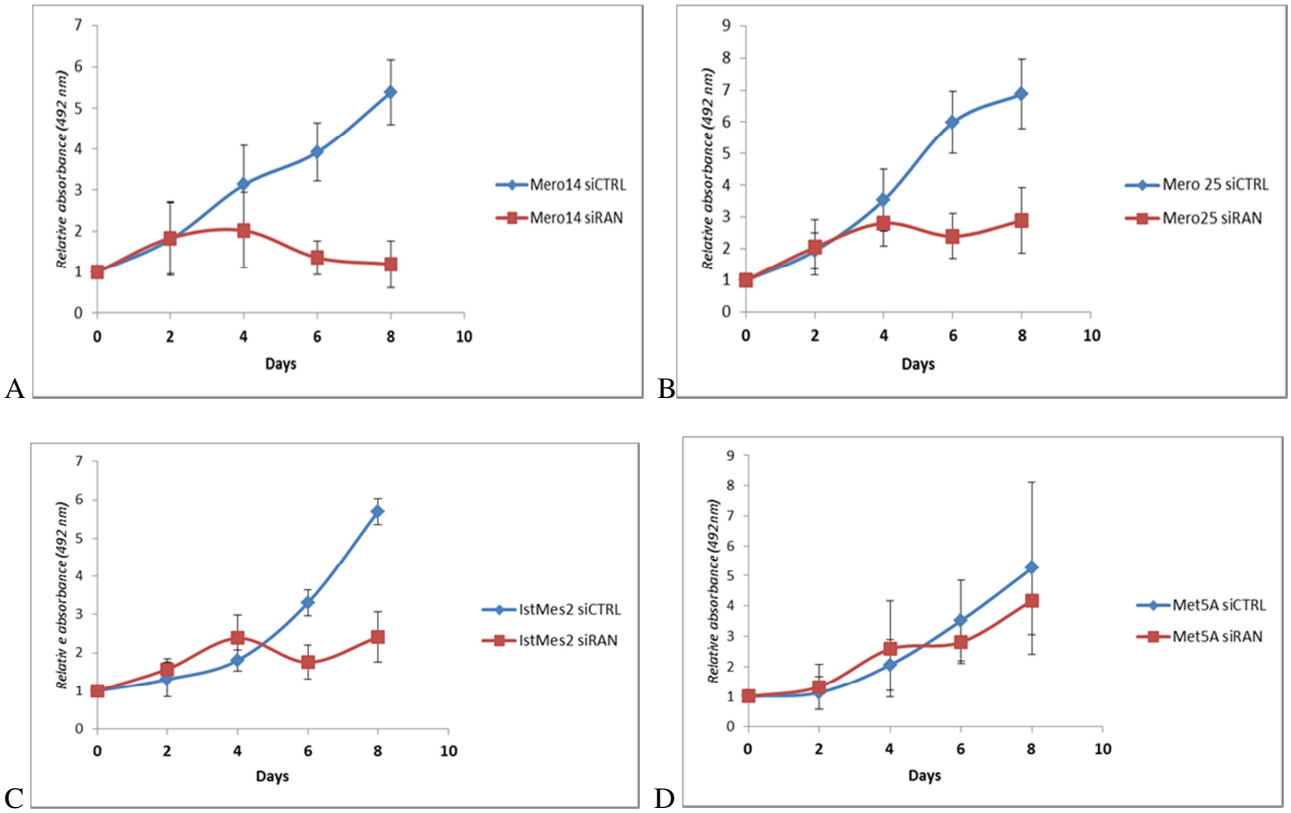
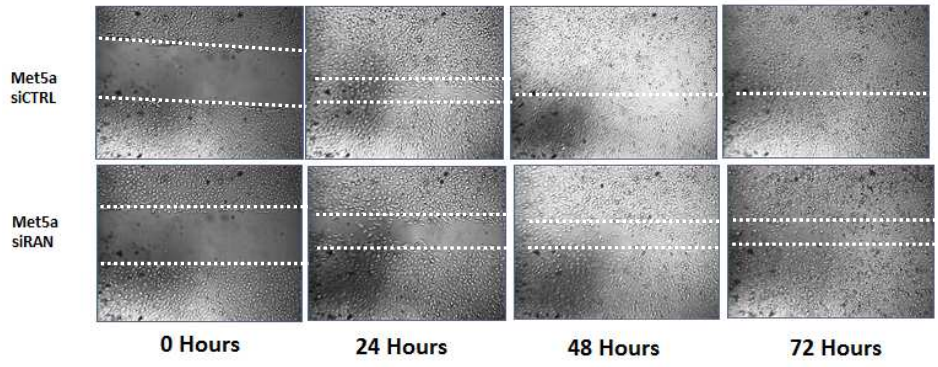


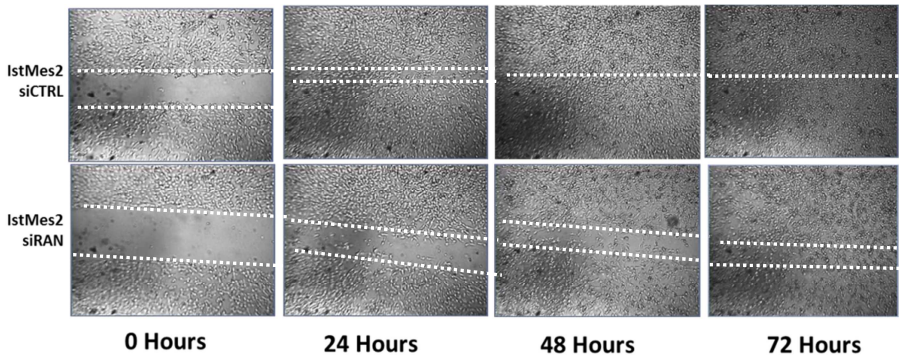
Fig. 60 Effects of *RAN* on the proliferation: On the left, proliferation assay curves of Mero25 (D), IstMes2 (G) and Met5A (L) cells treated with 50 nM of siCTRL (All star negative siRNA) and si*RAN*. Mero14 (A) has been treated with 20nM of siCTRL and si*RAN*, according to the transfection efficiency results. The acquisition of optical density has been made every two days (day 0, 2, 4, 6, 8) starting from the time of transfection (= day 0). Error bars represent SEM of three independent experiments, each done in triplicate.

RAN silencing and migration

After RAN silencing we observe a decrease of migration ability in Met5A (43,5%) and in IstMes2 (20,22%) at 24h. IstMes2 cells treated with si*RAN* showed, at 72h, an increased number of dead cells compared to the control; while the viability of Met5A cells seems not to be affected.



A



B

Fig. 61 Effects of *RAN* on migration A Met5A cells treated with 50nM of siCTRL, while at the bottom Met5A cells treated with 50 nM of si*RAN;* the acquisition has been made every 24h (0, 24, 48, 72 Hours) starting from the time of scratch (= 0 Hours). This is a representative image of one of the three independent experiments performed.**B** IstMes2 cells treated with 50nM of siCTRL , while at the bottom IstMes2 cells treated with 50 nM of si*RAN*; the acquisition has been made every 24h (0, 24, 48, 72 Hours) starting from the time of scratch (= 0 Hours).

RAN silencing and colony formation ability

Met5A cells, silenced with siRAN, were not significantly (p =0,08) affected by the treatment, while the MPM cell lines showed a greater response to RAN silencing with higher percentages of decrease: for Mero14 was 98,92% (p =4,7x10^{-5}), for Mero25 was 76,2% (p = 0,016) and for Istmes2 was 70,75% (p = 0,03).

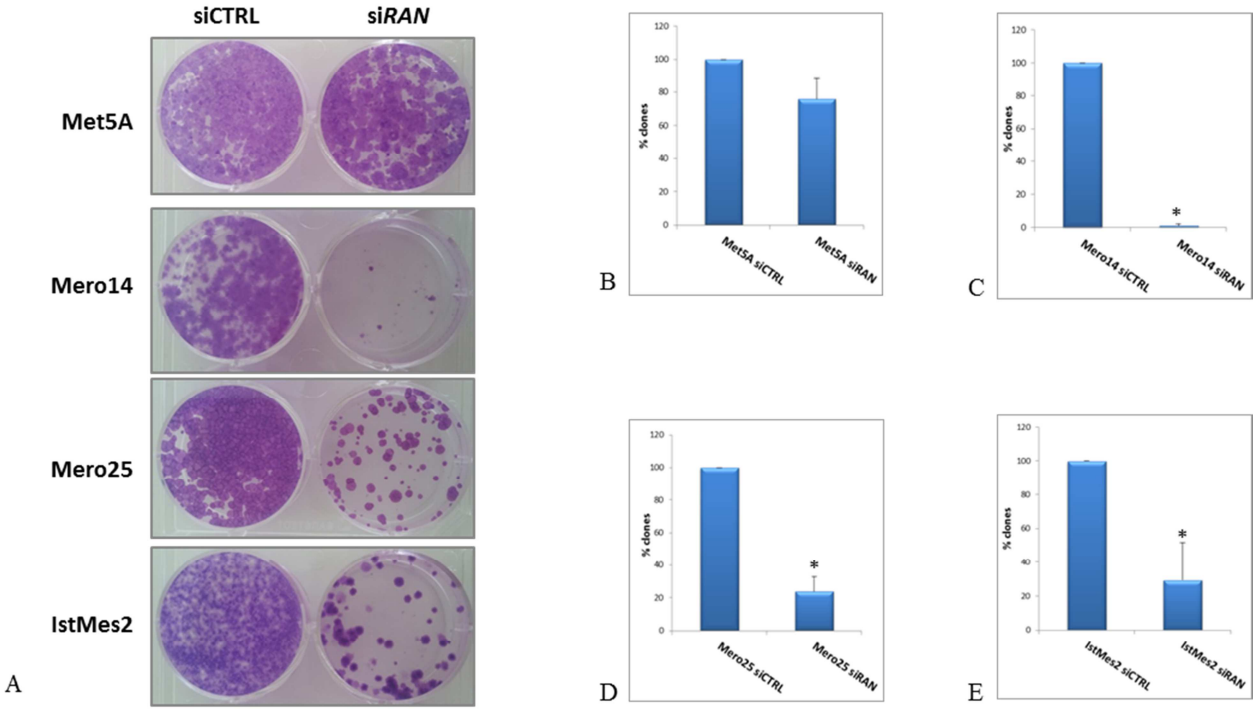


Fig.62:Effects of RANsilencing in the colony formation ability: A Pictures show the Met5A, Mero25 and IstMes2 cells, silenced with 50nM of siCTRL and si*SOD1* and Mero14 cells, silenced with 20nM of siCTRL and si*SOD1* fixed and stained 14 days after treatment. **B, C, D, E)** The histograms show the percentage of clones measured 14 days after silencing. Errors bars are SEM of the fold change from three independent experiments

RAN silencing and apoptosis

RAN silencing caused a statistical significant increment of caspase 3/7 activity in all the MPM cell lines; the non-malignant Met5A cell line showed a slight increase of 17,29% not statistically significant (p = 0,13). Mero14 caspase 3/7 activity increased by 66,26% (p = $4x10^{-4}$), in Mero25 the increment was of 43,95% (p = 0,017), in IstMes2 was of 114% (p = 0,01) and in NCI-H28 was of 64,36% (p = 0,046).

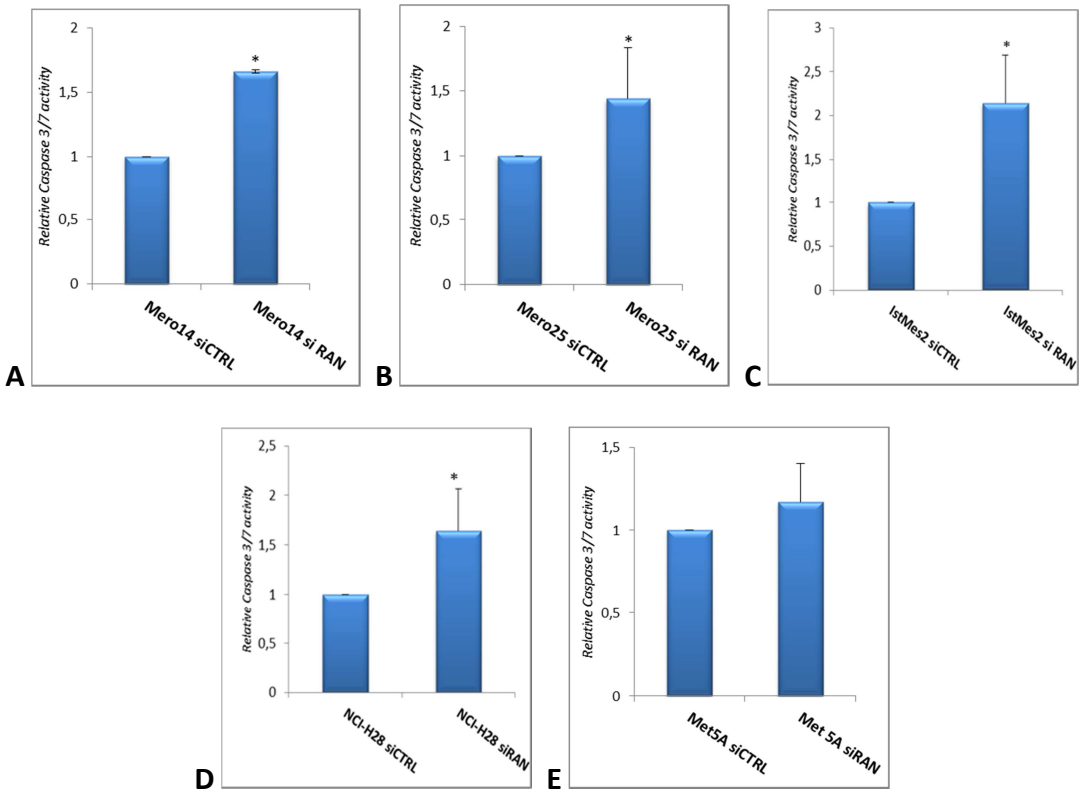
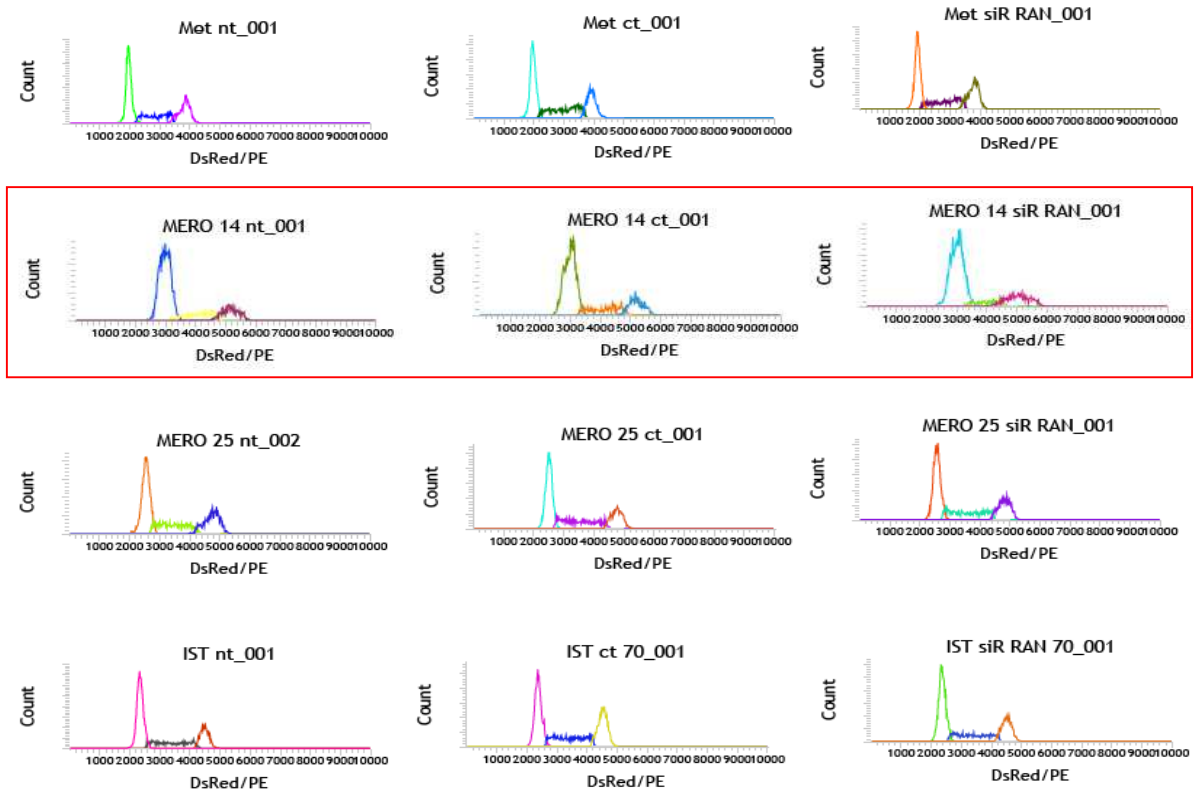


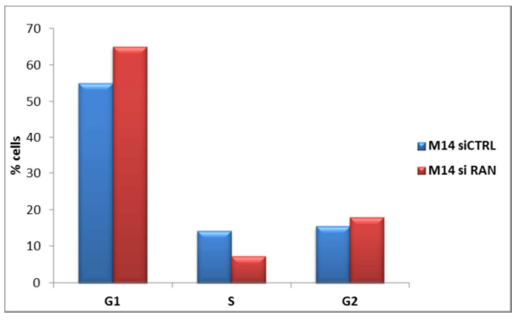
Fig 63. **Effects of *RAN* silencing on caspase 3/7 activity:** Relative fold change of caspase 3/7 activity measured 72h after transfection with 50nM of siCTRL and si*RAN* for Mero25 (B), IstMes2 (C), NCI-H28 (D) and Met5A (E) cell lines; and after transfection with 20nM of siCTRL and si*RAN* for Mero14 (A) cell line, according to the transfection efficiency results. Errors bars are SEM of the fold change from three independent experiments.

RAN silencing and cell cycle

The effect of *RAN*-silencing on the progression of cell cycle was evaluated through flow cytometry analysis. The preliminary analysis performed shows that in Mero14 cell line, si*RAN* induces a decrease in the percentage of cells in S phase, halving the proportion of cells compared to the control, and an increase of cells in G1 phase. This suggests a growth-promotion role of RAN in Mero14 cells. No significant effects were detected on Met5A, Mero-25 and IstMes2 cells.



A



B

Fig.64 Effects of *RAN* silencing on cell cycle: (A) Analysis of the cell cycle of Met5A (Met), Mero14, Mero25 and IstMes2 cells. The analysis has been performed in non-treated cells (nt), in cells treated with siCTRL (ct) and in cells treated with si*RAN*. (B) Histogram shows the distribution of Mero14 cells treated with 20nM of siCTRL and 20nM of si*RAN*. *RAN* silencing increased the proportion of cells in G0/G1 phase and halved the percentage of cells in S phase.

6.2.10 *CDH11* phenotypic analysis

CDH11: mRNA and protein levels.

One of the four mesothelioma cell lines analysed showed statistically significant upregulated levels of *CDH11* mRNA compared to Met5A expression levels (Mero25 fold change = 3,7; p = 0,032). IstMes2 showed a slight upregulation not statistically significant. Mero14 and NCI-H28 cells did not express *CDH11* mRNA. We did not observe the same pattern of up-regulation at protein level: Mero14 and IstMes2 cell lines showed higher levels compared to Met5A.

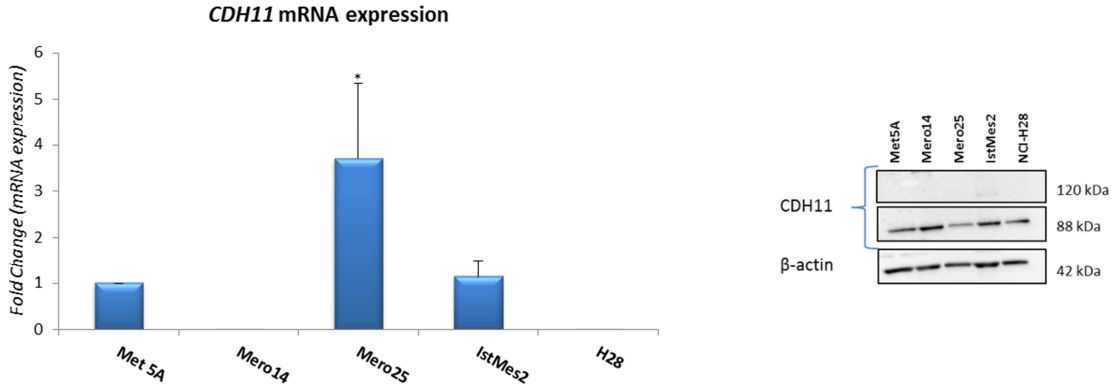


Fig.65 Basal expression level of *CDH11* in four MPM cell lines. On the left, RTqPCR showing fold change of quantitative mRNA levels of *CDH11* measured on MPM cell lines versus MeT-5A cells. Mean of *RPLP0*, *HPRT*, and *TBP* was used for normalization. Errors bars are SEM of the fold change from three independent experiments, each in triplicate. Only Mero25 showed statistically significant up-regulated levels of *CDH11* mRNA compared to Met5A expression levels. Mero14 and NCI-H28 cell lines did not express *CDH11* mRNA.

mRNA and protein expression after *CDH11* silencing

CDH11 silencing has been effective, at mRNA level, for all the cell lines. In Met5A the decrease of CDH11 mRNA levels has been of 86,48 % (p= 0,003), in Mero25 of 82,36% (p= 0,003) and in IstMes2 of 64,07% (p= 0,014). While, at protein level, only Mero25 and NCI-H28 showed a decrement of CDH11 protein 72h after the treatment with si*CDH11*.

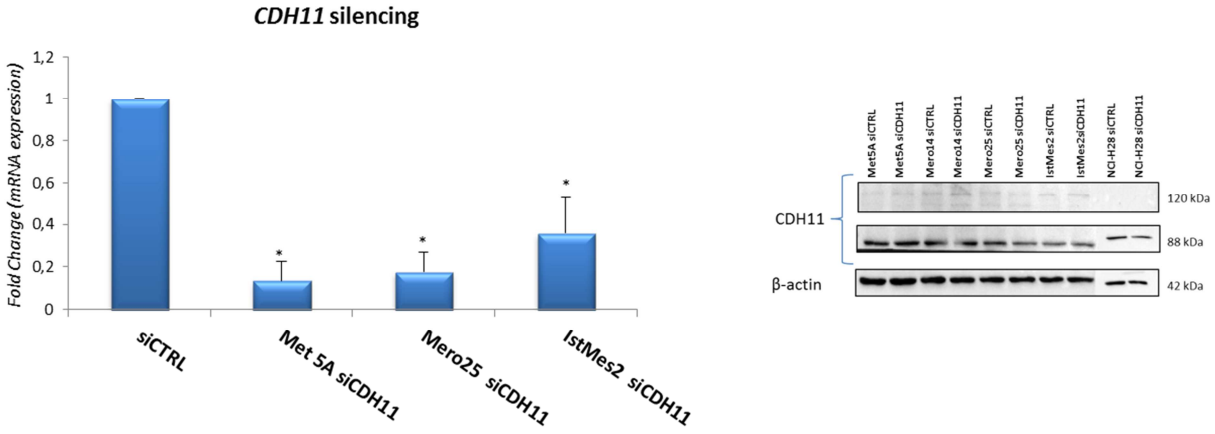


Fig. 66: Silencing of *CDH11*. On the left, RTqPCR showing fold change of quantitative mRNA levels of *CDH11* (72h after CDH11 transfection) in one mesothelial cell line (Met5A) and two mesothelioma cell lines versus the expression levels observed in the corresponding cell line treated with siCTRL (All Star Negative control siRNA). Mean of RPLP0, HPRT, and TBP was used for normalization. Errors bars are SEM of the fold change from three independent experiments, each in triplicate.

CDH11 silencing and proliferation

The proliferation rate of all the cell line treated has not been affected by si*CDH11* treatment.

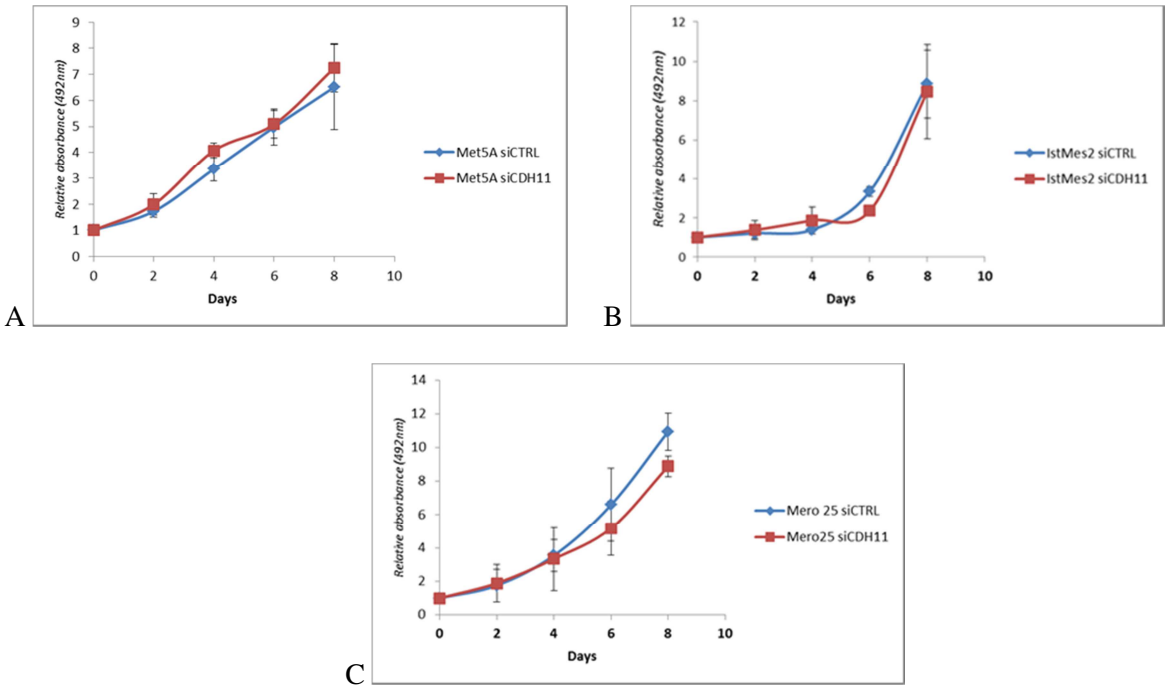


Fig. 67 Effects of *CDH11* on the proliferation: Proliferation assay curves of Met5A (A), Mero25 (B), and IstMes2 (C) cells treated with 50 nM of siCTRL and si*CDH11*. The acquisition of optical density has been made every two days (day 0, 2, 4, 6, 8) starting from the time of *CDH11* transfection (= day 0). Error bars represent SEM of three independent experiments, each done in triplicate.

CDH11 silencing and migration

CDH11 knockdown did not affect the migration ability of any of the cells treated.

CDH11 silencing and colony formation ability

CDH11 knockdown did not affect the colony formation ability of any of the cells treated.

CDH11 silencing and apoptosis

CDH11 silencing caused a statistical significant increment of caspase 3/7 activity in Mero25 while the non-malignant Met5A cell line did not show any change in caspase 3/7 activity. Mero25 caspase 3/7 activity increased by 53,86% (p = 0,007), in IstMes2 we did not observe any significant increment.

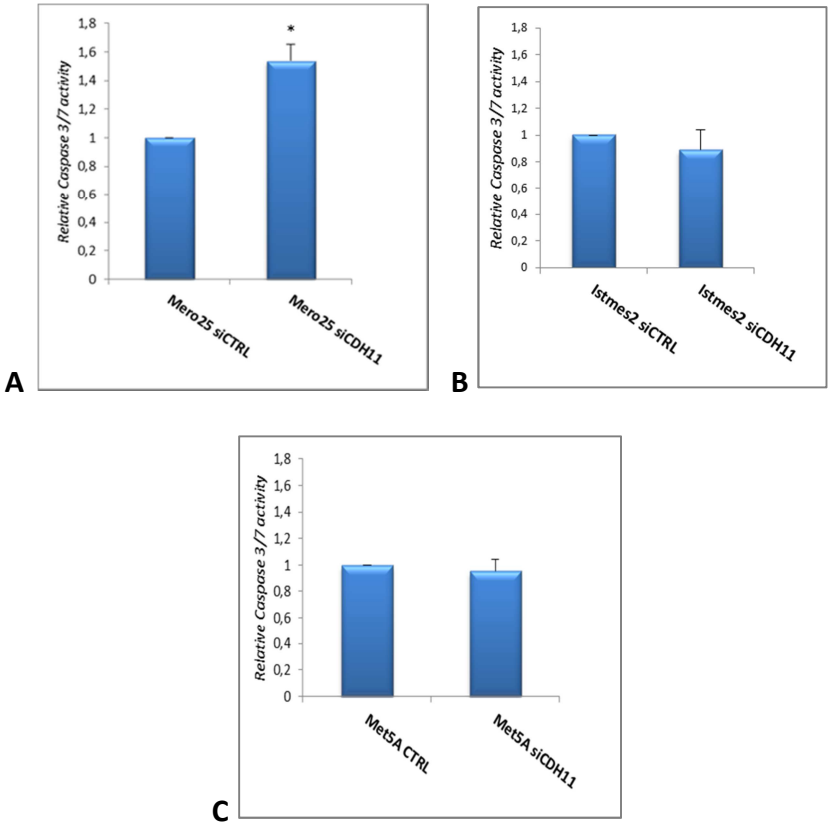


Fig 68. **Effects of *CDH11* silencing on caspase 3/7 activity** Relative fold change of caspase 3/7 activity measured 72h after *CDH11* transfection with 50nM of siCTRL and si*CDH11* for Mero25 (A), IstMes2 (B) and Met5A (C) cell lines. Errors bars are SEM of the fold change from three independent experiments.

6.2.11 *IMP3* phenotypic analysis

***IMP3*: mRNA and protein levels.**

Three MPM cell line showed statistically significant up-regulated levels of *IMP3* mRNA versus Met5A expression (Mero14, p = 0,041; IstMes2, p = 0,03; NCI-H28, p = 0,04). Mero25 cells showed a statistically significant downregulation versus Met5A levels (p = 0,017). Protein expression analysis confirmed the upregulations in Mero14 and in IstMes2 and the downregulation in Mero25.

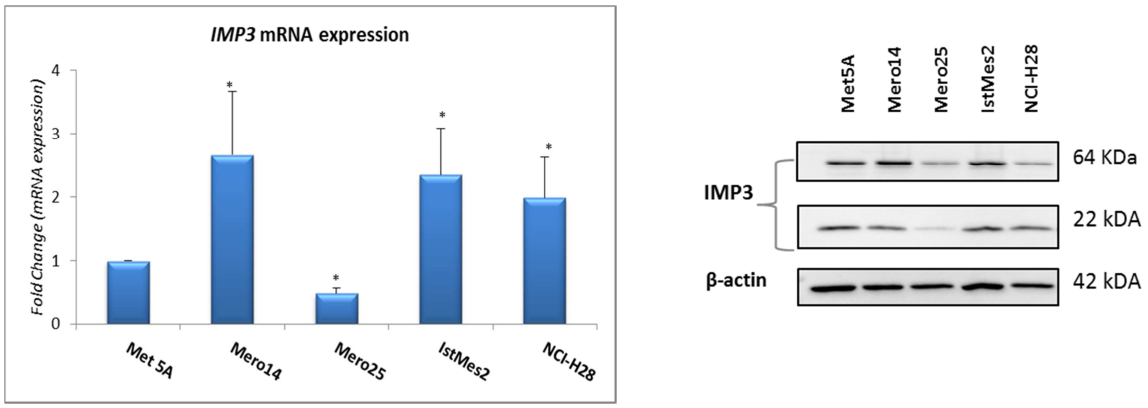


Fig.69 Basal expression level of *IMP3* in four MPM cell lines. On the left, RTqPCR showing fold change of quantitative mRNA levels of *IMP3* measured on MPM cell lines versus MeT-5A cells. Mean of *RPLP0*, *HPRT*, and *TBP* was used for normalization. Errors bars are SEM of the fold change from three independent experiments, each in triplicate. All the MPM cell lines express *IMP3* mRNA but only two MPM cell lines show a significant upregulation compared to *IMP3* levels in Met5A cell line. IstMes2 cells showed the highest expression levels of *IMP3* (p = 0,029) compared to Met5A expression levels, followed by Mero25 (p = 0,0004). Expression levels in Mero14 (p = 0,019) and NCI-H28 (p = 0,001) cells were downregulated compared to Met5A levels. On the right, the protein levels of IMP3 on MeT5A, Mero14, Mero25, IstMes2 and NCI-H28 cells. β-Actin was used as loading control. The protein levels were confirmed with two independent experiments.

mRNA and protein expression after *IMP3* silencing

IMP3 silencing was effective for all the cell lines: at mRNA level, downregulation versus the siCTRL was statistically significant for three MPM cell lines (decrease of 73,52% in Mero14, p= 0,0009; decrease of 41,72% in Mero25, p= 0,002; decrease of 76,53% in IstMes2, p= 0,007) but not for Met5A (decrease of 34,07%, p = 0,27) and NCI-H28 (decrease of 21,22%, p = 0,48).

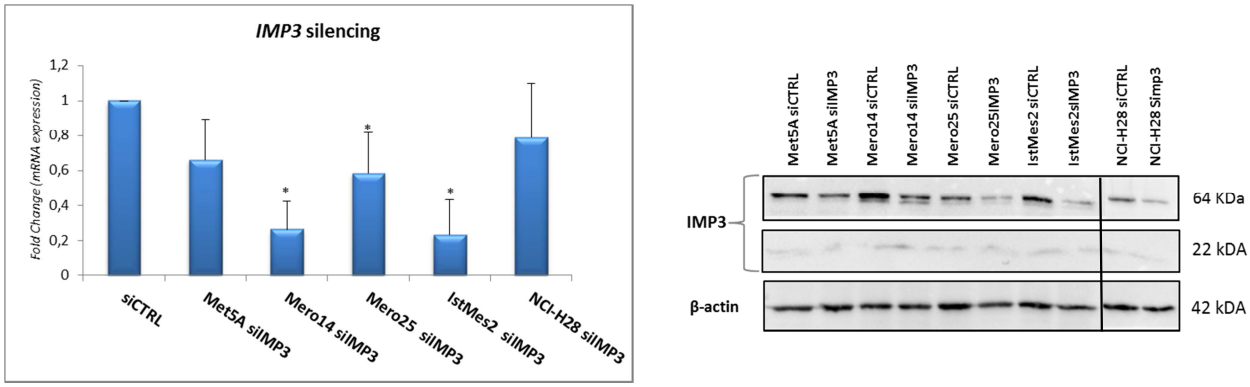


Fig. 70 Silencing of *IMP3*. On the left, RTqPCR showing fold change of quantitative mRNA levels of *IMP3* (72h after transfection) in one mesothelial cell line (Met5A) and four mesothelioma cell lines versus the expression levels observed in the corresponding cell line treated with siCTRL (All Star Negative control siRNA). Mean of RPLP0, HPRT, and TBP was used for normalization. Errors bars are SEM of the fold change from three independent experiments, each in triplicate. On the right, the protein levels of IMP3 after its depletion with *IMP3* siRNA versus the control, β-Actin was used as loading control. The protein levels were confirmed with two independent experiments.

***IMP3* silencing and proliferation**

In Met5A, Mero14 and Mero25 we did not observe any significant difference between the proliferation curves of the control and the silenced. The proliferation has been affected, in a statistically significant way, by IMP3 silencing in IstMes2 (p = 0,024) and NCI-H28 (p = 0,034) cells. The effects of silencing are noticeable from day 6 in both cell lines in all the three experiments performed. The proliferation in Istmes2 treated with si*IMP3* decreased by 32,31% at

day 8. A similar trend has been observed in NCI-H28 cell line: IMP3 silencing caused a decrease of 35,28% at day 8.

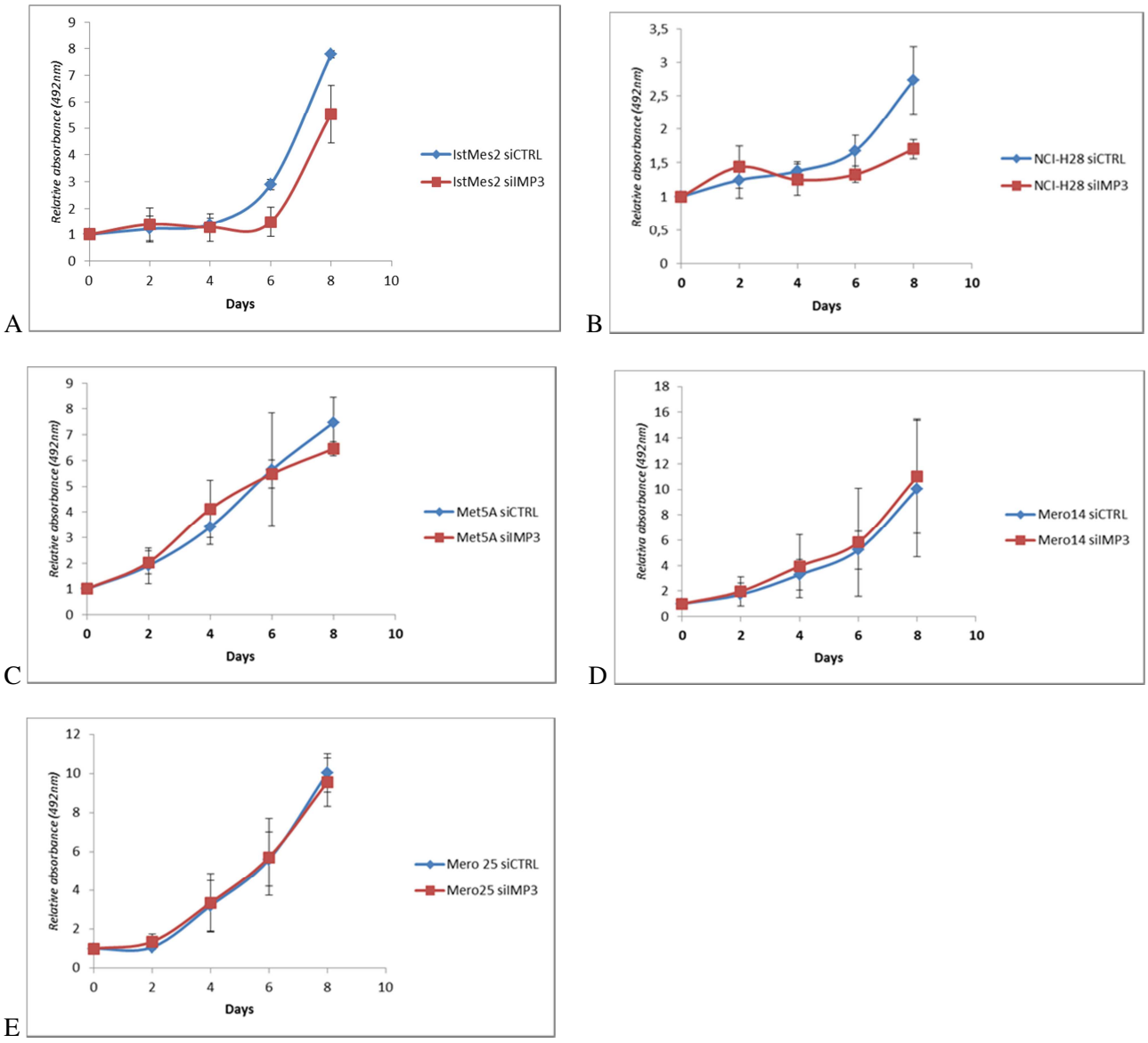


Fig. 71 Effects of *IMP3* on the proliferation: On the left, proliferation assay curves of IstMes2 (A), NCI-H28 (B), Met5A (C) and Mero25 (E) cells treated with 50 nM of siCTRL and si*IMP3*. Mero14 (D) cells has been treated with 20nM of siCTRL and si*IMP3*, according to the transfection efficiency results. The acquisition of optical density has been made every two days (day 0, 2, 4, 6, 8) starting from the time of transfection (= day 0). Error bars represent SEM of three independent experiments, each done in triplicate.

IMP3 silencing and colony formation ability

Only IstMes2 cells were affected by *IMP3* silencing showing a statistically significant decrease of 60,63% in number of colonies (p =0,035)

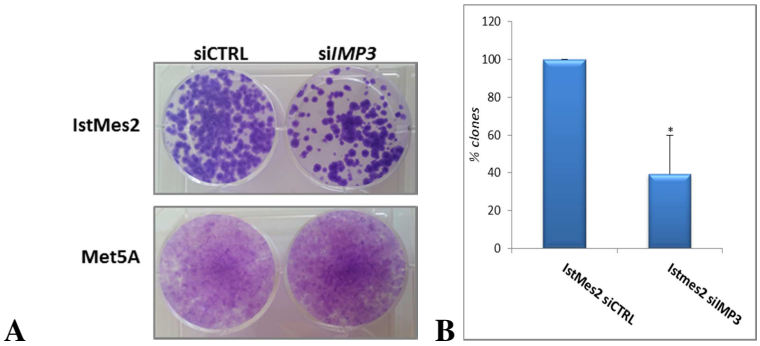


Fig.72 Effects of *IMP3* silencing in the colony formation ability: (A) Picture showing Istmes2 and Met5A cells, silenced with 50nM of siCTRL and si*IMP3,* fixed and stained 14 days after treatment. (B) Percentage of IstMes2 clones measured 14 days after silencing. Errors bars are SEM of the fold change from three independent experiments.

IMP3 silencing and apoptosis

Two MPM cell lines showed a statistically significant increment in caspase 3/7 activity after treatment with siIMP3 (increase of 51,17% in Mero25, p = 0,044; increase of 19,88% in Istmes2, p = 0,045). In none of the others cells treated (Met5A, Mero14 and NCI-H28) we observed any significant difference in caspase 3/7 activity after IMP3 silencing.

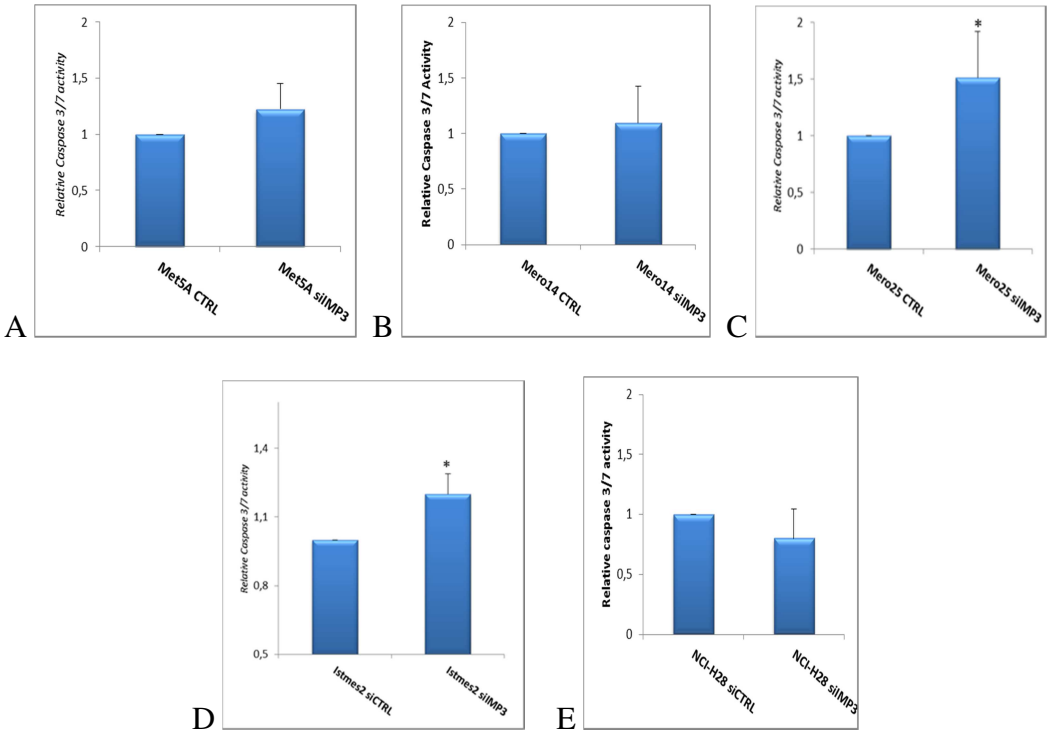
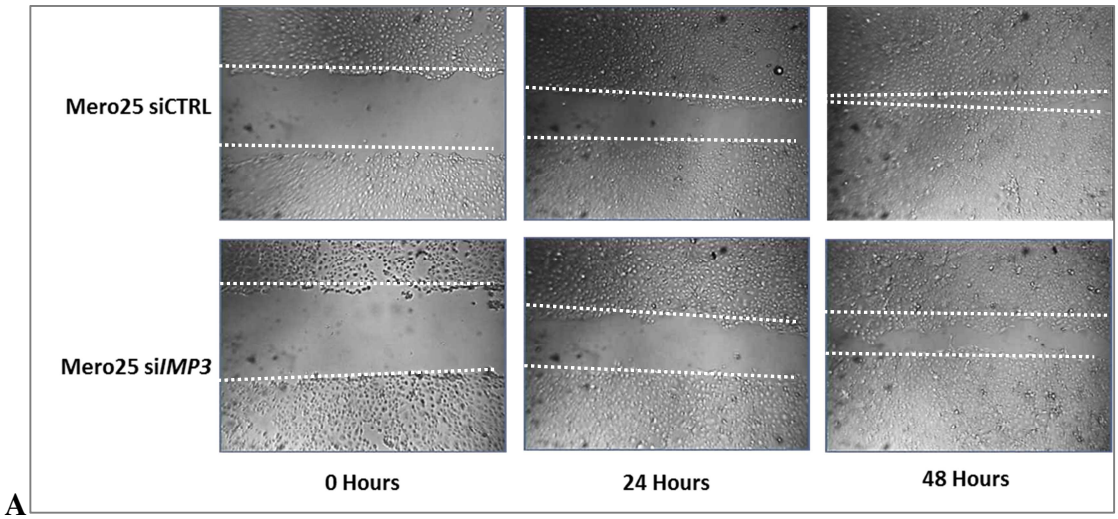


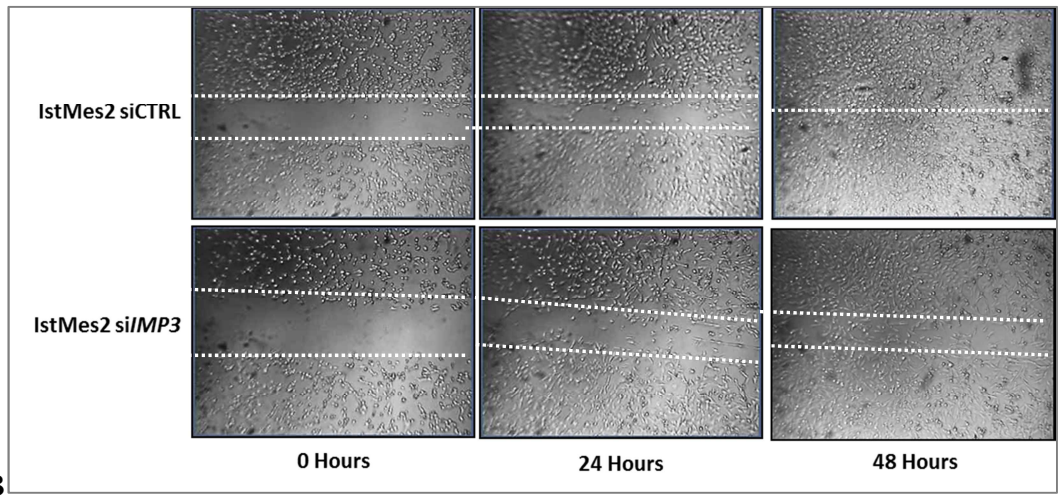
Fig 73. **Effects of *IMP3* silencing on caspase 3/7 activity:** Relative fold change of caspase 3/7 activity measured 72h after transfection with 50nM of siCTRL and si*IMP3* (A, C, D, E). (B) . Relative fold change of caspase 3/7 activity measured 72h after transfection with 20nM of siCTRL and siIMP3, according to efficiency results. Errors bars are SEM of the fold change from three independent experiments.

IMP3 silencing and migration

Mero25 cells silenced with siIMP3 decrease their migration ability by ~12% at 24h, this difference became more evident at 48h as shown in the picture (Fig. 74 A). The knockdown of IMP3 slightly decreased Istmes2 cells migration at 24h but only in two of the three independent experiment performed (Fig. 74B). NCI-H28 cells migration has been affected more than the others MPM cells: we observed a decrement in migration of 26,94% (Fig. 74 C). In Mero14 cells we observed an opposite trend: IMP3 silencing slightly increased their migration ability (~18% at 24h) as shown in picture (Fig. 74 D). While in Met5A we did not observe an evident difference between the control and the treatment (decrement of less than 4%) (Fig. 74 E).



A



B

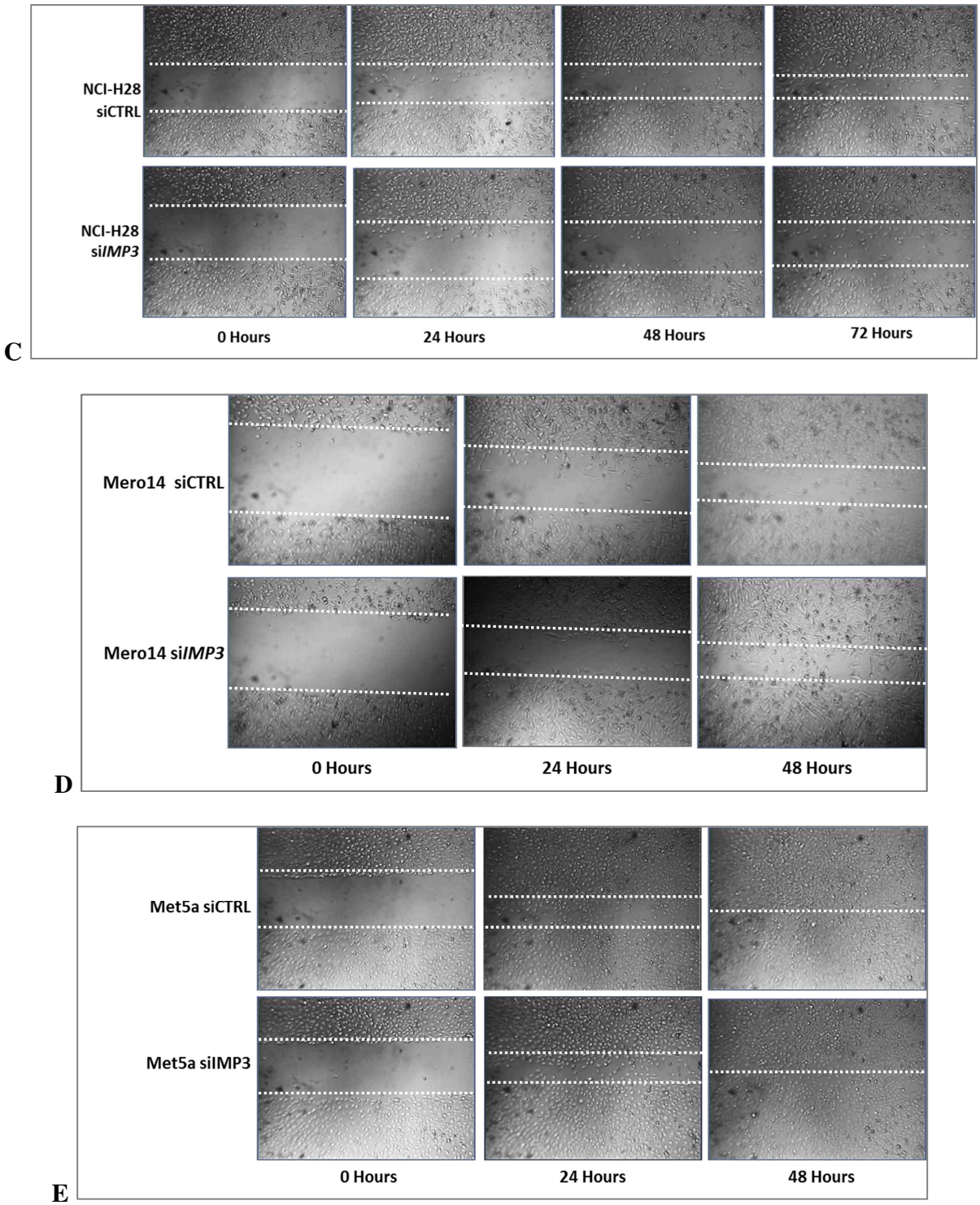


Fig. 74 Effects of *IMP3* silencing on migration: A, B, C, E) Mero25, IstMes2 and Met5A cells treated with 50nM of siCTRL, while at the bottom the same cells treated with 50 nM of si*IMP3;* the acquisition has been made every 24h (0, 24, 48, 72 Hours) starting from the time of scratch (= 0 Hours). This is a representative image of one of the three independent experiments performed.**D** Mero14 cells treated with 20nM of siCTRL , while at the bottom Mero14 cells treated with 20 nM of si*IMP3*; the acquisition has been made every 24h (0, 24, 48, 72 Hours) starting from the time of scratch (= 0 Hours).

6.2.12 *EIF4G1* phenotypic analysis

***EIF4G1*: mRNA and protein levels.**

Two MPM cell lines, Mero14 (p= 0,003) and IstMes2 (p = 0,026), showed statistically significant higher levels of *EIF4G1* mRNA compared to Met5A levels; while NCI-H28 cells showed lower *EIF4G1* levels (p=0,035) compared to Met5A.

EIF4G1 protein expression was high in Met5A and we did not observe up-regulated levels in MPM cell lines compared to the Met5A. Mero25 and IstMes2 cell lines, followed by Mero14 showed the higher expression levels among the MPM cell lines.

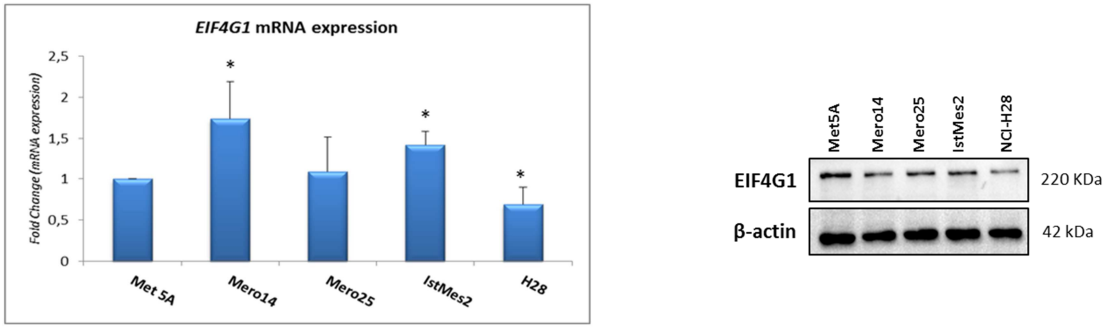


Fig. 75 Basal expression level of *EIF4G1* in four MPM cell lines. On the left, RTqPCR showing fold change of quantitative mRNA levels of *EIF4G1* measured on MPM cell lines versus MeT-5A cells. Mean of *RPLP0*, *HPRT*, and *TBP* was used for normalization. Errors bars are SEM of the fold change from three independent experiments, each in triplicate. Mero14 cells showed the highest expression levels of *EIF4G1* (p=0,003), followed by IstMes2 (p = 0,026) On the right, the protein levels of EIF4G1 on MeT-5A, Mero14, Mero25, IstMes2, and NCI-H28 cells. β-Actin was used as loading control. The protein levels were confirmed with two independent experiments.

mRNA and protein expression after *EIF4G1* silencing

EIF4G1 silencing has been effective, at mRNA level, in all the cell lines: *EIF4G1* expression, versus the control, decreased in Mero14 by 94,84% (p=4,32 x 10^{-7}), in Mero25 by 71,86% (p= 6,95 x 10^{-5}), in IstMes2 by 81,47% (p=2,47 x 10^{-6}), in Met5A by 68,90% (p= 0,001) and in NCI-H28 by 56,14% (p=0,040). At protein level only NCI-H28 cells showed protein expression similar to the control while all the others cells treated showed decreased expression levels.

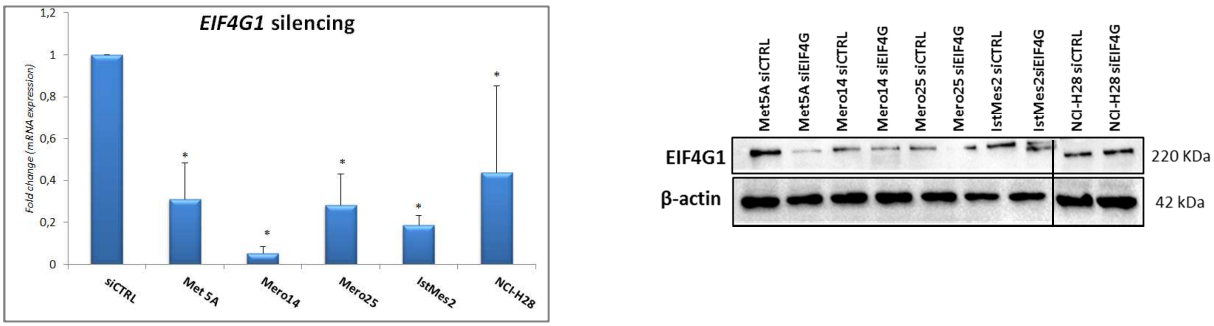


Fig.76 Silencing of *EIF4G1*. On the left, RTqPCR showing fold change of quantitative mRNA levels of *EIF4G1* in Met5A (p=0,002), Mero14 (p=0,001) and IstMes2 (p=0,00002) cell lines treated with si*EIF4G1* versus the corresponding cell line treated with siCTRL (All Star Negative control siRNA). Mean of *RPLP0*, *HPRT*, and *TBP* was used for normalization. Errors bars are SEM of the fold change from three independent experiments, each in triplicate. On the right, the protein levels of EIF4G1 after its depletion with *EIF4G1* siRNA versus the control, β-Actin was used as loading control. The protein levels were confirmed with two independent experiments.

EIF4G1 silencing and proliferation

EIF4G1 silencing affected the proliferation rate of two MPM cell lines, Mero25 ($p = 0{,}0008$) and IstMes2 ($p = p < 10^{-4}$), leading to a decrease of 25,05% at day 8 in Mero25 and to a decrease of proliferation of 62,66% at day 8 in IstMes2. Met5A, Mero14 and NCI-H28 proliferation rate has not been affected by si*EIF4G1* treatment.

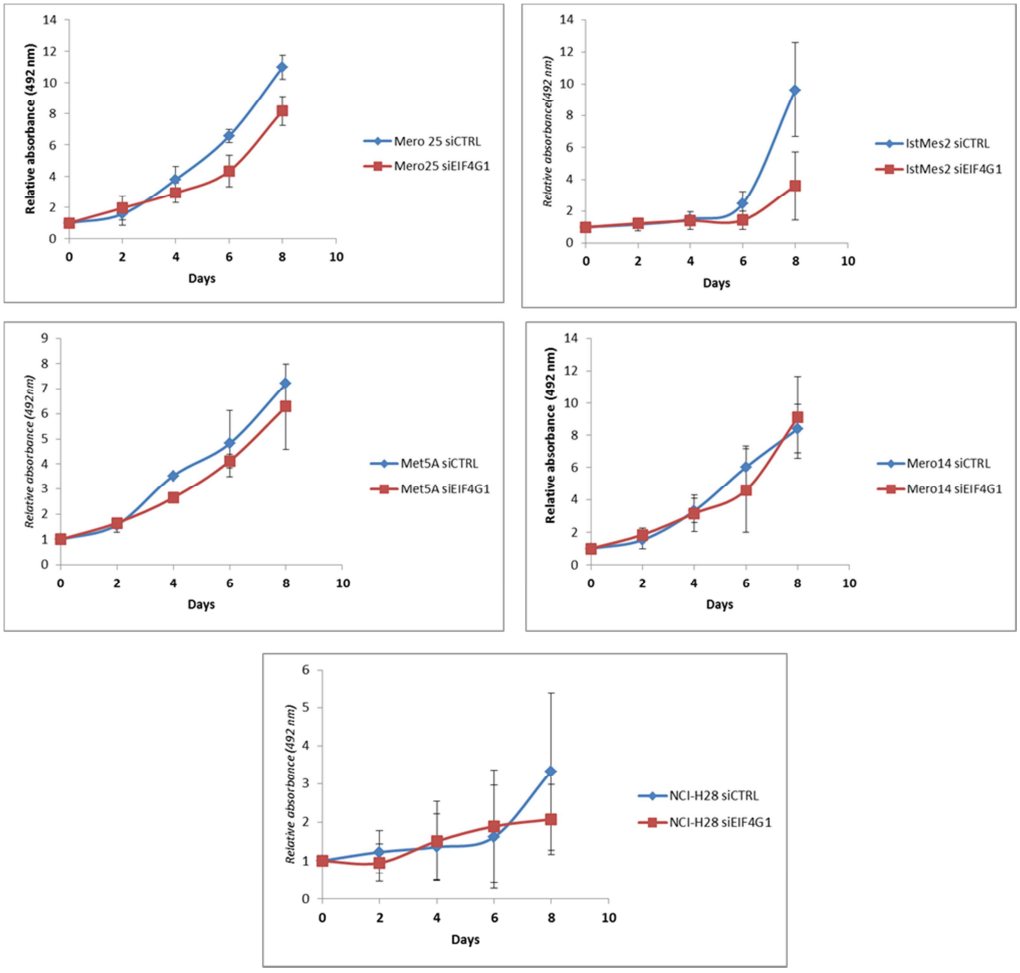


Fig. 77 Effects of *EIF4G1* on the proliferation: Proliferation assay curves of Mero25, IstMes2 , Met5A and NCI-H28 cells treated with 50 nM of siCTRL (All star negative siRNA) and si*EIF4G1*. Mero14 cells has been treated with 20nM of siCTRL and si*EIF4G1*, according to the transfection efficiency results. The acquisition of optical density has been made every two days (day 0, 2, 4, 6, 8) starting from the time of transfection (= day 0). Error bars represent SEM of three independent experiments, each done in triplicate.

EIF4G1 silencing and migration

After si*EIF4G1* treatment we observed a slight decrease (11,03%), not statistically significant, of migration ability only in Met-5A. The migration ability of MPM cell lines seems not to be affected by *EIF4G1* silencing.

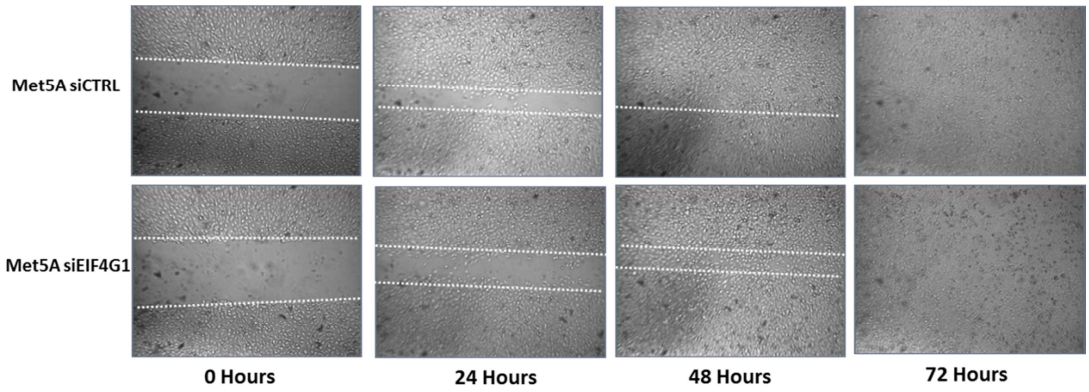


Fig. 78 Effects of *EIF4G1* on Met5A migration Met5A cells treated with 50nM of siCTRL, while at the bottom the same cells treated with 50 nM of si*EIF4G1;* the acquisition has been made every 24h (0, 24, 48, 72 Hours) starting from the time of scratch (= 0 Hours). This is a representative image of one of the three independent experiments performed.

EIF4G1 silencing and colony formation ability

We observed a decreased colony formation ability, 14 days after *EIF4G1* silencing, in Mero25 (p= 0,048) and Mero14 (p= 0,02), while the non-malignant Met5A cell line and the MPM IstMes2 (p= 0,08) cell line did not show significative differences after treatment.

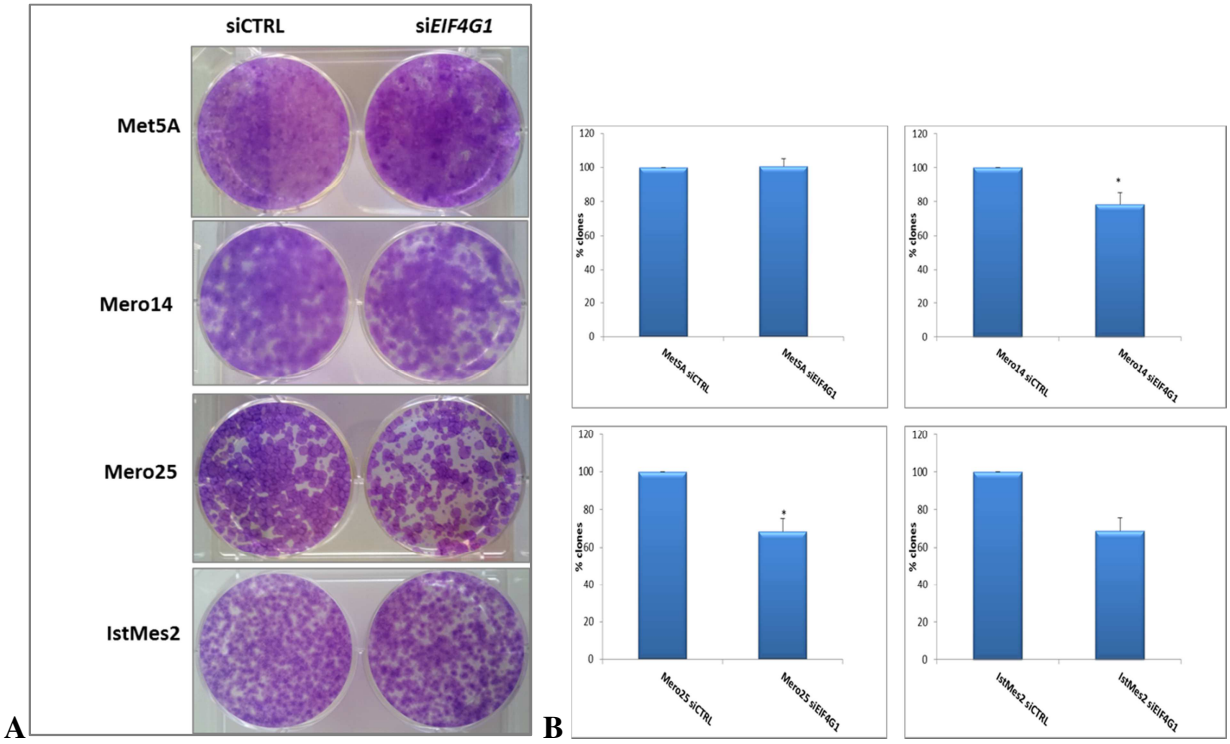


Fig. 79 Effects of *EIF4G1* on colony formation ability: (A) Picture showing Met5A, Mero25 and IstMes2 cells, silenced with 50nM of siCTRL and si*IMP3,* and Mero14 cells treated with 20nM of siCTRL and of si*IMP3,* fixed and stained 14 days after treatment. (B) Percentage of clones measured 14 days after silencing. Errors bars are SEM of the fold change from three independent experiments.

EIF4G1 silencing and apoptosis

The caspase 3/7 activity has been statistically significant affected in Met-5A and Mero14 with an increased cell death of 70,66% (p=0,049) and of 55,64% (p= 0,002), respectively. Mero25(p= 0,210),IstMes2 (p=0,10), and NCI-H28(p=0,26) showed a slight increase of caspase activity but not statistically significant.

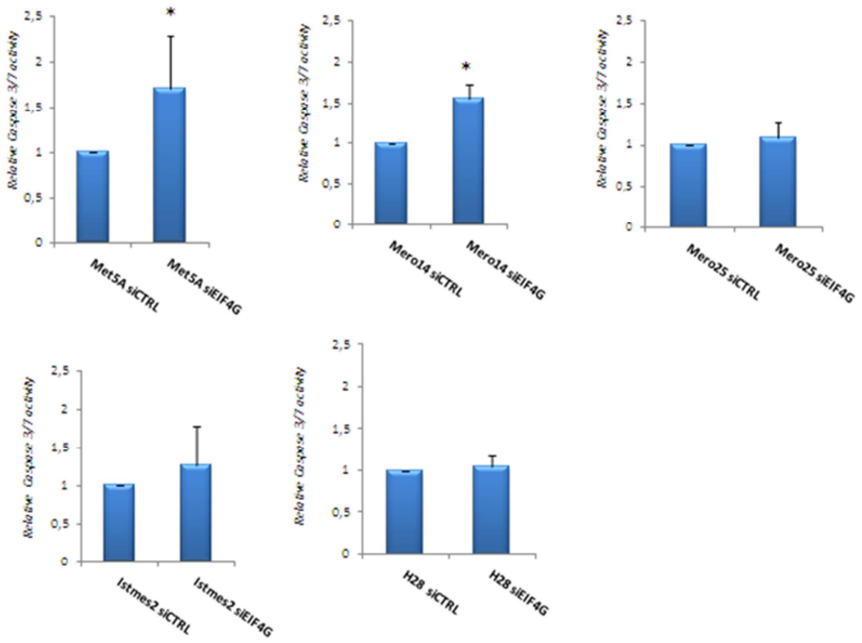


Fig. 80 Effects of *EIF4G1* silencing on caspase 3/7 activity: Relative fold change of caspase 3/7 activity measured 72h after transfection with 50nM of siCTRL and si*EIF4G1* for Met5A, Mero25, IstMes2 and NCI-H28 and relative fold change of caspase 3/7 activity measured 72h after transfection with 20nM of siCTRL and siEIF4G1, for Mero14. Errors bars are SEM of the fold change from three independent experiments.

6.2.13 *MCT4* phenotypic analysis.

***MCT4*: mRNA levels.**

MCT4 was expressed in all the MPM cell lines with statistically significant upregulated levels found in Mero14 and NCI-H28 cell lines (versus Met5A expression levels).

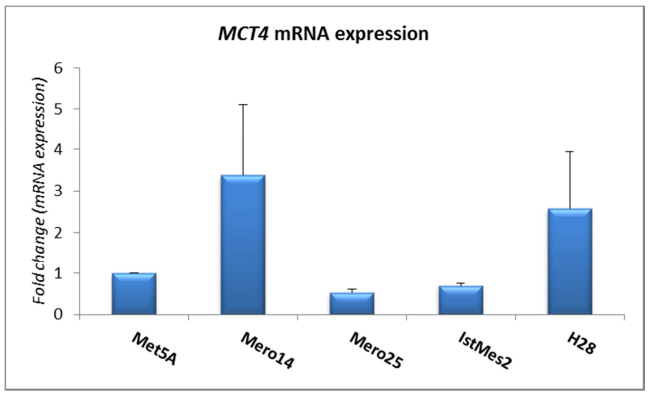


Fig. 81 Basal expression level of *MCT4* in four MPM cell lines. RTqPCR showing fold change of quantitative mRNA levels of *MCT4* measured on MPM cell lines versus MeT5A cells. Mean of *RPLP0*, *HPRT*, and *TBP* was used for normalization. Errors bars are SEM of the fold change from three independent experiments, each in triplicate. Mero14 and NCI-H28 cells showed statistically significant up-regulated levels of *MCT4* mRNA compared to Met5A expression levels; while Mero25 and IstMes2 showed downregulated mRNA levels compared to Met5A.

mRNA expression after *MCT4* silencing

MCT4 knockdown was statistically significant in all the cell lines: in Met5A with a reduction of 68,46% (p= 0,0013), in Mero-14 (p = 0,03) with 71,43% reduction of MCT4 mRNA, in Mero25 (p-value =0,01) with a reduction of 78,27%, in IstMes2 (p-value= 0,002) with a reduction of 90,5% and in NCI-H28 (p-value = 0,046) with 39,27% of reduction of MCT4 mRNA.

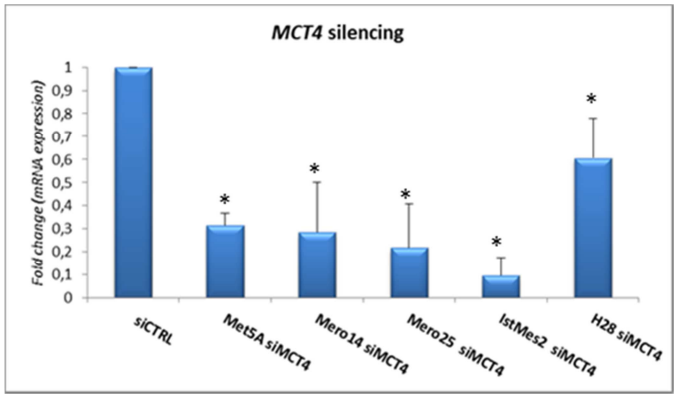


Fig. 82 Silencing of *MCT4:* RTqPCR showing fold change of quantitative mRNA levels of *MCT4* (72h after transfection) in one mesothelial cell line (Met5A) and four mesothelioma cell lines versus the expression levels observed in the corresponding cell line treated with siCTRL (All Star Negative control siRNA). Mean of RPLP0, HPRT, and TBP was used for normalization. Errors bars are SEM of the fold change from three independent experiments, each in triplicate.

MCT4 silencing and proliferation

MCT4 silencing affected the proliferation rate of all the mesothelioma cell lines, except NCI-H28, while the non-malignant cell line Met5A seems not to be affected by *MCT4* silencing. Mero14 showed a statistically significant decreased proliferation rate (p = 0.01) with a a decrement of 16,33% at day 8; Mero25 significantly decreased their proliferation rate (p = 0,0257) with a reduction of 25,1% at day 8; IstMes2 proliferation has been significantly affected by MCT4 silencing (p = 0,001) with a decrease of 61,12% at day 8.

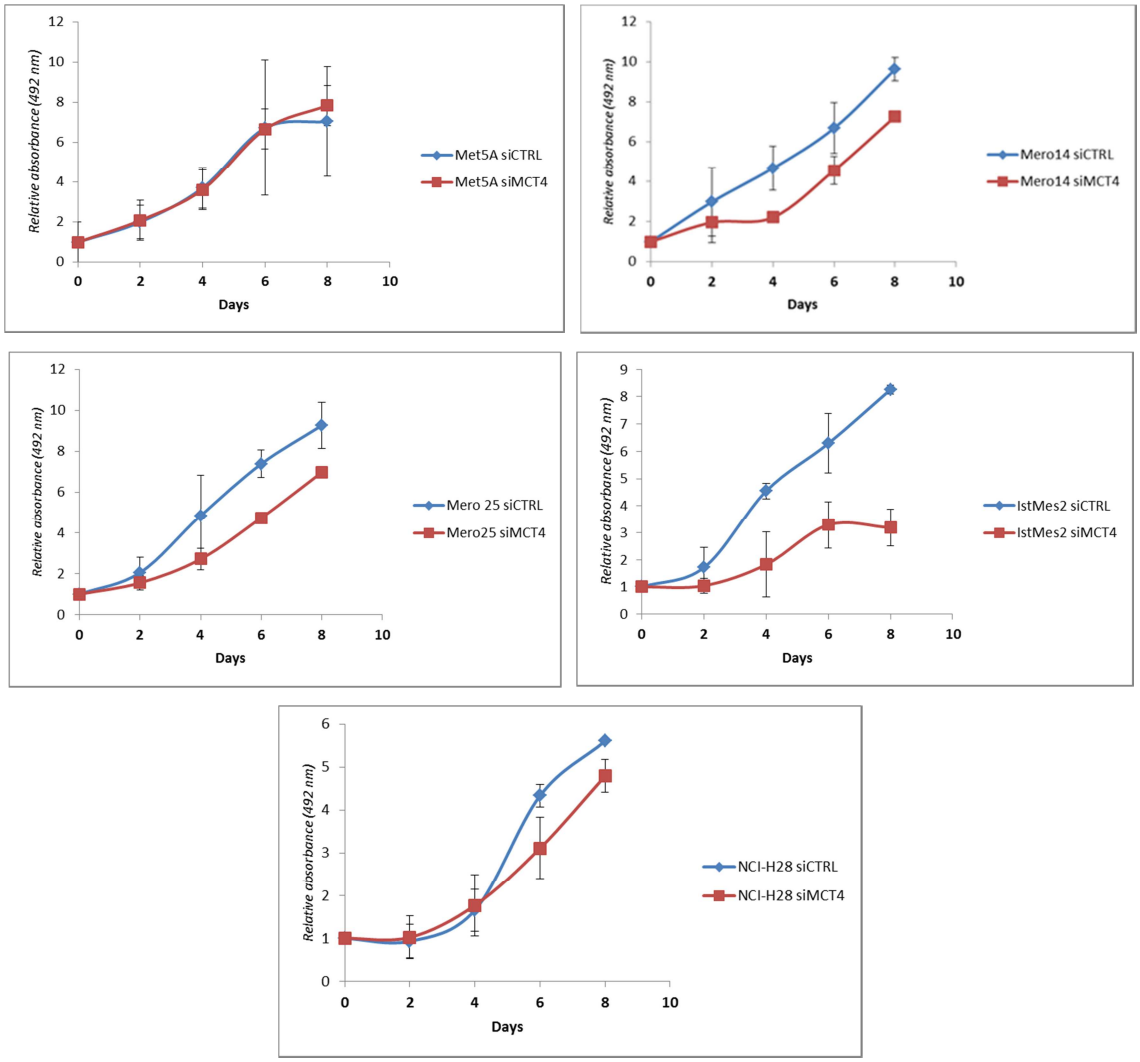


Fig. 83 Effects of *MCT4* on the proliferation: Proliferation assay curves of Met5A, Mero25, IstMes2 , and NCI-H28 cells treated with 50 nM of siCTRL (All star negative siRNA) and si*MCT4*. Mero14 cells has been treated with 20nM of siCTRL and si*MCT4*, according to the transfection efficiency results. The acquisition of optical density has been made every two days (day 0, 2, 4, 6, 8) starting from the time of transfection (= day 0). Error bars represent SEM of three independent experiments, each done in triplicate

MCT4 silencing and apoptosis

The caspase 3/7 activity increased by 81,4% after si*MCT4* treatment in IstMes2 cell line (p = 0,046) while in the others MPM cells treated we did not observe any significant change in caspase activity after the depletion of *MCT4*.

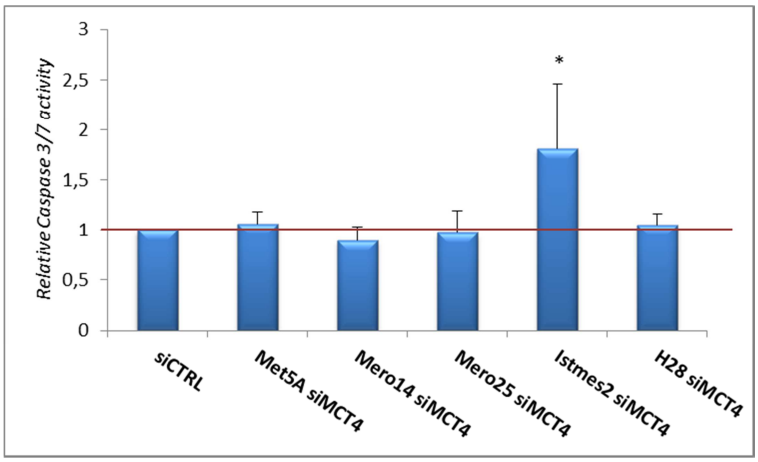
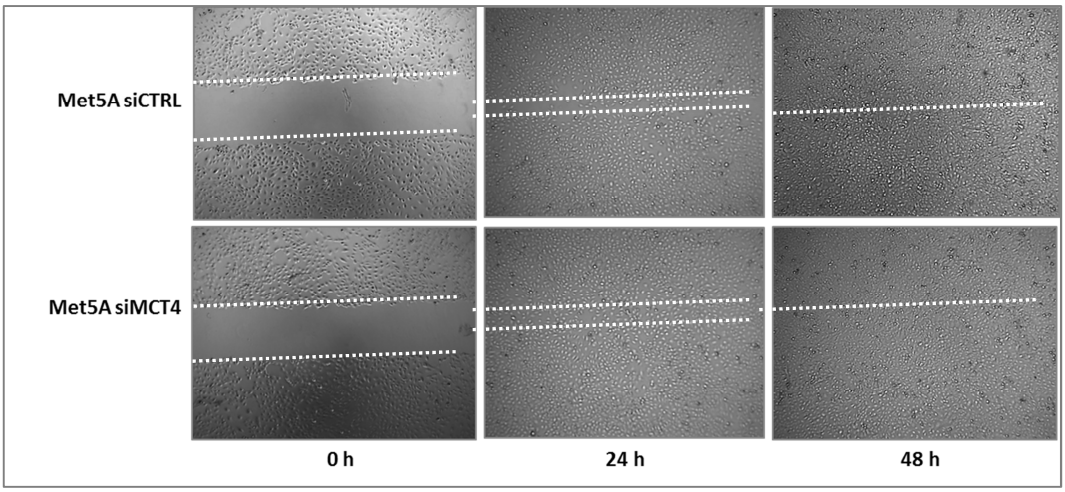


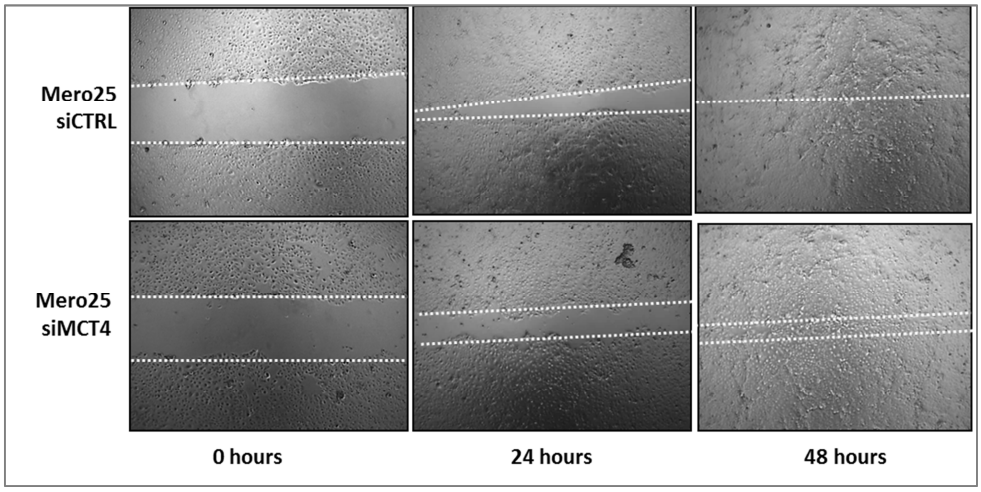
Fig. 84 Effects of *MCT4* silencing on caspase 3/7 activity: Relative fold change of caspase 3/7 activity measured 72h after transfection with 50nM of siCTRL and si*MCT4* for Met5A, Mero25, IstMes2 and NCI-H28 and relative fold change of caspase 3/7 activity measured 72h after transfection with 20nM of siCTRL and siMCT4, for Mero14. Errors bars are SEM of the fold change from three independent experiments.

MCT4 silencing and migration

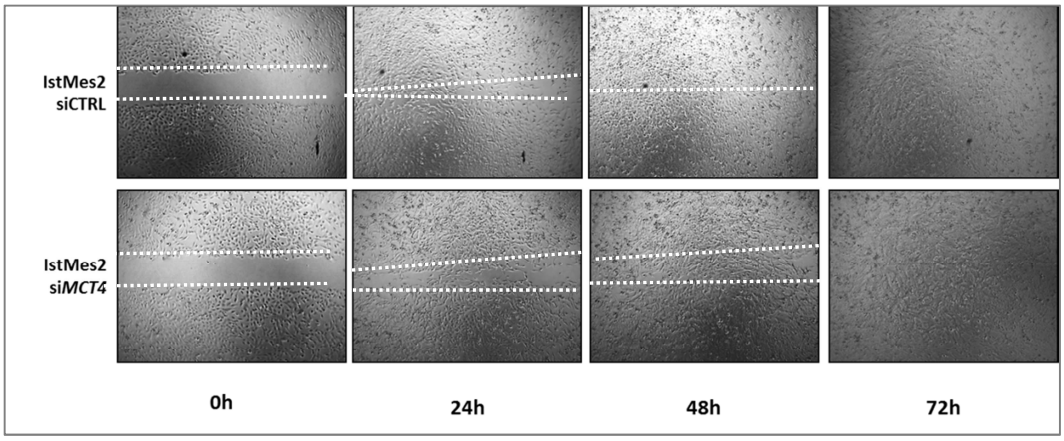
The migration ability of Met5A cells seems not to be affected by *MCT4* silencing, as shown in picture. While three MPM cell lines (Mero25, IstMes2 and NCI-H28) showed a decreased migration following the depletion of *MCT4*, respectively by 17,87%, 21,6% and 13,31%. Mero14 cells seems not to be affected by *MCT4* silencing. Here we report the pictures made with 4x magnification every 24h and 10x magnification at 24h.


Met5A siCTRL
Met5A siMCT4
0 h
24 h
48 h

A


Mero25
siCTRL
Mero25
siMCT4
0 hours
24 hours
48 hours

B


IstMes2
siCTRL
IstMes2
siMCT4
0h
24h
48h
72h

C

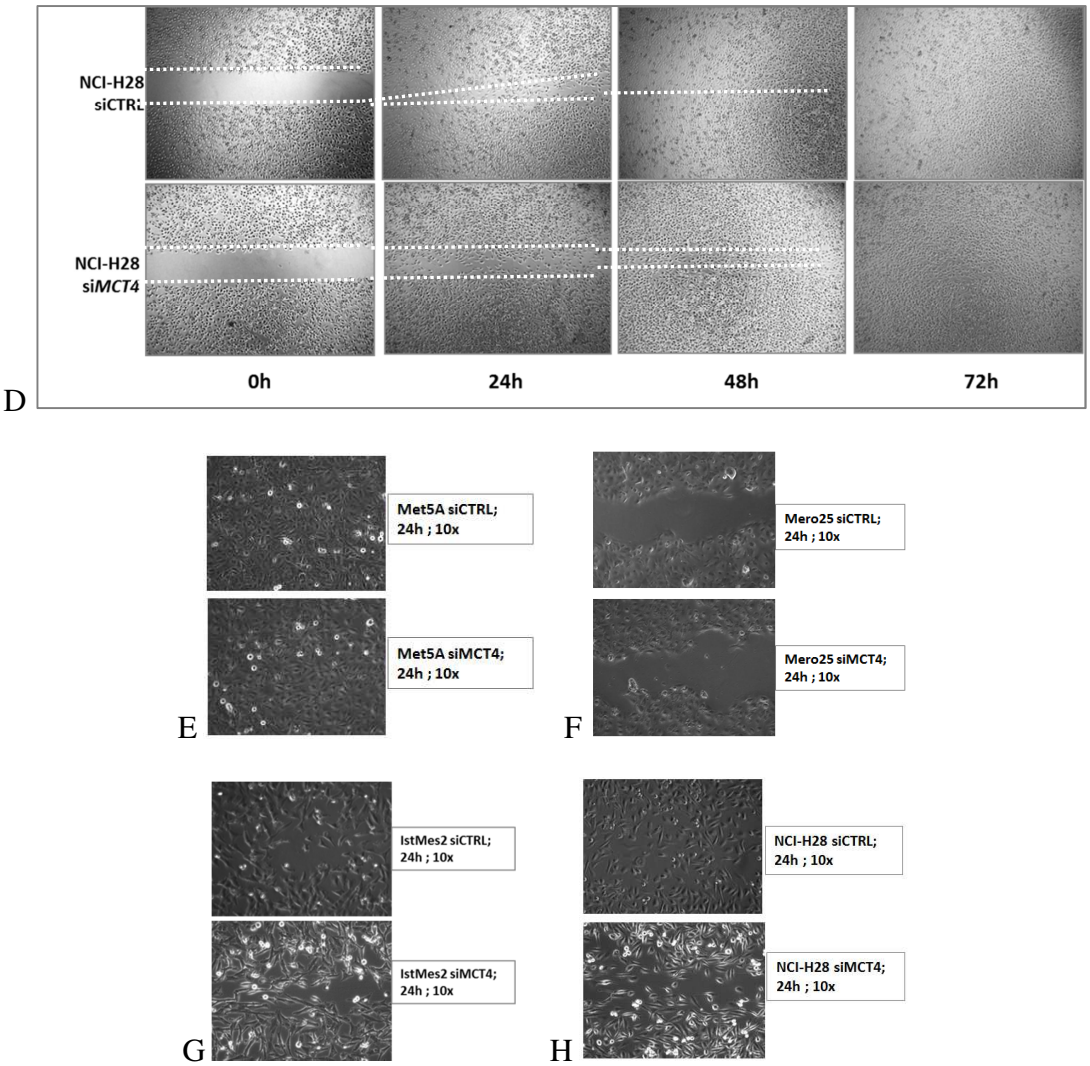


Fig. 85 Effects of *MCT4* on migration A, B, C, D) Met5A, Mero25, IstMes2 and NCI-H28 cells treated with 50nM of siCTRL, while at the bottom the same cells treated with 50 nM of si*MCT4;* the acquisition has been made every 24h (0, 24, 48, 72 Hours) starting from the time of scratch (= 0 Hours). These are representative images of one of the three independent experiments performed. **E, F, G, H)** 10x magnification of the middle area of the scratch for Met5A, Mero25, IstMes2 and NCI-H28, acquired 24h after scratch.

MCT4 silencing and colony formation ability

The colony formation ability has been affected in a statistically significant way by *MCT4* knockdown in two MPM cell lines: Mero25 (p= 0,014) and IstMes2 (p= 0,0106). Mero14 and Met5A cells did not show any statistically significant difference between siCTRL and siMCT4 in the three independent experiments performed.

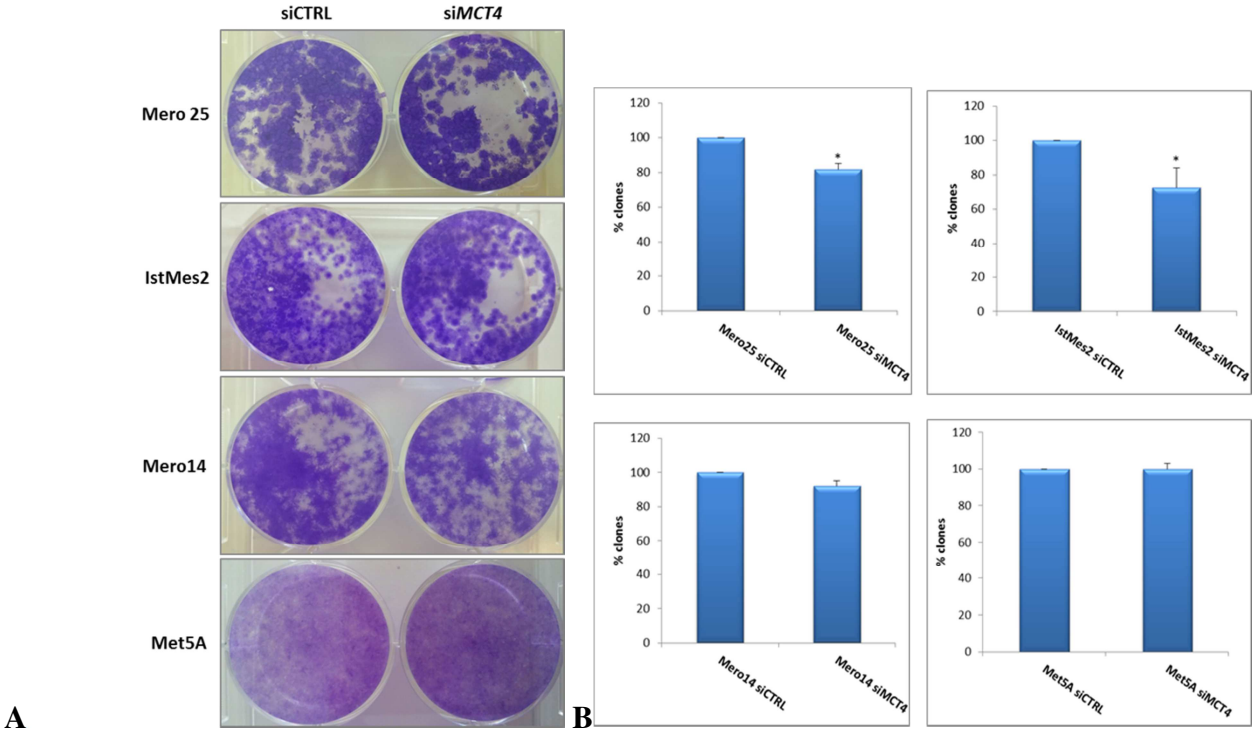


Fig. 86 Effects of *MCT4* on colony formation ability: (A) Picture showing, Mero25, IstMes2 and Met5A cells, silenced with 50nM of siCTRL and si*MCT4,* and Mero14 cells treated with 20nM of siCTRL and of si*MCT4,* fixed and stained 14 days after treatment. (B) Percentage of clones measured 14 days after silencing. Errors bars are SEM of the fold change from three independent experiments.

6.3 Tissue Microarray Immunohistochemistry

6.3.1 Evaluation of antibody specificity: western blot analysis

As shown in the picture (Fig. 87) BSG antibody seemed not specific for BSG protein in Hela extracts not treated with PNGase; for this reason we proceded with PNGase treatment to isolate the de-glycosylated protein. The treatment revealed the specificity of ab49493 (BSG antibody) for the de-glycosilated BSG protein.

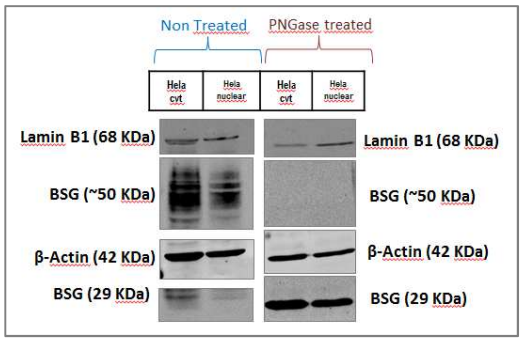


Fig. 87

CAIX antibody correctly identified CAIX protein as shown in Fig. 88.

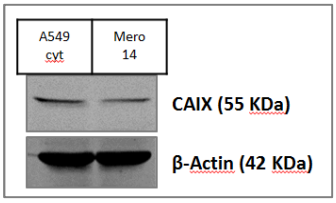


Fig. 88

CDH11 antibody correctly identified the molecular weight expected for CDH11 but showed a nuclear staining both in lung tissues and in nuclear protein extracts (Fig. 89). This was not in agreement with the datasheet of the antibody and with the literature, for this reason we did not proceed with TMA staining. Recently reported a weak CDH11 nuclear staining in epithelial tumour cells with a different antibody clone (Bùlow et al. 2015).

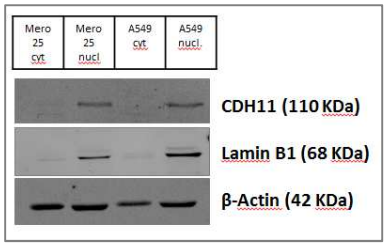


Fig. 89

ITGA4 antibody did not show specificity for ITGA4 protein in WB analysis (Fig. 90); ITGA4 molecular weight is 150KDa but after incubation with the antibody we only obtained one band around 28KDa. The manufacturer has tested the antibody through Western blot in Jurkat cells lysate, showing only one band around 150 KDa; for this reason we decided to test ITGA4 antibody in this cell line but we observed the same band at 28KDa (Fig. 91).

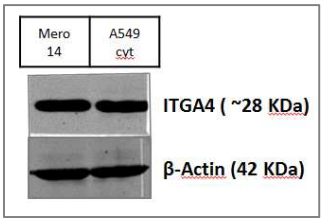


Fig. 90

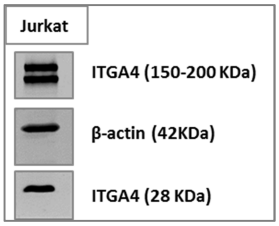


Fig. 91

MCT1 antibody correctly identified MCT1 protein in Hela and A549 cell cytosolic extracts (Fig. 92).

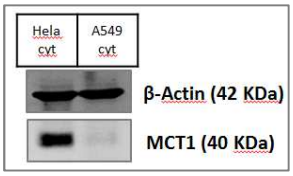


Fig 92

MCT4 antibody correctly identified MCT4 protein in Hela and A549 cell cytosolic extracts (Fig. 93).

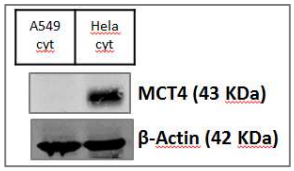


Fig. 93

THBS2 antibody correctly identified THBS2 protein in Mero14 and Mero25 cytosolic extracts (Fig. 94).

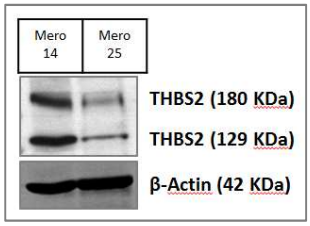
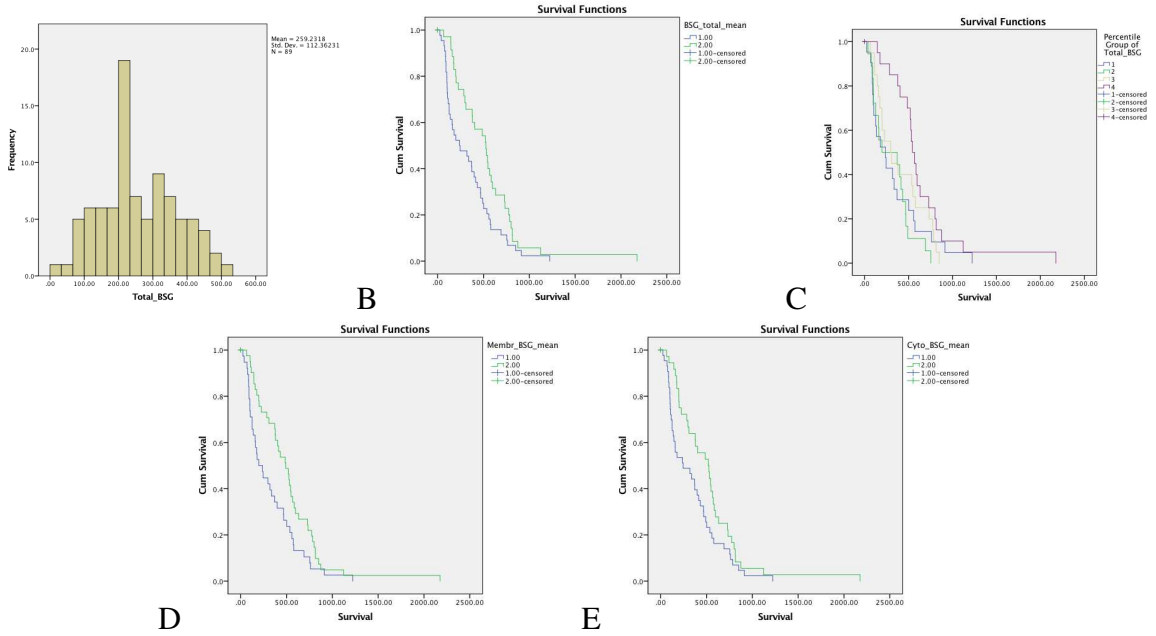
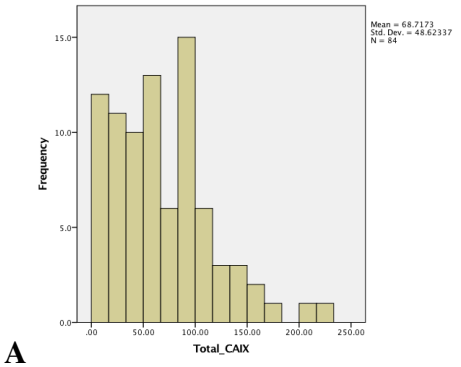


Fig. 94

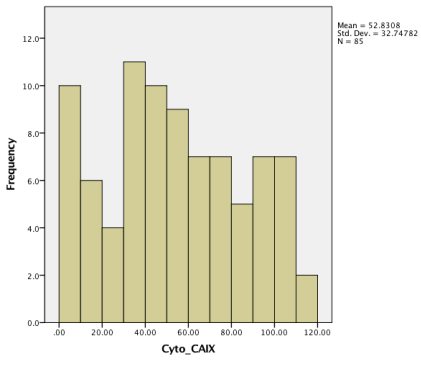
6.3.2 BSG:**Fig. 95** A) Distribution of BSG expression in MPM TMA. B) Kaplan-Meier survival analysis of total BSG expression; 1=expression levels lower the mean, 2=expression levels above the mean; LogRank = 0.018 C) Kaplan-Meier survival analysis of total BSG expression; Expression levels divided in quartiles. D) Kaplan-Meier survival analysis of membrane BSG expression; 1=expression levels lower the mean, 2=expression levels above the mean; LogRank = 0.019 (E) Kaplan-Meier survival analysis of cytoplasm BSG expression; 1=expression levels lower the mean, 2=expression levels above the mean; LogRank = 0.045



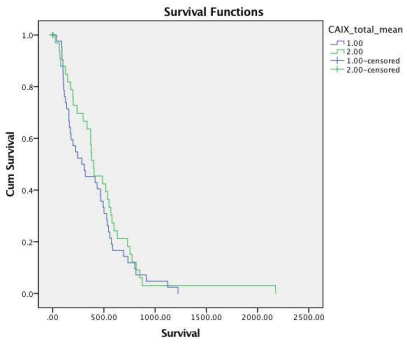
6.3.3 CAIX Fig. 96: A) Distribution of total CAIX expression in MPM TMA. B) Distribution of cytoplasmic CAIX expression in MPM TMA C) Kaplan-Meier survival analysis of total CAIX expression; 1=expression levels lower the mean, 2=expression levels above the mean; LogRank = 0.360 D) Kaplan-Meier survival analysis of total CAIX expression; Expression levels divided in quartiles. E) Kaplan-Meier survival analysis of cytoplasm CAIX expression; 1=expression levels lower the mean, 2=expression levels above the mean; LogRank = .740



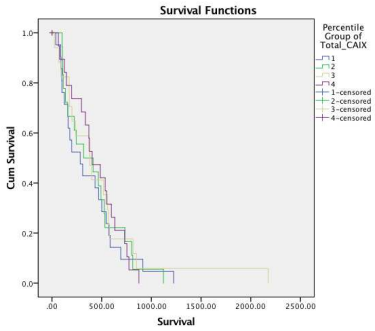
A



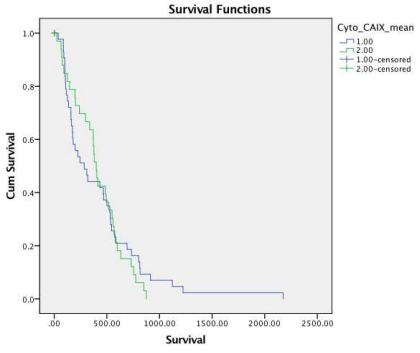
B



C

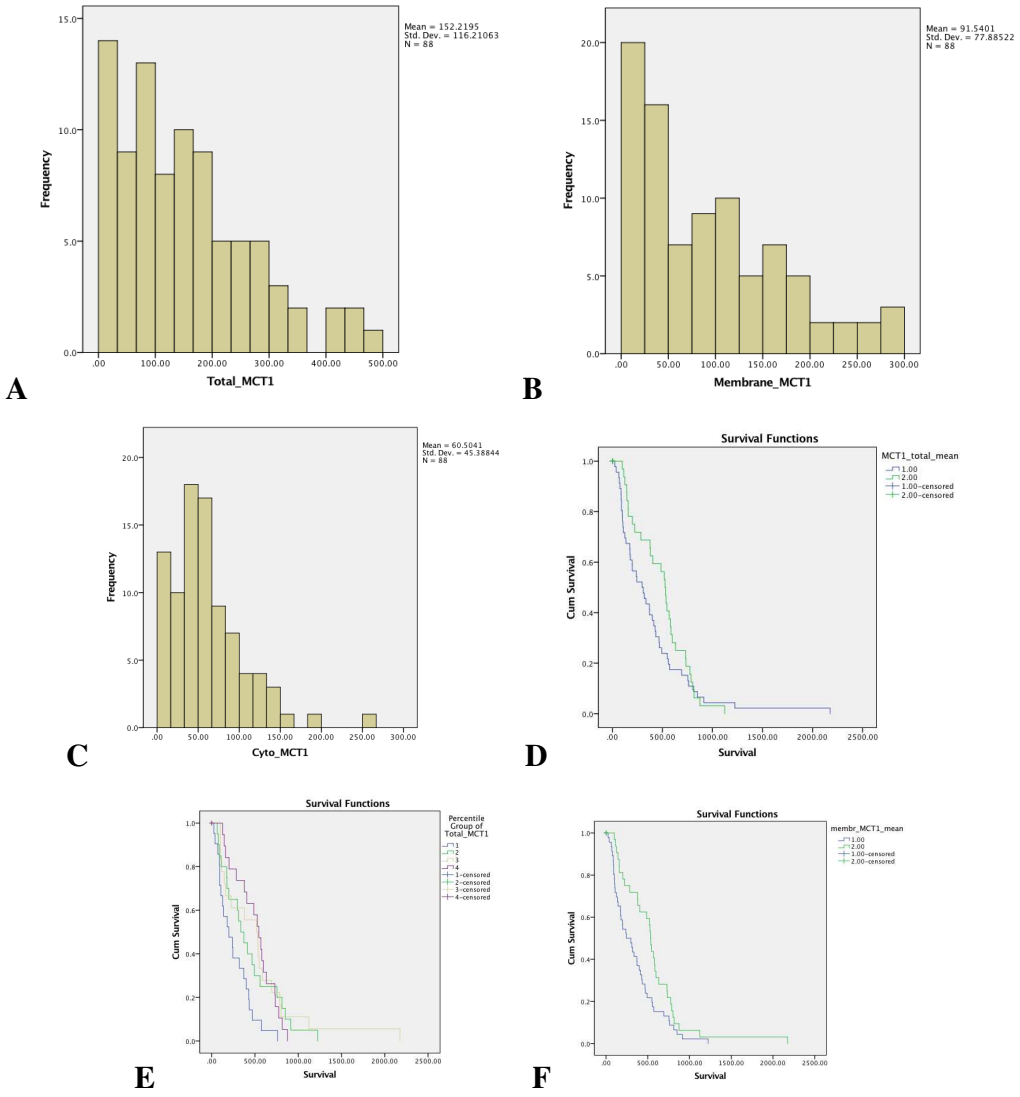


D



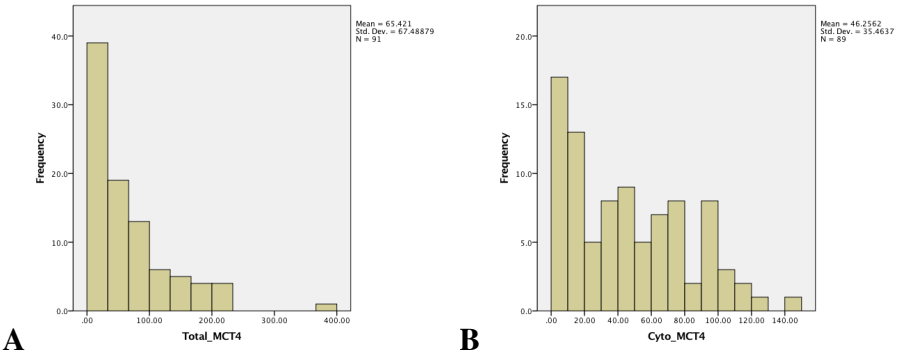
E

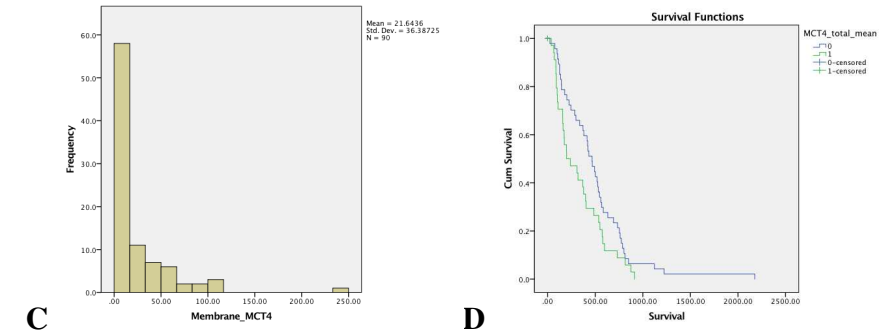
6.3.4 MCT1 Fig.97: A) Distribution of total MCT1 expression in MPM TMA. B) Distribution of membrane MCT1 expression in MPM TMA C) Distribution of cytoplasm MCT1 expression in MPM TMA. D) Kaplan-Meier survival analysis of total MCT1 expression; 1=expression levels lower the mean, 2=expression levels above the mean; LogRank =0.200 E) Kaplan-Meier survival analysis of total MCT1 expression; Expression levels divided in quartiles. F) Kaplan-Meier survival analysis of membrane MCT1 expression; 1=expression levels lower the mean, 2=expression levels above the mean; LogRank = 0.019

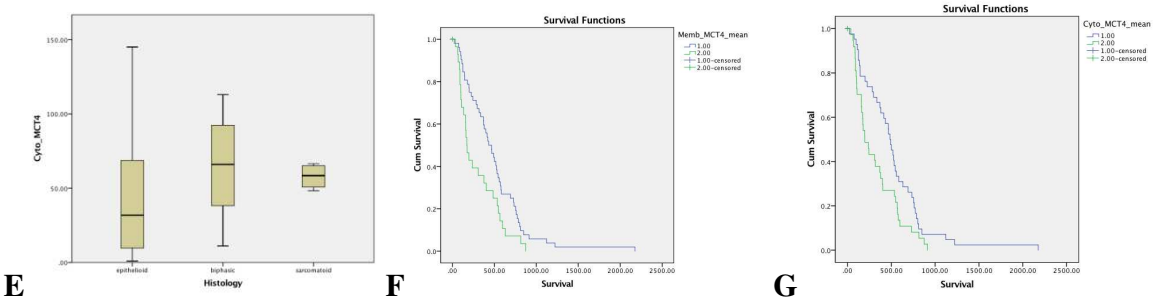


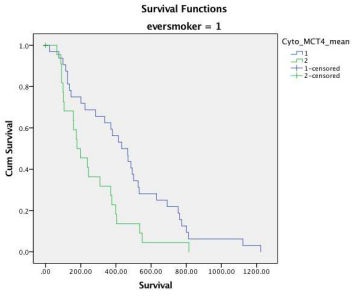
6.3.5 MCT4 Fig. 98: Interestingly cases with lower MCT4 expression showed longer survival. This relation is still observed in the group of eversmokers (fig H). A) Distribution of MCT4 expression in MPM TMA. B) Distribution of cytoplasm MCT4 expression in MPM TMA. C) Distribution of membrane MCT4 expression in MPM TMA. D) Kaplan-Meier survival analysis of total MCT4

expression; 0=expression levels lower the mean, 1=expression levels above the mean; LogRank = 0.049 E) Cytoplasm MCT4 distribution in the histopathological subtype F) Kaplan-Meier survival analysis of membrane MCT4 expression; 1=expression levels lower the mean, 2=expression levels above the mean; LogRank = 0.015 (G) Kaplan-Meier survival analysis of cytoplasm MCT4 expression; 1=expression levels lower the mean, 2=expression levels above the mean; LogRank = 0.020. H) Kaplan-Meier survival analysis of cytoplasm MCT4 expression in the selected group of eversmokers; 1=expression levels lower the mean, 2=expression levels above the mean.

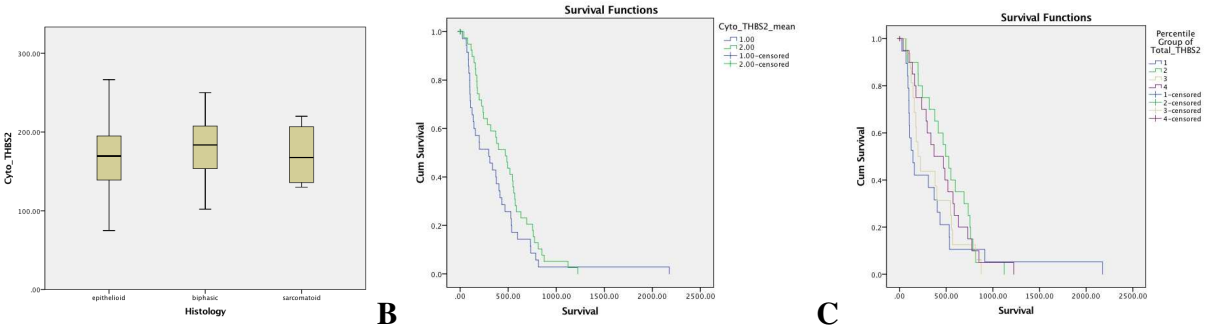








6.3.6 THBS2 Fig.99: A) Distribution of THBS2 expression in MPM TMA. B) Kaplan-Meier survival analysis of cytoplasm THBS2 expression; 1=expression levels lower the mean, 2=expression levels above the mean; LogRank = 0.115 C) Kaplan-Meier survival analysis of total THBS2 expression; Expression levels divided in quartiles.



A **B** **C**

6.3.7 Survival analysis

In table we report the estimated hazard ratio per 1 unit increase (with 95% confidence interval and p-value) for cytoplasm and membrane scoring of each of the five biomarkers.

Biomarker	Scoring type	Hazard ratio	p-value
THBS2	Membrane	1.002 (0.996-1.007)	0.567
	Cytoplasm	0.997 (0.991-1.003)	0.365
MCT4	Membrane	1.004 (0.995-1.014)	0.379
	Cytoplasm	1.004 (0.995-1.013)	0.412
CAIX	Membrane	0.998 (0.986-1.011)	0.803
	Cytoplasm	1.000 (0.991-1.009)	0.992
MCT1	Membrane	0.999 (0.994-1.003)	0.649
	Cytoplasm	0.998 (0.989-1.007)	0.679
BSG	Membrane	0.997 (0.994-1.001)	0.146
	Cytoplasm	1.001 (0.995-1.006)	0.820

There does not appear to be any significant associations between any of the biomarker scorings and survival time.

6.4 Evaluation of THBS2 and MCT4 expression in normal pleura samples

The different grade of THBS2 staining observed in the normal pleura samples and the intensity of staining observed in MPM tissues do not seem to confirm the upregulation found at mRNA level. It is worth of note that all the MPM tissues analysed in TMA expressed THBS2 and 45/84 cases showed THBS2 expression above the average expression level observed, with high intensity of staining.

Interestingly the staining with MCT4 of the non-neoplastic mesothelial cells of the normal pleura samples appeared negative as shown in pictures. While all the MPM tissues stained in TMA showed different grade of staining: in particular 34/91 MPM cases showed MCT4 expression above the average expression level observed, with high intensity of staining. This is a clear evidence of the upregulation of MCT4 in MPM.

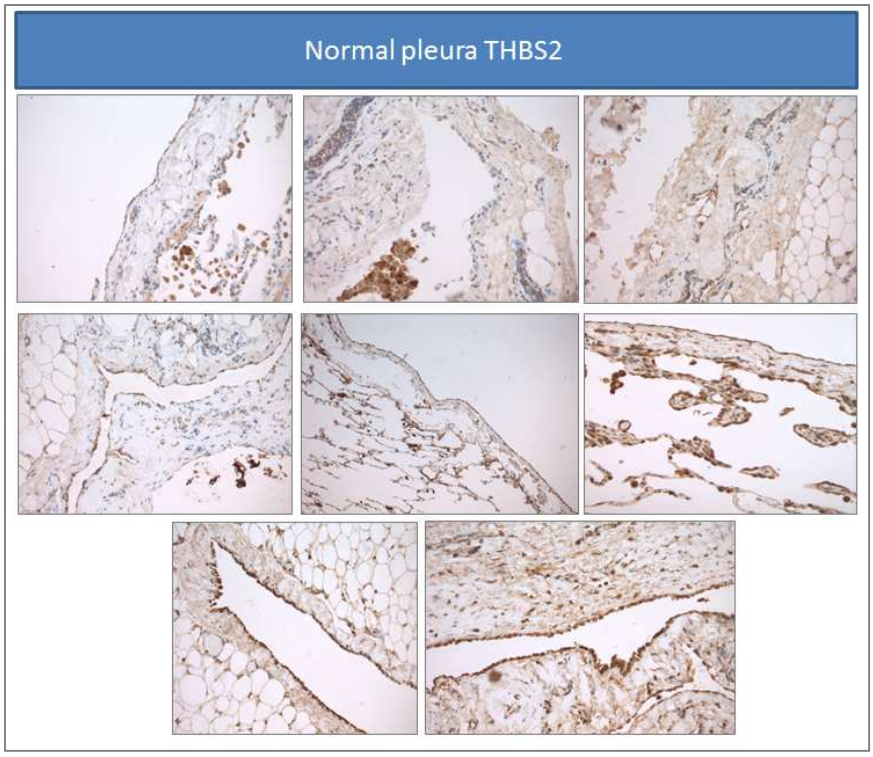


Fig 100 THBS2 staining in eight normal pleura samples. Mesothelial cells showed different grades of staining: from low/medium intensity, as shown in the first five pictures, to high intensity, as shown in the last three samples.



Fig 101 THBS2 staining in three MPM cases: MPM cells showed medium/high intensity of cytoplasm staining.

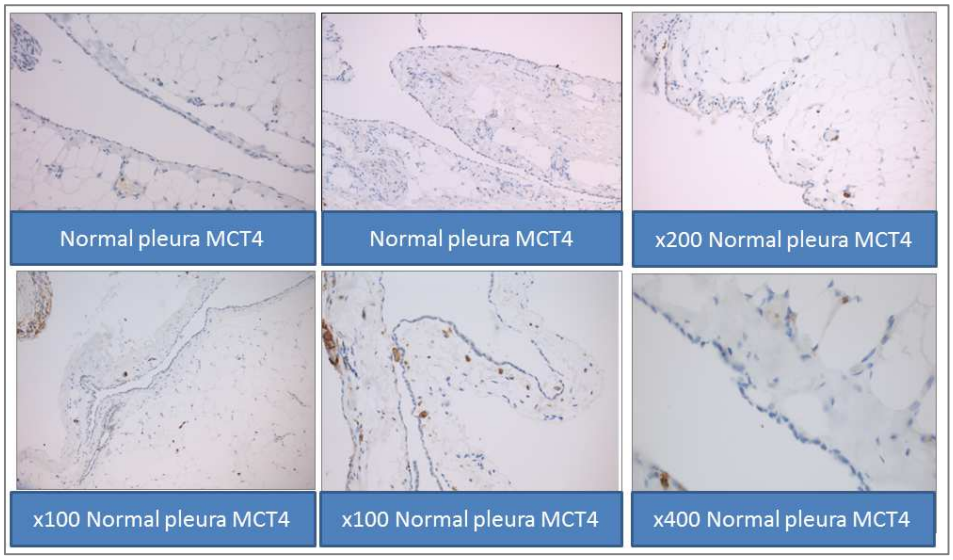


Fig. 102 MCT4 staining in six normal pleura samples. The normal mesothelial cells are completely negative for MCT4 antibody.

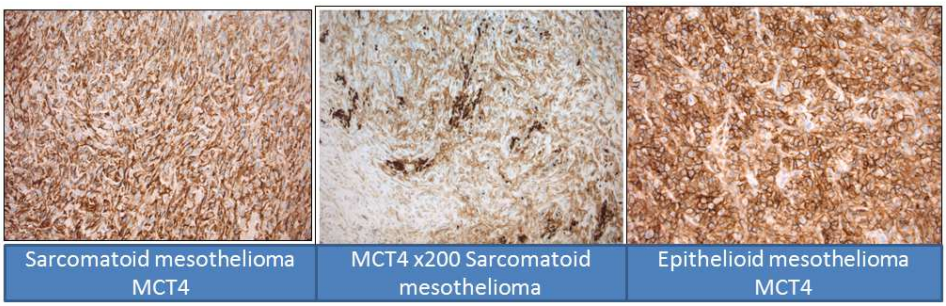


Fig. 103 MCT4 staining in three MPM cases. MPM cells show a high intensity of membrane and cytoplasm MCT4 staining.

7 Discussion

7.1 CCNO

The gene CCNO encodes a member of the cyclin protein family, and the encoded protein, called cyclin O, is involved in regulation of the cell cycle. This gene, was erroneously identified, in past, as a uracil DNA glycosylase (Muller et al. 1991); later it has been correctly (Muller et al. 1993) identified as a cyclin protein family member. The UNG2 symbol is also used as a specific protein isoform name for the UNG gene (GeneID 7374), so confusion exists in the scientific literature and in some databases for these two genes. There is little information in the literature on the expression and function of CCNO gene in cancer. Data from the Human Protein Atlas (http://www.proteinatlas.org/ENSG00000152669-CCNO/cancer) reports that CCNO protein expression has been detected with a medium-strong intensity of staining only in prostate cancer tissues while in all the others cancers tissues analyzed the staining was completely negative. Data from trascriptome studies and from the validation study performed in our laboratory shown an upregulation of this gene in MPM tissues and cell lines (Melaiu et al. 2011, 2015)

In our phenotypic screening CCNO resulted overexpressed in 4 MPM cell lines (Mero14, Mero25, NCI-H28 and Ren) versus MeT-5A. CCNO silencing affected, in a statistical significant way the proliferative rate and the colony formation ability of only Ren MPM cell line causing an increment of proliferation and of colonies number after treatment. The depletion of this gene did not affected the proliferation, the caspase activity, the colony formation and the migration of most of the MPM cells analysed. Thus, the overexpression of CCNO in MPM should be interpreted as an epiphenomenon and not as a factor of oncogenic conversion.

7.2 CFB

The gene Complement Factor B (*CFB*) encodes an extracellular protein belonging to the alternative pathway of complement activation. CFB expression has been associated with malignancies as the nasopharyngeal carcinoma (Xu et al. 2013; Seriramalun et al. 2010), the breast cancer (Haiman et al. 2013; Ruiz-Garcia et al. 2010) and the prostate cancer (Giusti et al.2014); however, the role in the occurrence of the malignant disease has never been investigated before. Regarding MPM, the gene has been found overexpressed in two independent trascriptome studies and in the validation study performed on MPM tissues and cell lines (Melaiu et al. 2011; 2015). Moreover in 2012 it has been observed that *CFB* expression is 10 fold higher in MPM spheroids, (that provide a more accurate representation of the physiology of the tumour) compared to the monolayer cultures (Kim

et al. 2012). Recently, has been observed that the exposure to the cytokine TNF (Tumour necrosis factor) of the human glomerular endothelial cells caused an increased expression of CFB (Sartain et al. 2016). It is known that TNF-α secretion is stimulated by HMGB1, in turn caused by asbestos induced cell necrosis (Carbone and Yang 2012). This finding could explain the overexpressed levels of CFB in MPM but do not explain the role played in the malignancy of the disease. For this reason we performed a phenotypic study on MPM cells. *CFB* resulted significantly overespressed at mRNA level only in Mero14 versus the MeT-5A; but at protein level the overexpression has been observed also in other three mesothelioma cell lines. The depletion of CFB in Mero14 did not show any significative change in proliferation, apoptosis, colony formation ability and migration despite the high efficiency of knockdown obtained at mRNA and protein level. These results suggest that CFB expression could be just a consequence of asbestos induced inflammation, that do not confers malignancy to MPM cells.

7.3 THBS2

The gene Thrombospondin 2 (THBS2) encodes the homotrimeric glycoprotein Trombospondin 2 that is secreted in the extracellular matrix (ECM). THBS2 interacts with many ECM proteins: thrombin, fibrinogen, heparin, fibronectin, plasminogen, laminin, collagen, various integrins, PDGFR, CD47 and MetalloProteases (MMP2 ed MMP9). It regulates the concentration of metalloproteases in the extracellular space, it takes part in the formation of the phagosome interacting with integrins, it modulates angiogenesis, cell/matrix focal adhesion and cell/cell adhesion (Bornstein et al. 2000). The expression of THBS2 has been related with various types of cancers: as the malignant ovarian tumour (Czekierdowski et al. 2008), the gastric cancer (Yang et al. 2007), the endometrial adenocarcinoma (Whitcomb et al. 2003), the adult acute lymphocytic leukemia (Garcia-Manero et al. 2002) and the non-small cell lung cancer (Metodieva et al. 2011); with many evidences of overexpression in cancer versus the non-malignant counterpart (Kim et al. 2010; Chang et al. 2016; Weng et al. 2016; Sun 2016)

In 2015 Naumnik found that NSCLC patients have higher serum concentrations of THBS2 (Naumnik et al. 2015). Moreover, high THBS2 immunoexpression has been significantly associated with advanced primary tumour status, nodal metastasis, and vascular invasion in urothelial carcinomas (Chang et al.2016) and with worse median survival in NSCLC patients (Weng et al. 2016).

However the specific role of THBS2 in cancer remains largely unclear: several studies reported an oncosuppressive role and at the same time, many studies reported its oncogenic role.

THBS2 may play a double-edged role in the progression of cancer, as it has been recently observed in lung adenocarcinoma (Weng et al. 2016).

In 1999 THBS2 has been proposed as an inhibitor of cancer proliferation and angiogenesis (Streit et al. 1999; Fontanini et al. 1999; Tokunaga et al. 1999). Subsequently in 2002 has been confirmed the inhibitory effect on proliferation and angiogenesis of induced trombospondin2 overexpression (Streit et al. 2002). More recently Chen and collaborators observed a decreased malignancy, associated with an increment of THBS2, in cervical cancer cells, after THBS2-target MiR-1246 depletion (Chen et al. 2014).

At the same time THBS2 expression has been associated with a more aggressive phenotype of epithelial ovarian tumour (Kodama et al. 2001) and of non-small cell lung cancer (Metodieva et al. 2011); furthermore THBS2 expression has been associated with an increased invasiveness of ductal breast carcinomas (Castellana et al. 2012), with a decreased survival, and with an increase of metastases (Cheon et al. 2014). Interestingly a recent study showed that THBS2 enhances metastatic colonization through the THBS2-dependent stromal niche activation via integrin signalling (del Pozo Martin et al. 2015)

In our experimental model we could not observe an effect on MPM cells migration ability after siTHBS2 treatment but we should consider that the scratch assay grossly oversimplifies the complex process of migration and invasion, lacking the tumour structural architecture and stromal components.

THBS2 has been found overexpressed at mRNA level in 3 independent trascriptome studies (Melaiu et al. 2011) and at mRNA level in MPM tissues and cell lines (Melaiu et al. 2015); and we confirmed the overexpression in three MPM cell lines (Mero14, Mero25 and Istmes2) versus the non-malignant Met-5A, with a level of expression, in Mero14, 300 times higher than Met5A. The different grade of THBS2 staining observed in the normal pleura samples and the intensity of staining observed in MPM tissues do not seem to confirm the upregulation found at mRNA level; but it is worth of note that all the MPM tissues analysed in TMA expressed THBS2 and 45/84 cases showed THBS2 expression above the average expression level observed, with high intensity of staining.

Interestingly we report a significative increase of caspase 3/7 activity after *THBS2* silencing with an increased cell death of 30%. Moreover we observed a significative decrease of proliferation and colony formation ability, respectively of 41% and of 66% after *THBS2* depletion in IstMes2 cells.

Thus the overexpression of *THBS2* in MPM seems to contribute to the malignant phenotype; to ascertain this role it would be useful to perform a phenotypic screening in a context of forced overexpression in a non-malignant mesothelial cell line (not expressing *THBS2*). The ambiguity of the roles of trombospondin has been attributed to the numerous interaction and pathways in which they take part, determining opposite functions (Bornstein et al. 1995; DiPietro 2000). For this reason a deeper understanding of the biology of mesothelioma would be useful to clarify the main interaction responsible of its aggressive phenotype.

7.4 TIMP3

The gene Tissue Inhibitor of Metallopeptidase 3 (TIMP3) codes for an inhibitor of matrix metalloproteinases (MMPs), a group of peptidase involved in the degradation of the extracellular matrix (ECM). TIMP3 protein is the only member of the family to be a component of the ECM, it can occur in two forms, a glycosylated (about 27 kDa) and the other non-glycosylated (approximately 24 kDa). Alterations of this gene are often found in the fundus dystrophy of Sorsby (SFD), an autosomal dominant disease that leads to blindness in adulthood. Few studies have investigated on the expression of TIMP3 in cancer: a downregulation of TIMP3 has been observed in renal cancer (Bachman, et al., 1999) and in secondary malignant glioblastoma (Nakamura, et al., 2005). Presumably it plays an anti-tumourigenic role (Bachman, et al., 1999; Nakamura, et al., 2005): TIMP3 is not only an inhibitor of MMPs, but also it negatively regulate ADAM-TS 5 (A disintegrin and metalloproteinase with THBS motif 5) and AGTR2 (angiotensine 2 Receptor type 2), two important proteins involved, respectively, in matrix degradation and the activation of proliferative pathways related to RAS (Huang, et al., 2014); moreover, the lack of TIMP3 seems to be associated with increased angiogenesis (Janssen, et al., 2008), it affected the adhesive, migratory and invasive capabilities of thyroid cancer cells and reduced the tumourigenicity by repressing angiogenesis and macrophage infiltration (Anania, et al., 2011). TIMP3 has an important role also in the resolution of inflammation caused by activation of the pathway of p38α (Black, et al., 2004; Zhong, et al., 2006). Further work reported that TIMP3 expression is induced by TGFβ (Qureshi, et al., 2005), an anti-inflammatory cytokine. In particular has been observed that TGFβ activates ERK 1/2 and JNK (c-Jun N-terminal Kinase) (Leivonen, et al., 2007; Ravanti et al., 1999), which in their turn, affect the activation of SMAD pathway leading to activation of TIMP3 (Leivonen, et al., 2013) (Fig). TIMP3, then, acts as a negative feedback regulator on the expression of p38α (Liu, et al., 2010), thus modulating the inflammation.

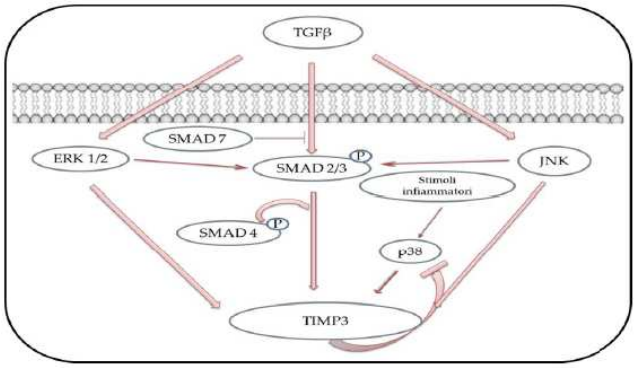


Fig.104: Signaling pathways downstream of TGFβ

The expression of TIMP3 in MPM resulted upregulated at mRNA level (Melaiu et al. 2011 and 2015) and we observed an overexpression in three MPM cell lines versus Met5A. Little is known about its role in the onset and in neoplastic progression. In particular, we may assume that in some types of cancer, the down-regulation of TIMP3 is due to the loss of activators (like SMAD proteins or some elements of the JNK pathway) and that this promotes growth because of the failure to inhibit the proliferative pathway. The overexpression found in MPM could be explained by the different molecular environment: in fact, MPM is characterized by a significant level of inflammation, in part due to chronic exposure to asbestos fibres, which causes a constitutive activation of p38α pathway (Swain, et al., 2004; Zhong, et al., 2006). p38α activation should lead to the negative feed-back through the over-expression of TIMP3. This suggests that in MPM the inhibitory activity of TIMP3 on p38 pathway could be lost and this would explain the high levels of expression of both p38 and TIMP3.

In Mero14 cells the depletion of TIMP3 leads to a drop of caspase levels and apoptotic activity; this result is in agreement with other studies that report TIMP3 as a pro-apoptotic agent (Baker, et al., 1998 and 1999; Bond, et al., 2000),that acts through a pathway dependent on FAK (Focal Adhesion Kinase- dependent) (Qi, et al., 2015). Furthermore, it has been observed that TIMP3 promotes apoptosis only in endothelial cells (EC) expressing KDR (Kinase insert domain receptor), but not in the EC expressing PDGFRB. (Qi, et al., 2015). This recent finding may explain why in the MPM cell lines, used in our phenotypic screening, the TIMP3 over-expression do not cause an intense apoptotic activity. In fact, the MPM cells often over-express PDGFRβ that may behave as an inhibitor of the apoptotic process, overriding the stimulus exercised by TIMP3. PDGFRβ is in fact able to hyper-stimulate the AKT pathway, known to be anti-apoptotic (Zhang, et al., 2003). In this hypotezized context it might be possible to interpret the reduction in the proliferative ability and

clonogenicity observed following TIMP3 silencing. In fact, we observed also an increase of senescence. In particular the reduction of proliferation rate could be explained by the fact that the cells in the absence of TIMP3 could go into pre-replicative senescence. A study on fibroblasts of mouse embryos TIMP3 - / - confirmed our hypothesis: when they are exposed to carcinogens, they go into senescence rather than apoptosis (Defamie, et al., 2014). In vivo, the loss of TIMP3 leads to reduced hepatic carcinogenesis due to an increased senescence of hepatocytes, in turn associated with early activation of three pathways: p38, p53 and NOTCH1 (Defamie, et al., 2014).

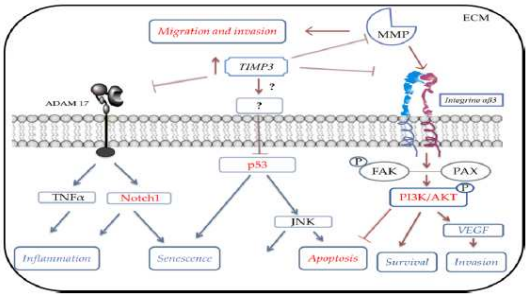


Fig. 105: Signaling pathways downstream of TIMP3

In the image above it can be seen that one of the most important functions of TIMP3 is to inhibit MMPs, not only involved in the degradation of ECM, but also in hyper -stimulation of pathways downstream integrin αVβ3. Furthermore it is able to inhibit the insertion in the membrane of integrin αVβ3, causing an anoikis, and at the same time, in an indirect manner, an inhibition of AKT pathways, implicated in the survival, proliferation and inhibiting apoptosis (Qi, et al., 2015) and of VEGF (Vascular Endothelial Growth Factor) involved in induction of angiogenesis (Chetty, et al., 2010).

Finally, it also seems to be involved in the resolution of inflammation: it seems that TIMP3 inhibits ADAM 17, a transmembrane dis-intregrin involved in the conversion of the TNF-R (Receptor) in sTNFα (Soluble Form) (Smookler, et al., 2006), and in the activation of Notch that is implicated both in inflammation and in senescence pathway (Liu, et al., 2012). Moreover, TIMP3 appears to block the action of p53 (Tront, et al., 2006) hampering the senescence caused by oxidative stress, cell damage and hyper stimulation of ERK and MAPK pathway (Itahana, et al., 2001; Rufini, et al, 2013). We can conclude that an up-regulation of TIMP3 might be useful to the cell to contrast the acquisition of a more aggressive phenotype, on one hand hindering invasion, migration and proliferation of cells, and on the other by activating the apoptosis. Our results show that its

depletion does not lead to increased malignancy in vitro, rather it seems to activate alternative pathway, such as that of senescence, which however seem to reduce the aggressiveness of MPM.

7.5 *SULF1*

The gene Sulfatase 1 (SULF1), encodes for an extracellular heparan sulfate endosulfatase that selectively removes 6-O-sulfate groups from heparan sulfate chains of heparan sulfate proteoglycans (HSPGs), it belongs to the sulfatase family and superfamily of aryl-sulfatase.

The expression of SULF1 in cancer has been found downregulated in some types of cancer, such as the hepato-cellular carcinoma (HCC), the ovarian (Roy, et al, 2014; He et al., 2014), the breast and the gastric cancer (Gopal, et al., 2012).

Several evidences highlight a tumour suppressor role of SULF1 (Lai, et al., 2008). In particular in breast cancer, under normoxic conditions, SULF1 plays its physiological role of endosulfatase on HS (Heparan Sulfate) reducing the FGF2 (Fibroblast Growth Factor 2) binding sites on the co-receptor (HSPGs) and consequently inhibiting the downstream pathways; while in hypoxic microenvironment (characteristic of solid tumours) HIF1α expression is stabilized and it, in turn, blocks the transcription of SULF1, over-activating the ERK pathways, and increasing cell migration, and invasion (Khurana, et al., 2011). Moreover, SULF1 appears to inhibit the formation of the ternary complex formed by HB-GF (Heparin Binding Growth Factor), its receptor (RTK) and its co-receptor (HSPG), reducing proliferation and cell growth. Thus the absence of SULF1 protein results in an up-regulation of the signals activated by ternary complex, resulting in hyper-proliferation (Lai, et al., 2003).

At the same time SULF1 resulted overexpressed in lung adenocarcinoma, hepatocellular carcinoma (Lai et al. 2004) and in brain, adrenal, epidermal (Bret, et al., 2011), pancreatic and gastric cancers (Hur et al., 2012). As previously reported, the prevailing view in the literature is that SULF1 is a negative regulator of tumourigenesis, but other studies on pancreatic cancer identify SULF1, together with SULF2, as enhancer of the autocrine signaling pathway of WNT, thus contributing to tumour growth (Nawroth, et al., 2007); moreover other studies confirm the role of SULF1 as a positive regulator of signaling pathways of oncogenes such as WNT (Dhoot GK, et al., 2001), BMP (Viviano, et al., 2004) and GDNF (Ai, et al., 2007).

Thus the ability of SULF1 to potentiate autocrine Wnt signaling appears to be the key factor for tumours driven by this canonical signaling pathway (Nawroth et al. 2007) furthermore it has been observed that SULF1 overexpression contributes to cancer cell proliferation, migration, and

invasion in colorectal cancer (Vicente et al. 2015). Increasing evidences suggest that wnt signaling in MPM play an important role in the neoplastic properties of mesothelioma cells and they found that targeting Wnt signaling can render mesothelioma cells more sensitive to cytotoxic drugs (Batra et al. 2006; Uematsu et al. 2007; Fox. et al. 2013).

In agreement with these studies, from our phenotypic screening it emerges that SULF1 is implicated (indirectly or directly) in promoting proliferation in MPM cells. In fact its depletion resulted in a reduced cell proliferation, in a reduced colony formation ability and in an increase in caspase activity. Recently has been observed that the overexpression of SULF1, promoting TGF-β-induced gene expression, induces epithelial-mesenchymal transition and enhances cell migration/invasiveness of hepatocellular carcinoma cells (Dhanasekaran et al. 2015). This finding could explain the reduction of the migratory ability that we observed in one of the two MPM cell lines treated with si*SULF1*, although it was not a statistically significant reduction.

From our data SULF1 appear to be positive regulator of tumour development but to better ascertain its role in MPM could be useful to test the involvement of SULF1 in Wnt and in TGF-β/SMAD signaling in MPM and to evaluate the involvement in tumour growth by overexpressing it in cells that lacked it.

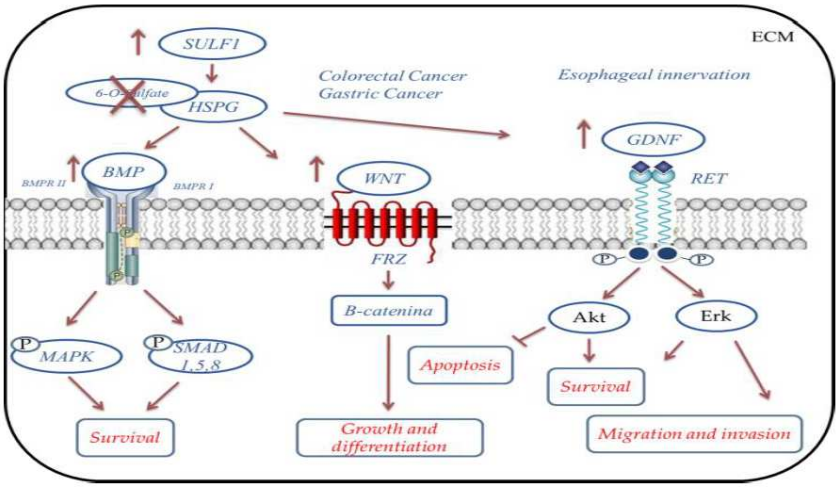


Fig. 106: Signaling pathways downstream of *SULF1*.

7.6 *PDGFRB*

The gene Platelet-derived Growth Factor Receptor Beta Polypeptide (PDGFRB), is localized in position 33.1 of the long arm of chromosome 5 (5q33.1) (Gene ID: 5159), encodes a tyrosine kinase surface receptor that binds the members of the PDGF family.

There are two isoforms of PDGFR receptor encoded by two different genes: PDGFRA e PDGFRB. The protein PDGFRβ plays an important role in the embryonic development, in cell proliferation, in differentiation, in cell survival, in chemotaxis, in cell migration (Nicolas G, et al., 2013) and in angiogenesis (Makihara, et al., 2014). Deregulated expression of PDGFRB has been associated with infant myofibromatosis (Martignetti, et al., 2013), idiopathic calcification of basal ganglia 4 (IBGC 4) (Arts, et al., 2015) and gastric adenocarcinoma (Drescher, et al., 2007). The pathway PDGF / PDGFRβ seems to play an important role in MPM carcinogenesis. In fact most of the MPM cell lines show PDGFRB gene overexpression, while in normal mesothelial cell lines PDGFRA expression is predominant (Langerak, et al., 1996). PDGFRB resulted overexpressed at mRNA level in transcriptome studies and in the validation performed in MPM tissues (Melaiu et al. 2011, 2015) and we confirmed PDGFRB up-regulation in 3 MPM cell lines. Moreover the phenotypic screening highlighted a pro-tumourigenic role of PDGFRB. In particular PDGFRB silencing lead to a decreased cell proliferation rate and a reduced colony formation ability of Mero14 and IstMes2. The increment of caspase activity in two MPM cell lines after siPDGFRB treatment suggest a survival role in MPM and the scratch assay revealed a significant decrease of migration ability in one MPM cell line. This is in agreement with studies that revealed an involvement of PDGFRβ not only in cell proliferation but also in chemotaxis of MPM: the inhibition of the active dimer PDGF-DD, that is a stimulator of PDGFRβ, showed that the inhibition of the activation of PDGFRβ caused the inhibition of MPM cell migration (Yaguchi, et al., 2010). Interestingly, in a previous study, has been observed that the selective inhibition of the PDGFR tyrosine kinase through STI571 slowed PDGF-mediated growth and leaded to apoptosis of osteosarcoma cells in vitro (McGary et al. 2002); moreover PDGFRB inhibition alone reduces spontaneous growth and metastasis in Ewing Sarcoma (EWS) (Wang et al. 2009). As shown in the picture, the downstream pathway of PDGFRB is involved in the regulation of cell growth, apoptosis and migration.

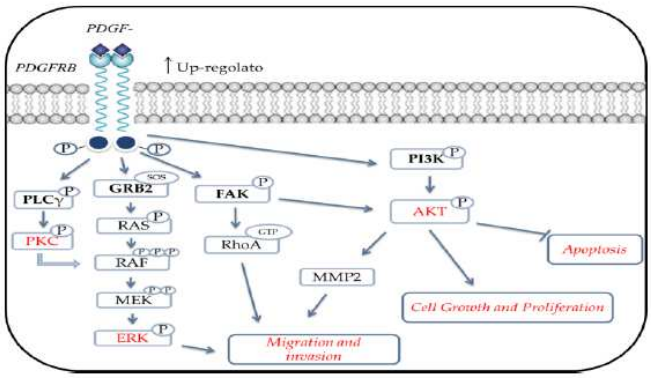


Fig. 107: Signalling pathways downstream of PDGFRB

As shown in picture, the activation of the receptor PDGFRB alters three different pathways activating the signalling pathway of Ras/Raf , of MAPK, of PI3K/AKT and of FAK.

The activation of PDGFRB receptor is caused by an autocrine mechanism (Hermanson, et al., 1992). The cancer cells, expressing PDGF and *PDGFRB* (instead of *PDGFRA*) activates the signalling pathways shown in picture (Zhang, et al., 2014). These leads to a proliferation stimuli and to the inhibition of apoptosis (Kennedy, et al., 1997; Zhang, et al., 2003; Okada, et al., 2012). Moreover PDGFRB has been associated with an increased expression of MMP2 correlated with increased cell migration, that anticipates EMT transition (Xu Z, et al., 2014; Seo KW,et al., 2013).

Thus, these results confirm the pro-tumourigenic role played by PDGFRB in cancer also in MPM malignancy.

7.7 ASS1

ASS1 is the argininosuccinate synthase 1 that catalyzes the penultimate step of the arginine biosynthetic pathway. In normal cells, ASS1 is a ubiquitous enzyme but its level of expression differs among different cell types and can be regulated by many extracellular factors. Levels of ASS vary markedly in a wide spectrum of tumour tissues as compared with their corresponding normal counterparts. Elevated levels of *ASS1* expression have been found in human epithelial ovarian cancer, in stomach cancer, in NSCLC and in colon cancer (Szlosarek et al. 2007; Rho et al. 2008). By contrast, reduced or undetectable levels of ASS1 have been found in the majority of melanoma, hepatocellular carcinoma (HCC), renal cell carcinoma, prostate cancers (Dillon et al. 2004), pancreatic cancer (Bowles et al. 2008) and in 50% of mesotheliomas (Szlosarek et al. 2006). The mechanisms that control ASS expression in these tumour types remain elusive. These ASS-negative

tumours are unable to synthesize their own arginine and, for this reason, they are sensitive to systemic Arg deprivation. The exposition of these tumours to Arg-degrading enzymes (as the pegylated arginine deaminasi or ADI-PEG20) has shown good response in ASS1-negative malignant melanoma (Ott et al. 2013) and HCC patients (Yang et al. 2010); the same strategy have been proposed for MPM ASS1-negative patients (Delage et al. 2010; Szlosarek et al. 2016; Burki 2016). The treatment with ADI-PEG20 gave a significant improvement in progression free survival (PFS) above the current standard of care (Szlosarek et al., 2013-2016); this is the first biomarker-driven study and first randomized trial in a decade, since the publication of antifolates with cisplatin (Vogelzang et al., 2003), to show a 50% reduction in the risk of disease progression in MPM patients.

Despite these promising results, the onset of drug-resistance limits the therapeutic efficacy: the re-expression of ASS1 has been associated with resistance to ADI-PEG20 treatment in melanoma (Feun et al., 2008; Tsai et al. 2009; Long et al., 2013) and the reactivation of ASS1 expression in lymphoma cell lines rescued them from ADI-PEG20 cytotoxicity (Delage et al. 2012). Tsai et al. observed that ASS1 expression is inducible by arginine deaminase treatment and that the overexpression of c-Myc induced ASS1 expression while HIF-1α suppressed c-Myc-induced ASS1 expression (Tsai et al. 2009).

Moreover ASS1 has been linked with chloroquine (an autophagy inhibitor drug) and cisplatin resistance: overexpression of ASS1 in mesothelioma cells reduced their sensitivity to chloroquine toxicity (Battisti et al. 2012); in ovarian cancer, the silencing of ASS1 has induced a resistance to platinum-induced cell death while, at the same time, sensitizing to arginine degradation (Nicholson et al. 2009); on the other hand cisplatin-resistant lung cancer cells showed high level of ASS1 expression (Wangpaichitr et al. 2012) and *ASS1* silencing in MPM spheroids increased the apoptotic response to cisplatin plus pemetrexed, (Barbone et al. 2016) rather suggesting an important contribution to the onset of cisplatin resistance.

ASS1 has been found overexpressed in mesothelioma tissues in three independent trascriptome studies (Melaiu et al. 2011) and in an independent set of mesothelioma tissues compared to non-malignant tissues, at mRNA level (Melaiu et al. 2015); ASS1 overexpression has been also found, at protein level, in paired samples, in mesothelioma tumour compared to adjacent normal tissues, furthermore ASS1 upregulation has been observed in mesothelioma spheroids compared to monolayer mesothelioma cells but not in the normal mesothelial cells (Barbone et al. 2016). These results suggest that a significant number of patients with mesothelioma will have elevated ASS1 expression. Likely ASS1 positive patient cannot benefit from many different therapeutic strategy

due to the onset of drug resistance previously described. Thus, while ASS1 deficiency is undoubtedly of interest in MPM, ASS1 overexpression also deserves attention. (Barbone et al 2016). Interestingly we observed that the depletion of *ASS1* in mesothelioma cell lines (showing *ASS1* overexpression compared to the non-malignant cell line Met5A) led to an increased caspase 3/7 activity compared to the treatment with siCTRL, suggesting an increment of apoptosis as recently observed in mesothelioma spheroids by Barbone (Barbone et al. 2016). Moreover we observed that *ASS1* silencing caused a significant decrease in proliferation and in colony formation ability of mesothelioma cells providing evidence for an important role of ASS1 in MPM malignancies.

7.8 *SOD1*

Emerging evidences from several groups report that *SOD1* is overexpressed in different types of cancers: in NSCLC (Glasauer et al. 2013), in lung adenocarcinoma (Somwar et al. 2011) and in breast cancer (Papa et al. 2014 (B)), in primary human leukemia cells and in primary ovarian cancer cells (Hileman et al. 2004); moreover it has been observed that in primary human multiple myeloma samples, increased gene expression of SOD1 correlated with cancer progression, high-risk disease, and adverse overall and event-free survival outcomes (Salem et al. 2015).

The upregulation of SOD protein expression was associated with the intrinsic oxidative stress of cancer cells (malignant cells in general are more active than normal cells in the production of ROS), likely SOD upregulation is a mechanism to tolerate increased ROS stress (Hileman et al. 2004). In breast cancer only SOD1, and not SOD2, is responsible of this protective mechanism: Papa et al. observed that during transformation of breast cancer cells they undergo a SOD switch from SOD2 to SOD1. In breast cancer the regulator of SOD2 activity, SIRT3, is usually decreased and this cause SOD2 downregulation that is promoted also by activation of oncogenes, such as Ras. In absence of SOD2, SOD1 activity increase to keep low ROS levels (Papa et al. 2014 (A))

SOD1 expression in MPM has not yet been studied extensively but results from two independent transcriptome studies and from the validation performed by our group on MPM tissues and cell lines confirmed the upregulation of *SOD1* in MPM compared to normal tissues (Melaiu et al. 2011 and 2015). It is known that MPM is an oxidative stress-induced cancer (Chew et al.2015; Benedetti et al. 2015) and recently has been observed that asbestos, one of the major etiological factor for MPM, induces oxidative stress (Pietrofesa et al. 2016). Likely a similar mechanism to that

suggested for breast cancer, could be responsible for SOD1overexpression in MPM tissues and cell lines.

In our experimental model SOD1 silencing caused an increment of caspase 3/7 activity in all the cell line treated; this was previously observed also by Huang (Huang et al. 2000) and, in lung cancer cells, by Somwar (Somwar et al.2011) and Glasauer (Glasauer et al. 2014); in particular Glasauer described a decrease of the antiapoptotic factor MCL1 as a consequence of H_2O_2-dependent activation of P38 MAPK after ATN-224 treatment (Glasauer et al. 2014);. Furthermore, SOD1 knockout influenced the proliferation rate of three mesothelioma cell lines, resulting in a decreased proliferation of Mero14, Mero25 and NCI-H28 cells and reducing Mero25 ability to form colonies. This is in agreement with the promotion of cell death and inhibition of cell proliferation by ATN-224 (a SOD1 specific inhibitor) verified in myeloid leukemia cells (Chen and Kan 2015). The inhibition of SOD1 by ATN-224 in leukemia cells increases intracellular oxidants, and induces peroxynitrite-dependent cell death decreasing viable cells number; moreover it also targets the mitochondria, decreasing both cytochrome c oxidase (CcOX) activity and mitochondrial membrane potential (Lee et al. 2013). On the other side, the overexpression of SOD1 in lung cancer cells promotes growth without affecting cell cycle progression and cells overexpressing SOD1 had a lower frequency of basal apoptosis, implying that SOD1 promotes growth by increasing survival (Somwar et al.2011). These findings support the notion that cells with increased SOD1 level may have a selective advantage during tumourigenesis (Somwar et al.2011).

It has been observed that the inhibition of SOD causes accumulation of cellular O(2-) and leads to free-radical-mediated damage to mitochondrial membranes, the release of cytochrome c from mitochondria and apoptosis of the cancer cells (Huang et al. 2000). These results indicate that targeting SOD may be a promising approach to the selective killing of cancer cells (Huang et al. 2000). The increase oxidative stress in cancer cell forces them to rely more on antioxidant enzyme for O(2)(-) elimination, making cancer cells more vulnerable to SOD1 inhibition than normal cells: interestingly SOD1 inhibition has the potential to selectively kill cancer cells by exploiting their vulnerability to damage by further ROS insult without causing substantial stress to normal cells with lower basal levels of ROS. Thus targeting the ability of cancer cells to adapt to and survive oxidative stress is an appealing therapeutic strategy (Hileman et al. 2004; Nicco et al. 2008; Trachootham et al. 2009) and that mechanism-based combinations of SOD inhibitors with free-radical-producing agents may have clinical applications (Huang et al. 2000).

Furthermore this therapeutic combination could be helpful in overcoming drug resistance as the upregulation of antioxidant defenses can impact drug resistance: Tome et al. demonstrated that

upregulation of SOD and catalase, in a lymphoma model , results in oxidative stress resistance and multi-drug chemoresistance (Tome et al. 2012). The knockdown of SOD1 sensitizes cisplatin-resistant human ovarian cancer cells suggesting that SOD1 is a key determinant of cisplatin resistance (Brown et al. 2008; Kim et al. 2010). Hour discovered that cisplatin, inducing the expression of CEBPD in human urothelial carcinoma cells, induces SOD1expression via direct promoter transactivation, leading to chemotherapy resistance (Hour et al. 2010).

Finally SOD1 promotes growth of cancer cells, including mesothelioma cells, and plays a survival role in cancer cells protecting them from the intrinsic high levels of ROS; moreover it has an important role in cisplatin resistance and modulation of its activity may overcome this resistance and ultimately lead to improved clinical outcomes in SOD1-overexpressing MPM.

7.9 *RAN*

RAN (ras-related nuclear protein) is a small GTP binding protein belonging to the RAS superfamily. It is abundantly expressed in many human cancers while in most normal tissues in vivo is present at low levels (Xia et al. 2008). *RAN* is overexpressed in lung cancer, where the expressional level on mRNA and protein in III stage tissues is higher than that of I and II stages in lung squamous cell carcinoma (Yan et al. 2010); it is overexpressed in NSCLC (Røe et al. 2010) with a higher expression level in highly invasive than in low invasive cells (Ning et al. 2013), in clear cell renal cell carcinoma (Abe et al. 2008), in ovarian cancer (Barre` s et al. 2010), in Pancreatic ductal adenocarcinoma (Saxena et al. 2013), in glioblastoma multiforme (Guvenc et al. 2013), in breast cancer (Vaidyanathan et al. 2016)

Interestingly, in breast cancer, the majority of RAN GTPase components are overexpressed and in particular those involved in nuclear export and mitotic spindle assembly but not nuclear import. The overexpression of these components strongly correlates with chromosome instability and marks poor breast cancer patient prognosis suggesting that, increased nuclear export *(of, for instance, pRb, p53, p73, BRCA1, p21, p27, E2F4, IκB, survivin)*, rather than spindle defects, mainly drives CIN and tumourigenesis of breast cancer (Vaidyanathan et al. 2016).

Regarding MPM, *RAN* gene has been found upregulated, in a statistical significant way, in three independent transcriptome studies on mesothelioma tissues (Melaiu et al. 2011) and these results has been further validated in an independent set of mesothelioma tissues and cell lines (Melaiu et al. 2015). Moreover it has been suggested as a new potential co-target for mesothelioma treatment (Røe et al. 2010).

Until now little is known about the role of *RAN* in malignant pleural mesothelioma; the present study revealed a high influence of RAN in the proliferation, in the apoptosis, in the colony formation ability of mesothelioma cells, highlighting an important role of this upregulated gene in the carcinogenesis of the MPM. Emerging evidences revealed that Ran signalling becomes a dominant pathway for tumour cell maintenance (Ly et al. 2010; Xia et al. 2008) in fact RAN ablation in different tumour cells triggered defects in mitotic spindle assembly, mitochondrial dysfunction with discharge of mitochondrial apoptogenic proteins, suppression of cell proliferation, decrease of cell adhesion and loss of cell viability by activation of caspase-dependent cell death (Kurisetty et al. 2008; Xia et al. 2008; Barres et al. 2010; Deng et al. 2013). Interestingly, despite the presence of RAN protein in non-tumourigenic Met5A cells, RAN silencing in this cell line did not elicit significant changes in proliferation, caspase activation and colony formation ability compared to the treatment with siCTRL. This result is in agreement with previous studies where Ran silencing in various normal cell types was well tolerated and did not cause mitotic defects or cell death suggesting a "cancer-specific" utilization of Ran signalling for maintenance of cell viability (Xia et al. 2008). These characteristics make it a suitable anti-cancer target (Røe et al. 2008) as suggested by Barres (Barres et al. 2010).

The reasons why non tumourigenic cells tolerate better *RAN* knockdown could be due, not only to the higher levels present in cancer tissues and cell lines but also to the interaction of RAN with oncogenic pathways in cancer cells: in fact the association of overexpression of Ran in clinical specimens with poor patient outcome is dramatically enhanced in cancers with c-Met or osteopontin expression, or with oncogenic mutations of Kras or PI3K/Akt/mTORC1 and/or Ras/MEK/ERK pathways (Yuen et al. 2012). Recently it has been suggested that cancer cells with an activated oncogenic pathways, including Met activation, require Ran for growth and survival: Yuen et al. observed that the knockdown of Ran leads to a reduction of Met receptor expression in several breast and lung cancer cell lines, suppressing HGF expression and the Met-mediated activation of the Akt pathway, as well as cell adhesion, migration, and invasion (Yuen et al. 2016) Moreover, Yuen showed that cancer cells with KRas activating mutation or Pten deletion are more sensitive to Ran-silencing induced apoptosis. In 2015 Schnepp et al. demonstrated that *RAN* is involved in promotion of neuroblastoma tumourigenesis through LIN28B-RAN-AURKA signalling and in particular the oncogene RAN is one of the most important downstream effectors of LIN28B. LIN28B increases RAN expression by promoting RAN Binding Protein 2 expression and by directly binding RAN mRNA and the resulting overexpression of RAN promotes the phosphorylation and activation of AURKA in neuroblastoma (Schnepp et al. 2015), as previously

observed by Tsai, in Xenopus model, and by Trieselmann, in Hela cells (Tsai et al., 2003; Trieselmann et al. 2003). Given that AURKA, as well as RAN, has been found upregulated in mesothelioma tissues, in three independent trascriptome studies (Melaiu et al. 2011) we could hypothesized a similar mechanism in MPM; it might be worth it to study in deep this pathway in MPM.

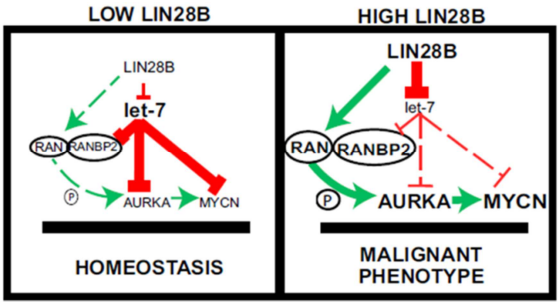


Fig. 108: RAN and malignant phenotype (Schnepp et al. 2015)

7. 10 *CDH11*

CDH11 gene encodes a type II classical cadherin from the cadherin superfamily, integral membrane proteins that mediate calcium-dependent cell-cell adhesion.

CDH11 expression is elevated in human brain tumours correlating with higher tumour grade and decreased patient survival. (Schulte et al. 2013). Moreover it seems to contribute to invasive phenotype as observed in breast cancer (Li et al. 2011; Luo et al. 2013) and in glioma by Delic (Delic et al. 2012); and to confirm this hypothesis, CDH11 has been found overexpressed in certain invasive tumours (Pishvaian et al., 1999; Chu et al., 2008; Huang et al., 2010). Earlier studies suggested that CDH11 was a candidate oncogene for some tumour types like prostate cancer (Chu et al., 2008; Huang et al., 2010), breast cancer (Pishvaian et al., 1999) and oral cancer (Choi et al., 2008). Conversely in 2010 has been proposed as a tumour suppressor in murine retinoblastoma as it promoted cell death in vivo and in vitro (Marchong et al. 2010) and in 2012 has been highlighted its pro-apoptotic properties and it was found to inhibit Wnt/β-catenin and AKT/Rho A signalling (Li et al. 2012). Regarding MPM, CDH11 has been found overexpressed in tissues and cell lines (Melaiu et al. 2011; 2015) and we confirmed the upregulation in two MPM cell lines at protein level. After CDH11 silencing we only observed a statistically significant increment of caspase activity in Mero25: the only cell lines that showed, simultaneously, a significant upregulation of CDH11 at mRNA level and a significant downregulation after treatment, both at mRNA and protein level. Mero25 cells silenced with si*CDH11* showed also a slight trend towards decreased proliferation,

although not statistically significant (p = 0,06). These results cannot define the role played by CDH11 in MPM carcinogenesis; in order to better clarify it, it would be useful to perform a phenotypic screening with others siRNA sequences and to evaluate the relations between Wnt/β-catenin and AKT/Rho A signalling with CDH11 in MPM.

7.11 *IMP3*

IMP3, also called IGF2BP3, is one of the three members of the IGF2 mRNA binding protein family (IGF2BPs) that exerts a post-transcriptional control of gene expression. In vitro studies revealed that IGF2BPs serve as post-transcriptional fine-tuners modulating the expression of genes implicated in the control of tumour cell proliferation, survival, chemo-resistance and metastasis (Lederer et al. 2014). IMP3 expression has been studied in many human neoplasms with growing evidence that it is a biomarker of enhanced tumour aggressiveness (Findeis-Hosey and Xu 2012). It is associated with aggressive and advanced cancers and is specifically expressed in malignant tumours but is not found in adjacent benign tissues (Gong et al. 2014). IMP3 is overexpressed in a large number of tumours: in triple-negative breast cancer (Walter et al. 2009; Sidoni et al. 2010), in cervical cancer (Danialan et al. 2013; Wei et al. 2013; Lastra et al 2014), in endometrial cancer (Mhawech-Fauceglia et al. 2010 and 2013; Fadare et al. 2013; Vercellini et al. 2013) in ovarian cancer (Zheng et al. 2008; Kobel et al. 2009), in colorectal cancer (Li et al. 2009; Lin et al. 2013), in prostate cancer (Ikenberg et al. 2010), in gastric adenocarcinoma (Wang et al. 2010), in different type of liver cancer (Hart et al. 2012; Shi et al. 2013; Chen et al. 2013; Wachter et al. 2012), in pancreatic cancer (Schaeffer et al. 2009), in thyroid cancer (Jin et al. 2010), in lung cancer (Bellezza 2009), in sarcoma (Do et al. 2008) and in lymphoid cancer (Hartmann et al. 2012). And in most of the cases the expression of IMP3 correlates with unfavourable prognosis and metastasis: it has been suggested as a progression marker in malignant melanoma and it seems to play an important role in the regulation of the biologic behaviour of this tumour (Pryor et al. 2008). Recently high IMP3 levels (together with high Lin28B) in breast cancer were associated with poor survival and higher risk of developing chemoresistance (Hsu et al. 2015) and were significantly associated with shorter periods of metastasis-free and disease-free survival in phyllodes tumours of the breast (Takizawa et al. 2016). Moreover extensive studies have shown that IMP3 oncoprotein is not only a prognostic biomarker but also a diagnostic molecule for different types of cancers (Findeis-Hosey and Xu 2011). Regarding MPM, different studies proposed IMP3 staining as a useful marker for distinguishing neoplastic cells from reactive mesothelial cells in effusion samples, alone (Ikeda et

al. 2010), or in combination with calretinin (Hanley et al. 2008), or with GLUT1 (Lee et al. 2013) and its overexpression in MPM has been confirmed by several studies (Hanley et al.2008; Ikeda et al. 2010; Ikeda et al. 2011; Shi et al.2011; Lee et al. 2013; Okazaki et al. 2013; Minato et a. 2014)
Different studies demonstrated that IMP3 expression promotes an aggressive phenotype of tumour-derived cells in vitro and its upregulated expression in aggressive malignancies provides strong evidence that is a powerful post-transcriptional oncogene enhancing tumour growth, drug-resistance and metastasis (Lederer et al. 2014): the expression of IMP3 is associated with epithelial-mesenchymal transition in breast cancer (Su et al. 2014), promotes tumour formation and invasion in oral squamous cell carcinoma (Lin et al.2011), enhanced proliferation and migration and significantly increased tumourigenesis and metastatic ability in nude mice (Sheen et al. 2015). It was also confirmed that IMP3 had an important role in melanoma invasion and metastasis through regulating HMGA2 mRNA expression (Sheen et al. 2015). In our experimental model we observed a possible role of IMP3 in promoting MPM proliferation and colony formation ability and this is in agreement with previous findings in others tumour models (Hsu et al. 2015; Lederer et al. 2014; Sheen et al. 2015). Moreover *IMP3* silencing induced caspase 3/7 activity in Mero25 and IstMes2 cells, suggesting a survival role of *IMP3* in MPM cells as previously observed by Liao in human chronic myeloid leukemia cells (Liao et al. 2011). IMP3 seems to influence also MPM migration ability as shown in Mero25 and IstMes2 cell lines by our study, and in pancreatic cancer cells by Pasiliao (Pasiliao et al. 2015) and in melanoma cells by Sheen (Sheen et al. 2015). These findings suggest IMP3 as powerful biomarker and candidate targets for MPM therapy.

RAN and _IMP3_ in mesothelioma, future perspectives.

Evidences from literature suggest that the overexpression of IMP3, observed in MPM, could be linked to RAN overexpression through LIN28B upregulation. LIN28B is overexpressed in cancer cells and it is known as a promoter of cancer cell proliferation and invasion (Madison et al. 2013; Shao et al. 2015). Hsu observed a correlation between high *IMP3* levels and high LIN28B levels with the poorest 5-year survival rates in ovarian cancer. Interestingly Nguyen demonstrated that IMP3 acts as an oncogene downstream of Lin28b, suggesting an important functional role of LIN28B in driving liver malignancy (Nguyen et al. 2014). The proteomic analysis performed by Hafner (Hafner et al. 2013) showed that IMP3 protein levels increased when LIN28B was overexpressed and decreased when LIN28B was knocked-down, providing evidence of a direct link between them.

Recently Schneppet demonstrated that LIN28B/let-7 indirectly promote RAN protein expression, one of the upregulated gene in MPM previously discussed, by promoting RAN Binding Protein 2 (RANBP2) expression and by directly binding RAN mRNA. Moreover has been observed a convergence of LIN28B and RAN signaling on Aurora kinase A activity.

The overexpression of Aurora kinase A, that is a cell-cycle control gene, has been related to a more aggressive clinical course of MPM (Lopez et al. 2006)

Interestingly has been demonstrated that Aurora kinase targeting in mesothelioma has an antiproliferative effect (Crispi et al. 2010) These results encourage us to further study the interaction between LIN28B/LET7/IMP3 and LIN28B/RAN/AURKA in mesothelioma. Potentially the inhibition of LIN28B in mesothelioma, downregulating both RAN and IMP3 expression levels, could impair cancer cell survival, growth and invasion providing a powerful approach to manage MPM.

7.12 *EIF4G1*

The protein encoded by this gene is a component of the multi-subunit protein complex EIF4F. eIF4F is a multi-subunit complex, the composition of which varies with external and internal environmental conditions. It is composed of at least EIF4A, EIF4E (cap-binding) and EIF4G1/EIF4G3. This complex facilitates the recruitment of mRNA to the ribosome, which is a rate-limiting step during the initiation phase of protein synthesis. This gene was found overexpressed in squamous cell carcinoma of the lung (Bauer et al. 2002; Comtesse et al. 2007) in chronic lymphocytic leukemia (Shull et al. 2015), in serous ovarian cancer (Li et al. 2016) and in non-small cell lung cancer (NSCLC) (Attar-Schneider et al. 2016). Its overexpression has been significantly associated with an advanced tumour stage in serous ovarian cancer (Li et al. 2016), with a pro-survival phenotype in chronic lymphocytic leukemia (Shull et al. 2015) and the coexpression of p-eIF4G with p-4EBP1 correlated with a high tumour proliferation rate in breast cancer (Rojo et al. 2007)

Overexpression of eIF4G1 seems to be responsible of malignant transformation (Fukuchi et al. 1997) and promotes formation of inflammatory breast cancer tumour emboli by enhancing translation of IRES-containing p120 mRNAs (Silvera et al. 2009); increased expression of EIF4G1 was found to selectively increase translation of survival, growth arrest, and DNA damage response mRNAs that are important in cell survival and DNA repair following genotoxic DNA damage, preventing autophagy and apoptosis (Badura et al. 2012); thus EIF4G1 expression promotes resistance to genotoxic DNA damage. In particular, Badura showed that EIF4G1 mediates a

transcriptional–translational feed-forward loop for HIF1α and survivin expression that promotes cell survival, in that Survivin transcription is stimulated by HIF1α, the mRNA of which shows strong EIF4G1-dependent IRES activity. Higher levels of EIF4G1 also establish a feed-forward pathway for increased cell survival through cell cycle arrest following DNA damage (Badura et al. 2012). Moreover EIF4G1 may contribute to the occurrence and metastasis of ovarian cancer and has been proposed as a potential therapeutic target for the treatment of ovarian cancer (Li et al. 2016).

Regarding MPM, EIF4G1 has been found overexpressed in two independent trascriptome studies and in the validation study performed by our group in MPM tissues (Melaiu et al. 2011; 2015) In 2009 has been observed that the EIF4F complex (to which EIF4G1 belongs) is stimulated in mesothelioma by the activation of both PI3K and ERK1/2 pathways after Insulin-like growth factor I (IGF-I) stimulation (Jacobson et al. 2009). The inhibition of the interaction between EIF4E and the scaffolding protein EIF4G1, inhibiting the formation of the active eIF4F complex and suppressing cap-mediated translation, resulted in significantly decreased tumourigenicity of murine xenografts and in the disruption of IGF-I-mediated growth, motility, and colony formation (Jacobson et al. 2009). In agreement with these findings, our phenotypic screening after *EIF4G1* silencing, revealed a decreased proliferation, colony formation and proliferation rate in some of the MPM cell lines analysed. Moreover the caspase 3/7 activity increased in two cell lines highlighting a survival role of this gene. Our results suggest a role in the malignancy of MPM but it is necessary to further understand how *EIF4G1* influences the translational control of genes involved in the pathogenesis of MPM and why it is overexpressed in MPM.

7.13 *MCT4 and MCT1, BSG, CAIX*

MPM is a highly chemoresistant cancer; several pathways and mechanisms are involved in drug resistance and the adaptation to hypoxia is one of the main factor that contributes to the resistance of cancer cells to chemotherapy and radiation treatment (Riganti et al. 2008; Maftouh et al. 2014). Increasingly evidences reports that MPM is a very hypoxic tumour (Giovannetti et al. 2016) with significant areas of hypoxia, particularly in dominant tumour masses (Francis et al. 2015). It is known that hypoxia induces a HIF- 1-mediated signaling cascade that results in nuclear translocation of HIF-1α, in the activation of hypoxia-regulated genes, including MCT1/4 and CAIX and in the"glycolytic switch" that results in increased production and export of lactate, leading to a decline in extracellular pH (McDonald et al. 2012)

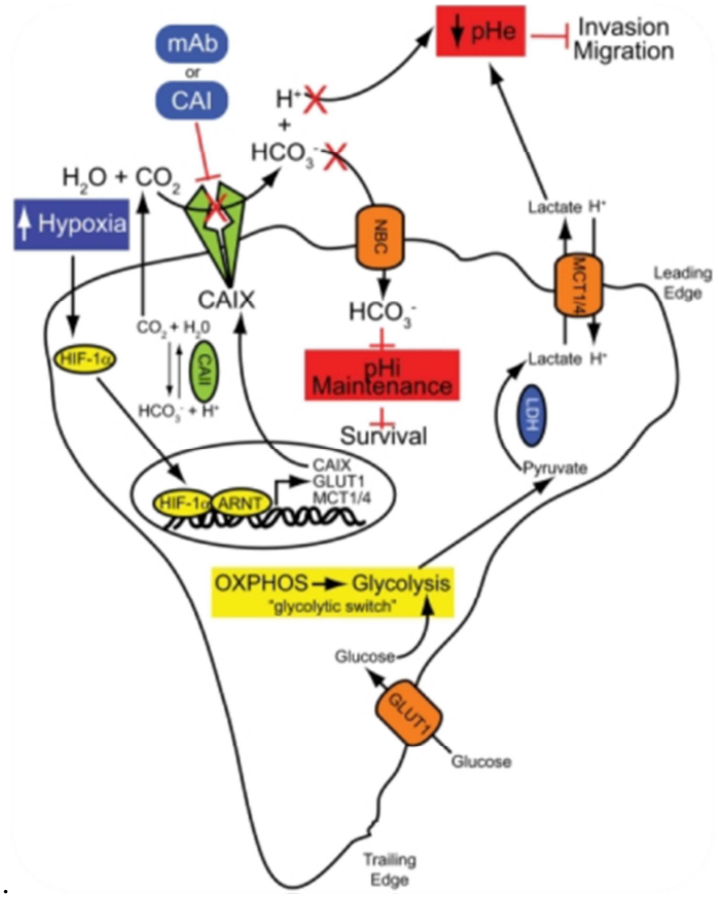


Fig. 109: Activation of hypoxia-regulated genes (MCT1, MCT4, CAIX and GLUT1).
Hypoxia induces HIF-1α traslocation and activation of hypoxia regulated genes, including MCT1, MCT4 and CAIX. Cells exposed to hypoxia change their metabolism toward a glicolitic pathway that leds to a decline in extracellular pH. (McDonald et al. 2012)

Increasing evidences report an important role of metabolic microenvironment in carcinogenesis: metabolic reprogramming is a hallmark of cancer and may offer novel treatment opportunities (Doherty et al. 2013); in particular MCT1 and MCT4 that resulted overexpressed in different types of cancers, were associated with shorter overall survival in melanoma (Pinheiro et al. 2016) and in oral cavity tumours (Simões-Sousa et al. 2016) and they has been proposed as new potential targets for anticancer therapy. (Chiche et al. 2013; Doherty et al. 2013). Interestingly MCT1 has a cooperative role with BSG in determining cisplatin resistance in bladder cancer (Afonso et al. 2015) and given its requirement for stabilizing and localizing MCTs to the cell membrane (Kirk et al. 2000), targeting BSG could be also an attractive antitumour strategy (Doherty et al. 2013). Moreover has been observed by Gallagher (Gallagher et al.2007) that the upregulation of BSG in metastatic cancer cells is coupled to the overexpression of MCT4 and their expression correlate with worse prognosis across many cancer types (Bovenzi et al. 2015), suggesting a molecular link between two hallmarks of metastatic cancer: the glycolytic switch and increased expression of BSG. It is known that tumour cells have an increased demand for nutrients and they overcome this necessity through an enhanced glycolysis associated with lactate production (Le Floch et al. 2011), for this reason tumour cells must find a way to eliminate lactic acid to prevent cellular acidification: this is achieved by the upregulation of MCT4, a H+-coupled lactate transporter (Ganapathy et al. 2009); MCT4 is not only important for the acid-resistant phenotype, but also for the hyper-glycolytic phenotype: by exporting newly formed lactate it allows continuous conversion of pyruvate to lactate and, therefore, continuous aerobic glycolysis (Pinheiro et al. 2012). *MCT4* is overexpressed in several types of cancer: in prostate cancer (Hao et al. 2010), in HPV-induced squamous cell carcinoma of the uterine cervix (Pinheiro et al. 2014), in stem-like glioblastoma cells (Lim et al. 2014) in adeno-NSCLC (Meijer et al. 2012) moreover the overexpression in prostate cancer is associated with poor prognosis (Pértega-Gomes et al. 2011) and its expression is increased in triple negative breast cancer and correlates independently with clinical outcome (Doyen et al. 2014). Interestingly, in our set of MPM cases, analysed through tissue microarray IHC, the cases with lower MCT4 expression showed longer survival and the non-malignant pleura samples did not express MCT4, thus MCT4 could be a specific and powerful target for MPM therapy. Recent evidence demonstrates that MCTs are involved in cancer cell uptake of chemotherapeutic agents, in this way they can act as "Trojan horses" mediating the entry of chemotherapeutic agent into the cells and selectively kill cancer cells (Baltazar et al. 2014).

MCT4 was highly overexpressed in MPM tissues compared to the mesothelial cells of the non-malignant pleura samples and its silencing revealed a survival role in IstMes2 cells, showing

increased caspase 3/7 activity and resulted in reduced tumour cell proliferation and migration. The others MPM cells did not showed increased caspase 3/7 activity but this do not mean that MCT4 do not have a survival role in MPM, infact in 2013 has been observed that MCT4 silencing in MPM cells did not affected caspase 3/7 activity but caused a significant increase in early apoptosis, detected as the annexin V-PEpositive and 7-AAD-negative population. All the MPM cells showed a dependence on MCT4 expression in maintaining their proliferation rate, in fact MCT4 silencing caused a significant decrease of proliferation in all the MPM cells treated, moreover it decreased the colony formation ability of the MPM cells treated; these results are in agreement with the previous findings made by Mogi (Mogi et al. 2013) in others MPM cell lines. *MCT4* silencing affected also the migration ability of MPM cells suggesting a potential involvement of MCT4 in the metastatic potential of cancer cells. Previous findings on lung cancer cells support this hypothesis: MCT4 seems to be involved in human cancer cell invasiveness, in fact the numbers of invading cells were potently decreased by transfection with siMCT4 (Izumi et al. 2011).

Our study suggests that MCT4 could be a clinically relevant target in MPM: it is highly expressed in MPM while normal pleura samples did not express it; it plays an important role in sustaining MPM cell proliferation and colony formation ability and seems to play also a role in facilitating MPM cell migration. Further study is required to confirm MCT4 overexpression and to elucidate how MCT4 inhibitor could affect MPM malignancy.

8 Conclusions and future perspectives

This work gives novel insights in the knowledge of the driver genes of MPM malignancy, improving the understanding of the biology of mesothelioma. The results obtained provided new potential therapeutic target (like RAN and IMP3) that may overcome the chemo- resistance of the current therapies (as cisplatin) leading to improved clinical outcomes in MPM. Moreover the MCT4 upregulation observed in MPM tissues compared to normal pleura prompted us to further study this target. Future studies will be performed by forcing the expression of specific genes with the expectation to notice opposite results as compared to those observed following gene silencing. Moreover, future studies could be aimed to better understand the interactions among overexpressed genes and to discover their metabolic pathways to gain kownledge on the mechanisms underlying the selective advantages gained by cancer cells.

REFERENCES

Abe H, Kamai T, Shirataki H, Oyama T, Arai K, et al. High expression of Ran GTPase is associated with local invasion and metastasis of human clear cell renal cell carcinoma. Int J Cancer. 2008;122:2391–2397.

Afonso J1,2, Santos LL3,4, Miranda-Gonçalves V1,2, Morais A5, Amaro T6, Longatto-Filho A1,2,7,8, Baltazar F1,2. CD147 and MCT1-potential partners in bladder cancer aggressiveness and cisplatin resistance. Mol Carcinog. 2015 Nov;54(11):1451-66. doi: 10.1002/mc.22222. Epub 2014 Sep 27.

Alberts Bruce, Johnson Alexander, Lewis Julian, Raff Martin, Roberts Keith, and Walter Peter. Molecular Biology of the Cell. 4th edition. DNA Repair. Bookshelf ID: NBK26879 (2002)

Anania MC , Sensi M, Radaelli E, Miranda C, Vizioli MG, Pagliardini S, Favini E, Cleris L, Supino R, Formelli F, Borrello MG, Pierotti MA, Greco A. TIMP3 regulates migration, invasion and in vivo tumourigenicity of thyroid tumour cells. Oncogene; 30(27):301123 (2011).

Attar-Schneider O, Drucker L, Gottfried M. Migration and epithelial-to-mesenchymal transition of lung cancer can be targeted via translation initiation factors eIF4E and eIF4GI. Lab Invest. 2016 Sep;96(9):1004-15. doi: 10.1038/labinvest.2016.77.

Bachman KE, Herman JG, Corn PG, Merlo A, Costello JF, Cavenee WK, Baylin SB, Graff JR. Methylation-associated silencing of the tissue inhibitor of metalloproteinase-3 gene suggest a suppressor role in kidney, brain, and other human cancers. Cancer Res.;59(4):798-802 (1999).

Badura M, Braunstein S, Zavadil J, Schneider RJ. DNA damage and eIF4G1 in breast cancer cells reprogram translation for survival and DNA repair mRNAs. Proc Natl Acad Sci U S A. 2012 Nov 13;109(46):18767-72. doi: 10.1073/pnas.1203853109. Epub 2012 Oct 29.

Baenke F, Dubuis S2, Brault C3, Weigelt B4, Dankworth B3, Griffiths B1, Jiang M5, Mackay A6, Saunders B5, Spencer-Dene B7, Ros S1, Stamp G7, Reis-Filho JS4, Howell M5, Zamboni N3, Schulze A Functional screening identifies MCT4 as a key regulator of breast cancer cell metabolism and survival. J Pathol. 2015 Oct;237(2):152-65. doi: 10.1002/path.4562.

Baker AH , Zaltsman AB, George SJ, Newby AC. Divergent effects of tissue inhibitor of metalloproteinase1, 2, or 3 overexpression on rat vascular smooth muscle cell invasion, proliferation, and death in vitro. TIMP3 promotes apoptosis. J Clin Invest;101(6):147887 (1998).

Baker AH, George SJ, Zaltsman AB, Murphy G, Newby AC. Inhibition of invasion and induction of apoptotic cell death of cancer cell lines by overexpression of TIMP-3. Br J Cancer; 79(9-10):1347-55 (1999).

Baltazar F1, Pinheiro C2, Morais-Santos F3, Azevedo-Silva J4, Queirós O5, Preto A4, Casal M4. Monocarboxylate transporters as targets and mediators in cancer therapy response. Histol Histopathol. 2014 Dec;29(12):1511-24. doi: 10.14670/HH-29.1511. Epub 2014 Jun 12.

Barbone D, Van Dam L, Follo C, Jithesh PV, Zhang SD, Richards WG, Bueno R, Fennell DA, Broaddus VC. Analysis of Gene Expression in 3D Spheroids Highlights a Survival Role for ASS1 in Mesothelioma. PLoS One. 2016 Mar 16;11(3):e0150044. doi: 10.1371/journal.pone.0150044.

Barrès V, Ouellet V, Lafontaine J, Tonin PN, Provencher DM, et al. An essential role for Ran GTPase in epithelial ovarian cancer cell survival. Mol Cancer. 2010;9:272.

Batra S, Shi Y, Kuchenbecker KM, He B, Reguart N, Mikami I, You L, Xu Z, Lin YC, Clément G, Jablons DM. Wnt inhibitory factor-1, a Wnt antagonist, is silenced by promoter hypermethylation in malignant pleural mesothelioma Biochem Biophys Res Commun. 2006 Apr 21;342(4):1228-32.

Battisti S, Valente D, Albonici L, Bei R, Modesti A, Palumbo C. Nutritional stress and arginine auxotrophy confer high sensitivity to chloroquine toxicity in mesothelioma cells. Am J Respir Cell Mol Biol. 2012 Apr;46(4):498-506. doi: 10.1165/rcmb.2011-0195OC.

Bauer C, Brass N, Diesinger I et al. Overexpression of the eukaryotic translation initiation factor 4G (eIF4G-1) in squamous cell lung carcinoma. Int J Cancer 2002;98:181–185.

Bellezza G., A. Cavaliere, A. Sidoni IMP3 expression in non-small cell lung cancer Hum Pathol, 40 (2009), pp. 1205–1206

Benedetti S, Nuvoli B, Catalani S, Galati R. Reactive oxygen species a double-edged sword for mesothelioma. Oncotarget. 2015 Jul 10;6(19):16848-65.

Berman DW, Crump KS. Update of potency factors for asbestos-related lung cancer and mesothelioma. Crit. Rev. Toxicol. 2008;38(Suppl. 1):1–47.

Bertino P, Carbone M, Pass H Chemotherapy of malignant pleural mesothelioma. Expert Opin Pharmacother. 2009 Jan; 10(1):99-107.

Bianchi C1, Giarelli L, Grandi G, Brollo A, Ramani L, Zuch C. Latency periods in asbestos-related mesothelioma of the pleura. Eur J Cancer Prev. 1997 Apr;6(2):162-6.

Bibby AC, Tsim S, Kanellakis N, Ball H, Talbot DC, Blyth KG, Maskell NA, Psallidas I. Malignant pleural mesothelioma: an update on investigation, diagnosis and treatment. Eur Respir Rev. 2016 Dec;25(142):472-486. doi: 10.1183/16000617.0063-2016.

Black RA. TIMP3 checks inflammation. Nat Genet.;36(9):934-5 (2004).

Blander G, de Oliveira RM, Conboy CM, Haigis M and Guarente L: Superoxide dismutase 1 knock-down induces senescence in human fibroblasts. J Biol Chem 278: 38966-38969, 2003.

Bond M, Murphy G, Bennett MR, Amour A, Knauper V, Newby AC, Baker AH. Localization of the death domain of tissue inhibitor of metalloproteinase-3 to the N terminus. Metalloproteinase inhibition is associated with proapoptotic activity. J Biol Chem.; 275(52):41358-63 (2000).

Bornstein P. Diversity of function is inherent in matricellular proteins: an appraisal of thrombospondin 1. J Cell Biol; 130(3):503-6 (1995).

Bornstein Paul, Themis R. Kyriakides, Zhantao Yang, Lucas C. Armstrong, and David E. Birk. Thrombospondin 2 Modulates Collagen Fibrillogenesis and Angiogenesis. J Investig Dermatol Symp Proc. 2000 Dec;5(1):61-6.

Bovenzi CD1, Hamilton J2, Tassone P2, Johnson J3, Cognetti DM2, Luginbuhl A2, Keane WM2, Zhan T4, Tuluc M5, Bar-Ad V6, Martinez-Outschoorn U3, Curry JM2. Prognostic Indications of Elevated MCT4 and CD147 across Cancer Types: A Meta-Analysis. Biomed Res Int. 2015;2015:242437. doi: 10.1155/2015/242437. Epub 2015 Dec 8.

Bowles TL, Kim R, Galante J, Parsons CM, Virudachalam S, Kunng HJ, Bold RJ. Pancreatic cancer cell lines deficient in argininosuccinate synthetase are sensitive to arginine deprivation by arginine deiminase. Int J Cancer 2008;123:1950-5.

Bret C , Moreaux J, Schved JF, Hose D, Klein B. SULFs in human neoplasia: implication as progression and prognosis factors. J Transl Med; 9:72. doi: 10.1186/14795876972 (2011) .

Brown DP, Chin-Sinex H, Nie B, Mendonca MS, Wang M. Targeting superoxide dismutase 1 to overcome cisplatin resistance in human ovarian cancer. Cancer Chemother Pharmacol. 2009 Mar;63(4):723-30. doi: 10.1007/s00280-008-0791-x.

BÜLOW CHARLOTTE VON,1 LETICIA OLIVEIRA-FERRER,1 THOMAS LÖNING,2 FABIAN TRILLSCH,1 SVEN MAHNER,1 and KARIN MILDE-LANGOSCH Cadherin-11 mRNA and protein expression in ovarian tumours of different malignancy: No evidence of oncogenic or tumour-suppressive function Mol Clin Oncol. 2015 Sep; 3(5): 1067–1072.Published online 2015 Jul 1. doi: 10.3892/mco.2015.593

Burki TK. Arginine deprivation for ASS1-deficient mesothelioma. Lancet Oncol. 2016 Oct;17(10):e423. doi: 10.1016/S1470-2045(16)30446-6.

Buuren S, Groothuis-Oudshoorn K. MICE: Multivariate imputation by chained equations in R. Journal of statistical software 2011;45(3).

Cacciotti,P., R.Libener, P.Betta, F.Martini, C.Porta, A.Procopio, L.Strizzi, L.Penengo, M.Tognon, L.Mutti, and G.Gaudino. 2001. SV40 replication in human mesothelial cells induces HGF/Met receptor activation: a model for viral-related carcinogenesis of human malignant mesothelioma. Proc. Natl. Acad. Sci. U. S. A 98: 12032-12037.

Capkova L, Koubkova L, Kodet R. Expression of carbonic anhydrase IX (CAIX) in malignant mesothelioma. An immunohistochemical and immunocytochemical study. Neoplasma. 2014;61(2):161-9.

Carbone M, Bedrossian CW. The pathogenesis of mesothelioma. Semin Diagn Pathol. 2006 Feb;23(1):56-60.

Carbone M, Yang H. Molecular pathways: targeting mechanisms of asbestos and erionite carcinogenesis in mesothelioma. Clin Cancer Res. 2012 Feb 1;18(3):598-604. doi: 10.1158/1078-0432.CCR-11-2259.

Carbone,M. and C.W.Bedrossian. 2006. The pathogenesis of mesothelioma. Semin. Diagn. Pathol. 23: 56-60.

Castellana B, Escuin D, Peiró G, Garcia-Valdecasas B, Vázquez T, Pons C, Pérez-Olabarria M, Barnadas A, Lerma E. ASPN and GJB2 Are Implicated in the Mechanisms of Invasion of Ductal Breast Carcinomas. J Cancer; 3:175-83 (2012).

Ceresoli, G.L.; Zucali, P.A.; Favaretto, A.G, Grossi, F., Bidoli, P., Del Conte, G., Ceribelli, A., Bearz, A., Morenghi, E., Cavina, R., Marangolo, M., Parra, H.J., Santoro, A. Phase II study of pemetrexed plus carboplatin in malignant pleural mesothelioma. J. Clin. Oncol. 2006, 24, 1443–1448.

Ceresoli, G.L.; Zucali, P.A.; Gianoncelli, L.; Lorenzi, E.; Santoro, A. Second-line treatment for malignant pleural mesothelioma. Cancer Treat. Rev. 2010, 36, 24–32.

Chang IW, Li CF, Lin VC3, He HL4, Liang PI5, Wu WJ6, Li CC6, Huang CN7. Prognostic Impact of Thrombospodin-2 (THBS2) Overexpression on Patients with Urothelial Carcinomas of Upper Urinary Tracts and Bladders. J Cancer. 2016 Jul 8;7(11):1541-9. doi: 10.7150/jca.15696. eCollection 2016.

Chen J, Yao D, Zhao S, He C, Ding N, Li L, Long F. MiR-1246 promotes SiHa cervical cancer cell proliferation, invasion, and migration through suppression of its target gene thrombospondin 2. Arch Gynecol Obstet (2014).

Chen Y.L., Y.M. Jeng, H.C. Hsu, H.S. Lai, P.H. Lee, P.L. Lai, et al. Expression of insulin-like growth factor II mRNA-binding protein 3 predicts early recurrence and poor prognosis in intrahepatic cholangiocarcinoma Int J Surg, 11 (2013), pp. 85–91

Chen YL, Kan WM. Down-regulation of superoxide dismutase 1 by PMA is involved in cell fate determination and mediated via protein kinase D2 in myeloid leukemia cells. Biochim Biophys Acta. 2015 Oct;1853(10 Pt A):2662-75. doi: 10.1016/j.bbamcr.2015.07.025.

Cheon DJ, Tong Y, Sim MS, Dering J, Berel D, Cui X, Lester J, Beach JA, Tighiouart M, Walts AE, Karlan BY, Orsulic S. A collagen-remodeling gene signature regulated by TGF-β signaling is associated with metastasis and poor survival in serous ovarian cancer. Clin Cancer Res; 20(3):711-23 (2014).

Chetty C., Lakka S.S., Bhoopathi P., and Rao J. S. MMP-2 Alters VEGF Expression via αVβ3 Integrin-Mediated PI3K/AKT Signaling in A549 Lung Cancer Cells. Int J Cancer; 127(5): 1081–1095 (2010).

Chew SH, Toyokuni S2. Malignant mesothelioma as an oxidative stress-induced cancer: An update. Free Radic Biol Med. 2015 Sep;86:166-78. doi: 10.1016/j.freeradbiomed.2015.05.002.

Chiche J1, Ricci JE, Pouysségur J. Tumour hypoxia and metabolism -- towards novel anticancer approaches. Ann Endocrinol (Paris). 2013 May;74(2):111-4. doi: 10.1016/j.ando.2013.02.004. Epub 2013 Apr 15.

Choi P, Jordan CD, Mendez E, Houck J, Yueh B, Farwell DG, et al. Examination of oral cancer biomarkers by tissue microarray analysis. Arch Otolaryngol Head Neck Surg. 2008;134:539–546.

Chu K, Cheng CJ, Ye X, Lee YC, Zurita AJ, Chen DT, et al. Cadherin-11 promotes the metastasis of prostate cancer cells to bone. Mol Cancer Res. 2008;6:1259–1267.

Comtesse N, Keller A, Diesinger I, Bauer C, Kayser K, Huwer H, Lenhof HP, Meese E. Frequent overexpression of the genes FXR1, CLAPM1 and EIF4G located on amplicon 3q26-27 in squamous cell carcinoma of the lung. Int J Cancer. 2007 Jun 15;120(12):2538-44.

Concha-Barrientos M et al. Selected occupational risk factors. In: Ezzati M et al, eds. *Comparative quantification of health risks: global and regional burden of diseases attributable to selected major risk factors*. Geneva, World Health Organization (WHO) 2004:1651-1801.

Creaney J, Dick IM, Yeoman D, Wong S, Robinson Auto-antibodies to β-F1-ATPase and vimentin in malignant mesothelioma.BW PLoS One.2011 ;6(10):e26515.doi: 10.1371/journal.pone.0026515. Epub 2011 Oct 17 (A).

Creaney J, Francis RJ, Dick IM, Musk AW, Robinson BW, Byrne MJ, Nowak AK. Serum soluble mesothelin concentrations in malignant pleural mesothelioma: relationship to tumor volume, clinical stage and changes in tumor burden. Clin Cancer Res. 2011 Mar 1;17(5):1181-9. doi: 10.1158/1078-0432.CCR-10-1929. Epub 2010 Dec 21 (B).

Crispi S, Fagliarone C, Biroccio A, D'Angelo C, Galati R, Sacchi A, Vincenzi B, Baldi A, Verdina A. Antiproliferative effect of Aurora kinase targeting in mesothelioma. Lung Cancer. 2010 Dec;70(3):271-9. doi: 10.1016/j.lungcan.2010.03.005.

Cristaudo A, Foddis R, Vivaldi A, Guglielmi G, Dipalma N, Filiberti R, Neri M, Ceppi M, Paganuzzi M, Ivaldi GP, Mencoboni M, Canessa PA, Ambrosino N, Chella A, Mutti L, Puntoni R. Clinical significance of serum mesothelin in patients with mesothelioma and lung cancer. Clin Cancer Res. 2007 Sep 1;13(17):5076-81.

Czekierdowski A, Czekierdowska S, Danilos J, Czuba B, Sodowski K, Sodowska H, Szymanski M, Kotarski J. Microvessel density and CpG island methylation of the THBS2 gene in malignant ovarian tumours. J Physiol Pharmacol;59 Suppl 4:53-65 (2008).

Dalton LE, Clarke HJ, Knight J, Lawson MH, Wason J, Lomas DA, Howat WJ, Rintoul RC, Rassl DM, Marciniak SJ. The endoplasmic reticulum stress marker CHOP predicts survival in malignant mesothelioma. Br J Cancer. 2013 Apr 2;108(6):1340-7. doi: 10.1038/bjc.2013.66.

Danialan R., M. Assaad, J. Burghardt, P. Newcomb, R.W. Cartun, S. Mandavilli The utility of PAX8 and IMP3 immunohistochemical stains in the differential diagnosis of benign, premalignant, and malignant endocervical glandular lesions Gynecol Oncol, 130 (2013), pp. 383–388

Defamie V, Sanchez O, Murthy A, Khokha R. TIMP3 controls cell fate to confer hepatocellular carcinoma resistance. Oncogene; 10.1038/onc.2014.339 (2014).

Delage B, Luong P, Maharaj L, O'Riain C, Syed N, Crook T, Hatzimichael E, Papoudou-Bai A, Mitchell TJ, Whittaker SJ, Cerio R, Gribben J, Lemoine N, Bomalaski J, Li CF, Joel S, Fitzgibbon J, Chen LT, Szlosarek PW. Promoter methylation of argininosuccinate synthetase-1 sensitises lymphomas to arginine deiminase treatment, autophagy and caspase-dependent apoptosis. Cell Death Dis. 2012 Jul 5;3:e342. doi: 10.1038/cddis.2012.83.

Delage B., D.A. Fennell, L. Nicholson, I. McNeish, N.R. Lemoine, T. Crook, P.W. Szlosarek, Arginine deprivation and argininosuccinate synthetase expression in the treatment of cancer, Int. J. Cancer 126 (2010) 2762–2772.

Delage B., D.A. Fennell, L. Nicholson, I. McNeish, N.R. Lemoine, T. Crook, P.W. Szlosarek, Arginine deprivation and argininosuccinate synthetase expression in the treatment of cancer, Int. J. Cancer 126 (2010) 2762–2772.

Delic S1, Lottmann N, Jetschke K, Reifenberger G, Riemenschneider MJ. Identification and functional validation of CDH11, PCSK6 and SH3GL3 as novel glioma invasion-associated candidate genes. Neuropathol Appl Neurobiol. 2012 Apr;38(2):201-12. doi: 10.1111/j.1365-2990.2011.01207.x.

Deraco M, Bartlett D, Kusamura S, et al. Consensus statement on peritoneal mesothelioma. J Surg Oncol 2008;98:268-72.

Dhanasekaran R, Nakamura I, Hu C, Chen G, Oseini AM, Seven ES, Miamen AG, Moser CD, Zhou W, van Kuppevelt TH, van Deursen JM, Mounajjed T, Fernandez-Zapico ME, Roberts LR. Activation of the transforming growth factor-β/SMAD transcriptional pathway underlies a novel tumour-promoting role of sulfatase 1 in hepatocellular carcinoma. Hepatology. 2015 Apr;61(4):1269-83. doi: 10.1002/hep.27658.

Dhoot GK , Gustafsson MK, Ai X, Sun W, Standiford DM, Emerson CP Jr. Regulation of Wnt signaling and embryo patterning by an extracellular sulfatase. Science; 293(5535):16636 (2001).

Dillon BJ, Prieto VG, Curley SA, Ensor CM, Holtsberg FW, Bomalaski JS, Clark MA. Incidence and distribution of argininosuccinate synthetase deficiency in human cancers: a method for identifying cancers sensitive to arginine deprivation. Cancer 2004;100:826-33.

Dipalma N, Luisi V, Di Serio F, Fontana A, Maggiolini P, Licchelli B, Mera E, Bisceglia L, Galise I, Loizzi M, Pizzigallo MA, Molinini R, Vimercati L. Biomarkers in malignant mesothelioma: diagnostic and prognostic role of soluble mesothelin-related peptide. Int J Biol Markers. 2011 Jul-Sep;26(3):160-5. doi: 10.5301/JBM.2011.8614.

DiPietro LA. Thrombospondin and Angiogenesis. Angiogenesis Inhibitors and Stimulators: Potential Therapeutic Implications; chapter 6 Taylor & Francis, 2000.

Do S.I., Y.W. Kim, H.R. Park, Y.K. Park Expression of insulin-like growth factor-II mRNA binding protein 3 (IMP3) in osteosarcoma Oncol Res, 17 (2008), pp. 269–272

Doherty JR, Cleveland JL. Targeting lactate metabolism for cancer therapeutics. J Clin Invest. 2013 Sep;123(9):3685-92. doi: 10.1172/JCI69741.

Doherty KJ, McKay C, Chan KK, El-Tanani MK. RAN GTPase as a target for cancer therapy: Ran binding proteins. Curr Mol Med. 2011;11:686–695.

Doyen J1, Trastour C2, Ettore F3, Peyrottes I3, Toussant N3, Gal J4, Ilc K5, Roux D5, Parks SK6, Ferrero JM7, Pouysségur J8. Expression of the hypoxia-inducible monocarboxylate transporter MCT4 is increased in triple negative breast cancer and correlates independently with clinical outcome. Biochem Biophys Res Commun. 2014 Aug 15;451(1):54-61. doi: 10.1016/j.bbrc.2014.07.050. Epub 2014 Jul 21.

Driscoll T et al. The global burden of diseases due to occupational carcinogens. American journal of Industrial Medicine, 2005, 48(6):419-431.

Duggan MA, Masters CB, Alexander F. Immunohistochemical differentiation of malignant mesothelioma, mesothelial hyperplasia and metastatic adenocarcinoma in serous effusions, utilizing staining for carcinoembryonic antigen, keratin and vimentin. Acta Cytol; 31(6):807-14 (1987).

Fadare O., S.X. Liang, M.A. Crispens, H.W. Jones, D. Khabele, K. Gwin, et al. Expression of the oncofetal protein IGF2BP3 in endometrial clear cell carcinoma: assessment of frequency and significance Hum Pathol, 44 (2013), pp. 1508–1515 3rd

Feun, L., You, M., Wu, C.J., Kuo, M.T., Wangpaichitr, M., Spector, S., and Savaraj, N. (2008). Arginine deprivation as a targeted therapy for cancer. Curr. Pharm. Des. 14, 1049–1057.

Findeis-Hosey JJ, Xu H. Insulin-like growth factor II-messenger RNA-binding protein-3 and lung cancer. Biotech Histochem. 2012 Jan;87(1):24-9. doi: 10.3109/10520295.2011.591831.

Findeis-Hosey JJ, Xu H. The use of insulin like-growth factor II messenger RNA binding protein-3 in diagnostic pathology. Hum Pathol 2011;42:303–14

Fontanini, G., L. Boldrini, A. Calcinai, S. Chine, M. Lucchi, A. Mussi, C. A. Angeletti, F. Basolo, and G. Bevilacqua. 1999. Thrombospondins I and II messenger RNA expression in lung carcinoma: relationship with p53 alterations, angiogenic growth factors, and vascular density. Clin. Cancer Res. 5:155–161.

Fox SA, Richards AK, Kusumah I, Perumal V, Bolitho EM, Mutsaers SE, Dharmarajan AM. Expression profile and function of Wnt signaling mechanisms in malignant mesothelioma cells. Biochem Biophys Res Commun. 2013 Oct 11;440(1):82-7. doi: 10.1016/j.bbrc.2013.09.025.

Francis RJ, Segard T2, Morandeau L3, Lee YC4, Millward MJ5, Segal A6, Nowak AK5. Characterization of hypoxia in malignant pleural mesothelioma with FMISO PET-CT. Lung Cancer. 2015 Oct;90(1):55-60. doi: 10.1016/j.lungcan.2015.07.015.

Fukuchi-Shimogori T1, Ishii I, Kashiwagi K, Mashiba H, Ekimoto H, Igarashi K. Malignant transformation by overproduction of translation initiation factor eIF4G. Cancer Res. 1997 Nov 15;57(22):5041-4.

Gallagher SM, Castorino JJ, Wang D, Philp NJ. Monocarboxylate transporter 4 regulates maturation and trafficking of CD147 to the plasma membrane in the metastatic breast cancer cell line MDA-MB-231. Cancer Res. 2007 May 1;67(9):4182-9.

Ganapathy V1, Thangaraju M, Prasad PD. Nutrient transporters in cancer: relevance to Warburg hypothesis and beyond. Pharmacol Ther. 2009 Jan;121(1):29-40. doi: 10.1016/j.pharmthera.2008.09.005. Epub 2008 Nov 1.

Garcia-Manero G, Daniel J, Smith TL, Kornblau SM, Lee MS, Kantarjian HM, Issa JP. DNA methylation of multiple promoter-associated CpG islands in adult acute lymphocytic leukemia. Clin Cancer Res; 8(7):2217-24 (2002).

Gibbs AR. Role of asbestos and other fibres in the development of diffuse malignant mesothelioma. Thorax. 1990 Sep;45(9):649-54.

Giusti I., Dolo V. Extracellular Vesicles in Prostate Cancer: New Future Clinical Strategies?. Biomed Res Int; 561571 (2014).

Glasauer A, Sena LA, Diebold LP, Mazar AP, Chandel NS. Targeting SOD1 reduces experimental non–small-cell lung cancer. J Clin Invest. 2014 Jan;124(1):117-28.

Gong Y, Woda BA, Jiang Z. Oncofetal protein IMP3, a new cancer biomarker. Adv Anat Pathol. 2014 May;21(3):191-200. doi: 10.1097/PAP.0000000000000021.

Gopal G, Shirley S, Raja UM, Rajkumar T. Endo-sulfatase Sulf-1 protein expression is downregulated in gastric cancer. Asian Pac J Cancer Prev; 13(2):6416 (2012).

Gordon GJ, Appasani K, Parcells JP, Mukhopadhyay NK, Jaklitsch MT, Richards WG, Sugarbaker DJ, Bueno R. Inhibitor of apoptosis protein-1 promotes tumor cell survival in mesothelioma. Carcinogenesis. 2002 Jun;23(6):1017-24.

Grigoriu BD, Chahine B, Vachani A, Gey T, Conti M, Sterman DH, Marchandise G, Porte H, Albelda SM, Scherpereel A. Kinetics of Soluble Mesothelin in Patients with Malignant Pleural Mesothelioma during Treatment. Am J Respir Crit Care Med; 179(10):950-4 (2009).

Grigoriu BD, Scherpereel A, Devos P, Chahine B, Letourneux M, Lebailly P, Grégoire M, Porte H, Copin MC, Lassalle P. Utility of Osteopontin and SerumMesothelin in Malignant Pleural Mesothelioma Diagnosis and Prognosis Assessment. Clin Cancer Res; 13(10):2928-35 (2007).

Guvenc, H., Pavlyukov, M.S., Joshi, K., Kurt, H., Banasavadi-Siddegowda, Y.K., Mao, P., Hong, C., Yamada, R., Kwon, C.H., Bhasin, D., et al. (2013). Impairment of glioma stem cell survival and growth by a novel inhibitor for Survivin-Ran protein complex. Clin. Cancer Res. 19, 631–642.

Haiman CA, Han Y, Feng Y, Xia L, Hsu C, Sheng X, Pooler LC, Patel Y, Kolonel LN, Carter E, Park K, Le Marchand L, Van Den Berg D, Henderson BE, Stram DO. Comparison of Breast Cancer to Healthy Control Tissue Discovers Novel Markers with Potential for Prognosis and Early Detection. PLoS Genet; 9(3) (2013).

Hanley Krisztina Z., Michael S. Facik , Patricia A. Bourne , Qi Yang , Betsy O. Spaulding , Thomas A. Bonfiglio, Haodong Xu. Utility of anti-L523S antibody in the diagnosis of benign and malignant serous effusions. Cancer 114 (1), 49-56. 2008 Feb 25.

Hao J1, Chen H, Madigan MC, Cozzi PJ, Beretov J, Xiao W, Delprado WJ, Russell PJ, Li Y. Co-expression of CD147 (EMMPRIN), CD44v3-10, MDR1 and monocarboxylate transporters is associated with prostate cancer drug resistance and progression. Br J Cancer. 2010 Sep 28;103(7):1008-18. doi: 10.1038/sj.bjc.6605839. Epub 2010 Aug 24.

Hart J., M. Parab, D. Mandich, R.W. Cartun, S. Ligato IMP3 immunocytochemical staining increases sensitivity in the routine cytologic evaluation of biliary brush specimens Diagn Cytopathol, 40 (2012), pp. 321–326

Hartmann E.M., S. Bea, A. Navarro, V. Trapp, E. Campo, G. Ott, et al. Increased tumour cell proliferation in mantle cell lymphoma is associated with elevated insulin-like growth factor 2 mRNA-binding protein 3 expression Mod Pathol, 25 (2012), pp. 1227–1235

He X, Khurana A, Roy D, Kaufmann S, Shridhar V. Loss of HSulf-1 expression enhances tumourigenicity by inhibiting Bim expression in ovarian cancer. Int J Cancer; 135(8):1783-9 (2014).

Henderson DW, Reid G, Kao SC, et al. Challenges and controversies in the diagnosis of mesothelioma: Part 1. Cytology-only diagnosis, biopsies, immunohistochemistry, discrimination between mesothelioma and reactive mesothelial hyperplasia, and biomarkers. J Clin Pathol; 66(10):847-53 (2013).

Hileman EO, Liu J, Albitar M, Keating MJ, Huang P. Intrinsic oxidative stress in cancer cells: a biochemical basis for therapeutic selectivity. Cancer Chemother Pharmacol. 2004 Mar;53(3):209-19.

Hollevoet K, Nackaerts K, Gosselin R, et al. Soluble mesothelin, megakaryocyte potentiating factor, and osteopontin as markers of patient response and outcome in mesothelioma. J Thorac Oncol; 6(11):1930-7 (2011).

Hollevoet K, Nackaerts K, Thas O, et al. The effect of clinical covariates on the diagnostic and prognostic value of soluble mesothelin and megakaryocyte potentiating factor. Chest 2012; 141: 477–484

Hollevoet K, Nackaerts K, Thimpont J, et al. Diagnostic performance of soluble mesothelin and megakaryocyte potentiating factor in mesothelioma. Am J Respir Crit Care Med 2010; 181: 620–625

Hour TC, Lai YL, Kuan CI, Chou CK, Wang JM, Tu HY, Hu HT, Lin CS, Wu WJ, Pu YS, Sterneck E, Huang AM. Transcriptional up-regulation of SOD1 by CEBPD: a potential target for cisplatin resistant human urothelial carcinoma cells. Biochem Pharmacol. 2010 Aug 1;80(3):325-34. doi: 10.1016/j.bcp.2010.04.007.

Hsu KF, Shen MR2, Huang YF1, Cheng YM1, Lin SH3, Chow NH4, Cheng SW4, Chou CY1, Ho CL4. Overexpression of the RNA-binding proteins Lin28B and IGF2BP3 (IMP3) is associated with chemoresistance and poor disease outcome in ovarian cancer. Br J Cancer. 2015 Jul 28;113(3):414-24. doi: 10.1038/bjc.2015.254.

Huang CF, Lira C, Chu K, Bilen MA, Lee YC, Ye X, et al. Cadherin-11 increases migration and invasion of prostate cancer cells and enhances their interaction with osteoblasts. Cancer Res. 2010;70:4580–4589.

Huang MM, Guo AB, Sun JF, Chen XL, Yin ZY. Angiotensin II promotes the progression of human gastric cancer. Mol Med Rep.; 9(3):1056-60 (2014).

Huang P, Feng L, Oldham EA, Keating MJ, Plunkett W. Superoxide dismutase as a target for the selective killing of cancer cells. Nature. 2000 Sep 21;407(6802):390-5.

Hur K , Han TS, Jung EJ, Yu J, Lee HJ, Kim WH, Goel A, Yang HK. Upregulated expression of sulfatases (SULF1 and SULF2) as prognostic and metastasis predictive markers in human gastric cancer. J Pathol; 228(1):8898 (2012).

Ikeda K, Tate G, Suzuki T, Kitamura T, Mitsuya T. Diagnostic usefulness of EMA, IMP3, and GLUT-1 for the immunocytochemical distinction of malignant cells from reactive mesothelial cells in effusion cytology using cytospin preparations. Diagn Cytopathol. 2011 Jun;39(6):395-401. doi: 10.1002/dc.21398. Epub 2010 May 27.

Ikeda K, Tate G, Suzuki T, Kitamura T, Mitsuya T. IMP3/L523S, a novel immunocytochemical marker that distinguishes benign and malignant cells: the expression profiles of IMP3/L523S in effusion cytology. Hum Pathol. 2010 May;41(5):745-50. doi: 10.1016/j.humpath.2009.04.030.

Ikenberg K, Fritzsche FR, Zuerrer-Haerdi U, Hofmann I, Hermanns T, Seifert H, Müntener M, Provenzano M, Sulser T, Behnke S, Gerhardt J, Mortezavi A, Wild P, Hofstädter F, Burger M, Moch H, Kristiansen G. Insulin-like growth factor II mRNA binding protein 3 (IMP3) is overexpressed in prostate cancer and correlates with higher Gleason scores. BMC Cancer. 2010 Jun 30;10:341. doi: 10.1186/1471-2407-10-341.

Itahana K, Dimri G, Campisi J. Regulation of cellular senescence by p53. Eur J Biochem.; 268(10):2784-91 (2001).

Izumi H1, Takahashi M, Uramoto H, Nakayama Y, Oyama T, Wang KY, Sasaguri Y, Nishizawa S, Kohno K. Monocarboxylate transporters 1 and 4 are involved in the invasion activity of human lung cancer cells. Cancer Sci. 2011 May;102(5):1007-13. doi: 10.1111/j.1349-7006.2011.01908.x. Epub 2011 Mar 7.

Jacobson BA, De A, Kratzke MG, Patel MR, Jay-Dixon J, Whitson BA, Sadiq AA, Bitterman PB, Polunovsky VA, Kratzke RA. Activated 4E-BP1 represses tumourigenesis and IGF-I-mediated activation of the eIF4F complex in mesothelioma. Br J Cancer. 2009 Aug 4;101(3):424-31. doi: 10.1038/sj.bjc.6605184. Epub 2009 Jul 14.

Janssen A, Hoellenriegel J, Fogarasi M, Schrewe H, Seeliger M, Tamm E, Ohlmann A, May CA, Weber BH, Stöhr H. Abnormal vessel formation in the choroid of mice lacking tissue inhibitor of metalloprotease-3. Invest Ophthalmol Vis Sci.; 49(7):2812-22 (2008).

Jin L., A.R. Seys, S. Zhang, M.R. Erickson-Johnson, C.W. Roth, B.R. Evers, et al. Diagnostic utility of IMP3 expression in thyroid neoplasms: a quantitative RT-PCR study Diagn Mol Pathol Am J Surg Pathol B, 19 (2010), pp. 63–69

Khurana A, Liu P, Mellone P, Lorenzon L, Vincenzi B, Datta K, Yang B, Linhardt RJ, Lingle W, Chien J, Baldi A, Shridhar V. HSulf-1 modulates FGF2- and hypoxia-mediated migration and invasion of breast cancer cells. Cancer Res; 71(6):2152-61 (2011).

Khurana A, Liu P, Mellone P, Lorenzon L, Vincenzi B, Datta K, Yang B, Linhardt RJ, Lingle W, Chien J, Baldi A, Shridhar V. HSulf-1 modulates FGF2- and hypoxia-mediated migration and invasion of breast cancer cells. Cancer Res; 71(6):2152-61 (2011).

Kim H, Phung Y, Ho M. Changes in Global Gene Expression Associated with 3D Structure of Tumours: An Ex Vivo Matrix-Free Mesothelioma Spheroid Model. PLoS One; 7(6) (2012).

Kim H, Watkinson J, Varadan V, Anastassiou D. Multi-cancer computational analysis reveals invasion-associated variant of desmoplastic reaction involving INHBA, THBS2 and COL11A1. BMC Med Genomics. 2010 Nov 3;3:51. doi: 10.1186/1755-8794-3-51.

Kim JW, Sahm H, You J, Wang M. Knock-down of superoxide dismutase 1 sensitizes cisplatin-resistant human ovarian cancer cells. Anticancer Res. 2010 Jul;30(7):2577-81.

Kirk P, Wilson MC, Heddle C, Brown MH, Barclay AN, Halestrap AP. CD147 is tightly associated with lactate transporters MCT1 and MCT4 and facilitates their cell surface expression. EMBO J. 2000; 19(15):3896–3904.

Klabatsa, A., Sheaff, M.T., Steele, J.P., Evans, M.T., Rudd, R.M., Fennell, D.A. Expression and prognostic significance of hypoxia-inducible factor 1α (HIF-1α) in malignant pleural mesothelioma (MPM). Lung Cancer 2006, 51, 53–59.

Kleinberg,L., A.K.Lie, V.A.Florenes, J.M.Nesland, and B.Davidson. 2007. Expression of inhibitor-of-apoptosis protein family members in malignant mesothelioma. Hum. Pathol. 38: 986-994.

Kobel M., H. Xu, P.A. Bourne, B.O. Spaulding, M. Shih Ie, T.L. Mao, et al. IGF2BP3 (IMP3) expression is a marker of unfavorable prognosis in ovarian carcinoma of clear cell subtype Mod Pathol, 22 (2009), pp. 469–475

Kodama J, Hashimoto I, Seki N, Hongo A, Yoshinouchi M, Okuda H, Kudo T. Thrombospondin-1 and -2 messenger RNA expression in epithelial ovarian tumour. Anticancer Res; 21(4B):2983-7 (2001).

Lai Jin-Ping, Dalbir S. Sandhu, Abdirashid M. Shire, and Lewis R. Roberts. The Tumour Suppressor Function of Human Sulfatase 1 (SULF1) in Carcinogenesis. J. Gastrointest Cancer; 39(14):149–158 (2008).

Lai JP, Chien JR, Moser DR, Staub JK, Aderca I, et al. hSulf1 Sulfatase promotes apoptosis of hepatocellular cancer cells by decreasing heparin-binding growth factor signaling. Gastroenterology. 2004;126:231–248.

Laplante M, Sabatini DM. mTOR signaling in growth control and disease. Cell. 2012 Apr 13;149(2):274-93. doi: 10.1016/j.cell.2012.03.017.

Lastra R.R., J.J. Ou, M.E. Reilly, W.D. Lawrence, Z.W. Baloch, J.S. Brooks, et al. Utility of ProExC and IMP3 immunocytochemical staining in atypical glandular cells of undetermined significance in liquid-based cervical cytology Diagn Cytopathol, 42 (2014), pp. 375–379

Le Floch R., J. Chiche, I. Marchiq, T. Naiken, K. Ilc, C.M. Murray, S.E. Critchlow, D. Roux, M.P. Simon, J. Pouyssegur, CD147 subunit of lactate/H+ symporters MCT1 and hypoxia-inducible MCT4 is critical for energetics and growth of glycolytic tumours, Proc. Natl. Acad. Sci. U.S.A. 108 (2011) 16663–16668.

Lederer M, Bley N, Schleifer C, Hüttelmaier S. The role of the oncofetal IGF2 mRNA-binding protein 3 (IGF2BP3) in cancer. Semin Cancer Biol. 2014 Dec;29:3-12. doi: 10.1016/j.semcancer.2014.07.006.

Lee AF, Gown AM, Churg A. IMP3 and GLUT-1 immunohistochemistry for distinguishing benign from malignant mesothelial proliferations. Am J Surg Pathol. 2013 Mar;37(3):421-6. doi: 10.1097/PAS.0b013e31826ab1c0.

Lee HY, Mohammed KA, Goldberg EP, Kaye F, Najmunnisa N. Silencing Receptor EphA2 Enhanced Sensitivity to Lipoplatin™ in Lung Tumour and MPM Cells. Cancer Invest. 2016 Aug 8;34(7):293-304. doi: 10.1080/07357907.2016.1201678.

Lee K, Briehl MM, Mazar AP, Batinic-Haberle I, Reboucas JS, Glinsmann-Gibson B, Rimsza LM, Tome ME. The copper chelator ATN-224 induces peroxynitrite-dependent cell death in hematological malignancies. Free Radic Biol Med. 2013 Jul;60:157-67. doi: 10.1016/j.freeradbiomed.2013.02.003.

Lee,A.Y., D.J.Raz, B.He, and D.M.Jablons. 2007. Update on the molecular biology of malignant mesothelioma. Cancer 109: 1454-1461.

Leivonen SK, Kähäri VM. Transforming growth factor-beta signaling in cancer invasion and metastasis. Int J Cancer; 121(10):2119-24 (2007).

Leivonen SK, Konstantinos Lazaridis, Julie Decock, Andrew Chantry, Dylan R. Edwards and Veli-Matti Kähäri. TGF-β-Elicited Induction of Tissue Inhibitor of Metalloproteinases (TIMP)-3 Expression in Fibroblasts Involves Complex Interplay between Smad3, p38α, and ERK1/2. PLoS One.; 8(2): e57474 (2013).

Leung,A.N., N.L.Muller, and R.R.Miller. 1990. CT in differential diagnosis of diffuse pleural disease. AJR Am. J. Roentgenol. 154: 487-492.

Li C., V. Zota, B.A. Woda, K.L. Rock, A.E. Fraire, Z. Jiang, et al. Expression of a novel oncofetal mRNA-binding protein IMP3 in endometrial carcinomas: diagnostic significance and clinicopathologic correlations Mod Pathol, 20 (2007), pp. 1263–1268

Li D., D. Yan, H. Tang, C. Zhou, J. Fan, S. Li, et al. IMP3 is a novel prognostic marker that correlates with colon cancer progression and pathogenesis Ann Surg Oncol, 16 (2009), pp. 3499–3506

Li L, Luo Q, Xie Z, Li G, Mao C, Liu Y1, Wen X, Yin N1, Cao J, Wang J1, Li L1, Yu J, Wang F, Yi P. Characterization of the Expression of the RNA Binding Protein eIF4G1 and Its Clinicopathological Correlation with Serous Ovarian Cancer. PLoS One. 2016 Sep 26;11(9):e0163447. doi: 10.1371/journal.pone.0163447.

Li L, Ying J, Li H, Zhang Y, Shu X, Fan Y, Tan J, Cao Y, Tsao SW, Srivastava G, Chan AT, Tao Q. The human cadherin 11 is a pro-apoptotic tumour suppressor modulating cell stemness through Wnt/β-catenin signaling and silenced in common carcinomas. Oncogene. 2012 Aug 23;31(34):3901-12. doi: 10.1038/onc.2011.541. Epub 2011 Dec 5.

Li Y1, Guo Z, Chen H, Dong Z, Pan ZK, Ding H, Su SB, Huang S. HOXC8-Dependent Cadherin 11 Expression Facilitates Breast Cancer Cell Migration through Trio and Rac. Genes Cancer. 2011 Sep;2(9):880-8. doi: 10.1177/1947601911433129.

Liao B, Hu Y, Brewer G. RNA-binding protein insulin-like growth factor mRNA-binding protein 3 (IMP-3) promotes cell survival via insulin-like growth factor II signaling after ionizing radiation. J Biol Chem. 2011 Sep 9;286(36):31145-52. doi: 10.1074/jbc.M111.263913.

Lim KS1, Lim KJ1, Price AC1, Orr BA2, Eberhart CG3, Bar EE4. Inhibition of monocarboxylate transporter-4 depletes stem-like glioblastoma cells and inhibits HIF transcriptional response in a lactate-independent manner. Oncogene. 2014 Aug 28;33(35):4433-41. doi: 10.1038/onc.2013.390. Epub 2013 Sep 30.

Lin CY, Chen ST, Jeng YM, Yeh CC, Chou HY, Deng YT, Chang CC, Kuo MY. Insulin-like growth factor II mRNA-binding protein 3 expression promotes tumour formation and invasion and predicts poor prognosis in oral squamous cell carcinoma. J Oral Pathol Med. 2011 Oct;40(9):699-705. doi: 10.1111/j.1600-0714.2011.01019.x.

Lin L., J. Zhang, Y. Wang, W. Ju, Y. Ma, L. Li, et al. Insulin-like growth factor-II mRNA-binding protein 3 predicts a poor prognosis for colorectal adenocarcinoma Oncol Lett, 6 (2013), pp. 740–744

Linch M, Gennatas S, Kazikin S, Iqbal J, Gunapala R, Priest K, Severn J, Norton A, Ayite B, Bhosle J, O'Brien M, Popat S. A serum mesothelin level is a prognostic indicator for patients with malignant mesothelioma in routine clinical practice. BMC Cancer. 2014 Sep 17;14:674. doi: 10.1186/1471-2407-14-674.

Liu H, Chen SE, Jin B, Carson JA, Niu A, Durham W, Lai JY, Li YP. TIMP3: a physiological regulator of adult myogenesis. J Cell Sci.;123(Pt 17):2914-21 (2010).

Liu ZJ, Tan Y, Beecham GW, Seo DM, Tian R, Li Y, Vazquez-Padron RI, Pericak-Vance M, Vance JM, Goldschmidt-Clermont PJ, Livingstone AS, Velazquez OC. Notch activation induces endothelial cell senescence and pro-inflammatory response: implication of Notch signaling in atherosclerosis. Atherosclerosis; 225(2):296-303 (2012).

Locke M, Ghazaly E2, Freitas MO1, Mitsinga M1, Lattanzio L3, Lo Nigro C3, Nagano A1, Wang J1, Chelala C1, Szlosarek P1, Martin SA4. Inhibition of the Polyamine Synthesis Pathway Is Synthetically Lethal with Loss of Argininosuccinate Synthase 1. Cell Rep. 2016 Aug 9;16(6):1604-13. doi: 10.1016/j.celrep.2016.06.097.

Long, Y., Tsai, W.B., Wangpaichitr, M., Tsukamoto, T., Savaraj, N., Feun, L.G., and Kuo, M.T. (2013). Arginine deiminase resistance in melanoma cells is associated with metabolic reprogramming, glucose dependence, and glutamine addiction. Mol. Cancer Ther. 12, 2581–2590.

López-Ríos F, Chuai S, Flores R, Shimizu S, Ohno T, Wakahara K, Illei PB, Hussain S, Krug L, Zakowski MF, Rusch V, Olshen AB, Ladanyi M. Global gene expression profiling of pleural mesotheliomas: overexpression of Aurora kinases and P16/CDKN2A deletion as prognostic factors and critical evaluation of microarray-based prognostic prediction. Cancer Res. 2006;66:2970–2979.

Low RN, Barone RM.. Combined diffusion-weighted and gadolinium-enhanced MRI can accurately predict the peritoneal cancer index preoperatively in patients being considered for cytoreductive surgical procedures. Ann Surg Oncol 2012;19:1394-401.

Luo D1, Wilson JM, Harvel N, Liu J, Pei L, Huang S, Hawthorn L, Shi H. A systematic evaluation of miRNA:mRNA interactions involved in the migration and invasion of breast cancer cells. J Transl Med. 2013 Mar 5;11:57. doi: 10.1186/1479-5876-11-57.

Ly TK, Wang J, Pereira R, Rojas KS, Peng X, et al. Activation of the Ran GTPase is subject to growth factor regulation and can give rise to cellular transformation. J Biol Chem. 2010;285:5815–5826.

Madison BB, Liu Q, Zhong X, Hahn CM, Lin N, Emmett MJ, Stanger BZ, Lee JS, Rustgi AK. LIN28B promotes growth and tumourigenesis of the intestinal epithelium via Let-7. Genes Dev. 2013 Oct 15;27(20):2233-45. doi: 10.1101/gad.224659.113.

Marchong MN1, Yurkowski C, Ma C, Spencer C, Pajovic S, Gallie BL. Cdh11 acts as a tumour suppressor in a murine retinoblastoma model by facilitating tumour cell death. PLoS Genet. 2010 Apr 22;6(4):e1000923. doi: 10.1371/journal.pgen.1000923.

Marinaccio A, Binazzi A, Cauzillo G, Cavone D, Zotti RD, Ferrante P, Gennaro V, Gorini G, Menegozzo M, Mensi C, Merler E, Mirabelli D, Montanaro F, Musti M, Pannelli F, Romanelli A, Scarselli A, Tumino R; Italian Mesothelioma Register (ReNaM) Working Group. Analysis of latency time and its determinants in asbestos related malignant mesothelioma cases of the Italian register. Eur J Cancer. 2007 Dec;43(18):2722-8. Epub 2007 Nov 5.

Marinaccio A, Montanaro F, Mastrantonio M et al. Predictions of mortality from pleural mesothelioma in Italy: a model based on asbestos consumption figures supports results from age-period-cohort models. Int J Cancer 2005;115(1):142-47

Meijer TW1, Schuurbiers OC, Kaanders JH, Looijen-Salamon MG, de Geus-Oei LF, Verhagen AF, Lok J, van der Heijden HF, Rademakers SE, Span PN, Bussink J. Differences in metabolism between adeno- and squamous cell non-small cell lung carcinomas: spatial distribution and prognostic value of GLUT1 and MCT4. Lung Cancer. 2012 Jun;76(3):316-23. doi: 10.1016/j.lungcan.2011.11.006. Epub 2011 Dec 6.

Melaiu O, Cristaudo A, Melissari E, Di Russo M, Bonotti A, Bruno R, Foddis R, Gemignani F, Pellegrini S, Landi S. A review of transcriptome studies combined with data mining reveals novel potential markers of malignant pleural mesothelioma. Mutat Res. 2012 Apr-Jun;750(2):132-40. doi: 10.1016/j.mrrev.2011.12.003.

Melaiu O, Melissari E, Mutti L, Bracci E, De Santi C, Iofrida C, Di Russo M, Cristaudo A, Bonotti A, Cipollini M, Garritano SI, Foddis R, Lucchi M, Pellegrini S, Gemignani F, Landi S. Expression status of candidate genes in mesothelioma tissues and cell lines. Mutat Res. 2015 Jan;771:6-12. doi: 10.1016/j.mrfmmm.2014.11.002.

Metodieva SN, Nikolova DN, Cherneva RV, Dimova II, Petrov DB, Toncheva DI. Expression analysis of angiogenesis-related genes in Bulgarian patients with early-stage non-small cell lung cancer. Tumouri; 97(1):86-94 (2011).

Metodieva SN, Nikolova DN, Cherneva RV, Dimova II, Petrov DB, Toncheva DI. Expression analysis of angiogenesis-related genes in Bulgarian patients with early-stage non-small cell lung cancer. Tumouri; 97(1):86-94 (2011).

Mhawech-Fauceglia P., F.R. Herrmann, H. Rai, N. Tchabo, S. Lele, I. Izevbaye, et al. IMP3 distinguishes uterine serous carcinoma from endometrial endometrioid adenocarcinoma Am J Clin Pathol, 133 (2010), pp. 899–908

Mhawech-Fauceglia P., L. Yan, S. Liu, T. Pejovic ER+/PR+/TFF3+/IMP3− immunoprofile distinguishes endometrioid from serous and clear cell carcinomas of the endometrium: a study of 401 cases Histopathology, 62 (2013), pp. 976–985

Minato H, Kurose N, Fukushima M, Nojima T, Usuda K, Sagawa M, Sakuma T, Ooi A, Matsumoto I, Oda M, Arano Y, Shimizu J. Comparative immunohistochemical analysis of IMP3, GLUT1, EMA, CD146, and desmin for distinguishing malignant mesothelioma from reactive mesothelial cells. Am J Clin Pathol. 2014 Jan;141(1):85-93. doi: 10.1309/AJCP5KNL7QTELLYI.

Mineo TC, Ambrogi V. Malignant pleural mesothelioma: factors influencing the prognosis. Oncology (Williston Park). 2012 Dec;26(12):1164-75.

Mogi A, Koga K, Aoki M, Hamasaki M, Uesugi N, Iwasaki A, Shirakusa T, Tamura K, Nabeshima K. Expression and role of GLUT-1, MCT-1, and MCT-4 in malignant pleural mesothelioma. Virchows Arch. 2013 Jan;462(1):83-93. doi: 10.1007/s00428-012-1344-6. Epub 2012 Nov 28.

Mori T, Tajima K, Hirama M, Sato T, Kido K, Iwakami S, Sasaki S, Iwase A, Shiomi K, Maeda M, Hino O, Takahashi K. The N-ERC index is a novel monitoring and prognostic marker for advanced malignant pleural mesothelioma. J Thorac Dis. 2013;5(2):145–148.

Muller SJ, Caradonna S. Cell cycle regulation of a human cyclin-like gene encoding uracil-DNA glycosylase. J Biol Chem; 268(2):1310-9 (1993).

Muller SJ, Caradonna S. Isolation and characterization of a human cDNA encoding uracil-DNA glycosylase. Biochim Biophys Acta; 1088(2):197-207 (1991).

Nakamura M, Ishida E, Shimada K, Kishi M, Nakase H, Sakaki T, Konishi N. Frequent LOH on 22q12.3 and TIMP-3 inactivation occur in the progression to secondary glioblastomas. Lab Invest.;85(2):165-75 (2005).

Nawroth Roman, Annemieke van Zante, Sara Cervantes, Michael McManus, Matthias Hebrok, Steven D. Rosen. Extracellular Sulfatases, Elements of the Wnt Signaling Pathway, Positively Regulate Growth and Tumourigenicity of Human Pancreatic Cancer Cells. PLoS ONE; DOI: 10.1371 (2007).

Nguyen LH, Robinton DA, Seligson MT, Wu L, Li L, Rakheja D, Comerford SA5, Ramezani S6, Sun X6, Parikh MS1, Yang EH1, Powers JT2, Shinoda G2, Shah SP2, Hammer RE7, Daley GQ8, Zhu H9. Lin28b is sufficient to drive liver cancer and necessary for its maintenance in murine models. Cancer Cell. 2014 Aug 11;26(2):248-61. doi: 10.1016/j.ccr.2014.06.018.

Nicco C, Laurent A, Chereau C, Weill B, Batteux F: Differential modulation of normal and tumour cell proliferation by reactive oxygen species. Biomed Pharmacother 2005;59:169-174.

Nicholson LJ, Smith PR, Hiller L, Szlosarek PW, Kimberley C, Sehouli J, Koensgen D, Mustea A, Schmid P, Crook T. Epigenetic silencing of argininosuccinate synthetase confers resistance to platinum-induced cell death but collateral sensitivity to arginine auxotrophy in ovarian cancer. Int J Cancer. 2009 Sep 15;125(6):1454-63. doi: 10.1002/ijc.24546.

Ning J, Liu W, Zhang J, Lang Y, Xu S. Ran GTPase induces EMT and enhances invasion in non-small cell lung cancer cells through activation of PI3K-AKT pathway. Oncol Res. 2013;21(2):67-72. doi: 10.3727/096504013X13747716581417.

O'Regan AW, Serlin D, Berman JS. Asbestos exposure and serum osteopontin. N Engl J Med; 354:304-5 (2006).

of serum samples unmasks reduced expression of alpha-2 macroglobulin and complement factor B in patients with nasopharyngeal carcinoma. Electrophoresis; 31(14):2388-95 (2010).

Okazaki Y, Nagai H, Chew SH, Li J, Funahashi S, Tsujimura T, Toyokuni S. CD146 and insulin-like growth factor 2 mRNA-binding protein 3 predict prognosis of asbestos-induced rat mesothelioma. Cancer Sci. 2013 Aug;104(8):989-95. doi: 10.1111/cas.12185. Epub 2013 May 26.

Orengo AM, Spoletini L, Procopio A, Favoni RE, De Cupis A, Ardizzoni A, Castagneto B, Ribotta M, Betta PG, Ferrini S, Mutti L. Establishment of four new mesothelioma cell lines: characterization by ultrastructural and immunophenotypic analysis. Eur Respir J. 1999 Mar;13(3):527-34.

Ott PA, Carvajal RD, Pandit-Taskar N, Jungbluth AA, Hoffman EW, Wu BW, Bomalaski JS, Venhaus R, Pan L, Old LJ, Pavlick AC, Wolchok JD. Phase I/II study of pegylated arginine deiminase (ADI-PEG 20) in patients with advanced melanoma. Invest New Drugs. 2013 Apr;31(2):425-34. doi: 10.1007/s10637-012-9862-2.

Papa L, Hahn M, Marsh EL, Evans BS, Germain D. SOD2 to SOD1 switch in breast cancer. J Biol Chem. 2014 Feb 28;289(9):5412-6. doi: 10.1074/jbc.C113.526475. (A)

Papa L, Manfredi G, Germain D. SOD1, an unexpected novel target for cancer therapy. Genes Cancer. 2014 Apr;5(1-2):15-21. (B)

Pasiliao CC, Chang CW, Sutherland BW, Valdez SM, Schaeffer D, Yapp DT, Ng SS. The involvement of insulin-like growth factor 2 binding protein 3 (IMP3) in pancreatic cancer cell migration, invasion, and adhesion. BMC Cancer. 2015 Apr 11;15:266. doi: 10.1186/s12885-015-1251-8.

Pass HI, Lott D, Lonardo F, et al. Asbestos exposure, pleural mesothelioma, and serum osteopontin levels. N Engl J Med; 353:1564 -73 (2005).

Patergnani S, Giorgi C, Maniero S, Missiroli S, Maniscalco P, Bononi I, Martini F, Cavallesco G, Tognon M, Pinton P. The endoplasmic reticulum mitochondrial calcium cross talk is downregulated in malignant pleural mesothelioma cells and plays a critical role in apoptosis inhibition. Oncotarget. 2015 Sep 15;6(27):23427-44.

Pértega-Gomes N1, Vizcaíno JR, Miranda-Gonçalves V, Pinheiro C, Silva J, Pereira H, Monteiro P, Henrique RM, Reis RM, Lopes C, Baltazar F. Monocarboxylate transporter 4 (MCT4) and CD147 overexpression is associated with poor prognosis in prostate cancer. BMC Cancer. 2011 Jul 25;11:312. doi: 10.1186/1471-2407-11-312.

Peto J, Decarli A, La Vecchia C, Levi F, Negri E. The European mesothelioma epidemic. Br J Cancer. 1999 Feb;79(3-4):666-72.

Pietrofesa RA, Velalopoulou A, Albelda SM, Christofidou-Solomidou M. Asbestos Induces Oxidative Stress and Activation of Nrf2 Signaling in Murine Macrophages: Chemopreventive Role of the Synthetic Lignan Secoisolariciresinol Diglucoside (LGM2605). Int J Mol Sci. 2016 Mar 1;17(3):322. doi: 10.3390/ijms17030322.

Pinheiro C, Garcia EA, Morais-Santos F, Scapulatempo-Neto C, Mafra A, Steenbergen RD, Boccardo E, Villa LL, Baltazar F, Longatto-Filho A1. Lactate transporters and vascular factors in HPV-induced squamous cell carcinoma of the uterine cervix. BMC Cancer. 2014 Oct 8;14:751. doi: 10.1186/1471-2407-14-751.

Pinheiro C, Longatto-Filho A, Azevedo-Silva J, Casal M, Schmitt FC, Baltazar F. Role of monocarboxylate transporters in human cancers: state of the art. J Bioenerg Biomembr. 2012 Feb;44(1):127-39. doi: 10.1007/s10863-012-9428-1.

Pinheiro C, Longatto-Filho A, Soares TR, Pereira H, Bedrossian C, Michael C, Schmitt FC, Baltazar F. CD147 immunohistochemistry discriminates between reactive mesothelial cells and malignant mesothelioma. Diagn Cytopathol. 2012 Jun;40(6):478-83. doi: 10.1002/dc.22821.

Pinheiro C, Longatto-Filho A, Soares TR, Pereira H, Bedrossian C, Michael C, Schmitt FC, Baltazar F. CD147 immunohistochemistry discriminates between reactive mesothelial cells and malignant mesothelioma. Diagn Cytopathol. 2012 Jun;40(6):478-83. doi: 10.1002/dc.22821.

Pinheiro C, Miranda-Gonçalves V, Longatto-Filho A, Vicente AL, Berardinelli GN2, Scapulatempo-Neto C, Costa RF1, Viana CR6, Reis RM, Baltazar F, Vazquez VL. The metabolic microenvironment of melanomas: Prognostic value of MCT1 and MCT4. Cell Cycle. 2016 Jun 2;15(11):1462-70. doi: 10.1080/15384101.2016.1175258. Epub 2016 Apr 22.

Pishvaian MJ, Feltes CM, Thompson P, Bussemakers MJ, Schalken JA, Byers SW. Cadherin-11 is expressed in invasive breast cancer cell lines. Cancer Res. 1999;59:947–952.

Poulikakos PI, Xiao GH, Gallagher R, Jablonski S, Jhanwar SC, Testa JR. Re-expression of the tumor suppressor NF2/merlin inhibits invasiveness in mesothelioma cells and negatively regulates FAK. Oncogene. 2006;25(44):5960–8. Epub 2006/05/03.

Pryor JG, Bourne PA, Yang Q, Spaulding BO, Scott GA, Xu H. IMP-3 is a novel progression marker in malignant melanoma. Mod Pathol. 2008 Apr;21(4):431-7. doi: 10.1038/modpathol.3801016.

Qi JH, Anand-Apte B. Tissue inhibitor of metalloproteinase-3 (TIMP3) promotes endothelial apoptosis via a caspase-independent mechanism. Apoptosis; (2015).

Quimby BB, Dasso M. The small GTPase Ran: interpreting the signs. Curr Opin Cell Biol. 2003;15:338–344.

Qureshi HY, Sylvester J, El Mabrouk M, Zafarullah M. TGF-beta-induced expression of tissue inhibitor of metalloproteinases-3 gene in chondrocytes is mediated by extracellular signal-regulated kinase pathway and Sp1 transcription factor. J Cell Physiol.; 203(2):345-52 (2005).

Ramsey ML, Yuh BJ, Johnson MT, Yeldandi AV, Zynger DL. Carbonic anhydrase IX is expressed in mesothelioma and metastatic clear cell renal cell carcinoma of the lung. Virchows Arch. 2012 Jan;460(1):89-93. doi: 10.1007/s00428-011-1178-7.

Ravanti L, Häkkinen L, Larjava H, Saarialho-Kere U, Foschi M, Han J, Kähäri VM. Transforming growth factor-beta induces collagenase-3 expression by human gingival fibroblasts via p38 mitogen-activated protein kinase. J Biol Chem.;274(52):37292-300 (1999).

Rena O, Boldorini LR, Gaudino E, Casadio C. Epidermal growth factor receptor overexpression in malignant pleural mesothelioma: prognostic correlations. J Surg Oncol. 2011 Nov 1;104(6):701-5. doi: 10.1002/jso.21901.

Rho JH, Qin S, Wang JY, Roehrl MH Proteomic expression analysis of surgical human colorectal cancer tissues: up-regulation of PSB7, PRDX1, and SRP9 and hypoxic adaptation in cancer J Proteome Res, 2008

Riganti C, Doublier S, Aldieri E, Orecchia S, Betta PG, Gazzano E, Ghigo D, Bosia A. Asbestos induces doxorubicin resistance in MM98 mesothelioma cells via HIF-1alpha. Eur Respir J. 2008 Aug;32(2):443-51. doi: 10.1183/09031936.00090407.

Robinson BW, Creaney J, Lake R, Nowak A, Musk AW, de Klerk N, Winzell P, Hellstrom KE, Hellstrom I. Mesothelin-family proteins and diagnosis of mesothelioma. Lancet; 362(9396):1612-6 (2003).

Robinson BW, Lake RA: Advances in malignant mesothelioma. N Engl J Med 2005, 353:1591-1603.

Røe OD, Anderssen E, Sandeck H, Christensen T, Larsson E, Lundgren S. Malignant pleural mesothelioma: genome-wide expression patterns reflecting general resistance mechanisms and a proposal of novel targets. Lung Cancer. 2010 Jan;67(1):57-68. doi: 10.1016/j.lungcan.2009.03.016.

Rojo F, Najera L, Lirola J, Jiménez J, Guzmán M, Sabadell MD, Baselga J, Ramon y Cajal S. 4E-binding protein 1, a cell signaling hallmark in breast cancer that correlates with pathologic grade and prognosis. Clin Cancer Res. 2007 Jan 1;13(1):81-9.

Rosenzweig KE.. Current readings: improvements in intensity-modulated radiation therapy for malignant pleural mesothelioma. Semin Thorac Cardiovasc Surg 2013;25:245-50.

Roy D, Mondal S, Wang C, He X, Khurana A, Giri S, Hoffmann R, Jung DB, Kim SH, Chini EN, Periera JC, Folmes CD, Mariani A, Dowdy SC, Bakkum-Gamez JN, Riska SM, Oberg AL, Karoly ED, Bell LN, Chien J, Shridhar V. Loss of HSulf-1 promotes altered lipid metabolism in ovarian cancer. Cancer Metab; 2:13 doi: 10.1186/2049-3002-2-13 (2014).

Roushdy-Hammady,I., J.Siegel, S.Emri, J.R.Testa, and M.Carbone. 2001. Genetic-susceptibility factor and malignant mesothelioma in the Cappadocian region of Turkey. Lancet 357: 444-445.

Rufini A, Tucci P, Celardo I, Melino G. Senescence and aging: the critical roles of p53. Oncogene; 32(43):5129-43 (2013).

Ruiz-Garcia E, Scott V, Machavoine C, Bidart JM, Lacroix L, Delaloge S, Andre F].Br J Cancer. Feb 2, 2010; 102(3): 462–468. Published online Jan 12,2010. doi: 10.1038/sj.bjc.6605511 PMCID: PMC2822945

Rusch VW, Giroux D. Do we need a revised staging system for malignant pleural mesothelioma? Analysis of the IASLC database. Ann Cardiothorac Surg. 2012 Nov;1(4):438-48. doi: 10.3978/j.issn.2225-319X.2012.11.10.

Saad RS, Cho P, Liu YL, Silverman JF. The value of epithelial membrane antigen expression in separating benign mesothelial proliferation from malignant mesothelioma: a comparative study. Diagn Cytopath; 32(3):156-9 (2005).

San-Millan I1,2, Brooks GA3. Reexamining cancer metabolism: Lactate production for carcinogenesis could be the purpose and explanation of the Warburg effect. Carcinogenesis. 2016 Dec 17. pii: bgw127.

Santarelli L, Strafella E, Staffolani S, et al. Association of MiR-126 with soluble mesothelinrelated peptides, a marker for malignant mesothelioma. PloS One; 6:e18232 (2011).

Sartain SE, Turner NA, Moake JL. TNF Regulates Essential Alternative Complement Pathway Components and Impairs Activation of Protein C in Human Glomerular Endothelial Cells J Immunol. 2016 Jan 15;196(2):832-45. doi: 10.4049/jimmunol.1500960.

Saxena S, Gandhi A, Lim PW, Relles D, Sarosiek K, Kang C, Chipitsyna G, Sendecki J, Yeo CJ, Arafat HA1. RAN GTPase and Osteopontin in Pancreatic Cancer. Pancreat Disord Ther. 2013 Apr 1;3(1):113.

Schnepp RW, Khurana P, Attiyeh EF, Raman P, Chodosh SE, Oldridge DA, Gagliardi ME, Conkrite KL, Asgharzadeh S, Seeger RC, Madison BB, Rustgi AK, Maris JM, Diskin SJ. A LIN28B-RAN-AURKA Signaling Network Promotes Neuroblastoma Tumourigenesis. Cancer Cell. 2015 Nov 9;28(5):599-609. doi: 10.1016/j.ccell.2015.09.012.

Schulte JD, Srikanth M, Das S, Zhang J, Lathia JD, Yin L, Rich JN, Olson EC, Kessler JA, Chenn A. Cadherin-11 regulates motility in normal cortical neural precursors and glioblastoma. PLoS One. 2013 Aug 7;8(8):e70962. doi: 10.1371/journal.pone.0070962. eCollection 2013.

Sekido,Y. 2008. Molecular biology of malignant mesothelioma. Environ. Health Prev. Med. 13: 65-70.

Seriramalu R, Pang WW, Jayapalan JJ, Mohamed E, Abdul-Rahman PS, Bustam AZ, Khoo AS, Hashim OH. Application of champedak mannose-binding lectin in the glycoproteomic profiling

Shao Y, Zhang L, Cui L, Lou W, Wang D, Lu W, Jin D, Liu T. LIN28B suppresses microRNA let-7b expression to promote CD44+/LIN28B+ human pancreatic cancer stem cell proliferation and invasion. Am J Cancer Res. 2015 Aug 15;5(9):2643-59.

Sheen YS, Liao YH1, Lin MH2, Chu CY3, Ho BY1, Hsieh MC1, Chen PC1, Cha ST4, Jeng YM5, Chang CC6, Chiu HC1, Jee SH1, Kuo ML4, Chu CY1. IMP-3 promotes migration and invasion of melanoma cells by modulating the expression of HMGA2 and predicts poor prognosis in melanoma. J Invest Dermatol. 2015 Apr;135(4):1065-73. doi: 10.1038/jid.2014.480. Epub 2014 Nov 7.

Shi J., H. Liu, H.L. Wang, J.W. Prichard, F. Lin Diagnostic utility of von Hippel-Lindau gene product, maspin, IMP3, and S100P in adenocarcinoma of the gallbladder Hum Pathol, 44 (2013), pp. 503–511

Shi M1, Fraire AE, Chu P, Cornejo K, Woda BA, Dresser K, Rock KL, Jiang Z. Oncofetal protein IMP3, a new diagnostic biomarker to distinguish malignant mesothelioma from reactive mesothelial proliferation. Am J Surg Pathol. 2011 Jun;35(6):878-82. doi: 10.1097/PAS.0b013e318218985b.

Shigematsu Y, Hanagiri T, Kuroda K, Baba T, Mizukami M, Ichiki Y, Yasuda M, Takenoyama M, Sugio K, Yasumoto K. Malignant mesothelioma-associated antigens recognized by tumour-infiltrating B cells and the clinical significance of the antibody titers. Cancer Sci; 100(7):1326-34 (2009).

Shiomi K, Miyamoto H, Segawa T, et al. Novel ELISA system for detection of N-ERC/mesothelin in the sera of mesothelioma patients. Cancer Sci 2006; 97: 928–932

Shull AY, Noonepalle SK, Awan FT, Liu J, Pei L2, Bollag RJ2,4, Salman H2,5, Ding Z6, Shi H1,2. RPPA-based protein profiling reveals eIF4G overexpression and 4E-BP1 serine 65 phosphorylation as molecular events that correspond with a pro-survival phenotype in chronic lymphocytic leukemia. Oncotarget. 2015 Jun 10;6(16):14632-45.

Sidoni A., F. Cartaginese IMP3 expression in triple-negative breast carcinoma Hum Pathol, 41 (2010), pp. 1355–1356 author reply 6-7

Silvera D, Arju R, Darvishian F, Levine PH, Zolfaghari L, Goldberg J, Hochman T, Formenti SC, Schneider RJ. Essential role for eIF4GI overexpression in the pathogenesis of inflammatory breast cancer. Nat Cell Biol. 2009 Jul;11(7):903-8. doi: 10.1038/ncb1900. Epub 2009 Jun 14.

Simeonova PP, Luster MI. Iron and reactive oxygen species in the asbestos-induced tumor necrosis factor-alpha response from alveolar macrophages. Am J Respir Cell Mol Biol. 1995 Jun;12(6):676-83.

Simões-Sousa S, Granja S, Pinheiro C, Fernandes D, Longatto-Filho A, Laus AC, Alves CD, Suárez-Peñaranda JM, Pérez-Sayáns M, Lopes Carvalho A, Schmitt FC, García-García A, Baltazar F Prognostic significance of monocarboxylate transporter expression in oral cavity tumours. Cell Cycle. 2016 Jul 17;15(14):1865-73. doi: 10.1080/15384101.2016.1188239. Epub 2016 May 27.

Smookler DS, Mohammed FF, Kassiri Z, Duncan GS, Mak TW, Khokha R. Tissue inhibitor of metalloproteinase 3 regulates TNF-dependent systemic inflammation. J Immunol.; 176(2):721-5 (2006).

Somwar R, Erdjument-Bromage H, Larsson E, Shum D, Lockwood WW, Yang G, Sander C, Ouerfelli O, Tempst PJ, Djaballah H, Varmus HE. Superoxide dismutase 1 (SOD1) is a target for a small molecule identified in a screen for inhibitors of the growth of lung adenocarcinoma cell lines. Proc Natl Acad Sci U S A. 2011 Sep 27;108(39):16375-80. doi: 10.1073/pnas.1113554108

Stamenkovic I, Yu Q. Merlin, a "magic" linker between extracellular cues and intracellular signaling pathways that regulate cell motility, proliferation, and survival. Curr Protein Pept Sci. 2010 Sep;11(6):471-84.

Stayner L, Kuempel E, Gilbert S, Hein M, Dement J. An epidemiological study of the role of chrysotile asbestos fibre dimensions in determining respiratory disease risk in exposed workers. Occup. Environ. Med. 2008;65(9):613–619.

Sternlicht MD, Werb Z. How matrix metalloproteinases regulate cell behavior. Annu Rev Cell Dev Biol; 17: 463–516 (2001).

Streit M, Riccardi L, Velasco P, Brown LF, Hawighorst T, Bornstein P, Detmar M. Thrombospondin-2: a potent endogenous inhibitor of tumour growth and angiogenesis. Proc NatlAcad Sci USA; 96(26):14888-93 (1999).

Streit M, Stephen AE, Hawighorst T, Matsuda K, Lange-Asschenfeldt B, Brown LF, Vacanti JP, Detmar M. Systemic inhibition of tumour growth and angiogenesis by thrombospondin-2 using cell-based antiangiogenic gene therapy. Cancer Res; 62(7):2004-12 (2002).

Su P, Hu J, Zhang H1, Li W1, Jia M1, Zhang X1, Wu X1, Cheng H1, Xiang L1, Zhou G1. IMP3 expression is associated with epithelial-mesenchymal transition in breast cancer. Int J Clin Exp Pathol. 2014 May 15;7(6):3008-17. eCollection 2014.

Swain WA, O'Byrne KJ, Faux SP. Activation of p38 MAP kinase by asbestos in rat mesothelial cells is mediated by oxidative stress. Am J Physiol Lung Cell Mol Physiol.;286(4): L859-65 (2004).

Szlosarek P.W., Klabatsa A., Pallaska A., Sheaff M., Smith P., Crook T., Grimshaw M.J., Steele J.P., Rudd R.M., Balkwill F.R., Fennell D.A. In vivo loss of expression of argininosuccinate synthetase in malignant pleural mesothelioma is a biomarker for susceptibility to arginine depletion. Clin. Cancer Res. 2006;12:7126–7131.

Szlosarek PW, Grimshaw MJ, Wilbanks GD, Hagemann T, Wilson JL, Burke F, Stamp G, Balkwill FR Aberrant regulation of argininosuccinate synthetase by TNF-alpha in human epithelial ovarian cancer Int J Cancer, 2007

Szlosarek PW, Steele JP, Nolan L, Gilligan D, Taylor P, Spicer J, Lind M, Mitra S, Shamash J, Phillips MM, Luong P, Payne S, Hillman P, Ellis S, Szyszko T, Dancey G, Butcher L, Beck S, Avril NE, Thomson J, Johnston A, Tomsa M, Lawrence C, Schmid P, Crook T, Wu BW,

Bomalaski JS, Lemoine N, Sheaff MT, Rudd RM, Fennell D, Hackshaw A. Arginine Deprivation With Pegylated Arginine Deiminase in Patients With Argininosuccinate Synthetase 1-Deficient Malignant Pleural Mesothelioma: A Randomized Clinical Trial. JAMA Oncol. 2016 Sep 1. doi: 10.1001/jamaoncol.2016.3049.

Takizawa K, Yamamoto H, Taguchi K, Ohno S, Tokunaga E, Yamashita N, Kubo M, Nakamura M, Oda Y. Insulin-like growth factor II messenger RNA-binding protein-3 is an indicator of malignant phyllodes tumour of the breast. Hum Pathol. 2016 Sep;55:30-8. doi: 10.1016/j.humpath.2016.04.007.

Thurneysen C, Opitz I, Kurtz S, Weder W, Stahel RA, Felley-Bosco E. Functional inactivation of NF2/merlin in human mesothelioma. Lung cancer. 2009;64(2):140–7.

Tokunaga T, Nakamura M, Oshika Y, Abe Y, Ozeki Y, Fukushima Y, Hatanaka H, Sadahiro S, Kijima H, Tsuchida T, et al. Thrombospondin 2 expression is correlated with inhibition of angiogenesis and metastasis of colon cancer. Br J Cancer. 1999;79:354–359. doi: 10.1038/sj.bjc.6690056.

Tomasson K, Gudmundsson G, Briem H3, Rafnsson V4Malignant mesothelioma incidence by nation-wide cancer registry: a population-based study. J Occup Med Toxicol. 2016 Jul 26;11:37. doi: 10.1186/s12995-016-0127-4. eCollection 2016.

Tome ME, Frye JB, Coyle DL, Jacobson EL, Samulitis BK, Dvorak K, Dorr RT, Briehl MM. Lymphoma cells with increased anti-oxidant defenses acquire chemoresistance. Exp Ther Med. 2012;3:845–852.

Trachootham D, Alexandre J, Huang P. Targeting cancer cells by ROS-mediated mechanisms: a radical therapeutic approach? Nat Rev Drug Discov. 2009;8:579–591.

Travis W.D., E.Brambilla, H.K.Muller-Hermelink, et al. 2004. WHO classification of tumours. Pathology and genetics of tumours of the lung, pleura, thymus, and heart. WHO classification of tumours. IARCPress, International Agency for Research on Cancer: Lyon, France, 128-136.

Trieselmann, N., Armstrong, S., Rauw, J., and Wilde, A. (2003). Ran modulates spindle assembly by regulating a subset of TPX2 and Kid activities including Aurora A activation. J. Cell Sci. 116, 4791–4798.

Tront JS, Hoffman B, Liebermann DA. Gadd45a suppresses Ras-driven mammary tumourigenesis by activation of c-Jun NH2-terminal kinase and p38 stress signaling resulting in apoptosis and senescence. Cancer Res.;66(17):8448-54 (2006).

Tsai WB, Aiba I, Lee SY, Feun L, Savaraj N, Kuo MT Resistance to arginine deiminase treatment in melanoma cells is associated with induced argininosuccinate synthetase expression involving c-Myc/HIF-1alpha/Sp4. Mol Cancer Ther. 2009 Dec; 8(12):3223-33.

Tsai, M.Y., Wiese, C., Cao, K., Martin, O., Donovan, P., Ruderman, J., Prigent, C., and Zheng, Y. (2003). A Ran signalling pathway mediated by the mitotic kinase Aurora A in spindle assembly. Nat. Cell Biol. 5, 242–248.

Uematsu K, Seki N, Seto T, Isoe C, Tsukamoto H, Mikami I, You L, He B, Xu Z, Jablons DM, Eguchi K. Targeting the Wnt signaling pathway with dishevelled and cisplatin synergistically suppresses mesothelioma cell growth Anticancer Res. 2007 Nov-Dec;27(6B):4239-42.

Vaidyanathan S, Thangavelu PU, Duijf PH. Overexpression of Ran GTPase Components Regulating Nuclear Export, but not Mitotic Spindle Assembly, Marks Chromosome Instability and Poor Prognosis in Breast Cancer. Target Oncol. 2016 Oct;11(5):677-686.

Vaishnaw,A.K., J.Gollob, C.Gamba-Vitalo, R.Hutabarat, D.Sah, R.Meyers, F.T.de, and J.Maraganore. 2010. A status report on RNAi therapeutics. Silence. 1: 14.

Vercellini P., F.M. Cribiu, A. Del Gobbo, M.L. Carcangiu, E. Somigliana, S. Bosari The oncofetal protein IMP3: a novel biomarker and triage tool for premalignant atypical endometriotic lesions Fertil Steril, 99 (2013), pp. 1974–1979

Versnel MA, Hoogsteden HC, Hagemeijer A, Bouts MJ, van der Kwast TH, et al. (1989) Characterization of three human malignant mesothelioma cell lines. Cancer Genet Cytogenet. 42(1): 115–28

Vicente CM, Lima MA, Yates EA, Nader HB, Toma L Enhanced tumourigenic potential of colorectal cancer cells by extracellular sulfatases. Mol Cancer Res. 2015 Mar;13(3):510-23. doi: 10.1158/1541-7786.MCR-14-0372. Epub 2014 Dec 4.

Viviano BL, Paine-Saunders S, Gasiunas N, Gallagher J, Saunders S. Domain-specific modification of heparan sulfate by Qsulf1 modulates the binding of the bone morphogenetic protein antagonist Noggin. J Biol Chem; 279(7):5604-11 (2004).

Vogelzang NJ, Rusthoven JJ, Symanowski J, Denham C, Kaukel E, Ruffie P, Gatzemeier U, Boyer M, Emri S, Manegold C, Niyikiza C, Paoletti P. Phase III study of pemetrexed in combination with cisplatin versus cisplatin alone in patients with malignant pleural mesothelioma. J Clin Oncol. 2003 Jul 15;21(14):2636-44.

Vogelzang, N.J.; Rusthoven, J.J.; Symanowski, J., Denham, C., Kaukel, E., Ruffie, P., Gatzemeier, U., Boyer,M., Emri, S.,Manegold, C.,Niyikiza, C., Paoletti, P. Phase III study of pemetrexed in combination with cisplatin versus cisplatin alone in patients with malignant pleural mesothelioma. J. Clin. Oncol. 2003, 21, 2636–2644.

Wachter D.L., G. Kristiansen, C. Soll, C. Hellerbrand, K. Breuhahn, F. Fritzsche, et al. Insulin-like growth factor II mRNA-binding protein 3 (IMP3) expression in hepatocellular carcinoma. A clinicopathological analysis with emphasis on diagnostic value Histopathology, 60 (2012), pp. 278–286

Walter O., M. Prasad, S. Lu, R.M. Quinlan, K.L. Edmiston, A. Khan IMP3 is a novel biomarker for triple negative invasive mammary carcinoma associated with a more aggressive phenotype Hum Pathol, 40 (2009), pp. 1528–1533

Wang L., H.G. Li, Z.S. Xia, J. Lu, T.S. Peng IMP3 is a novel biomarker to predict metastasis and prognosis of gastric adenocarcinoma: a retrospective study Chin Med J (Engl), 123 (2010), pp. 3554–3558

Wangpaichitr M, Sullivan EJ, Theodoropoulos G, Wu C, You M, Feun LG, Lampidis TJ, Kuo MT, Savaraj N. The relationship of thioredoxin-1 and cisplatin resistance: its impact on ROS and oxidative metabolism in lung cancer cells. Mol Cancer Ther. 2012 Mar;11(3):604-15. doi: 10.1158/1535-7163.MCT-11-0599.

Wei Q., B. Fu, J. Liu, J. Xu, T. Zhao Combined detection of p16(INK4a) and IMP3 increase the concordance rate between cervical cytologic and histologic diagnosis Int J Clin Exp Pathol, 6 (2013), pp. 1549–1557

Weng TY, Wang CY, Hung YH, Chen WC, Chen YL, Lai MD. Differential Expression Pattern of THBS1 and THBS2 in Lung Cancer: Clinical Outcome and a Systematic-Analysis of Microarray Databases. PLoS One. 2016 Aug 11;11(8):e0161007. doi: 10.1371/journal.pone.0161007. eCollection 2016.

Whitcomb BP, Mutch DG, Herzog TJ, Rader JS, Gibb RK, Goodfellow PJ. Frequent HOXA11 and THBS2 promoter methylation, and a methylator phenotype in endometrial adenocarcinoma. Clin Cancer Res; 9(6):2277-87 (2003).

World Health Organization. Elimination of asbestos related disease. WHO/SDE/OEH/0603 (September 2006).

Xia F, Lee CW, Altieri DC. Tumour cell dependence on Ran-GTP-directed mitosis. Cancer Res. 2008 Mar 15;68(6):1826-33. doi: 10.1158/0008-5472.CAN-07-5279.

Xu CZ, Shi RJ, Chen D, Sun YY, Wu QW, Wang T, Wang PH. Potential biomarkers for paclitaxel sensitivity in hypopharynx cancer cell. Int J Clin Exp Pathol; 6(12):2745-56 (2013).

Yan TD, Haveric N, Carmignani CP, et al. Computed tomographic characterization of malignant peritoneal mesothelioma. Tumouri 2005;91:394-400.

Yan Z, Li Z, Yao W, Wu W, Wu Y. Expression and clinical significance of Ran in lung squamous carcinoma tissues. Wei Sheng Yan Jiu. 2010 Sep;39(5):583-5.

Yang H, Bocchetta M, Kroczynska B, Elmishad AG, Chen Y, Liu Z, Bubici C, Mossman BT, Pass HI, Testa JR, Franzoso G, Carbone M. TNF-alpha inhibits asbestos-induced cytotoxicity via a NF-kappaB-dependent pathway, a possible mechanism for asbestos-induced oncogenesis. Proc Natl Acad Sci U S A. 2006 Jul 5;103(27):10397-402.

Yang S, Shin J, Park KH, Jeung HC, Rha SY, Noh SH, Yang WI, Chung HC. Molecular basis of the differences between normal and tumour tissues of gastric cancer. Biochim Biophys Acta; 1772(9):1033-40 (2007).

Yang TS, Lu SN, Chao Y, Sheen IS, Lin CC, Wang TE, Chen SC, Wang JH, Liao LY, Thomson JA, Wang-Peng J, Chen PJ, Chen LT. A randomised phase II study of pegylated arginine deiminase (ADI-PEG 20) in Asian advanced hepatocellular carcinoma patients. Br J Cancer. 2010 Sep 28;103(7):954-60. doi: 10.1038/sj.bjc.6605856.

Yasumitsu A, Tabata C, Tabata R, et al. Clinical significance of serum vascular endothelial growth factor in malignant pleural mesothelioma. J Thorac Oncol; 5:479-83 (2010).

Yip CK, Murata K, Walz T, Sabatini DM, Kang SA. Structure of the human mTOR complex I and its implications for rapamycin inhibition. Mol Cell. 2010 Jun 11;38(5):768-74. doi: 10.1016/j.molcel.2010.05.017.

Young B, Purcell C, Kuang YQ, Charette N, Dupré DJ. Superoxide Dismutase 1 Regulation of CXCR4-Mediated Signaling in Prostate Cancer Cells is Dependent on Cellular Oxidative State. Cell Physiol Biochem. 2015;37(6):2071-84. doi: 10.1159/000438566.

Yuen HF, Chan KK1, Platt-Higgins A2, Dakir el-H1,3, Matchett KB1, Haggag YA1,4, Jithesh PV5, Habib T5, Faheem A6, Dean FA7, Morgan R3, Rudland PS2, El-Tanani M3. Ran GTPase promotes cancer progression via Met receptor mediated downstream signaling. Oncotarget. 2016 Oct 3. doi: 10.18632/oncotarget.12420.

Zhang SX, Gozal D, Sachleben LR Jr, Rane M, Klein JB, Gozal E. Hypoxia induces an autocrine-paracrine survival pathway via platelet-derived growth factor (PDGF)-B/PDGFbeta receptor/phosphatidylinositol 3-kinase/Akt signaling in RN46A neuronal cells. FASEB J; 17(12):1709-11 (2003).

Zheng W., X. Yi, O. Fadare, S.X. Liang, M. Martel, P.E. Schwartz, et al. The oncofetal protein IMP3: a novel biomarker for endometrial serous carcinoma Am J Surg Pathol, 32 (2008), pp. 304–315

Zhong J, Gencay MM, Bubendorf L, Burgess JK, Parson H, Robinson BW, Tamm M, Black JL, Roth M. ERK1/2 and p38 MAP kinase control MMP-2, MT1-MMP, and TIMP action and affect cell migration: a comparison between mesothelioma and mesothelial cells. J Cell Physiol.; 207(2):540-52 (2006).

Zucali,P.A. and G.Giaccone. 2006. Biology and management of malignant pleural mesothelioma. Eur. J. Cancer 42: 2706-2714.

Zucali,P.A., G.L.Ceresoli, V.F.De, M.Simonelli, E.Lorenzi, L.Gianoncelli, and A.Santoro. 2011. Advances in the biology of malignant pleural mesothelioma. Cancer Treat. Rev. 37: 543-558.